Development of an LC-MS/MS method for the analysis of triacylglycerols from meat and application in the discrimination of cooked meat products

HASLINA HASAN

A thesis submitted in partial fulfilment of the requirement for the degree of Doctor of Philosophy at the University of York

Department of Chemistry
University of York

June 2010

Abstract

A single stage reversed phase high performance liquid chromatography (RP HPLC) separation of animal fat triacylglycerols (TAGs) has been developed for coupling with atmospheric pressure chemical ionization tandem mass spectrometry using an ion trap mass spectrometer. The method developed offers significant improvements on existing methods for TAG analysis, giving better resolution of TAGs with similar equivalent carbon number (ECN), and good separation of TAGs with odd ECN and TAG regioisomers of animal fats. Although the analysis times for chromatographic analysis of these TAGs are long, this is compensated by better separation of highly unsaturated TAGs. Development of an ultra high performance liquid chromatography method has reduced the run time by half, while maintaining separation and resolution. The TAG profiles of fats reflect their fatty acid (FA) compositions, showing a high proportion of unsaturated FAs for chicken and pork, whereas, saturated FAs are dominant in the major TAGs detected in beef and lamb. The improved RP HPLC separation of TAGs developed in this study has been shown to give more reliable discrimination of different animal species than previous methods including analysis of FAs as the methyl esters and RP HPLC separations of intact TAGs. All animal species separated well in the principal component analysis (PCA) plot of TAG profiles, whereas in the PCA plot of FA, chicken plots very close to pork fat, particularly ham. The profiles of TAGs in animal species highlight a number of components that are important for species discrimination.

The meat products of different species (beef, pork, chicken and lamb) cooked by microwave, roasting and currying are separated well in the PCA scores plot. This work shows that the discrimination of meat from different animal species is possible for both raw and cooked meat products, and reveals that the differences produced by the various cooking methods were less than the variations observed between species. The loadings values for the scores plot of TAGs for raw and cooked meat products are similar to the raw meat in different animal species and have the same important descriptors for discrimination. Hence, analysis of intact TAGs in cooked food products has considerable potential for detection of adulteration of cooked meat-based food products.

CONTENTS

Title page		i
Abstract		ii
Contents		iii
List of tables		viii
List of figures		x
Symbol and abbreviations		xvii
Acknowledgement		xix
Author's declaration		xx
Chapter 1	**: Introduction**	**1**
1.1	Food authenticity and adulteration	2
1.2	Recent developments in food authentication and the detection of adulteration	3
1.3	Nomenclature and structures of TAGs	6
1.4	TAG distributions in animal fats	9
1.5	Separation of complex TAGs mixture	11
	1.5.2 Gas chromatography	11
	1.5.1.1 Separation of FAs	11
	1.5.1.2 Separation of TAGs	11
	1.5.2 High performance liquid chromatography	13
	1.5.2.1 Separation of TAGs by single stage HPLC	13
	1.5.2.2 Separation of positional isomers of TAGs	14
1.6	Limitations of current studies	15
1.7	Background on instrumentation	16
	1.7.1 Gas chromatography	16
	1.7.2 Reversed phase high performance liquid chromatography (RP HPLC)	17

1.7.3 Mass spectrometry 19
1.7.3.1 Atmospheric pressure chemical ionization 19
1.7.3.2 Electrospray ionization 21
1.7.3.3 Ion trap mass spectrometry (ITMS) 22
1.7.3.4 Multistage tandem mass spectrometry (MS^n) 24
1.7.3.5 Collision-induced dissociation (CID) 25

1.8 Aims of the research 26

Chapter 2 :Development of single stage RP HPLC-APCIMS/MS separation of TAGs 27

2.1 Introduction and aims 28

2.2 Results and discussion 31
2.2.1 Structural characterization of TAG standards of OOP* and OPO 31
2.2.1.1 Mass spectra of OOP* and OPO standards 31
2.2.1.2 Collision induced dissociation (CID) of OOP* and OPO standards in MS^2 32
2.2.1.3 CID of OPO and OOP* standard in MS^3 36
2.2.2 MS of TAGs in beef and pork fats by direct infusion 39
2.2.3 Development of a single stage RP HPLC-MS/MS separation of TAGs 42
2.2.3.1 Development of RP HPLC separation of TAGs from beef fat 42
2.2.3.2 MS spectra of separated TAGs from RPHPLC-APCI MS 59
2.2.3.3 CID of ammoniated TAG ions in MS^2 of beef and pork fat 64
2.2.3.4 CID of DAG product ions in MS^3 76
2.2.3.5 TAG profiles of beef and pork fat 77

2.2.4 RP HPLC-APCI MS/MS separation of regioisomers of TAGs from beef, pork, chicken and lamb fat 83
2.2.4.1 Chromatographic separation of TAG isomers from beef, pork, chicken and lamb fat 83
2.2.4.2 Mass spectra of separated TAG isomers from beef fat 86
2.2.4.3 Regioisomer compositions of TAGs of beef, lamb, pork and chicken fats 95
2.2.5 UHPLC vs. HPLC for separating TAGs of beef fat sample 99

2.3 Conclusions 102

Chapter 3 :FA and TAG variations in different anatomical location of pigs and different animal species 104

3.1 Introduction and aims 105

3.2 Results and discussion 107
3.2.1 FA profiles of beef, lamb, chicken and pork fats 107
3.2.2 FA profiles from different anatomical locations of pork adipose tissues 112
3.2.3 TAG profiles of beef, lamb, chicken and pork 119
3.2.4 TAG profiles of adipose tissue for different anatomical locations of pork 126
3.2.5 PCA of FAME and TAG profiles for different animal species 131
3.2.5.1 PCA of FAMEs for beef, lamb, chicken and pork 131
3.2.5.2 PCA of TAGs for beef, lamb, chicken and pork 134
3.2.6 PCA of FAME and TAG profiles of adipose tissue from different anatomical locations of pork 139
3.2.6.1 PCA of FAMEs of adipose tissue from different anatomical locations of pork 139

3.2.6.2 PCA of TAGs of adipose tissue from different anatomical locations of pork 142

3.3 Conclusions 145

Chapter 4 : Analysis of TAGs for discrimination of cooked meat products 148

4.1 Introduction and aims 149

4.2 Results and discussion 152

4.2.1 RP HPLC-APCI MS/MS separation of TAGS from cooked meat products of beef, lamb, chicken and pork 152

4.2.2 Evaluation of regioisomer of TAGs resolved from cooked meat products 157

4.2.3 TAG variations of raw and cooked meat products 159

4.2.4 PCA of TAG profiles for raw and different cooking methods of beef, lamb, chicken and pork 170

4.2.4.1 PCA of TAGs for raw and cooked beef 170

4.2.4.2 PCA of TAGs for raw and cooked lamb 173

4.2.4.3 PCA of TAGs for raw and cooked chicken 175

4.2.4.4 PCA of TAGs for raw and cooked pork 178

4.2.5 PCA of TAG profiles for raw and cooked meat products 180

4.3 Conclusions 190

Chapter 5 : Overall conclusions and future work 192

5.1 Overall conclusions 193

5.2 Future work 198

Chapter 6 : Experimental **200**

6.1 Chemicals 201
6.1.1 Reagents and standards 201
6.1.2 Sampling 201
6.1.2.1 Different anatomical locations of adipose tissue 201
6.1.2.2 Raw/uncooked meat samples 203
6.1.2.3 Cooked meat products 203
6.1.3 Extraction procedure 204
6.1.3.1 Solvent extraction (Liquid-liquid extraction). 204
6.1.3.2 Accelerated Solvent Extraction (ASE). 205
6.1.4 Hydrolysis and methylation of the fat extract. 206

6.2 Instrumentation 207
6.2.1 GC/FID 207
6.2.2 HPLC-LCQ ion trap 209
6.2.3 RSLC-HCT 210
6.2.4 HPLC– HCT ultra ETD 211

6.3 Statistical analysis 211

References **212**

LIST OF TABLES

Chapter 1

Table 1.1 Scientific names, chemical formula, carbon numbers (CN) and double bond number (DB) and chemical structures of TAGs. 8

1.2 Abbreviations, trivial names, scientific names, carbon numbers: double bond number and chemical formula of common FAs in animal fats. 10

Chapter 2

Table 2.1 Relative abundances of product ions of TAG standard OOP and OPO in solvent with ammonium acetate added: a) $[OP]^+$ b) $[OO]^+$ and c) the relative DAG ratio $[OP]^+/ [OO]^+$ under APCI and ESI conditions. 35

2.2 Proportions of 2-propanol and acetonitrile in the mobile phase of a) Dugo et al., 2006 and variations in gradient profile employed in this study (Method A), b) as modified in this study (Method B). 43

2.3 HPLC columns tested for separation of TAGs from beef fat, ordered according to decreasing particle size. 43

2.4 Proportions of chloroform and acetonitrile in the mobile phase Method C and D for the separation of TAGs from beef fat, a) Fauconnot et al., 2004 (Method C), b) as modified in this study (Method D). 48

2.5 Proportions of dichloromethane and acetonitrile in the mobile phase of Method E and F eluted on the a) Apex ODS column (Method E), b) Genesis C18 column (Method F) for separating the TAGs from beef fat. 50

2.6 Proportions of dichloromethane and acetonitrile in the mobile phase of a) Method G, b) Method H on the Waters Spherisorb ODS2 columns for separating the TAGs of beef fat. 53

2.7 TAG identifications from ammoniated molecules, $[M+NH_4]^+$, protonated molecules, $[M + H]^+$, and DAG product ions, $[M-RCO_2]^+$ of beef and pork fats analysed by RP HPLC-APCI MS/MS using the method developed in Section 2.2.3.1 (Method H). 74

2.8 RCO^+ ions observed in the mass spectra of beef and pork fat. 76

2.9	Percentages of TAG isomers resolved from beef, lamb, chicken and pork fat.	96
2.10	The mobile phase gradient for separation of TAGs on the Ultimate 3000 RS (Dionex) UHPLC system with two RSLC Acclaim 120 C18 2.2 um (2.1 x 100 mm, 2.2 μm) columns (Method I).	99

Chapter 3

Table 3.1	Mean percentages of FAMEs for different anatomical locations of pork adipose tissues.	113
3.2	Mean percentages of TAGs for different animal species analysed by RP HPLC-APCI MS/MS (Method J; Chapter 6; Section 6.2.4).	120
3.3	The mean percentage of TAGs for different anatomical locations of pork fat (Method J; Chapter 6; Section 6.2.4).	127

Chapter 4

Table 4.1	Mean percentages of TAGs from raw and cooked meat products of pork, chicken, beef and lamb.	156
4.2	Percentages of resolved regioisomer of TAGs from raw and cooked beef	157
4.3	The percentages of separated TAG isomers from raw and cooked lamb	158
4.4	Reassessed proportions of TAGs for chicken curry after subtracting possible TAGs from rapeseed oil.	166
4.5	The reassessed proportions of TAGs for beef curry^{+} after considering the TAGs from rapeseed oil and TAGs for beef curry $^{++}$ after subtracting possible TAGs from rapeseed oil.	182

Chapter 6

Table 6.1	Chromatographic conditions used in the determination of FAMEs for split injector.	207
6.2	Chromatographic conditions used in the determination of FAMEs for on column.	208
6.3	The mobile phase gradient for HPLC for separation of TAGs.	209

6.4 The mobile phase gradient for Ultimate 3000 RS (Dionex) RSLC for separation of TAGs (Method I). 210

6.5 The mobile phase gradient for Dionex Ultimate 3000 HPLC for separation of TAGs (Method J). 211

LIST OF FIGURES

Chapter 1

Figure 1.1 Generalized structure of a triacylglycerol, R^{1-3} represent alkyl groups. 6

1.2 van Deemter plot, illustrating the evolution of particle sizes (2006 Waters Corporation). 18

1.3 Generalised schematic diagram of an APCI source, illustrating the formation of ions (modification from Covey et al., 1986). 20

1.4 The cross section of ion trap (modification of March, 1997). 22

1.5 The regions of stability in the quadrupole ion trap (Jonscher et al., 1997) 24

Chapter 2

Figure 2.1 Direct infusion of OPO dissolved in acetonitrile:methanol (70:30) with added ammonium acetate a) APCI-MS spectrum of OPO b) ESI-MS spectrum of OPO. 32

2.2 a) APCI-MS^2 spectrum of ammoniated OPO, b) ESI-MS^2 spectrum of ammoniated OPO. (Both were from direct infusion of OPO dissolved in acetonitrile:methanol (70:30) with added ammonium acetate). (PI = precursor ion). 34

2.3 a) APCI-MS^3 spectrum of *m/z* 603, b) APCI-MS^3 spectrum of *m/z* 577. (Both were from direct infusion of OPO dissolved in acetonitrile:methanol (70:30) with added ammonium acetate; PI = precursor ion). 37

2.4 a) ESI-MS^3 spectrum of *m/z* 603, b) ESI-MS^3 spectrum of *m/z* 577. (Both were from direct infusion of OPO dissolved in acetonitrile:methanol (70:30) with added ammonium acetate; PI = precursor ion). 38

2.5 Direct infusion of an extract of pork fat in acetonitrile and methanol (70:30) with ammonium acetate addition, a) ESI-MS spectrum (all ions are ammoniated TAGs). b) APCI-MS spectrum. 40

2.6 Direct infusion of an extract of beef fat in acetonitrile and methanol (70:30) with ammonium acetate addition, a) ESI-MS spectrum (all ions are ammoniated TAGs). b) APCI-MS spectrum. 41

2.7 a) RP HPLC-APCI MS chromatogram of TAGs from beef fat with regions of the chromatogram assigned according to ECN (modified from Dugo et al., 2006). b) RP HPLC-APCI MS chromatogram of TAGs from beef fat on the Apex ODS column using the mobile phase system of Dugo et al., 2006 (Method A; Table 2.2a, labelled $^{+}$). 44

2.8 RP HPLC-APCI MS chromatogram of TAGs from beef fat eluted with the mobile phase Method B (Table 2.2b) on the a) Apex ODS column. b) Genesis C18 column. 46

2.9 RP HPLC-APCI MS chromatograms of TAGs from beef fat on the Apex ODS column eluted using a) chloroform and acetonitrile (Method C; Table 2.4a), b) modified proportion of chloroform and acetonitrile (Method D; Table 2.4b). 49

2.10 RP HPLC-APCI MS chromatogram of TAGs from beef fat a) on the Apex ODS column eluted with the mobile phase in Method E (Table 2.5a), b) on the Genesis C18 column eluted with the mobile phase in Method F (Table 2.5b). 52

2.11 RP HPLC-APCI MS chromatogram of TAGs from beef fat on the Waters Spherisorb ODS2 column a) eluted with the mobile phase of Method G (Table 2.6a), b) eluted with the mobile phase of Method H (Table 2.6b). 56

2.12 a) RP HPLC-APCI MS chromatogram of TAGs from pork fat (modified from Dugo et al., 2006). b) RP HPLC-APCI MS chromatogram of TAGs from pork fat on the Waters Spherisorb ODS2 column eluted with the mobile phase of Method H (Table 2.6b). 58

2.13 RP HPLC-APCI MS chromatograms of a) beef fat. b) pork fat. 60

2.14 a) EIC of dominant peaks in pork fat, b) the spectrum across the peak with *m/z* 900.4, c) the spectrum across the peak with *m/z* 874.4 and d) the spectrum across the peak with *m/z* 876.4. 61

2.15 a) EIC of trisaturated TAGs in beef fat, and APCI-MS spectra for b) peak 1; *m/z* 824 to 825, c) peak 2; *m/z* 852 to 853, d) peak 4; *m/z* 880 to 881. 63

2.16 a) EIC from MS, MS^2 and mass range chromatograms of beef fat, AAA type TAGs are labelled b) MS^2 spectrum from ammoniated TAG at *m/z* 902 and c) MS^2 spectrum from ammoniated TAG at *m/z* 908 (PI=precursor ion). 65

2.17 a) EIC from MS and MS^2 of pork fat labelled with ABA type TAGs and MS^2 spectra from ammoniated TAGs at b) *m/z* 883, c) *m/z* 876, d) *m/z* 890 and e) *m/z* 880 (PI=precursor ion). 67

2.18 a) EIC from MS and MS^2 of beef fat labelled with AAB type TAGs and MS^2 spectra from ammoniated TAGs at b) *m/z* 876.3, c) *m/z* 904.4, d) *m/z* 852.4, e) *m/z* 906.4 and f) *m/z* 880.4 (PI=precursor ion; Rel. ab. = relative abundance). 69
ABC TAGs

2.19 a) EIC from MS and MS^2 of pork fat labelled with ABC type TAGs and MS^2 spectra from ammoniated TAGs at b) *m/z* 874.4, c) *m/z* 878.4 and d) *m/z* 892.4 (PI=precursor ion; Rel. ab. = relative abundance). 72

2.20 Structures of LPO* and DAG product ions including possible resonance structures. 73

2.21 RP HPLC-APCI MS chromatograms of a) beef fat and b) pork fat labelled with identified TAG peaks on the Waters Spherisorb ODS2 column eluted with the mobile phase of Method H (Section 2.2.3.1; Table 2.6b). 78

2.22 Base peak at *m/z* 877.5 for coeluted LLLn* and LnLnO* compound in pork fat and EICs for mass ranges corresponding to the DAG product ions. 79

2.23 Base peak chromatogram and EIC at *m/z* 848 to *m/z* 849 for OPPo* which partially coeluted with LPO*. 80

2.24 RP HPLC-APCI MS chromatogram of beef fat labelled with 8 groups of separated regioisomers of TAGs eluted with the mobile phase of Method H (Section 2.2.3.1; Table 2.6b). 84

2.25 RP HPLC-APCI MS chromatograms of TAG isomers from beef, lamb, chicken and pork fat eluted with the mobile phase of Method H (Section 2.2.3.1; Table 2.6b). 84

2.26 RP HPLC-APCI MS chromatogram of POM*/PMO* isomers in beef fat and MS^2 spectra (PI = precursor ion). 86

2.27 RP HPLC-APCI MS chromatogram of OOP*/OPO isomers from beef fat and insert MS^2 spectra (PI = precursor ion). 87

2.28 RP HPLC-APCI MS chromatogram of POP/OPP* isomers in beef fat and insert MS^2 spectra (PI = precursor ion). 88

2.29 RP HPLC-APCI MS chromatogram of OOS*/OSO isomers in beef fat and insert MS^2 spectra (PI = precursor ion). 89

2.30 RP HPLC-APCI MS chromatogram of SOP*/SPO* isomers from beef fat and insert MS^2 spectra (PI = precursor ion). 90

2.31 RP HPLC-APCI MS chromatogram of SPMa*/SMaP* isomers from beef fat and insert MS^2 spectra (PI = precursor ion). 91

2.32 RP HPLC-APCI MS chromatogram of SOS/SSO* isomers from beef fat and insert MS^2 spectra (PI = precursor ion). 92

2.33 RP HPLC-APCI MS chromatogram of SSMa*/SMaS isomers from beef fat and insert MS^2 spectra (PI = precursor ion). 93

2.34 RP HPLC-APCI MS chromatogram and insert MS^2 spectra of SLO* isomers; SLO*, SOL* and LSO* from pork fat (PI = precursor ion). 94

2.35 a) RP HPLC-APCI MS chromatogram and EIC for all ions present for OOS*/OSO isomers of lamb fat and b) the histogram of area percent for OOS* and OSO isomers. 95

2.36 UHPLC-APCI MS chromatogram of TAGs from beef fat sample on the two RSLC acclaim 120 C18 (2.1x100mm, 2.2μm) columns with the mobile phase of Method I (Table 2.10). 101

2.37 HPLC-APCI MS chromatogram of TAGs from beef fat sample on the two Waters Spherisorb ODS2 (4.6x150mm,3μm) columns with the mobile phase of Method H (Section 2.2.3.1). 101

Chapter 3

Figure 3.1 GC chromatograms of FAMEs for a) lamb b) beef c) chicken and d) pork fat. 108

3.2 a) Percentages of FAMEs for beef, lamb, chicken and pork. b) Percentages of FAMEs for beef, lamb, chicken and pork (rescale to low relative abundance FAMEs). 109

3.3 Relationships between mean of SFA and PUFA in animal fats. 111

3.4 a) Percentages of FAMEs for different anatomical location of pork b) Percentages of FAMEs for different anatomical location of pork 114

rescaled to low percentage of FAMEs).

3.5 a) Percentages of FAMEs for SC fats of pork b) Percentages of FAMEs for IM fats of pork. 116

3.6 Relationships between mean of MUFA and SFA from different anatomical locations of pork adipose tissues. 117

3.7 Relationships between mean of MUFA and PUFA from different anatomical locations of pork adipose tissues. 118

3.8 Chromatograms of TAGs for a) Chicken, b) Pork, c) Beef and d) Lamb. 119

3.9 Histograms for the proportions of TAGs for pork, chicken, beef and lamb. 122

3.10 Histograms for the proportions of TAGs of a) pork and chicken b) beef and lamb c) pork and beef and d) chicken and lamb. 124

3.11 Chromatograms of TAGs for a) BIM, b) BSC, c) HIM and d) HSC (Refer to Table 3.3 for identification of TAGs peak). 126

3.12 Histograms of the percentages of TAGs for a) different location of pork b) different location of pork (rescaled to low relative abundance of TAGs). 130

3.13 PCA scores plot of FAMEs in different animal species. 132

3.14 a) Loadings plot for PC1 of FAMEs for different animal species b) Loadings plot for PC2 of FAMEs for different animal species 132

3.15 a) PCA scores plot of TAGs in different animal species, b) Loadings plot for PC1 of TAGs for different animal species, c) Loadings plot for PC2 of TAGs for different animal species. 136

3.16 Plots of PC1 vs. PC2 loadings values from PCA scores plot of TAGs from different animal species. 137

3.17 PCA scores plot of FAMEs for different anatomical locations of pork fats (n = 9 for each location). 140

3.18 a) Loadings plot for PC1 of FAMEs for different locations of pork. b) Loadings plot for PC2 of FAMEs for different locations of pork. 140

3.19 The PCA scores plot of FAMEs for three different pigs (A, B and C). (n=24 for each animal). 141

3.20 PCA scores plot for TAGs of different pork fat locations (*n*=6 for each location). 143

3.21 a) Loadings plot for PC1 of TAGs for different locations of pork. b) Loadings plot for PC2 of TAGs for different locations of pork. 143

3.22 PCA scores plot of TAGs for three different pigs (A, B and C). (n=16 for each animal). 144

Chapter 4

Figure 4.1 Chromatograms of TAGs from raw and cooked beef products. (Refer Table 4.1 for peak identifications). 154

4.2 Chromatograms of TAGs from raw and cooked lamb products. (Refer Table 4.1 for peak identifications). 154

4.3 Chromatograms of TAGs from raw and cooked chicken products. (Refer Table 4.1 for peak identifications). 155

4.4 Chromatograms of TAGs from raw and cooked pork products. (Refer Table 4.1 for peak identifications). 155

4.5 Percentage of TAGs for a) raw and cooked beef, b) beef curry with rapeseed oil c) raw and cooked beef normalised to OOP* and d) the reproduced histogram of TAGs proportion for raw and cooked beef with reassessed beef curry. 161

4.6 Percentages of TAGs for a) raw and cooked lamb, b) raw and cooked lamb normalised to SOP*. 163

4.7 Percentage of TAGs for a) raw and cooked chicken, b) chicken curry and rapeseed oil c) raw and cooked chicken normalised to LPO* and d) reproduced histogram of TAGs proportion for raw and cooked chicken with reassessed chicken curry. 167

4.8 Percentage of TAGs for a) raw and cooked pork, b) raw and cooked pork normalised to LPO* and c) raw and cooked pork with all pork locations of ham, belly, loin and shoulder. 169

4.9 a) PCA scores plot of TAGs for raw and cooked beef (excluding the vegetable oil for curry samples, b) loadings plot for PC1, c) loadings plot for PC2. 171

4.10 PCA scores plot of TAGs for raw and cooked beef with reassessed beef curry. 172

4.11 a) PCA scores plot of TAGs for raw and cooked lamb, b) loadings 174

plot for PC1, c) loadings plot for PC2.

4.12 a) PCA scores plot of TAGs for raw and cooked chicken, b) loadings plot for PC1 and c) loadings plot for PC2 176

4.13 PCA scores plot of TAGs for raw and cooked chicken with reassessed chicken curry. 177

4.14 a) PCA scores plot of TAGs for raw and cooked pork, b) loadings plot for PC1 c) loadings plot for PC2. 179

4.15 PCA scores plot of TAGs for raw and cooked meat products including the beef curry^{+} (label $^{+}$ in beef curry indicates the contribution of rapeseed oil has been incorporated in the TAG profiles) 180

4.16 a) PCA scores plot of TAGs for raw and cooked meat products, b) loadings plot for PC1, c) loadings plot for PC2. 185

4.17 Plots of PC1 vs. PC2 loadings values from PCA scores plot of TAGs from raw and cooked meat products 187

4.18 a) PCA scores plot of TAGs for raw and cooked meat products including reassessed beef^{++} and chicken curry. b) loadings plot for PC1 c) loadings plot for PC2. 189

Chapter 6

Figure 6.1 Diagram identifying the four different locations of pig adipose tissue (modified from Metayer et al., 1998). b) Subcutaneous, intermuscular and intramuscular adipose tissues from sliced dry-cured Iberian ham (Timon et. al., 2001). 202

SYMBOL AND ABBREVIATIONS

AAS	atomic absorption spectroscopy
APCI	atmospheric pressure chemical ionisation
CID	collision induced dissociation
CI	chemical ionization
CN	carbon numbers
DAG	diacylglycerols
DB	double bond number
DNA	deoxyribonucleic acid
DSC	differential scanning calorimetry
ELISA	enzyme-linked immune sorbent assay
ELSD	evaporative light scattering detector
ECL	equivalent chain length
ECN	equivalent carbon number
EIC	extracted ion chromatogram
ESI	electrospray ionisation
FAMEs	fatty acid methyl esters
FA	Fatty acid
FDAAA	Food and Drug Administration Amendments Act
FERA	Food and Environment Research agency
FFA	free fatty acid
FID	flame ionization detector
FT-ICR	fourier transform - ion cyclotron resonance
GC	gas chromatography
GLC	gas liquid chromatography
HCA	hierarchical cluster analysis
HPLC	high performance liquid chromatography
HTGC	high temperature capillary gas chromatography
ICR	ion cyclotron resonance
i.d.	internal diameter
IR	infrared spectroscopy
IRMS	isotope ratio mass spectrometry

ITMS	ion trap mass spectrometry
L	length
LC	liquid chromatography
LDA	linear discriminant analysis
LOD	limit of detection
MS	mass spectrometry
MS/MS	tandem mass spectrometry
MS^n	Multistage tandem mass spectrometry
m/z	mass to charge ratio
NMR	nuclear magnetic resonance
NP	normal phase
PCA	principal component analysis
PCR	polymerase chain reaction
PLS	partial least squares
PN	partition number
RI	refractive index
RP	reversed phase
SEM	scanning electron microscopy
SIMCA	soft independent modelling of class analogy
SNIF-NMR	site-specific natural isotope fractionation nuclear magnetic resonance
t_R	retention time
TAG	Triacylglycerol
UHPLC	ultra high performance liquid chromatography
UV	ultraviolet
UV/Vis	ultraviolet-visible spectroscopy

ACKNOWLEDGEMENT

Thank you to Malaysian Agricultural Research & Development Institute (MARDI) for sponsoring me. A special thanks to my supervisor Brendan Keely for all the help and guidance throughout this project. Phil, Trevor and Ed for helping me with GC and MS, Julie for the PCA, thanks. A heartfelt grateful to my colleagues: Matt, Chris, Suleman, Neung, Denise, Andy, Angela, Kim, Yao and Salina for the help and encouragement. My love and gratitude to my parents (Hasan and Saadiah), my parents in law (Abdul Halim and Radiyah), my siblings: Ita, An, Nim, Ayus and Mam. Lastly to my husband, Rafil and my special angels Nabilah and Ahmad for pulling me through when things were tough, I love you all.

AUTHOR'S DECLARATION

I hereby declare that the work described in this thesis is my own, except where otherwise acknowledged, and has not been submitted previously for a degree at this or any other university.

Haslina Hasan

CHAPTER 1

Introduction

1.1 Food authenticity and adulteration

In food production, the assessment of raw materials and the final product is important for maintaining overall high standards of food quality (in terms of sensory, stability and nutritional value), safety (microbiology, contaminants and toxins), and authenticity (Kamm et al., 2001; Van Ruth et al., 2010). Authentication is the process of proving that something is true, genuine or valid (Soanes et al., 2005) and food authentication is the process by which food products are verified as complying with their label descriptions; labelling and compositional regulations may differ from country to country (Dennis, 1998). The authentication process is important at all levels of production, from raw materials to finished products which strictly comply with labelling. It encompasses authenticity of ingredients, natural components, absence of extraneous substances, production technology, geographical and botanical origin, production year and genetic identity (Kamm et al., 2001). Authenticity is important for a number of reasons including legal compliance, economic reasons, constant quality, safe ingredients and religious observance (e.g. halal, kosher). Applying accurate specifications for raw materials and selecting suppliers that have quality assurance in place, in combination with regular audits of the supplier, certificates of analysis and periodical analytical checks, can guarantee or ensure the authenticity of food products.

Food adulteration is one of the most common problems in food authenticity and has usually been carried out for financial gain. Food adulteration includes the addition of substances to food in order to increase its bulk and reduce the cost of production, with intent to defraud the purchaser (Bender, 2009). It ranges from the simple addition of natural compounds to much more serious cases of contamination with harmful substances (Defernez et al., 1995). On the other hand, contamination may occur accidentally (i.e. cross-contamination in factories which produce several products, in which case the added substance is usually below 1-2% of the total amount). In some cases adulteration may pose a safety risk to the consumer.

Quality standards have been established for preventing or minimizing the adulteration of food products, specifically by enforcing the requirement for quality labels (labelling) on foods to ensure that it is properly described. The USA Food and Drugs Act of 1906 was the first of more than 200 laws that constitute one of the world's most comprehensive and effective networks of public health and consumer protection (US Food and Drug Administration, FDA, US Department of Health and Human Services) and the latest

amendment was in 27 September 2007: the Food and Drug Administration Amendments Act (FDAAA) of 2007. In the UK, the Food Standards Agency has a statutory objective to protect public health and consumers' other interests in relation to food and drink. The production, processing, distribution, retail, packaging and labelling of food stuffs are governed by numerous laws, regulations, codes of practice and guidance. The Food and Environment Research agency (FERA) in the UK is responsible for routine monitoring and actively engaged in developing new techniques for food assurance and traceability. The rights of the consumer and food producer/processor regarding food adulteration or deceptive practices in food production are set out in a recent European Union regulation regarding food safety and traceability (Official Journal of EC, 2002; Reid et al., 2006). In Malaysia, the Food Act, 1983 and the Food Regulation Act 1985 are enforced by the Food Safety and Quality Division of the Ministry of Health, to ensure that food sold in the country complies with the minimum quality standards so that it is safe and produced using proper technology (pamphlet-standard section, Ministry of Health, Malaysia; 06 January 2007).

Consideration of the authenticity of food includes the species of origin (from which a food was made), the geographical origin (mostly relevant for high grade olive oil), substitution, commercial treatment and compliances with legal requirements (product standards).

1.2 Recent developments in food authentication and the detection of adulteration.

The development of new and sophisticated/updated techniques for the authentication or detection of adulteration of food products has increased with increasing consumer awareness of food quality and safety issues and the importance of maintaining fair competition among food producers and manufacturers. Four classes of food and food products have been identified as the major concerns in developing the techniques for detecting adulteration and determining authenticity: meat and meat products, milk and dairy products, cereals and edible oils and fat. There are also similar methods used for fruit and fruit products, fish and fish products, coffee, wines and spirits and honey.

The recent developments in the determination of food authenticity and adulteration issues have been subject to periodic review (Reid et al., 2006; Cordella et al., 2002; Ulberth and Buchgraber, 2000; Dennis, 1998). Discussions include the principal techniques that have been successfully applied to food authentication and the detection

of adulteration, namely scanning electron microscopy (SEM), ultraviolet-visible spectroscopy (UV/Vis), atomic absorption spectroscopy (AAS), infrared spectroscopy (IR), nuclear magnetic resonance (NMR)), isotopic analysis (site-specific natural isotope fractionation-nuclear magnetic resonance (SNIF-NMR) and isotope ratio mass spectrometry (IRMS), chromatography (gas chromatography, GC and high performance liquid chromatography, HPLC), DNA-based technology (polymerase chain reaction, PCR) and thermal analysis (differential scanning calorimetry, DSC). The techniques applied are dependent on the food matrix and compound analyzed.

There are difficulties in attempting to detect adulterants that have approximately the same chemical composition as the original food product. To overcome this, the instrumental techniques used are frequently associated with the use of chemometrics such as principal component analysis (PCA), linear discriminant analysis (LDA), soft independent modelling of class analogy (SIMCA), and partial least squares (PLS) to compare similarities or differences of sample data with the authentic product. An alternative approach is to find specific marker compounds in the products; this could be particular chemical constituents or morphological components (Cordella et al., 2002). The ideal marker should be specific to the adulterant and absent in the authentic product. Not many chemical markers fulfil these criteria and the natural variability in the chemical composition precludes having one discriminative marker for each type of product. At the same time, food processing and treatment may greatly influence its chemical composition. Authenticity assessment is a difficult task which, in most cases, requires the measurement of several markers and must take into account natural and technology-induced variations (Kamm et al., 2001).

Despite the biological complications and risk of diseases associated with the consumption of animal fats, there is a growing tendency among some countries to blend vegetables oils with animal fats such as lard (pork fat) and tallow (beef fat), either for the purpose of adulteration or for product development (Marikkar et al., 2002). It has, therefore become essential to develop methods for monitoring the presence of animal fats in food in order to safeguard the interest of the health-conscious masses, particularly in those countries where vegetarianism is widely practiced. Food products containing pork and lard are a great concern for Islamic and Orthodox Jewish religions, while those mixed with tallow are prohibited in the Hindu religion. Also, pregnant women and people with particular allergies need to know exactly what is declared on the label.

In meat authentication, animal parts used in the product and the presence of fat, water or connective tissues which are not defined as meat should be declared in product labelling. Legislative authorities establish that meat products must be accurately labelled regarding species content. The problem of adulteration of meat products includes the substitution of one species for another, the addition of low quality meat (mechanically recovered meat) and the use of cheaper protein sources such as those of vegetable origin (Lees, 2003). Meat species adulteration in ground and mixed products has been a widespread problem in retail markets (Asensio et al., 2008). The main analytical methods for species identification include:

a) electrophoretic methods – separation of protein by the use of homogenous gel, concentration-gradient gels and pH-gradient gels (Hitchcock and Crimes, 1985).
b) genetic, DNA (deoxyribonucleic acid)-based technologies using PCR are the most specific and sensitive methods for meat species identification (Asensio et al., 2008).
c) immunological techniques, e.g. ELISA (enzyme-linked immune sorbent assay) is an immunological technique that involves an enzyme (a protein that catalyzes a biochemical reaction) to detect the presence of an antibody or an antigen in a sample (Asensio et al., 2008).
d) chromatographic techniques, e.g. fatty acid (FA) and triacylglycerol (TAG) profiling by gas chromatography (GC) and high performance liquid chromatography (HPLC).

In meat and meat products, FA and TAG profiles have been used for classification and as indicators of purity, as well as parameters for authenticity assessment (Lees, 2003). TAGs are the most abundant form of natural lipids in animal fats (more than 96%). Also present are minor compounds including diacylglycerol (DAG), free fatty acid (FFA), phospholipids, cholesterol, carotene and vitamins K and E (Wood et al., 2008). Animal fats comprise complex mixtures of TAGs, reflecting various different adipose tissues sites. The main fat deposits in animals are located in the subcutaneous tissue and abdominal cavity and TAGs constitute over 90% of adipose tissue (Wood et al., 2008).

1.3 Nomenclature and structures of TAGs

Triacylglycerols comprise three FAs esterified to a glycerol backbone. Glycerol is a trihydric alcohol (containing three hydroxyl groups) that can combine with up to three fatty acids. TAGs are typically described in abbreviated form by combination of the three FAs XYZ where X designates the FA in the *sn*-1 position, Y the FA in the *sn*-2 position and Z that in the *sn*-3 position (Fig. 1.1). The FAs may differ in their chain-length, degree of unsaturation and distribution among the *sn*-1, *sn*-2 and *sn*-3 positions.

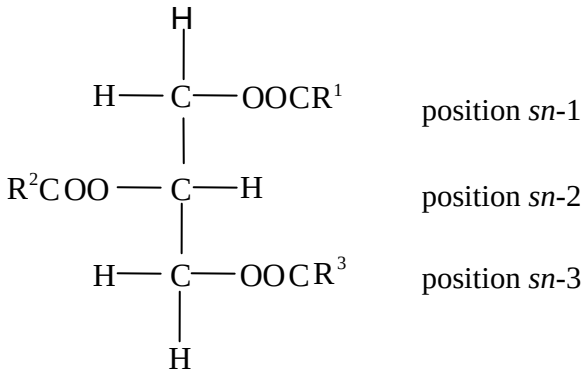

Figure 1.1: Generalized structure of a triacylglycerol, R^{1-3} represent alkyl groups.

The stereochemistry of TAGs can be described by a stereochemical or stereospecific numbering (*sn*) system, as recommended by the IUPAC-IUB Commission on Biochemical Nomenclature (CBN): The Nomenclature of Lipids (Recommendations 1976). In a Fischer projection of a natural L-glycerol derivative, the secondary hydroxyl group is shown to the left of C-2 and the carbon atom above this becomes C-1, that below becomes C-3, and the prefix "*sn"* is placed before the stem name of the compound (Sovova et al., 2008). A "rac" prefix indicates that the middle FA in the abbreviation is attached at the *sn*-2 position, while the remaining two acids are equally divided between the *sn*-1 and *sn*-3 position, yielding a racemic mixture of two enantiomers (Gutierrez and Barron, 1995). A 'β' prefix indicates that the middle fatty acid in the abbreviation esterifies the β- or *sn*-2 position. For example:

a) *sn*-PLS *sn*-1- palmitoyl -2- linoleoyl -3-stearoylglycerol.

b) rac-PLS equal proportions of *sn*-PLS and *sn*-SLP.

c) β-PLS *sn*-PLS and *sn*-SLP in any proportion.

The molecule structures of TAGs, including the distribution of FAs between the different stereospecific positions, have nutritional (e.g. fat digestion and absorption), biochemical (e.g. biosynthesis) and technological (e.g. physical properties such as crystal structure, melting point) importance (Laakso, 2002). TAGs present in animal fat include 1,3-dioleoyl-2-linoleoylglycerol (OLO), 1-linoleoyl-2-palmitoyl-3-oleoylglycerol (LPO), trioleoylglycerol OOO), and 1,3-dioleoyl-2-palmitoylglycerol (OPO). The scientific names, chemical formula, carbon numbers (CN) and double bond number (DB) and chemical structures of TAGs are simplified in Table 1.1.

Table 1.1: Scientific names, chemical formula, CN, DB and chemical structures of TAGs. The structures represent *cis* and *trans* of the FAs.

Scientific names	Chemical formula	CN:DB	Chemical structures
a)1,3-dioleoyl-2-linoleoylglycerol (OLO, C18:1/C18:2/C18:1)	$C_{57}H_{102}O_6$	54:4	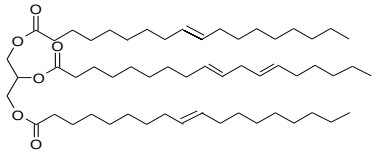
b)1-linoleoyl-2-palmitoyl-3-oleoylglycerol. (LPO, C18:2/C16:0/C18:1)	$C_{55}H_{100}O_6$	52:3	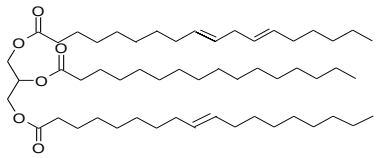
c)Trioleoylglycerol (OOO,C18:1/C18:1/C18:1)	$C_{57}H_{104}O_6$	54:3	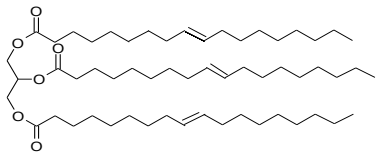
d)1,3-dioleoyl-2-palmitoylglycerol (OPO, C18:1/C16:0/C18:1)	$C_{55}H_{102}O_6$	52:2	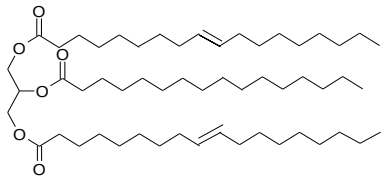
e)1-oleoyl-2,3-dipalmitoyl-rac-glycerol. (OPP, C18:1/C16:0/C16:0)	$C_{53}H_{100}O_6$	50:1	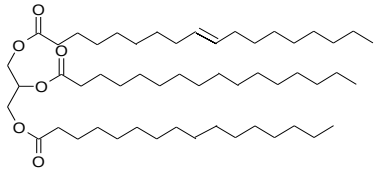
f) 1- palmitoyl -2-linoleoyl -3-stearoylglycerol. (PLS, C16:0/C18:2/C18:0)	$C_{55}H_{102}O_6$	52:2	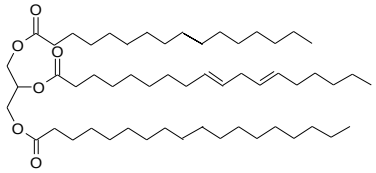
g) 1-stearoyl-2-palmitoyl-3-oleoylglycerol. (SPO, C18:0/C16:0/C18:1)	$C_{55}H_{104}O_6$	52:1	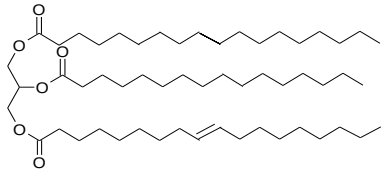

1.4 TAG distributions in animal fats.

In general, lipids are a diverse group of biological substances made up primarily of non-polar compounds (triglycerides, diglycerides, monoglycerides and sterols) and more polar compounds (free fatty acids, phospholipids and sphingolipids). They bind covalently to carbohydrates and proteins to form glycolipids and lipoproteins, respectively (Manirakiza et al., 2001). FA positional distribution patterns in animal TAGs vary depending on dietary fat intake, which can alter the TAG profiles of animal fat deposits; the types of animal, because the positional distribution patterns are not the same, and vary between different body tissues in the same animal (Litchfield, 1972).

Animal lipids come from two different sources: exogenous lipids ingested in food (nearly all are TAGs) and endogenous lipids synthesised by animal tissues (these include a high proportion of polar lipids, mainly phospholipids; Gutierrez and Barron, 1995). A previous study classified FAs according to their accumulation pattern in different tissues according to six selected markers: C18:2 *n*-6 (omega 6; marker of dietary supply), C16:0 (marker of the de novo synthesis), C18:1 *n*-9 (marker of Δ-9 (delta 9) desaturase activity), C20:4 *n*-6 (marker of Δ-6 desaturase activity), C16:1 *n*-7 and C20:3 *n*-3 (marker of competition for Δ-9 desaturase and Δ-6 desaturase between *n*-3 and *n*-6, polyunsaturated, PUFA) (Pascual et al., 2007). Those authors showed that the remainder of the FAs are highly correlated to one of the six markers. In pigs linoleic acid (C18:2) is derived entirely from the diet and it passes through the stomach unchanged before being absorbed into the blood stream in the small intestine and incorporated into tissues (Wood et al., 2008). In ruminants, C18:2 is degraded to monounsaturated (MUFA) and saturated FAs in the rumen by microbial biohydrogenation and only about 10% is incorporated into tissue lipids. Oleic acid (C18:1*cis*) is the major FA in meat and is formed from stearic acid (C18:0) by the enzyme stearoyl Co-A desaturase, a major lipogenic enzyme (Wood et al., 2008). The double bonds in unsaturated FAs are usually *cis*, conferring low melting points to these FAs. In ruminants, a significant proportion of double bonds are *trans* as a result of biohydrogenation in the rumen. Vaccenic acid, C18:1 *trans*, is a major FA produced by biohydrogenation of C18:2 *n*-6. This FA is converted to conjugated linoleic acid (CLA, 18:2 9_*cis*, 11_*trans*) in adipose tissue by the enzyme stearoyl Co-A desaturase (Wood et al., 2008). FAs present in animal fats, including the trivial names, scientific names, carbon numbers and number of double bonds is listed in Table 1.2.

Table 1.2: Abbreviations, trivial names, scientific names, carbon numbers: double bond number and chemical formula of common FAs in animal fats.

Abbreviations	Trivial Names	CN:DB	Chemical formula	Scientific Names
M	Myristic acid	14:0	$C_{14}H_{28}O_2$	Tetradecanoic acid
My	Myristoleic	14:1	$C_{14}H_{26}O_2$	9-Tetradecenoic acid
-	-	15:0	$C_{15}H_{30}O_2$	Pentadecanoic acid
-	-	15:1	$C_{15}H_{28}O_2$	10-Pentadecenoic acid
P	Palmitic acid	16:0	$C_{16}H_{32}O_2$	Hexadecanoic acid
Po	Palmitoleic acid	16:1	$C_{16}H_{30}O_2$	9-Hexadecenoic acid
Ma	Margaric acid	17:0	$C_{17}H_{34}O_2$	Heptadecanoic acid
Mo	Heptadecenoic Acid	17:1	$C_{17}H_{32}O_2$	10-Heptadecenoic Acid
S	Stearic acid	18:0	$C_{18}H_{36}O_2$	Octadecanoic acid
O	Oleic acid	18:1	$C_{18}H_{34}O_2$	9-Octadecenoic acid
L	Linoleic acid	18:2	$C_{18}H_{32}O_2$	9,12-Octadecadienoic acid
Ln	Linolenic acid	18:3	$C_{18}H_{30}O_2$	9,12,15-Octadecatrienoic acid
G	Gadoleic acid	20:1	$C_{20}H_{38}O_2$	9-Eicosenoic acid

1.5 Separation of complex TAGs mixture

In principle, there are two possible methods for the identification of TAGs: LC-MS or GC-MS analysis of the intact TAGs or analysis of the FAs after transesterification. When analysing TAGs it is important to consider the FA chain lengths, degree of unsaturation, double bond position (including the *cis*/*trans* configuration of the double bond) and position of the FA on the glycerol backbone. Chromatographic separation techniques are often required to resolve the complex mixtures of TAGs. The two most useful techniques for separating TAGs mixture are discussed below.

1.5.1 Gas chromatography

1.5.1.1 Separation of FAs

Capillary GC has been the most commonly used approach for the evaluation of FA compositions. In order to analyze the FAs it is necessary to transform them into less polar, more volatile analytes, normally methyl esters (Tranchida et al., 2007). Methyl esters are prepared by methylation in a methanolic medium that can be carried out with alkaline, acid or alkaline and acid catalysis, or another alternative is methylation with diazomethane (Aparicio and Aparicio-Ruiz, 2000). Polyethylene glycol-type stationary phase have proved effective for the separation of the most important saturated and polyunsaturated FAs. In order to achieve full separation of geometrical and conjugated FA isomers long columns, up to 100 m, with high polarity phases (i.e. bis-cyanopropyl polysiloxane) are required (Tranchida et al., 2007).

1.5.1.2 Separation of TAGs

Separation in GC occurs first according to the boiling point and then according to the molecule weights of the components. The first GC analysis of natural TAGs was performed by Kuksis and McCarthy (1962) utilising glass or stainless steel packed. The capillary column for TAGs was introduced in the 1970s and Tvrzicka et al. (1994) summarized a number of advantages of capillary columns over packed columns (i.e. better separation efficiencies, quantitative recovery, shorter analysis time and longer lifetimes of chemically bonded stationary phases). Currently, fused silica capillary columns protected by a coating of temperature resistant polyimide are generally used (Buchgraber et al., 2004).

The ECL (equivalent chain length) or ECN concept was originally introduced for GC analysis of fatty acid methyl esters (FAMEs) and was later adopted for HPLC. These values were found to be useful for identification of TAGs separated by capillary GC (Rezanka and Mares, 1991). The use of high temperature capillary gas chromatography (HTGC) permits analysis of the intact TAG molecules. Separation of TAGs according their total acyl carbon number and, within each CN, according to the degree of unsaturation can be achieved using HTGC if polarizable stationary phases are used (Aichholz et al., 1998). One such stationary phase is an immobilized OV-22 (65% phenyl methyl polysiloxane) polymer, which becomes more polar with increasing temperature and is stable up to 360ºC (Evershed, 1996). Although HTGC has been used for many years, there are drawbacks to this approach, particularly for TAGs with numerous sites of unsaturation, which are subject to degradation at the temperatures used for HTGC (Byrdwell, 2005). The decomposition products of the TAGs can be seen in the chromatogram, in particular when the column is overloaded and at higher temperatures (Mayer and Lorbeer, 1997). Free FAs and diglyceride-like compounds, probably enol esters are formed (Buchgraber et al., 2004). TAGs with long FA chains and/or oxygen containing functional groups require higher temperatures which often produce substantial column bleed in HTGC. Repeat measurements of PPP on columns coated with different stationary phase indicated that the bleeding rate of the columns were quite similar (0.1 to 0.3 µg/min mg; Mayer and Lorbeer, 1997). Those author used cold on-column injection at 60ºC, the oven was programmed to 280 ºC at 20ºC/min and then to 410 or 420ºC at 4ºC/min. The first chromatograms devoid of signs of decomposition were reported by Kuksis and McCarthy (1962) who improved the separation technique by employing direct injection onto the column. Further limitation of HTGC for analysing TAGs includes baseline instability and rapid column aging because of the need for elevated oven temperatures (Marzilli et al., 2003).

The integration of chromatographic and spectroscopic analytical techniques is important for analyzing FAs and TAGs, hence separation by a GC is typically coupled with detection by mass spectrometry (MS).

1.5.2 High performance liquid chromatography

1.5.2.1 Separation of TAGs by single stage HPLC.

Over the years advances in liquid chromatography have been used successfully for separation of TAGs. Thus, TLC was employed to separate different categories of lipids according to their functional groups, argentation LC (with $AgNO_3$) to separate TAGs according to degree of unsaturation and reversed phase LC to separate TAGs according to both unsaturation and carbon number (Gutierrez and Barron, 1995). Two different separation modes of partition HPLC; normal phase (NP) and reversed phase (RP) have been applied in lipid analysis. Attempts to use NP HPLC for TAGs separation had limited success and the technique is not commonly used (Buchgraber et al., 2004). RP HPLC is the most commonly employed chromatographic technique for separating mixtures of TAGs (Gutierrez and Barron, 1995). Stationary phases with 10 μm, 5 μm, and 3 μm particle size packing materials are usually used. Various octylsilyl (OS or C8) and octadecylsilyl (ODS or C18) columns have been employed.

Two LC separation mechanisms have been found to be most useful for resolving TAGs, including the positional isomers: reversed-phase (C18) and complexation with silver ions (argentation chromatography). Silver ion chromatography separates the TAGs according to the degree of unsaturation and the basis for separation is the ability of the π-electrons in the double bonds on the FA chains to interact with the silver ions on the stationary phase and form stable polar complexes. As the number of double bonds increases so does the complex formation effect and hence retention (Gutierrez and Barron, 1995). The first mechanism separates TAG on the basis of their ECN or partition number (PN). TAGs with the same ECN (e.g. PLO and OLO) are easily separated by argentation chromatography (PLO: DB=3; OLO:DB=4) but not easily by RP-HPLC. The reverse is true for TAGs with the same DB number, e.g. POO and SOO. These cannot be separated by argentation chromatography but are easily separated by RP-HPLC as their ECNs are 48 and 50 (Van der Klift et al., 2008).

1.5.2.2 Separation of positional isomers of TAGs.

The development of efficient methods to determine positional isomers of individual TAG species is important especially if isolation of pure TAG compounds is needed: for isotopic analysis of individual TAG or for understanding biological functions such as absorption, metabolism and atherogenic potential (tendency for deposition on the artery walls), all of which may be influenced by FA position in TAGs (Malone and Evans, 2004). The TAG structure is also important in lipid chemistry for formulating nutritious food products via use of particular lipids as food ingredients or nutritional supplements (Buchgraber et al., 2004).

The positional analysis of TAGs has traditionally been performed through hydrolysis of the outer two FAs, *sn*-1/3 positions (by enzymatic methods) and subsequent HPLC analysis of the remaining two monoglycerides and free fatty acids. This laborious traditional method requires separation of TAGs, fraction collection, enzymatic digestion of each fraction, and the separation and analysis of the DAGs and free FA hydrolysis products in each of the digested fractions (Li et al., 2006). The first approach was introduced by Brockerhoff (1967) and employed pancreatic lipase or a Grignard reagent to partially hydrolyze TAGs. These methods are cumbersome and time consuming and only provide information on the overall 2-position composition of a mixture rather than information on each molecule (Mottram, 2005). The use of enzymatic methods for analysing TAGs is very well suited to micromethods for working directly with samples such as serum. Nevertheless, the usefulness of the method is limited to measuring serum TAG levels: it is difficult to apply to lipid extracts and the organic solvents used interfere with enzymatic reactions (Gutierrez and Barron, 1995). The combination of enzymatic analysis with several different analytical techniques such as argentation TLC, HPLC, HPLC-GC and HPLC-MS gave valuable information for determining the stereospecific composition of TAGs in natural fats (Gutierrez and Barron, 1995). In addition, the compositions of FA in the *sn*-2 position of TAGs in animal fats of lamb and pork fat were determined by lipase degradation and validated by HPLC-APCI MS (Mottram et al., 2001).

1.6 Limitations of current studies

The first difficulty of current approaches for the HPLC analysis of TAGs is the separation of components having the same ECN or PN. Despite the improvements in efficiency using small particle sizes (3µm), poorly resolved or even unresolved TAG pairs or groups still exist, especially in highly complex mixtures of natural fats. The second difficulty is the simultaneous analysis of TAGs differing in molecular structure and with a broad range of ECN values: good resolution and reasonable analysis times for the range from the least strongly retained TAGs to the most strongly retained can be difficult to achieve. The third difficulty is a limitation of the detector; refractive index (RI) and ultraviolet (UV) have been used with HPLC for fat analyses, however most lipids have little or no UV and visible light absorption (Segal, 2006). Thus, it is necessary to use evaporative light scattering detector (ELSD) or combine with MS. Until recently, the chromatographic methods did not resolve TAGs according to the FA distributions on the glycerol backbone, exception for silver ion chromatography where only limited resolution was possible (Sovova et al., 2008).

1.7 Background on instrumentation

1.7.1 Gas chromatography

Gas chromatography or gas liquid chromatography (GLC) uses a carrier gas (e.g. H_2, N_2, He) as a mobile phase, and a liquid stationary phase (e.g. cyanopropylphenyl dimethyl polysiloxane, carbowax polyethyleneglycol, biscyanopropyl cyanopropylphenyl polysiloxane and diphenyl dimethyl polysiloxane) coated onto the walls of a borosilicate glass for fused silica capillary. Nonpolar stationary phases of the polysiloxane type, marketed under a number of different brand names (DB-1, HP-1, CP-SIL 5 CB, BP-1 etc. for 100% dimethyl polysiloxane and OV-3, DB-5, HP-5, CP-SIL 8 CB, BP-5 etc. for 5% phenyl/95% dimethyl polysiloxane), are commonly used. These columns only separated TAGs according to their carbon number and do not allow for complete separation of components. Higher polarity stationary phases improve the TAG separation and some allow the separation of TAGs with different degrees of unsaturation: the prepared fused silica capillary column coated with 75% diphenyl/ 25% dimethyl polysiloxane enabled better resolution of TAGs differing only by one double bond (Mayer and Lorbeer, 1997). These columns (high polarity stationary phase of cyanopropyl polysiloxane, OV-275, CP Sil88) cannot tolerate the high temperatures necessary for TAG work even though they give separation of saturated and unsaturated FAs.

In general, GC is used for the separation of volatile compounds, though, many involatile substances such as amino acids, steroids and fatty acids can be derivatized to form volatile substances that can be separated by GC. The resolution (R_S) of the two components as peaks on the chromatogram is characterized by equation 1.1.

$$R_S = \frac{2\Delta t'_R}{W_1 + W_2}$$ (Equation 1.1; Grob, 1985)

Where $\Delta t'_R = t'_{R2} - t'_{R1}$ (retention time for component 1 and 2) and W is the peak width for both components. The resolution can also be expressed as an influence of retention factor, selectivity and column efficiency or number of theoretical plate. Loss of resolution can be caused by various factors that lead to band broadening, which controls the shape of the concentration profile of the peak, peak (width), affecting column efficiency.

The efficiency of the column depends on the nature and flow-rate of the carrier gas, column dimensions, liquid-phase thickness and column temperature. Notably, however, the nature and velocity of the carrier gas (hydrogen, helium or nitrogen) are the most important considerations (Christie, 1990).

1.7.2 Reversed phase high performance liquid chromatography (RP HPLC)

HPLC uses high pressures to force a liquid mobile phase through a closed column packed with micrometer sized particles. In RP HPLC the mobile phase is polar while the stationary phase is non-polar (e.g. C18 or octadecylsilane (ODS), C8 (octyl), phenyl etc.) and is chemically bonded to a porous support matrix of silica. The analytes are injected onto the head of the column and interact with the stationary phase through non-polar interactions, thus the least polar analytes elute last from the column. The degree of separation between two peaks can be measured quantitatively by calculating the resolution (R_s) using Equation 1.1 (Section 1.7.1).

The number of theoretical plates or column efficiency is calculated by Equation 1.2, where L is the column length and H is the height equivalent to a theoretical plate. The column efficiency increases with N where larger N values give narrower peaks and better separation. Efficiency of the LC system can be expressed as HETP (h*eight equivalent to a theoretical plate*).

$$N=L/HETP \qquad \text{(Equation 1.2)}$$

The evolution of packing materials used to effect separations in the LC column is an important factor in LC and the principle is governed by the van Deemter equation (Equation 1.3), where u is the average velocity of the mobile phase, A, B, and C are factors which contribute to band broadening: A is Eddy diffusion, B is longitudal diffusion and C is resistance to mass transfer. The van Deemter equation is an empirical formula that describes the relationship between linear velocity (flow rate) and height equivalent to a theoretical plate (HETP, or column efficiency). The equation predicts that column efficiency increases with decreasing particle size. This, however, leads to a rapid increase in back pressure. Accordingly, a pump capable of delivering solvent smoothly and reproducibly at a pressure range greater than that provided by HPLC instruments and which can compensate for solvent compressibility, was developed. The new

technique was named ultra high performance liquid chromatography or UHPLC. By utilizing very high pressures the technique enables the use of stationary phases with particle sizes of less than 2.5 μm. In early 2004, the first commercially available UPLC system that embodied these requirements was described for the separation of various pharmaceutical related small organic molecules, proteins, and peptides; it is called the ACQUITY UPLC™ System (Swartz, 2005).

$$\mathrm{HETP} = A + B / u + C u \qquad \text{(Equation 1.3)}$$

With the development of other commercial instrumentation the term UHPLC has recently been introduced to describe the generic approaches for improved chromatographic performance with fast, sensitive and high resolution separations through use of smaller particle sizes and high pressures. The decrease in particle size possible with UHPLC provides not only increased efficiency, but also the ability to work at increased linear velocity without a loss of efficiency, providing both resolution and speed. The van Deemter curve can be used to investigate chromatographic performance (Fig. 1.2). As the particle size decreases to less than 2.5 μm, not only is there a significant gain in efficiency; but the efficiency does not diminish at increased flow rates or linear velocities (Swartz, 2005).

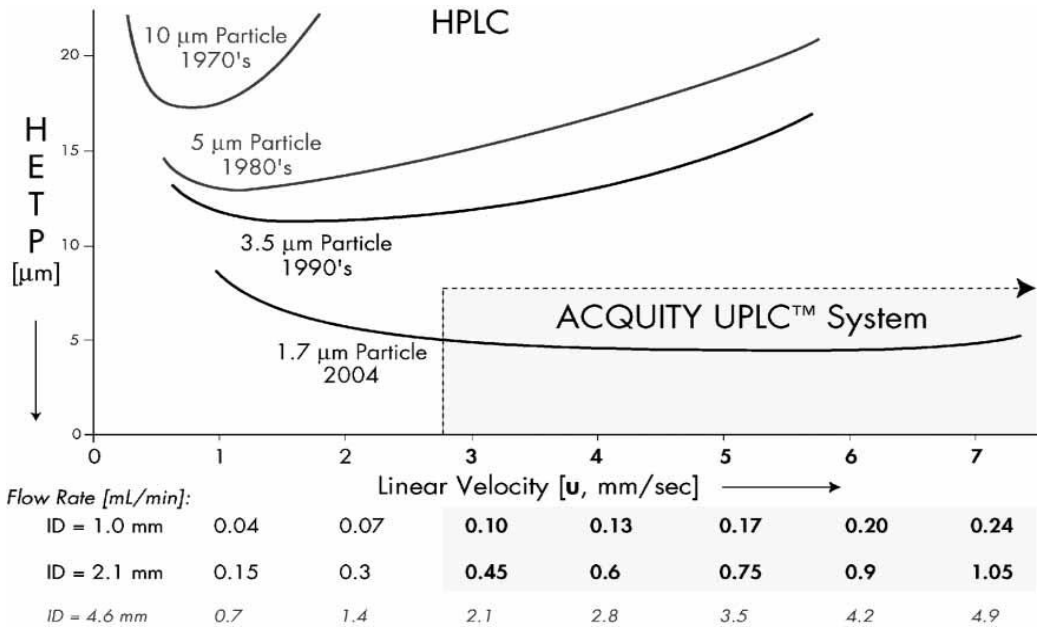

Figure 1.2: van Deemter plot, illustrating the evolution of particle sizes (2006 Waters Corporation).

The first TAG separation by UHPLC was reported on vegetable oils and lard (Leskinen et al., 2007) and later Leskinen et al. (2010) described the positional distribution of FAs in TAGs in vegetables oils using UHPLC. Thus, it is now possible to take full advantage of chromatographic principles to run separations using shorter columns and/or higher flow rates for increased speed with superior resolution and response.

1.7.3 Mass spectrometry

Atmospheric pressure chemical ionisation (APCI) and electrospray ionisation (ESI) are the most commonly used ionization methods for the analysis of TAGs by HPLC-MS due to the relatively simple mass spectra generated (i.e. very few fragmentations) and the possibility of identifying the positional isomers. While both positive ESI and APCI can result in a charged analyte, the process of ionization for each technique is very different. With ESI, protonation of the analyte occurs in the liquid phase. With APCI, a protonated solvent molecule donates a proton to the analyte in the gas phase.

1.7.3.1 Atmospheric pressure chemical ionization

The first application of APCI-MS to TAG analysis was reported by Tyrefors et al., (1993) with prior separation of TAGs by supercritical fluid chromatography (SFC). Byrdwell and Emken (1995) first coupled APCI MS with HPLC. APCI is similar to conventional chemical ionization (CI) in that it involves a solvent-mediated ionisation process (Byrdwell, 2005) in which the vaporized LC mobile phase acts as the CI reagent gas and ionizes the sample. Importantly, CI uses gas-phase ion-molecule reactions at reduced pressure, whereas APCI operates at atmospheric pressure.

The components of APCI include the sample inlet capillary, spray nozzle, heated vaporizer and corona discharge needle (Fig. 1.3). The liquid sample from HPLC or direct infusion enters the APCI source via a capillary and is converted into a mist of fine droplets through a combination of gentle heating and pneumatic nebulization. A make up/sheath of nitrogen gas sweeps the mixture of droplets and vapour towards the ion formation region, held at atmospheric pressure. A corona discharge needle carrying a high voltage facilitates the ionization (protonation) of trace amounts of water vapour. The charged species ionize the analyte (i.e. by protonation forming protonated molecules, $[M + H]^+$) and the resulting ions are transported to the mass analyzer.

The series of reactions occurring in pure nitrogen with traces of water at pressures of 0.5 to 4 torr (thus including atmospheric pressure) were described by Good et al. (1970) and the mechanism of $(H_2O)_nH_+$ formation is as follows (Byrdwell, 2005):

$$N_2 + e \rightarrow N_2^+ + 2e$$
$$N_2^+ + 2N_2 \rightarrow N_4^+ + N_2$$
$$N_4^+ + H_2O \rightarrow 2N_2 + H_2O^+$$
$$H_2O^+ + H_2O \rightarrow H_3O^+ + OH$$
$$H_3O^+ + H_2O + N_2 \rightarrow H^+(H_2O)_2 + N_2$$
$$H^+(H_2O)_2 + H_2O + N_2 \rightarrow H^+(H_2O)_3 + N_2$$
$$H^+(H_2O)_{n-1} + H_2O + N_2 \rightarrow H^+(H_2O)_n + N_2 \qquad \text{(Equation 1.4)}$$

Any chemical species present in the source such as the incorporated buffer, postcolumn additive, sparging liquid or other additives can react with each other and with the analyte. These species can also take part in ion forming reactions at atmospheric pressure either by proton transfer, or by attaching themselves to produce adducts (ions), e.g. sodium adducts, $[M + Na]^+$. Also, soft decomposition reactions sometimes occur, producing a series of fragment ions. In general, APCI is better suited for the ionization of non-polar, volatile low molecular weight molecules while ESI is better suited for more polar, non-volatile molecules.

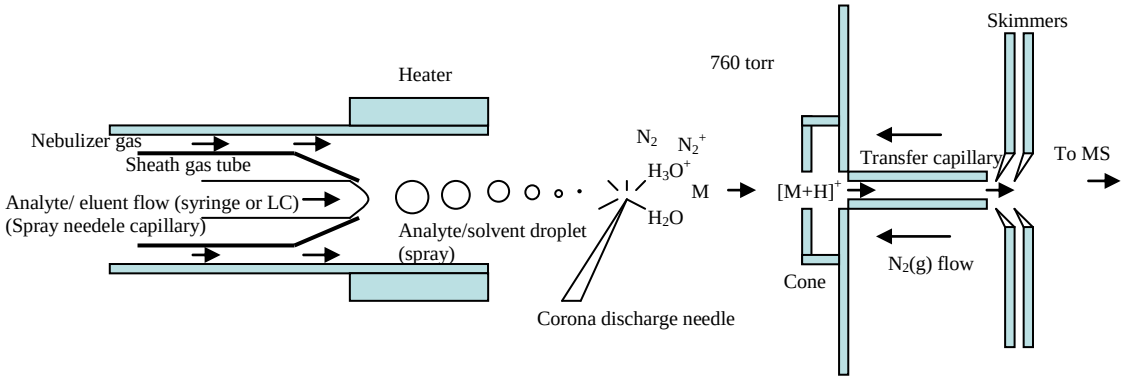

Figure 1.3: Generalised schematic diagram of an APCI source, illustrating the formation of ions (modification from Covey et al., 1986).

1.7.3.2 Electrospray ionization

TAGs are neutral molecules that are not readily ionized under ESI conditions without the use of a reagent buffer to promote adduct formation. Analysis of TAG by ESI-MS was first performed by Duffin and Henion (1991) by direct infusion with sodium acetate and ammonium acetate addition.

The liquid sample from LC or direct infusion enters the ESI source through an inlet capillary which is threaded down the centre of a stainless steel needle. The high voltage applied to the needle charges the surface of the drops emerging from the needle, which disperse into a fine spray of charged droplets. The nebulizing gas used to spray the solution aids in the evaporation of the solvent from the charged droplets. There are two models for formation of gas phase ions from electrosprayed solution: the "ion evaporation" (or ion desorption) model proposed by Iribarne and Thomson (1976) and "charge residue" model proposed by Dole et al. (1968). The first stage of both models involves solvent evaporation and droplet fission at the Rayleigh limit to produce smaller charged droplets. Rather than ions evaporating out of the shrinking droplets, the charge residue model assumes that solvent evaporation and Rayleigh fission continue until there is essentially one analyte ion per droplet (Byrdwell, 2005). The ion evaporation model is applied to small analyte molecules, while the charge residue model was developed to describe the ionization behaviour of large macroions. Thus, it is ion evaporation that is responsible for producing gas-phase TAG adduct ions from the sprayed effluents. The ions are accelerated towards the entrance capillary by an attracting potential.

The electrospray ionization source on the LCQ Deca ion trap MS employs a linear geometry, instead of the orthogonal orientation adopted in later designs, e.g. HCT ultra ETD II. In the linear geometry, the spray direction is in line with the bore of the heated capillary inlet. The orthogonal orientation reduces the contamination going through the mass spectrometer.

1.7.3.3 Ion trap mass spectrometry (ITMS)

The ion trap is a mass analyzer and the conventional quadrupole ion trap consists of three hyperbolic electrodes: a ring electrode and two electrically connected end cap electrodes (entrance and exit) forming a hyperboloidal geometry. Fig. 1.4 is a cross-section of the ion trap showing the dimensions of r_o and z_o, where r_o is the radius of the ring electrode in the central horizontal plane and $2z_o$ is the separation of the two end-cap electrodes measured along the axis of the ion trap (March, 1997).

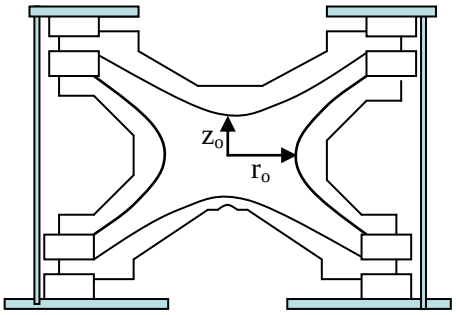

Figure 1.4: The cross section of ion trap (modification of March, 1997).

An oscillating electric potential applied to the ring electrode (termed the fundamental rf potential which has a constant frequency but variable amplitude) focuses ions toward the centre of the trap by creating a parabolic (saddle shaped) potential surface inside the trapping volume. Typically, the end cap electrodes are held at ground potential. The ions are trapped in a stable oscillating trajectory, axially and radially. For an ideal quadrupole field, $r_o^2=2z_o^2$. Development work in the early days of ion trap manufacture led to the electrodes of the ion trap being truncated in order to obtain a practical working instrument (March, 1997). In order to compensate this stretching of the ion trap, the trapping parameters can be calculated by using the actual values of r_o and z_o by the Mathieu equations as follows ($r_o^2 \neq 2z_o^2$):

$$a_z = \frac{-16eU}{m(r_o^2 + 2z_o^2)\omega^2}$$

$$q_z = \frac{8eV}{m(r_o^2 + 2z_o^2)\omega^2}$$ (Equation 1.5; March, 1997; Stafford et al., 1984)

a_u and q_u are dimensionless parameters in the Mathieu equation, where u represents the coordinate axes x, y and z. Ω is equal to $2\pi f$, where f is the frequency in hertz and U and V are the amplitudes of the applied dc and rf voltages, respectively. For the majority of commercial ion traps, r_o is either 1.00 or 0.707 cm. In LCQ ion trap instruments, r_o is 0.707 cm and z_o is 0.785 cm so that the geometry is stretched by 57% (Jonscher and Yates, 1997).

To measure the *m/z* value of a molecule in an ion trap, the molecule must be ionized, trapped, ejected and detected. Ions can only be stored in the ion trap if their trajectories are stable in the r (radial) and z (axial) direction simultaneously. One region of stability in which radial and axial stability overlaps is shown in Fig. 1.5 and ions will be stably trapped anywhere within that region, which is plotted a_z versus q_z. The mass-selective instability mode of operation utilizes no dc voltage; thus, the mass spectrometer is operated on the line $a_z = 0$. Ion trajectories become unstable in the axial direction but remain stable in the radial direction when the $q_z = 0.908$ (Termed Q_{eject}; Jonscher and Yates, 1997). Ions are ejected through holes in the endcap electrodes and detected by an electron multiplier. A mass spectrum is generated by sequentially ejecting ions from low to high *m/z*. The ejection of ions from the potential well is accomplished by ramping the amplitude of a radiofrequency (rf) potential applied to one of the ion trap electrodes in a linear fashion. This has the effect of increasing the q_z value for each of the ions. This translates to an increase in the ion's oscillation in the axial direction and each ion will, in order of increasing *m/z*, reach the critical q_z value (Q_{eject}). At this point the amplitude of the ion's oscillation in the z direction exceeds the physical dimensions of the trap and the ion is ejected. Each ion species is ejected at a specific amplitude of the fundamental rf (March, 1997) from low to high *m/z*.

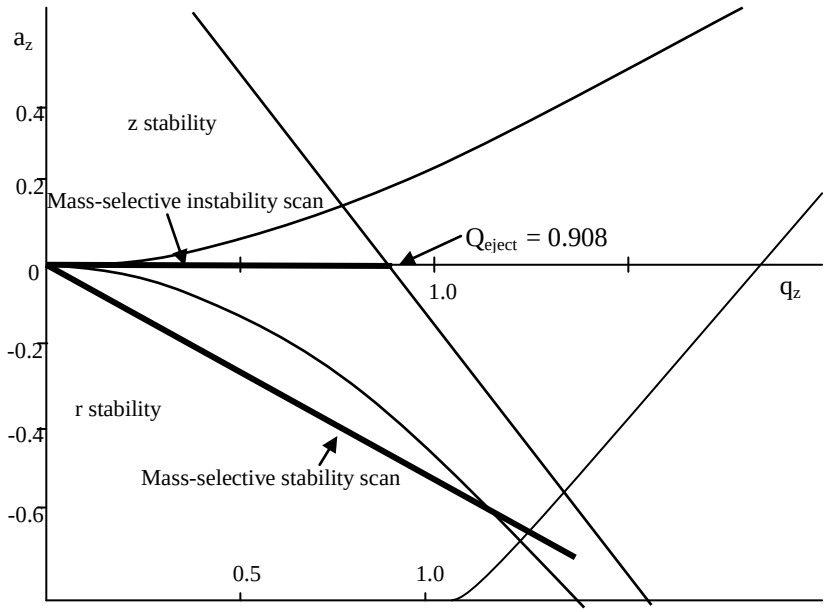

Fig.1.5: The regions of stability in the quadrupole ion trap (Jonscher and Yates, 1997)

1.7.3.4 Multistage tandem mass spectrometry (MS^n)

There are two main categories of instruments that allow tandem mass spectrometry (MS/MS) experiments: the first is MS/MS which can be affected in space where two mass spectrometers are assembled in tandem (e.g. two mass-analysing quadrupoles, two magnetic analyser or hybrids containing one magnetic and one quadrupole spectrometer). For example the triple quadrupole, where the precursor is selected by the first quadrupole, dissociated in the second quadrupole (functioning as a collision cell) and the product ions are analysed by the third quadrupole. The second category are analysers capable of storing ions (ion cyclotron resonance (ICR) and quadrupole ion trap) which allow the selection of particular ions by ejection of all others (Hoffman, 1996) and by carrying out operations temporarily within the same physical space. Multistage tandem mass spectrometry (MS^n) allows the dissociation of product ions from MS/MS if further dissociation is required. This technique can only be performed with ion trap and FT-ICR instruments. The process can be repeated a number of times, resulting in a series of MS^n spectra.

1.7.3.5 Collision-induced dissociation (CID)

Collision-induced dissociation (CID) also called collision-activated dissociation (CAD) of ions in a mass spectrometer is an important technique for ion structure determination and complex mixture analysis. CID has been used with quadrupole, ion cyclotron resonance and time-of-flight mass analyzers as well as in ion traps which allow time dependent rather than space-dependent tandem MS.

The CID process involves collisional activation of ions with an inert gas and subsequent dissociation to various product ions depending on the amount of energy transferred to the ion (Shukla and Futrell, 1993). The first CID mass spectra reported by Jennings (1968) and Haddon and Mclaffer (1968) were on metastable ions which can be dissociated in commercial mass spectrometers by introducing collision gas into field-free region. This led to the development of the CID technique in mass spectrometers. These studies together with work by Beynon et al. (1973) showed that CID spectra were qualitatively similar to those from electron ionization and provided definitive information on fragmentation pathways. Product ion abundances from CID were successfully used to distinguish various isomeric structures (Shukla and Futrell, 1993).

The precursor ion undergoes repeated collisions with the collision gas, which accumulates as potential/internal energy of the molecule until the dissociation threshold is reached and product ions are formed. The process involved in CID of a precursor ion has two steps: collisional activation, where a fraction of the ion's kinetic energy is transferred into internal energy (Eq. (1.4)) and unimolecular dissociation of the internally excited/activated ion (Eq. (1.5)). The ions are activated by collision, and therefore are induced to dissociate:

$$M_1^{+}{}_{(\text{precursor ion})} + X_{(\text{neutral collision partner})} \rightarrow M_1^{+}{}^{*}{}_{(\text{activated precursor ion})} + X_{(\text{neutral collision partner})} \quad (1.4)$$

$$M_1^{+}{}^{*}{}_{(\text{activated precursor ion})} \rightarrow M_3^{+}{}_{(\text{dissociation product ions})} + \text{neutrals} \quad (1.5)$$

The collision gas is a chemically inert gas such as helium, argon, xenon, nitrogen or carbon dioxide. In an ion trap, if these product ions need to be dissociated further they are isolated in the ion trap and subsequently dissociated in another round of CID. The process may be repeated to observe product ions of product ions, over several generations.

1.8 Aims of the research

The overall aim of this study was to improve on current methods for the separation of TAGs, especially those having identical masses or the same ECNs, by combining RP HPLC with APCI and ion trap MS. The requirement for the method was that it would be suitable for the analysis of complex mixtures of TAGs in animal fats and cooked meat products. The proposed application for the method was the detection of adulteration in cooked meat products where the thermal processing limits the use of DNA technologies to identify different species of meat products. The development of such a method would also support a wide range of studies on metabolism, biosynthesis, and degradation of individual TAG species within biological systems. An underlying objective was to determine the extent to which the improved characterization of TAG profiles improves discrimination within and between different animal species.

CHAPTER 2

Development of single stage RP HPLC-APCIMS/MS separation of TAGs

2.1 Introduction and aims

Introduction

The first RP-HPLC separation of TAGs with identification by APCI-MS demonstrated analysis of mixtures of homogeneous (monoacid) triglyceride standards containing fatty acids with zero to three double bonds (Byrdwell and Emken, 1995). The coupling of chromatographic and spectroscopic analytical techniques, in particular, separation by HPLC with detection by mass spectrometry is important for analyzing FAs and TAGs. RP HPLC permits fractionation or separation of complex mixture of TAGs, and online MS provides detailed information about the molecular mass, the FA composition and the position of the FAs within TAG molecules. The combination of MS with HPLC is also important to provide identification of non- or partially resolved TAG peaks (Jakab et al., 2002).

The main advantage in the use of MS is that quantitative information about the positional distribution of FA in individual TAGs can be obtained directly without any enzymatic treatment of the sample (Leskinen et al., 2007). Other HPLC detection techniques, including ELSD and UV, have been used but these detection methods cannot discriminate partially or completely co-eluting compounds. Furthermore it is necessary to employ standards to identify the compounds, of which not all are available. The failure to resolve overlapping peaks can cause some TAG species to be overestimated while others go unidentified. A specific shortcoming of the UV detector is that many suitable solvents for HPLC separation, such as chloroform, acetone, ethyl acetate and toluene, cannot be used since they absorb strongly between 200 and 237 nm, which overlaps with the detection window for TAGs. Refractive index (RI) and infrared (IR) detectors have been used in simple TAG analysis. RI detection gave low response and stability and is not suitable for gradient elution while IR detector may produce substantial baseline drift. Furthermore, some of the detectors do not respond equally to all TAGs, e.g. UV detection exhibits more absorbance signal from unsaturated TAGs than from saturated ones (Byrdwell, 2005).

Several studies have reported separation of TAGs from animal fats by RPHPLC coupled with an APCI ionization source as the interface to a triple quadrupole MS analyzer (Fauconnot et al., 2004; Dugo et al., 2006; Kallio et al., 2001; Mottram et al., 2001 and Leskinen et al., 2007). There is, however, evidence of co-elution in the chromatograms

produced. The combination of APCI and an ion-trap MS analyzer for RP HPLC analysis of TAGs has been reported for plant oil samples (Holcapek et al., 2003 and Brydwell et al., 2002), but there are no reports relating to animal fat analysis.

Recently, RP HPLC-APCI MS (Byrdwell et al., 1996; Mottram et al., 2001; Holcapek et al., 2003 and Fauconnot et al., 2004) and RP HPLC-ESI MS/MS (Hvattum., 2001; Byrdwell and Neff, 2002 and Malone and Evans, 2004) methods have been developed to perform positional analysis on individual TAG species without separation. The ESI MS/MS of ammoniated TAGs, in which DAG ions are formed, has been used for the analysis of various TAG regioisomers in fats and oils (Leskinen et al., 2010; Leskinen et al., 2007 and Malone and Evans, 2004). The APCI MS/MS methods are shown to be unusable for these analyses because of the very low extent of formation of precursor ions (protonated TAGs) from saturated TAGs (Mottram and Evershed, 1996 and Byrdwell and Emken, 1995) and because the formation of DAG ions in CID of protonated TAGs has been shown not to be dependent on the FA positional distribution (Leskinen et al., 2007). The APCI MS of ammoniated TAGs has been shown to give comparable results to ESI MS/MS (Byrdwell and Neff, 2002 and Holcapek et al., 2003).

Analysis of TAG regioisomers by MS has been achieved by analyzing linear calibration plots of fractional DAG fragment intensities vs. the fractional composition of binary mixtures of standards (Malone and Evans, 2004; Li et al., 2005 and Fauconnot et al., 2004). However, as the regioisomers were not separated, the MS/MS spectra across the chromatographic peaks of co-eluting regioisomers give composite spectra. Thus, it is difficult to retrieve the relative abundance data from the composite spectra.

Regiospecific characterisation of the TAGs in animal fats has been performed using HPLC-APCI-MS by Mottram et al. (2001), who determined the identification of FAs in the *sn*-2 position by lipase degradation and validated the HPLC-APCI-MS method for determining the *sn*-2 FAs from the relative intensities of DAG fragment ions in lamb and pork fat. The compositions of the TAG fraction of lard, tallow and a mixture of both were determined using a multidimensional HPLC RP HPLC-UV and silver ion HPLC-APCI MS and the technique was shown to allow discrimination of tallow in lard via the *sn*-POP/*sn*-PPO ratio (Dugo et al., 2006). The combination of RP HPLC and Ag HPLC allowed the resolution of critical pairs and isomers in rice oil due to the different retention mechanism of TAGs under these two distinct HPLC modes (Dugo et al., 2004). Separation of the regioisomers of the synthetic monosaturated and disaturated TAGs

POP-PPO and PLP-PPL was demonstrated for the first time on a single RP HPLC column (Momchilova et al., 2004). To date, there is no report for complete separation of regioisomers in animal fat.

Aims

The aims of the work described in this chapter were:

a) to improve on current methods for the separation of TAGs especially those having identical masses or the same ECNs, by combining RP HPLC with APCI and ion trap MS.
b) to separate and identify the regioisomers of TAGs in different type of animal fats (beef, lamb, chicken and pork fat) using single stage RP HPLC-APCI MS/MS (also known as one step or one dimensional HPLC).
c) to develop an ultra high performance liquid chromatography (UHPLC) method to improve the resolution and speed of analysis for TAGs in animal fats by single stage UHPLC-APCI MS/MS.

2.2 Results and discussion

The three letter code of TAGs includes the suffix * where more than one regioisomer can exist in a form that can, potentially, be separated chromatographically.

2.2.1 Structural characterization of TAG standards of OOP* and OPO.

2.2.1.1 Mass spectra of OOP and OPO standards*

The TAG standards OPO and OOP* were dissolved in different solvents (acetonitrile, methanol, dichloromethane and chloroform) with and without addition of ammonium acetate (NH_4Ac). The ESI and APCI-MS spectra of the two standards were examined by direct infusion on a Finnigan LCQ ion trap mass spectrometer analyzer. In the absence of ammonium acetate in the mobile phase, the protonated TAGs $[OOP^* + H]^+$ and $[OPO + H]^+$ at *m/z* 859 and DAG fragment ions were present for acetonitrile, methanol and dichloromethane under APCI conditions. No protonated TAGs or DAG fragment ions were observed under ESI conditions.

The ammoniated TAG, $[M + NH_4]^+$ at *m/z* 876 was generated at 100% relative abundance for both standards in all solvents when ammonium acetate was added to the mobile phase under ESI condition. In addition to the ammoniated TAG, protonated TAG and DAG ions are present in the MS spectrum of OPO and OOP* standards under APCI conditions (see for example OPO; Fig. 2.1a). No protonated TAG was observed for either standard under ESI conditions (Fig. 2.1b). Under ESI, sodium adduct $[M + Na]^+$ were commonly observed produced ions at *m/z* 881 and *m/z* 1740, corresponding to the sodium adduct $[M + Na]^+$ and sodium adduct dimer $[2M + Na]^+$, with no fragmentation. The sodium adducts are attributed to sodium being present as an impurity in the mass spectrometer and/or extract. The dimers occur more frequently when the concentration of the analyte is high (compare well with Segall et al., 2006).

a)

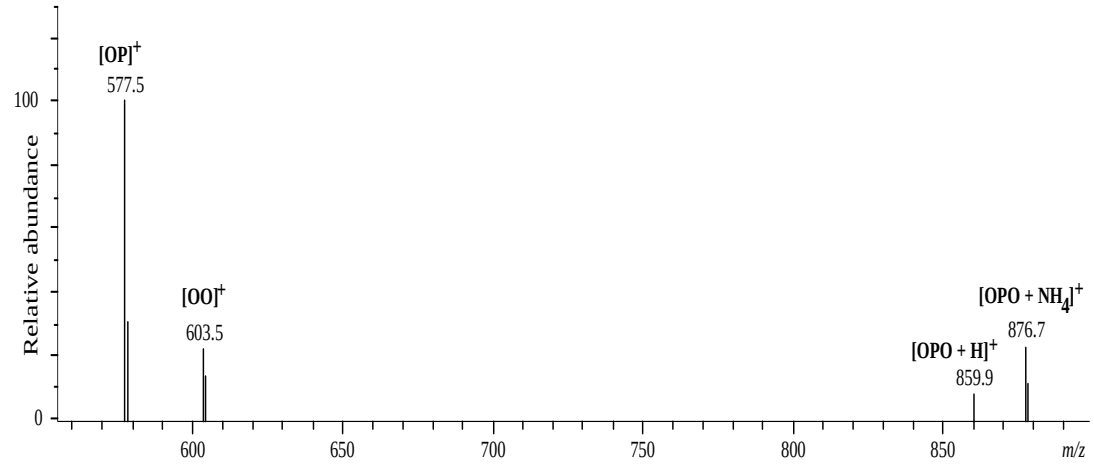

b)

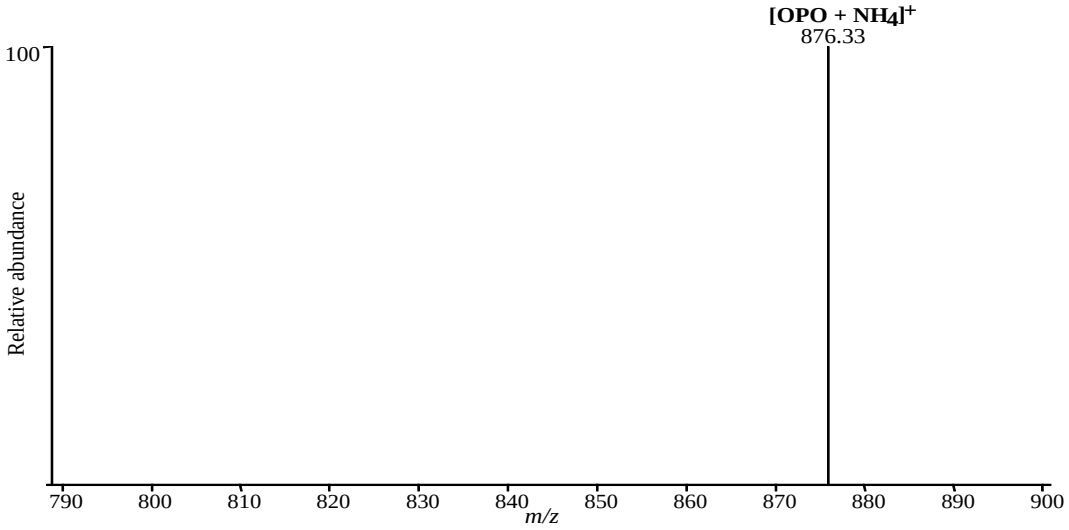

Figure 2.1: Direct infusion of OPO dissolved in acetonitrile:methanol (70:30) with added ammonium acetate a) APCI-MS spectrum of OPO b) ESI-MS spectrum of OPO.

2.2.1.2 Collision induced dissociation (CID) of OOP and OPO standards in MS^2.*

Both standards were subjected to CID following APCI and ESI under direct infusion with the purpose of examining the dissociation of the ionised standards formed by the two different ionization process.

APCI

CID of the $[OPO + NH_4]^+$ and $[OOP^* + NH_4]^+$ formed by APCI with ammonium acetate added in the solvent yielded their protonated TAGs, $[OPO + H]^+$ and $[OOP^* + H]^+$ and two DAG ions in MS^2 (Fig. 2.2a). In MS^2, the loss of NH_3 (17 Da) is evident from the ammoniated TAG producing the protonated TAG at *m/z* 859. The ions $[OP]^+$ at *m/z* 577

and $[OO]^+$ at *m/z* 603 result from combined loss of NH_3 and oleic and palmitic FAs, respectively; $[M + NH_4 – NH_3 - RCOOH]^+$. CID of the protonated TAG in the solvent without ammonium acetate added produced the same two DAG ions in MS^2 and undissociated protonated TAG.

ESI

Under ESI condition, $[OPO + NH_4]^+$ and $[OOP* + NH_4]^+$ produced two DAG product ions in MS^2: $[OP]^+$ at *m/z* 577 and $[OO]^+$ at *m/z* 603 (see for example OPO; Fig. 2.2b). CID of the ammoniated TAG from solvent with added ammonium acetate produced the same ions as seen under APCI. The absence of protonated TAG in the MS spectrum under ESI conditions precluded dissociation of the protonated molecule. The $[M + Na]^+$ ion where present (data not shown) did not dissociate readily, indicating them to be more stable than the ammoniated adduct, $[M + NH_4]^+$. Dissociation of the sodiated molecule at *m/z* 881 produced the palmitoyl oleoyl glycerol sodium product ion $[M + Na - RCOOH]^+$ (*m/z* 599) and sodium diolein (*m/z* 625), by loss of oleic and palmitic acids, respectively. The mass spectra also indicate the losses of the sodium salts of oleic and palmitic acids; $[M + Na -RCOONa]^+$, producing $[OP]^+$ (*m/z* 577) and $[OO]^+$ (*m/z* 603), respectively.

For both ionization sources, $[OP]^+$ and $[OO]^+$ were produced in the same relative proportions in all of the solvents with ammonium acetate added, and the relative abundances for both ions were compared with the data from previous published reports (Table 2.1a and b). The relative abundances of $[OP]^+$ and $[OO]^+$ dissociated from OPO and OOP* under APCI and ESI conditions are comparable to the published studies (Marzilli et al., 2003; Byrdwell and Neff, 2002 and Holcapek et al., 2003) indicating the tandem MS approach to be robust.

The relative abundance ratios for DAG ions, $[OP]^+/ [OO]^+$ in the solvent with and without ammonium acetate addition and from both ionization sources were calculated and compared with the published studies (Table 2.1c). The comparison reveals that for solvent with added ammonium acetate, dissociation of the standard in MS^2 is consistent with previous studies both for APCI and ESI. The data confirm that the fatty acid group in the *sn*-2 position is approximately five times less likely to be lost for OPO and two times less likely for OOP*. This dissociation behaviour is important for identification of regioisomers.

a)

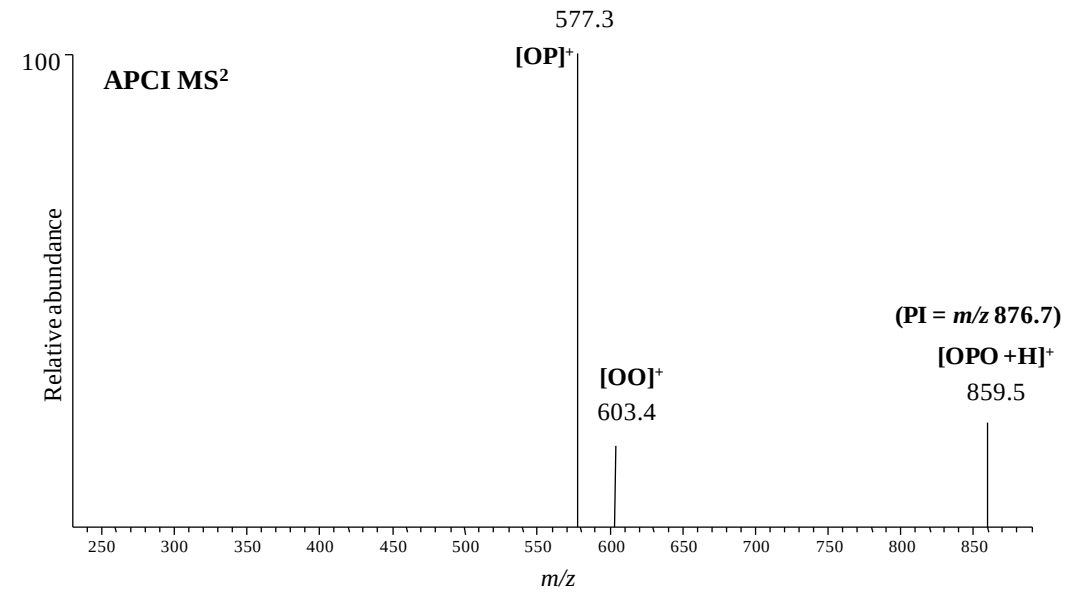

b)

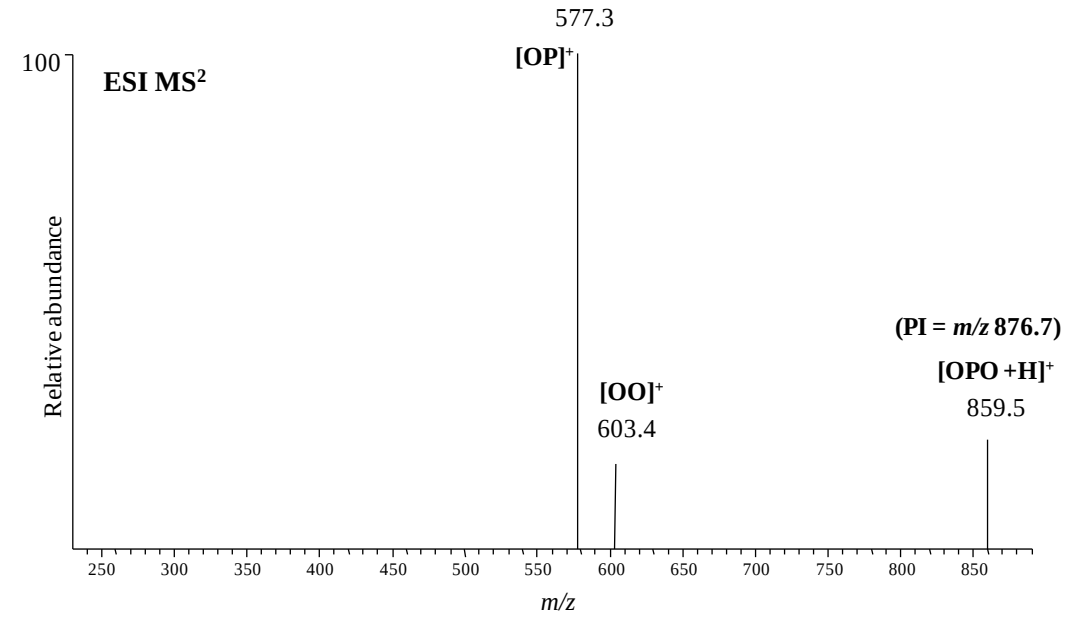

Figure 2.2: a) APCI-MS^2 spectrum of ammoniated OPO, b) ESI-MS^2 spectrum of ammoniated OPO. (Both were from direct infusion of OPO dissolved in acetonitrile:methanol (70:30) with added ammonium acetate). (PI = precursor ion).

Table 2.1: Relative abundances of product ions of TAG standard OOP and OPO in solvent with ammonium acetate added: a) $[OP]^+$ b) $[OO]^+$ and c) the relative DAG ratio $[OP]^+/[OO]^+$ under APCI and ESI conditions.

a)

Standard	Solvent	$[OP]^+$	
		ESI# &APCI# (MS^2)	Ref ([a]), ([b]), ([c])
OPO	All	100	100
OOP*	All	100	100

b)

Standard	Solvent	$[OO]^+$						
		ESI# (MS^2)	APCI# (MS^2)	Marzilli et al., 2003[a] (ESI-MS^2)	Byrdwell and Neff, 2002[b]		Holcapek et al., 2003[c]	
					ESI-MS^2	APCI-MS	ESI-MS^2	APCI-MS
OPO	All	20	20	20	24.4	16.7	15.7	20.6
OOP*	All	60	53	58	67.7	50.7	67.4	45.5

c)

standard	Solvent	APCI# MS^2 (without NH_4Ac added)	APCI and ESI (with ammonium acetate)						
			APCI# MS^2 and ESI# MS^2	APCI# MS	Marzilli et al., 2003[a] (ESI MS^2)	Byrdwell and Neff, 2002[b]		Holcapek et al., 2003[c]	
						ESI-MS^2	APCI-MS	ESI-MS^2	APCI-MS
OPO	DCM MeCN:DCM MeCN:MeOH MeOH MeCN	2.3:1 5.3:1 5:1 2:1 4.3:1	5:1##	5:1 3:1 4:1	5:1	4:1	6:1	6.4:1	5:1
OOP*	DCM MeCN:DCM MeCN:MeOH MeOH MeCN	1.6:1 1.4:1 1.2:1 1.2:1 1.4:1	2:1##	1.6:1 1.3:1 1:1 1.4:1 1.3:1	2:1	1.5:1	2:1	1.5:1	2.2:1

Results from the present study

All solvents gave similar ratio.

[a] acetonitrile: methanol (70:30) with 10mM ammonium acetate

[b] dichloromethane-with 20mM ammonium formate solution in H_2O/ACN (1:4)

[c] hexane:2-propanol (1:1) with 1mM ammonium acetate

In the absence of ammonium acetate in the solvent, the OPO and OOP* standards gave inconsistent $[OP]^+$/ $[OO]^+$ ratios in APCI MS^2 and the ratios were different for different solvents. By contrast, the OPO and OOP* standards in all solvent with added ammonium acetate gave a consistent ratio for $[OP]^+$/ $[OO]^+$ under APCI and ESI conditions. These results indicate that ammonium acetate is required to produce APCI spectra with a consistent dissociation ratio for $[OP]^+$/ $[OO]^+$ in MS^2 for the OPO and the OOP* standards. In ESI, ammonium acetate needs to be added to all of the solvents used. Furthermore, with the ammonium acetate added, the ammonium ions result in improve ionization and consequent enhancement in the response and signal stability. Notably, APCI gave higher signal intensity in MS to MS^3 than ESI, especially with acetonitrile as the solvent.

The use of HPLC grade chloroform as the solvent (without ammonium acetate addition) gave a base peak at *m/z* 901 for both APCI and ESI, a 43 *m/z* difference from the protonated molecules of the OPO and OOP* standards. The same peak was detected with standards in distilled chloroform and anhydrous chloroform with ethanol as a stabilizer. The dissociation of *m/z* 901 in MS^2 did not produce DAG ions as expected. Thus, chloroform cannot be used as a solvent for analysis of TAGs.

2.2.1.3 CID of OPO and OOP standard in MS^3.*

Similar product ions are present in the APCI and ESI MS^3 spectra of OPO and OOP*, although with different relative intensities. The DAG ions from the ammoniated molecules gave rise to ions in the MS^3 spectra corresponding to: $[RCO]^+$ (*m/z* 239 and 265), $[RCO\text{-}H_2O]^+$ (*m/z* 221 and 247), $[RCO+74]^+$ (*m/z* 313 and 339), and $[RCO+74\text{-}H_2O]^+$ (*m/z* 295 and 321). The major product ion in both the APCI and ESI MS^3 spectra from the DAG ion $[OO]^+$ (*m/z* 603) is *m/z* 265 $[O]^+$ (Figs 2.3a and 2.4a). Other product ions were observed at *m/z* 247, $[O\text{-}18]^+$; 339, $[O+74]^+$; and 321 $[O+74\text{-}18]^+$, reflecting the presence of the O atom in all of the product ions. The APCI MS^3 spectrum of *m/z* 577 (Fig 2.3b) and ESI MS^3 spectrum (Fig 2.4b) show product ions at *m/z* 239, $[P]^+$; 221, $[P\text{-}18]^+$; 313, $[P+74]^+$ and 295 $[P+74\text{-}18]^+$, corresponding to the equivalent product ions resulting from the presence of the FA P in the DAG ion. The loss of 74 Da from $[OP]^+$and $[OO]^+$, giving product ions at *m/z* 503 and 529, respectively represents the glycerol backbone of the TAG molecule in the form of the elements of $C_3H_6O_2$ as observed in the ESI-MS, MS^2 and MS^3 spectra of the TAG standards of OPO and OOP* (Marzilli et al., 2003). No corresponding data for APCI are available in the literature.

a)

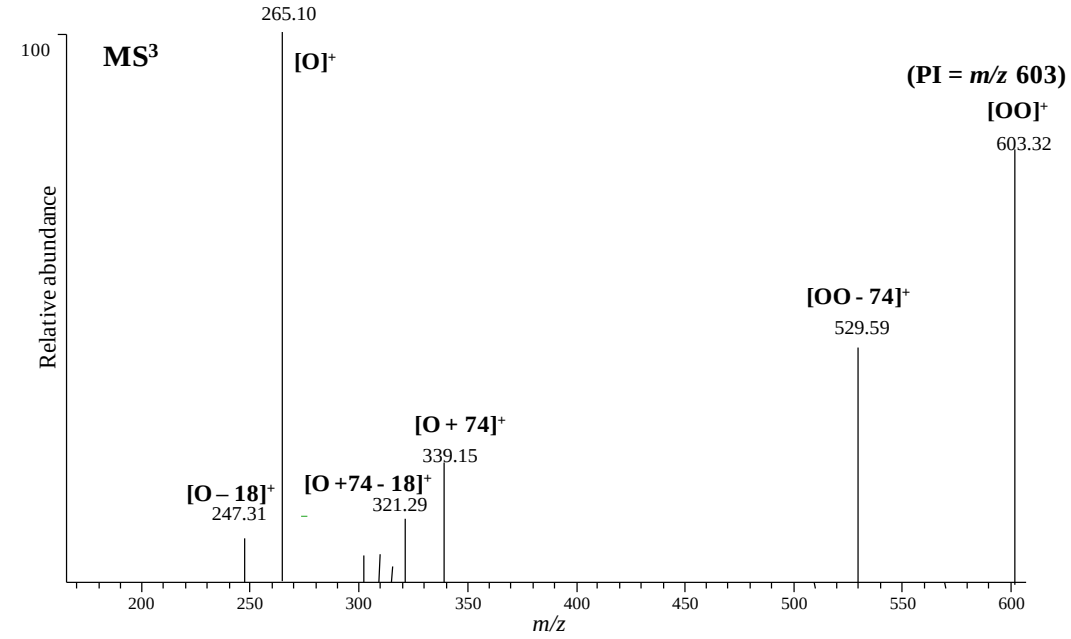

b)

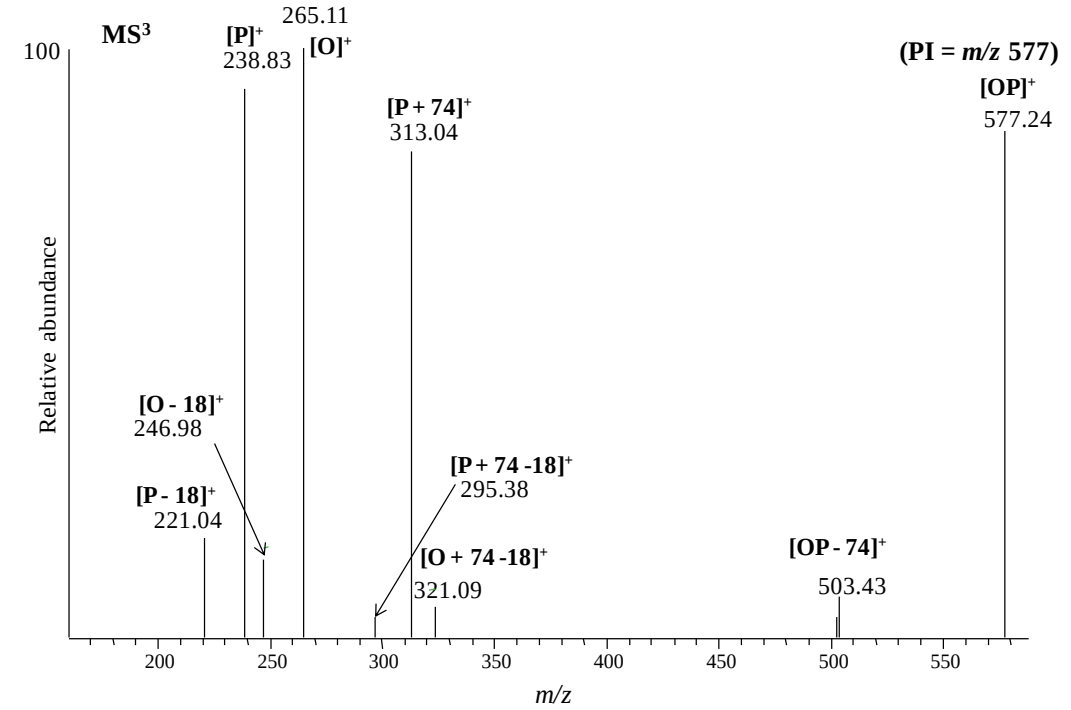

Figure 2.3: a) APCI-MS^3 spectrum of *m/z* 603, b) APCI-MS^3 spectrum of *m/z* 577. (Both were from direct infusion of OPO dissolved in acetonitrile:methanol (70:30) with added ammonium acetate; PI = precursor ion).

a)

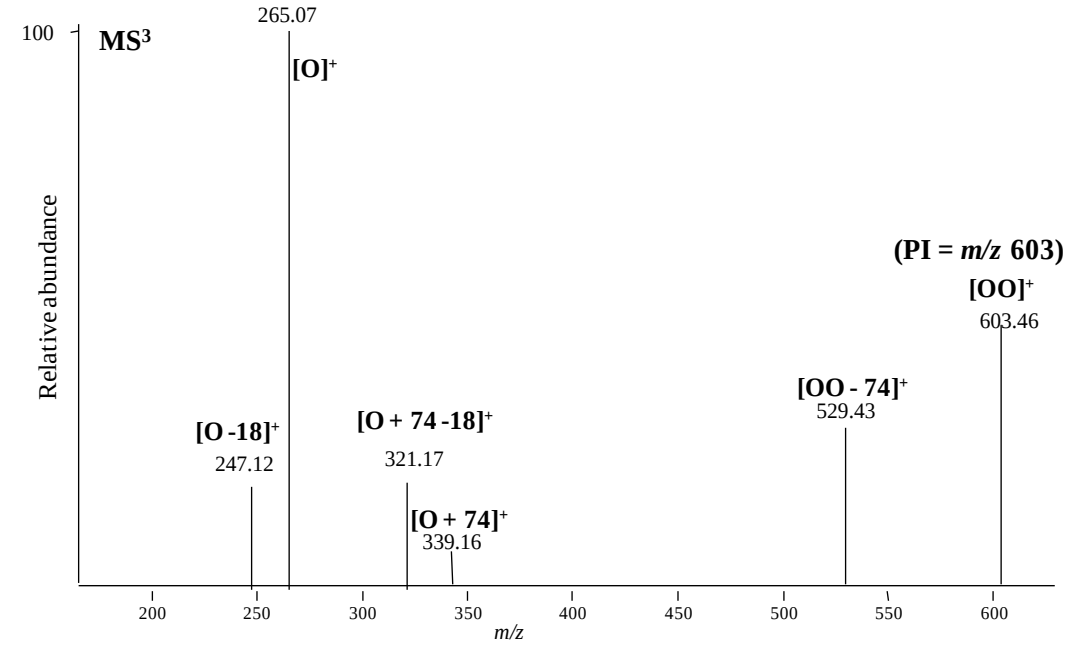

b)

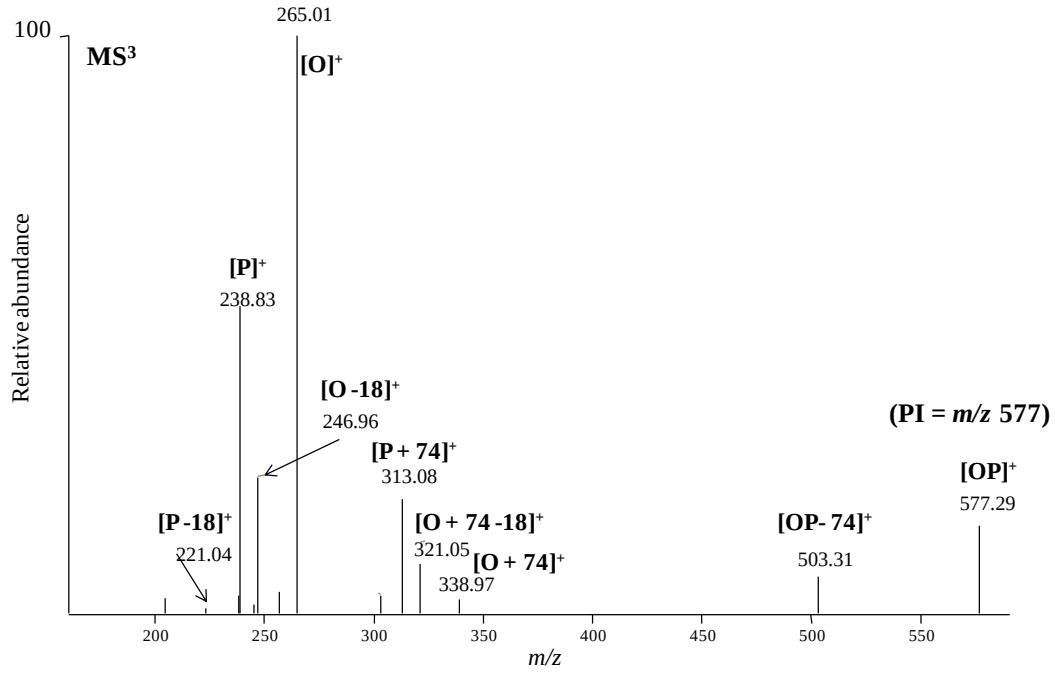

Figure 2.4: a) ESI-MS^3 spectrum of *m/z* 603, b) ESI-MS^3 spectrum of *m/z* 577. (Both were from direct infusion of OPO dissolved in acetonitrile:methanol (70:30) with added ammonium acetate; PI = precursor ion).

2.2.2 MS of TAGs in beef and pork fats by direct infusion

Pork and beef fat were extracted with chloroform and methanol (2:1) and the extracts were analysed by direct infusion in acetonitrile and methanol (70:30) using APCI and ESI on a Finnigan LCQ employing post column addition of ammonium acetate. The ESI spectra show only ammoniated TAGs, whereas the APCI spectra show both ammoniated and protonated molecules (Fig. 2.5 and 2.6). Apart from differences in ion relative abundance, the profiles of pork and beef are very similar. The APCI spectra are labelled with the carbon numbers of the TAGs as determined from the *m/z* of the ammoniated molecules.

The ammoniated (labelled ✻ in Figs. 2.5b and 2.6b) and protonated (labelled • in Figs. 2.5b and 2.6b) TAGs formed in the APCI source occur between *m/z* 822 to 906 in pork fat and *m/z* 803 to 908 in beef fat. The pork and beef fat spectra both show the ammoniated molecule at *m/z* 876 as the most abundant ion. The next two most abundant ions in pork are *m/z* 874 and 900 and in beef fat are *m/z* 902 and 874. There are also dominant peaks at *m/z* 857 and *m/z* 883 in pork fat, corresponding to protonated TAG molecules with CN values of 52 and 54, respectively. The dominant protonated TAGs in beef fat are *m/z* 859 and *m/z* 885 which also have CN values of 52 and 54, respectively. The ammoniated TAGs at *m/z* 876 also represent the most abundant ions formed in the ESI source for pork and beef fat. Other dominant ammoniated TAGs occur at *m/z* 878, 874 and 848 for pork fat and at *m/z* 878, 904 and 850 for beef fat.

Every ion in the spectrum may represent either a single TAG molecule or several: many TAGs have the same mass. Due to the similarities in the spectra obtained by direct infusion, the samples were introduced via LC to separate the TAG compounds prior to detection by MS. Even though ESI have simpler spectra than APCI (absence of protonated molecules), APCI was used in this study because of the presence of sodium interference in the ESI which produced sodium adducts and sodium adduct dimers.

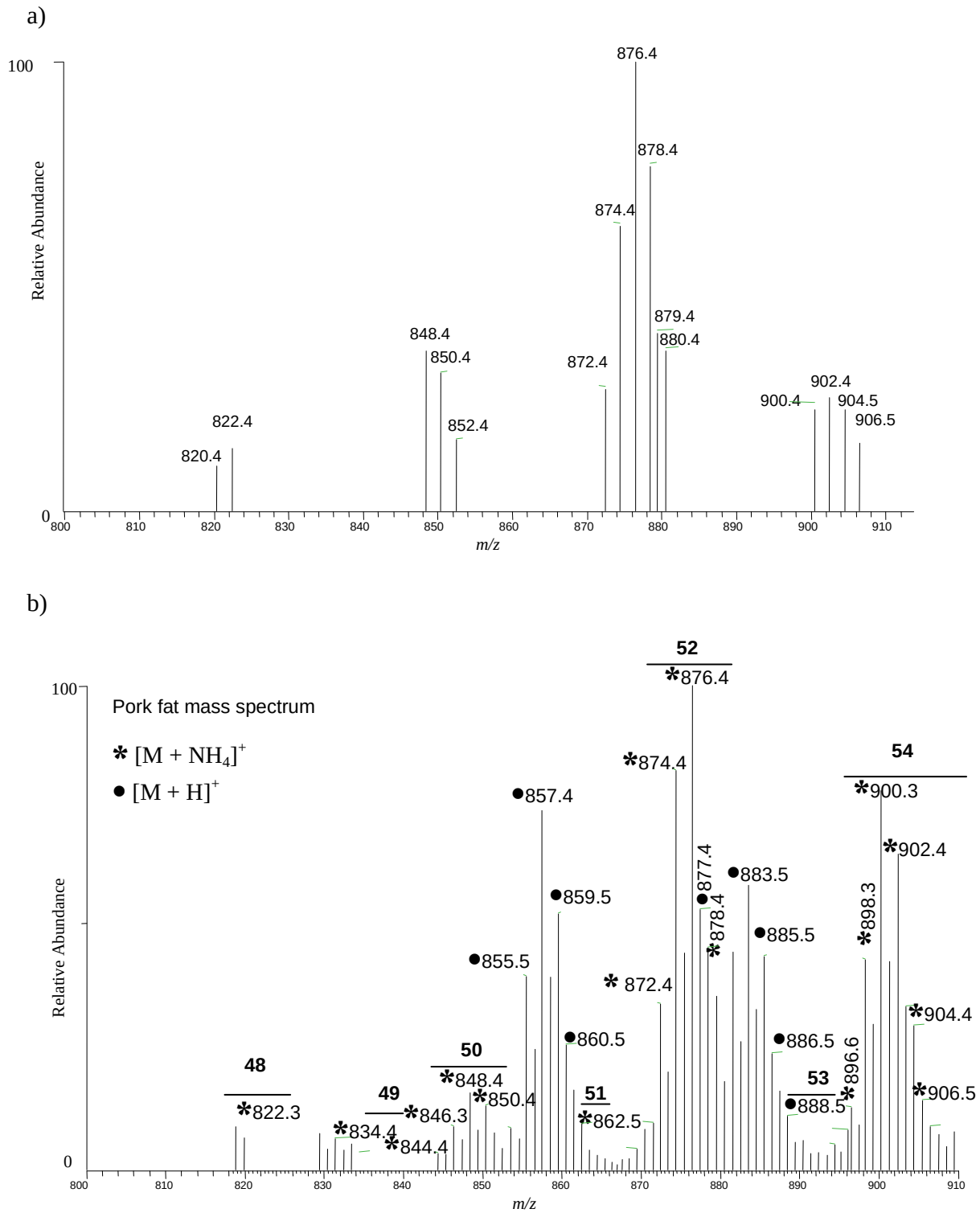

Figure 2.5: Direct infusion of an extract of pork fat in acetonitrile and methanol (70:30) with ammonium acetate addition, a) ESI-MS spectrum (all ions are ammoniated TAGs). b) APCI-MS spectrum.

a)

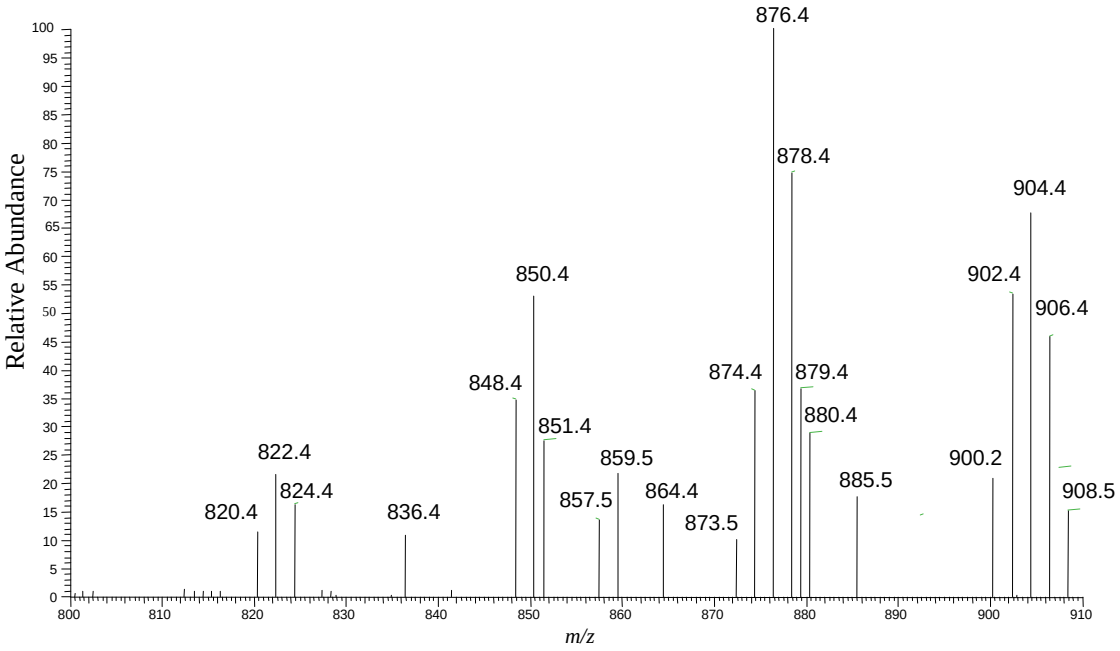

b)

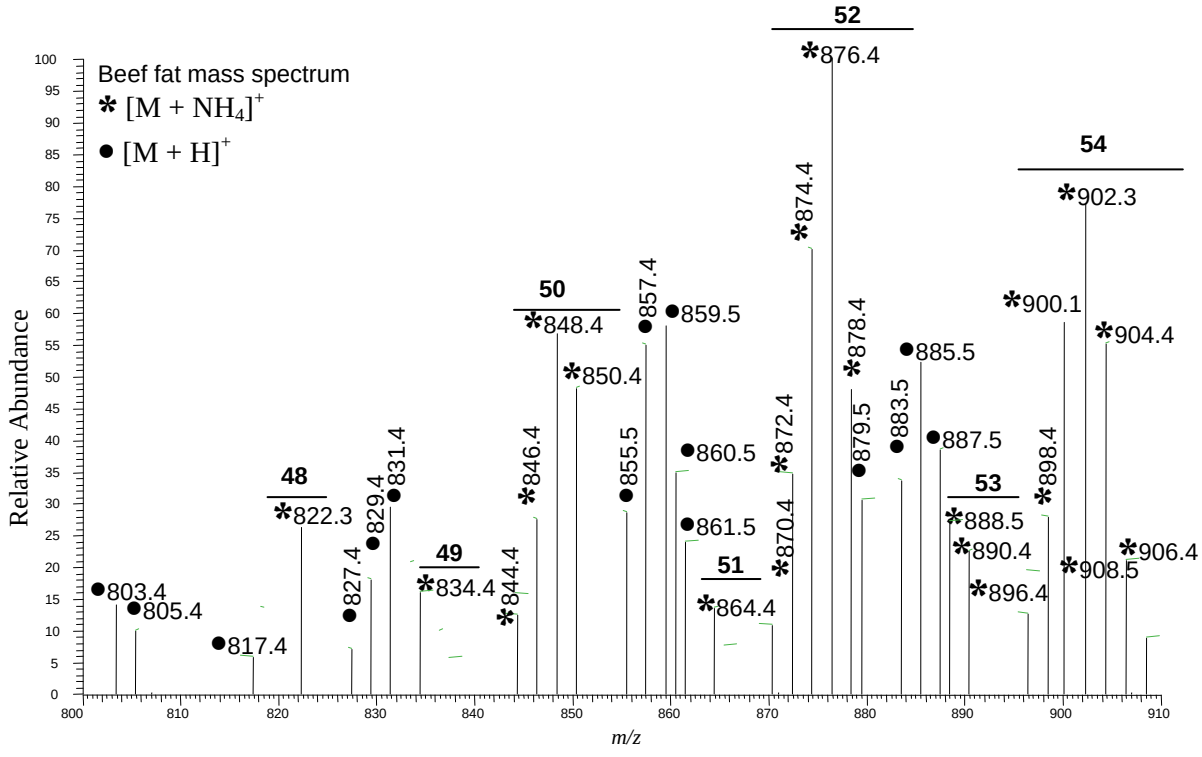

Figure 2.6: Direct infusion of an extract of beef fat in acetonitrile and methanol (70:30) with ammonium acetate addition, a) ESI-MS spectrum (all ions are ammoniated TAGs). b) APCI-MS spectrum.

2.2.3 Development of a single stage RP HPLC-MS/MS separation of TAGs.

2.2.3.1 Development of RP HPLC separation of TAGs from beef fat.

As a starting point for development of an HPLC method separating TAGs of animal fats, a published method for separating lard and beef fat was selected (Dugo et al., 2006; Fig. 2.7a). That method used two Supelco Discovery HS C18 columns (250 mm x 4.6 mm, 5 µm) eluted with a mobile phase gradient comprising 2-propanol and acetonitrile (labelled $^{+}$, Table 2.2). The method achieves separation of TAGs according to their ECN, components with ECN between 46 and 52 being discriminated with retention times increasing with ECN (Fig. 2.7a). Within each group of compounds of a particular ECN several components are resolved (e.g. OOO, OOP*, POP and MPS for ECN 48). Notably, however, a number of small shoulders can be seen on several of the peaks (e.g. peaks 5, 6 and 7; Fig. 2.7a), indicating that separation and resolution are not optimal. In order to develop an improved separation, three distinct chromatographic phases were investigated (Table 2.3). All phases examined were C18 materials with differences in particle size and carbon loading being two important variables. The columns available for the study were of differing length and results are discussed accordingly. All of the columns were evaluated using a solvent extract from the same sample of beef fat. Finnigan MAT SpectraSystem P4000 HPLC coupled to a Finnigan LCQ ion trap mass spectrometer with the APCI sources were used for the method development. Briefly, the fat was extracted with chloroform and methanol and reduced to dryness after which the extract was stored in a freezer until use. For initial screening of the different phases the fat was dissolved in mobile phase for injection. The Apex ODS and Genesis C18 columns were each evaluated using the mobile phase gradient employed by Dugo et al., 2006 (labelled $^{+}$, Method A, Table 2.2a), adapted where shorter column lengths were used (labelled * for Apex ODS column and ** for Genesis C18 column, Method A, Table 2.2a) and with APCI MS detection employing post column addition of ammonium acetate to enhance ionization response.

Table 2.2: Proportions of 2-propanol and acetonitrile in the mobile phase of a) Dugo et al., 2006 and variations in gradient profile employed in this study (Method A), b) as modified in this study (Method B).

Time (min)	Flow rate (mL/min)	2-propanol	Acetonitrile
a) Method A			
0	1	30	70
30[+] (15*, 9**)	1	40	60
50[+] (25*, 15**)	1	55	45
75[+] (38*, 23**)	1	70	30
90[+] (45*, 27**)	1	70	30
b) Method B			
0	0.5	54	46
75	0.5	65	35

[+] gradient time of Dugo et al., 2006

* gradient time for Apex ODS column

** gradient time for Genesis C18.

Table 2.3: HPLC columns tested for separation of TAGs from beef fat, ordered according to decreasing particle size.

Particle size (µm)	% C loading	Columns	Dimensions
5	10	Jones Apex Octadecyl	250 mm x 4.6 mm
4	18	Genesis C18	150 mm x 4.6 mm
3	11.5	Waters Spherisorb ODS2	150 mm x 4.6 mm

The Apex ODS and Genesis C18 columns failed to separate the components with the same ECN using the gradient employed by Dugo et al., 2006 (Method A; Table 2.2a). The ECN values were determined from the spectrum produced from MS across each peak in the chromatogram. Very limited separation of the TAGs having the same ECN

was observed in both columns, showing several peaks appearing as shoulders (e.g. the broad peak for ECN 52 corresponds to peaks 12 and 13, which were not separated, Fig. 2.7b). Very familiar chromatography was observed on the Genesis C18 column but with a shorter run time of about 24 min. A peak for TAGs with ECN 54 was observed on both the Apex ODS and Genesis C18 columns: no such peak was observed by Dugo et al., 2004.

a)

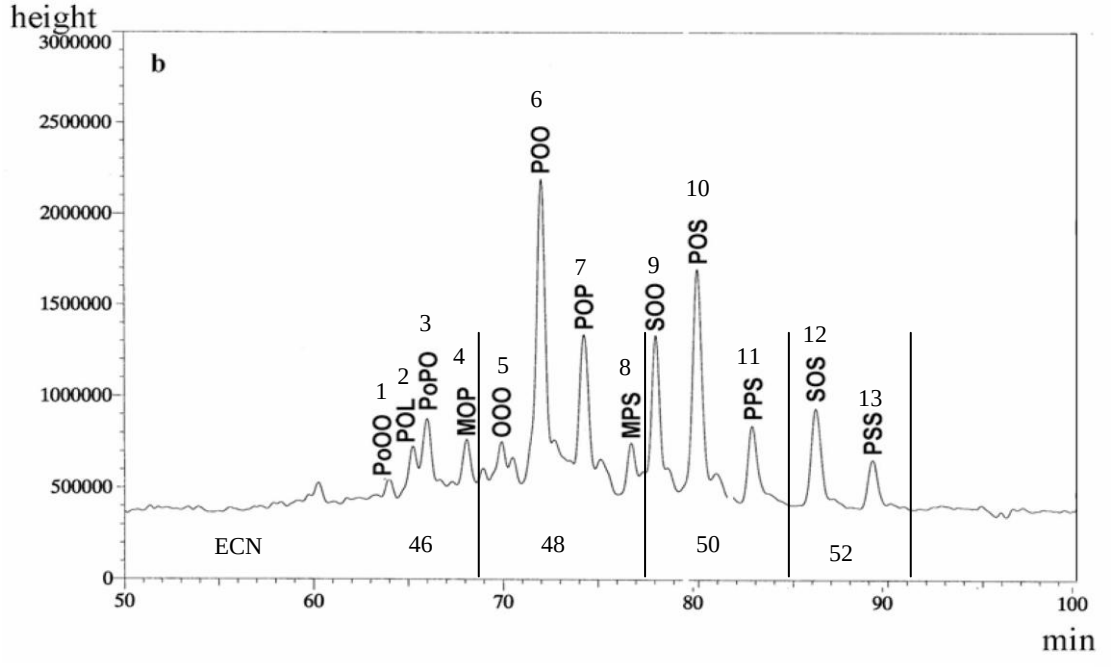

b)

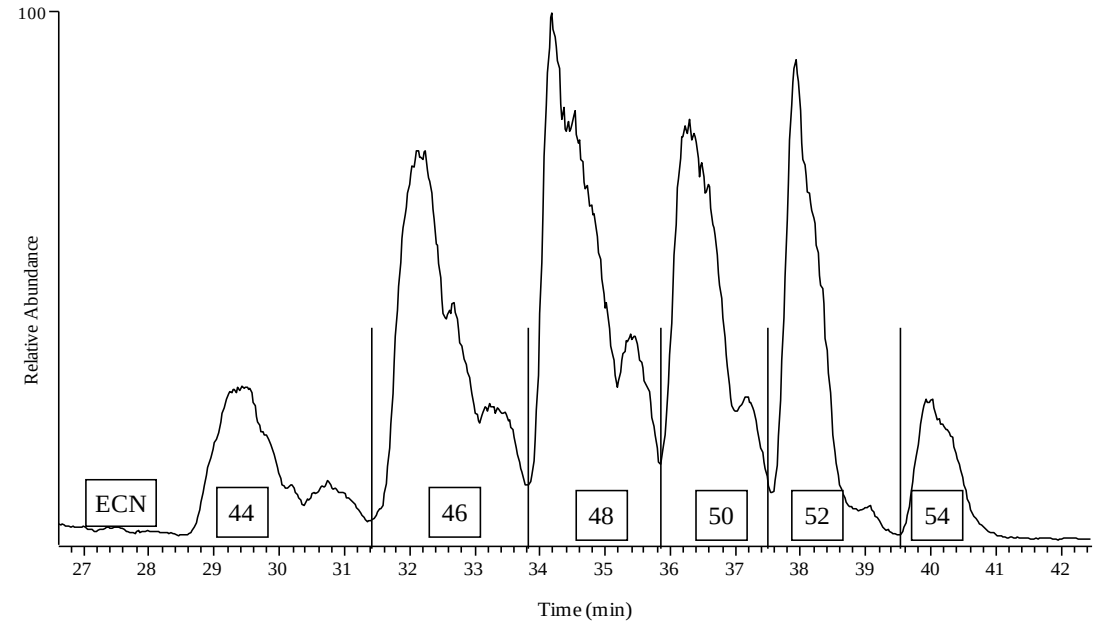

Figure 2.7: a) RP HPLC-APCI MS chromatogram of TAGs from beef fat with regions of the chromatogram assigned according to ECN (modified from Dugo et al., 2006). b) RP HPLC-APCI MS chromatogram of TAGs from beef fat on the Apex ODS column using the mobile phase system of Dugo et al., 2006 (Method A; Table 2.2a, labelled $^{+}$).

Different proportions of 2-propanol were evaluated, varying from 30 to 70% by volume with 5% increments. The values between 50 to 65% give the best separation on the Apex ODS and Genesis C18 columns. This region was further explored with 1% increments and the optimum composition was found starting at 54% 2-propanol and increasing to 65% by 75 min with both columns (Method B; Table 2.2b).

The separation and resolution of TAGs having the same ECN were improved on both columns tested (e.g. peaks 9, 10, 11 for ECN 50 and peaks 12 and 13 for ECN 52, Fig 2.8a and b). Peak 13 is almost completely separated from peak 12, though none of the peaks are better resolved than the published method. Notably, the resolution and peak shape for the TAGs is not as good as in the published method. There is, however, a small improvement in assignment with TAGs of ECN 44, which is dominated by LLP*, and ECN 54 (SSS) being detected in the present study. The two columns examined have different advantages and capabilities for separating TAGs. For example, the resolution of peaks 12 and 13 and peaks 10 and 11 are better on the Genesis C18 column whereas the separation of peaks 9 and 10 is better on the Apex ODS column. Interestingly, in the region for ECN 44, PPoPo* is dominant on the Genesis C18 column whereas LLP* dominates on the Apex ODS column. Both columns were explored further for separation of TAGs.

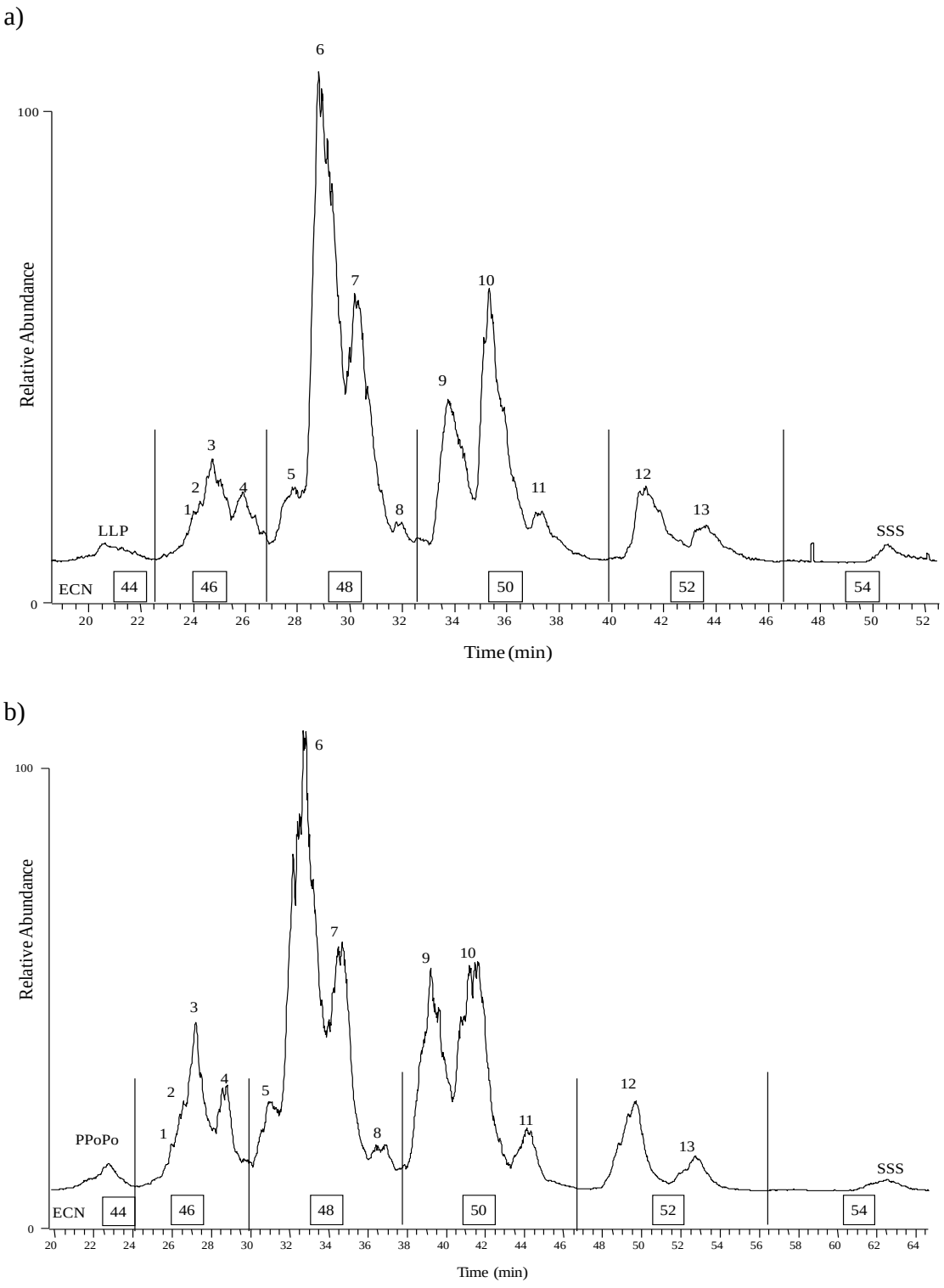

Figure 2.8: RP HPLC-APCI MS chromatogram of TAGs from beef fat eluted with the mobile phase Method B (Table 2.2b) on the a) Apex ODS column. b) Genesis C18 column.

Since partial resolution was observed, other factors that may limit the resolution were considered critically. The effect on the chromatographic resolution of the solvent used to dissolve the beef fat sample (the sample solvent) was examined. The initial mobile phase has been suggested to be the ideal sample solvent (Tsimidou and Macrae, 1985) and all proceeding analyses were performed using the initial mobile phase. Three non polar solvents, chloroform, dichloromethane and hexane were each evaluated as additives to the sample solvent to increase the solubility of TAGs. The use of non polar solvent is suggested if working with highly saturated TAGs and for situations where TAGs exhibit low solubility in the initial mobile phase. Sharper peaks will improve resolution and may result from combinations of polar and non polar solvents dissolving highly unsaturated and saturated TAGs equally effectively. Hexane is a more apolar solvent than chloroform and dichloromethane. The combination of hexane:acetonitrile:2-propanol (1:1:1,v/v/v) for the sample solvent gave slightly sharper peaks than with the same combination replacing chloroform and dichloromethane. This sample solvent combination was used throughout the subsequent development of the separation.

The mobile phase combination of 2-propanol and acetonitrile gave worse resolution and peak shape for all of the TAGs than in the published method. Also, the peaks of polar and non polar TAGs were broadened. This can be attributed in part to the low solubility of TAGs; especially the highly saturated components, in the mobile phase system making this combination not optimal. In RP HPLC of TAGs the mobile phase has a major effect on the separation through competition with the stationary phase. Thus, increased or decreased solubility of TAGs in the mobile phase can enhance or retard their separation and affect peak width. Chlorinated solvents (dichloromethane, chloroform, 1,2-dichloroethane), benzene and tetrahydrofuran have been added to improve the solubility of TAGs in the base solvent, changing mobile phase polarity and increasing peak selectivity (Barron et al., 1987).

Chloroform was introduced to the mobile phase system replacing 2-propanol, the proportion being determined according to Fauconnot et al., 2004 (Method C; labelled $^{+}$, Table 2.4a) with the addition of 6 min separation time on the final gradient. Those authors analyzed vegetable oil and animal fats using a Restek Ultra C18 (250 cm x 2.1 mm, 5 µm) column. In the present study, the TAGs with the same ECN co-eluted in a single peak (Fig. 2.9a), none of the peaks being better resolved than the published method. The Apex ODS and Genesis C18 columns gave similar separation behaviour to each other. Even though the TAGs with equal ECN were not separated, peaks of odd

ECN (45, 47, 49, 51 and 53) were observed. These peaks were not observed in the previous method (Fauconnot et al., 2004). Also, the TAGs with ECN value of 42 are observed in the chromatogram. The proportion of chloroform was adjusted, varying from 5 to 80% by volume with 5% increments. Changing the proportion of chloroform did not improve the separation dramatically. Even a constant value of 5% chloroform for the whole run did not improve the resolution. The composition between 5 to 50% gave the best separation and this region was further explored with 1% increments and the optimum composition, starting at 5% chloroform and and increasing to 40% by 75 min (Method D; Table 2.4b), gave a chromatogram with slightly resolved TAG compounds of similar ECN but with loss of separation of TAGs with the odd ECN (Fig. 2.9b).

Table 2.4: Proportions of chloroform and acetonitrile in the mobile phase Method C and D for the separation of TAGs from beef fat, a) Fauconnot et al., 2004 (Method C), b) as modified in this study (Method D).

Time (min)	Flowrate (mL/min)	Chloroform	Acetonitrile	NH_4Ac in MeOH (10 mM)
a)[+] Method C				
0	0.25	20	80	0
7	0.25	40	60	0
33	0.25	40	60	0
34	0.25	20	80	0
b) Method D				
0	1	5	95	Post column
75	1	40	60	(4 µL/min)

[+] Fauconnot et al., 2004.

a)

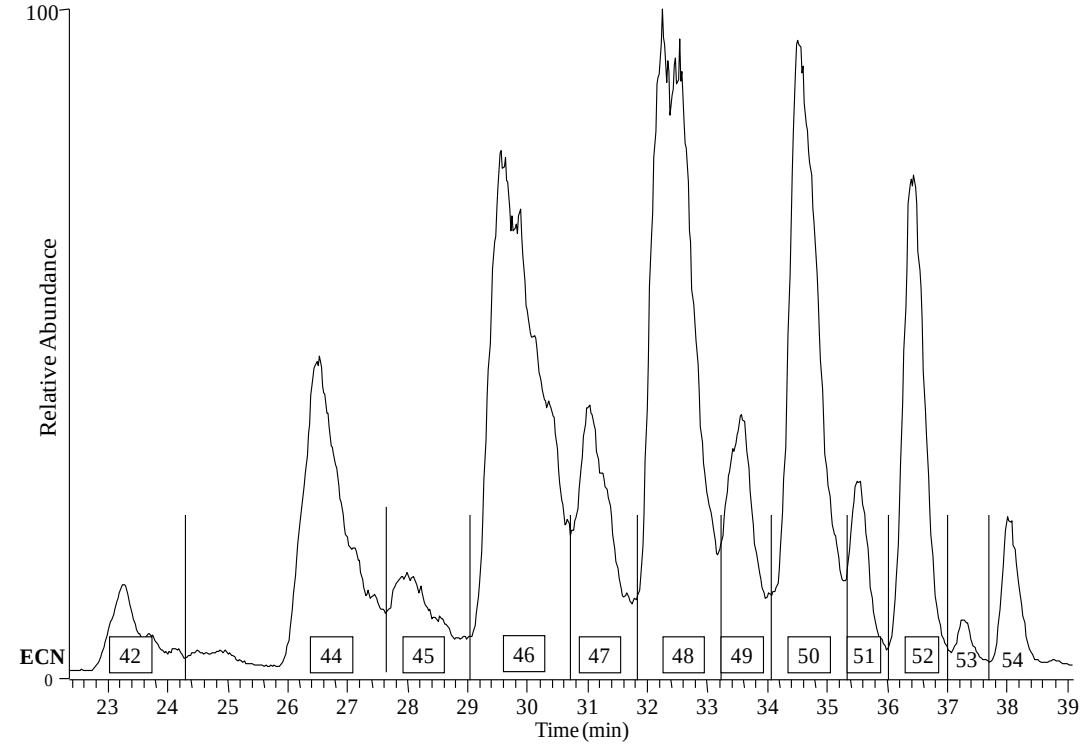

b)

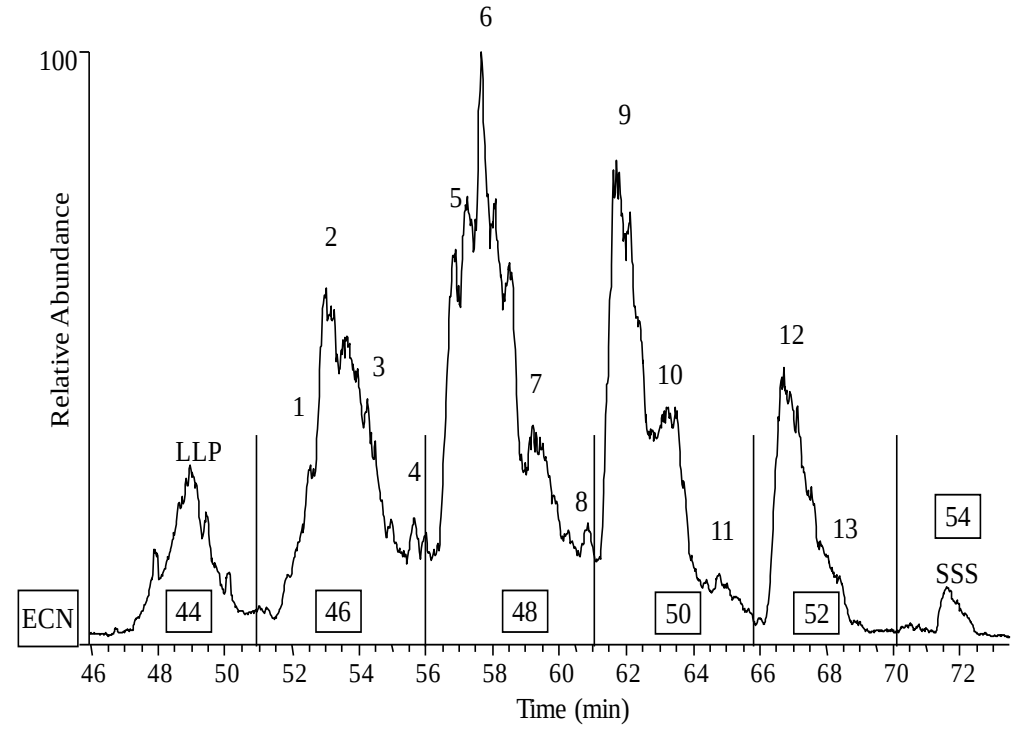

Figure 2.9: RP HPLC-APCI MS chromatograms of TAGs from beef fat on the Apex ODS column eluted using a) chloroform and acetonitrile (Method C; Table 2.4a), b) modified proportion of chloroform and acetonitrile (Method D; Table 2.4b).

The replacement of 2-propanol by chloroform in the mobile phase gave worse resolution for TAGs having similar ECN. This suggests that introducing a more apolar solvent than chloroform to the mobile phase may improve the solubility of TAGs by changing the mobile phase polarity, which may improve peak selectivity. Dichloromethane was introduced into the mobile phase system, replacing chloroform, and different proportions of dichloromethane were evaluated, varying from 20 to 50% by volume with 5% increments. The values between 35 to 40% give the best separation on the Apex ODS and Genesis C18 columns. This region was further explored with 1% increments and the optimum composition was found starting at 35% dichloromethane and increasing to 38% by 110 min with the Apex ODS column (Method E; Table 2.5a; Fig. 2.10a). The optimum composition with the Genesis C18 column started at 35% dichloromethane and increasing to 36% by 110 min (Method F; Table 2.5b; Fig. 2.10b). The Genesis C18 column, which has smaller particle size and a column length 3/5 that of the Apex ODS column, required 2% less dichloromethane for complete elution of TAGs. The increment in the proportion of dichloromethane was only 1% for 110 min or about 0.01% for every min with Genesis C18 column and 3% for 110 min or about 0.03% per min with Apex ODS column. This provides a very slow increase in elutrophic strength leading to slower elution of highly unsaturated and saturated TAGs and improving the resolution. Ammonium acetate (10 mM) at a flow rate of 4 µl/min was added post column to enhance ionization and hence, response. The combination of hexane:acetonitrile:2-propanol (1:1:1,v/v/v) was used as sample solvent for the beef fat.

Table 2.5: Proportions of dichloromethane and acetonitrile in the mobile phase of Method E and F eluted on the a) Apex ODS column (Method E), b) Genesis C18 column (Method F) for separating the TAGs from beef fat.

Column	Time (min)	Flowrate (ml/min)	Dichloromethane (%)	Acetonitrile (%)
a) Method E	0	0.5	35	65
(Apex ODS)	110	0.5	38	62
b) Method F	0	0.5	35	65
(Genesis C18)	110	0.5	36	64

The Apex ODS column using Method E separated some of the components having the same ECN (e.g. Peaks 9, 10, 11 for ECN 50 and peaks 12 and 13 for ECN 52; Fig. 2.10a). Here, better separation of peaks 3 and 4, peaks 7 and 8, peaks 10 and 11 and peaks 12 and 13 was observed than in the separation on the same column with the mobile phase based on 2-propanol (Fig. 2.8a). Notably, the resolution of peaks 12 and 13 is much better with dichloromethane (*Rs* = 1.42) than with 2-propanol (*Rs* = 0.8). Nevertheless, the resolution and peak shape for the TAGs is not as good as in the published Methods (e.g. for peaks 6 and 7, *Rs* = 0.8 and for peaks 9 and 10, *Rs* = 1.0 compared with 1.6 and 2.0 in Dugo et al., 2006 and 1.04 and 1.7 in Fauconnot et al., 2004). Due to the limited ability of the Apex ODS column to separate the TAGs, this column was not evaluated further.

The chromatogram of TAGs on the Genesis C18 column eluted using Method F (Fig. 2.10b) shows better separation of TAGs having the same ECN than with the 2-propanol-based mobile phase (Fig. 2.8b). In the region for ECN 44, LLP* is dominant rather than PPoPo* which dominated this region on the same column eluted with 2-propanol. The almost complete separation with dichloromethane suggests that the PPoPo* peak observed with 2-propanol elution is broadened, i.e. both peaks, LLP* and PPoPo*, have narrower peaks with dichloromethane present in the mobile phase. Overall, the separation of TAGS on the Genesis C18 column was much better with dichloromethane elution (Method F) than with 2-propanol (Method B), with better separation for TAGs having the same ECN (from ECN 44 to 52) and several additional peaks being observed between the dominant peaks (e.g. between peaks 4 and 5, 6 and 7, 7 and 8). The improvement in separation of the most apolar compounds can be attributed to the presence of dichloromethane in the mobile phase increasing the solubility of the most apolar TAGs. An increase in separation of TAGs with ECN 48 and above was observed (e.g. peaks 6 and 7, 8 and 9) and the resolution of peaks 6 and 7 (*Rs* = 2.0) is slightly better than in the published methods (*Rs* = 1.6) in Dugo et al. (2006) and (*Rs* = 1.04) in Fauconnot et al. (2004). Peaks 9 and 10 and peaks 12 and 13 are also better resolved (*Rs* = 2.5 and 2.3 compared with 2.0 for both (Dugo et al., 2006) and *Rs* = 1.7 and 2.2 (Fauconnot et al., 2004). The separation of an additional peaks between peaks 8 and 9 and two peaks between peaks 11 and 12 and the presence of a number of smaller shoulders on some of the peaks (e.g. peaks of 5, 6, 7, 9 and 10) indicates improved separation. Attempts to further separate those peaks and to improve separation of TAGs with an ECN below 48 were unsuccessful with the Genesis C18 column. Fairly, the

peaks are still broadened compared with those obtained by Dugo et al. (2006), being almost double the peak width.

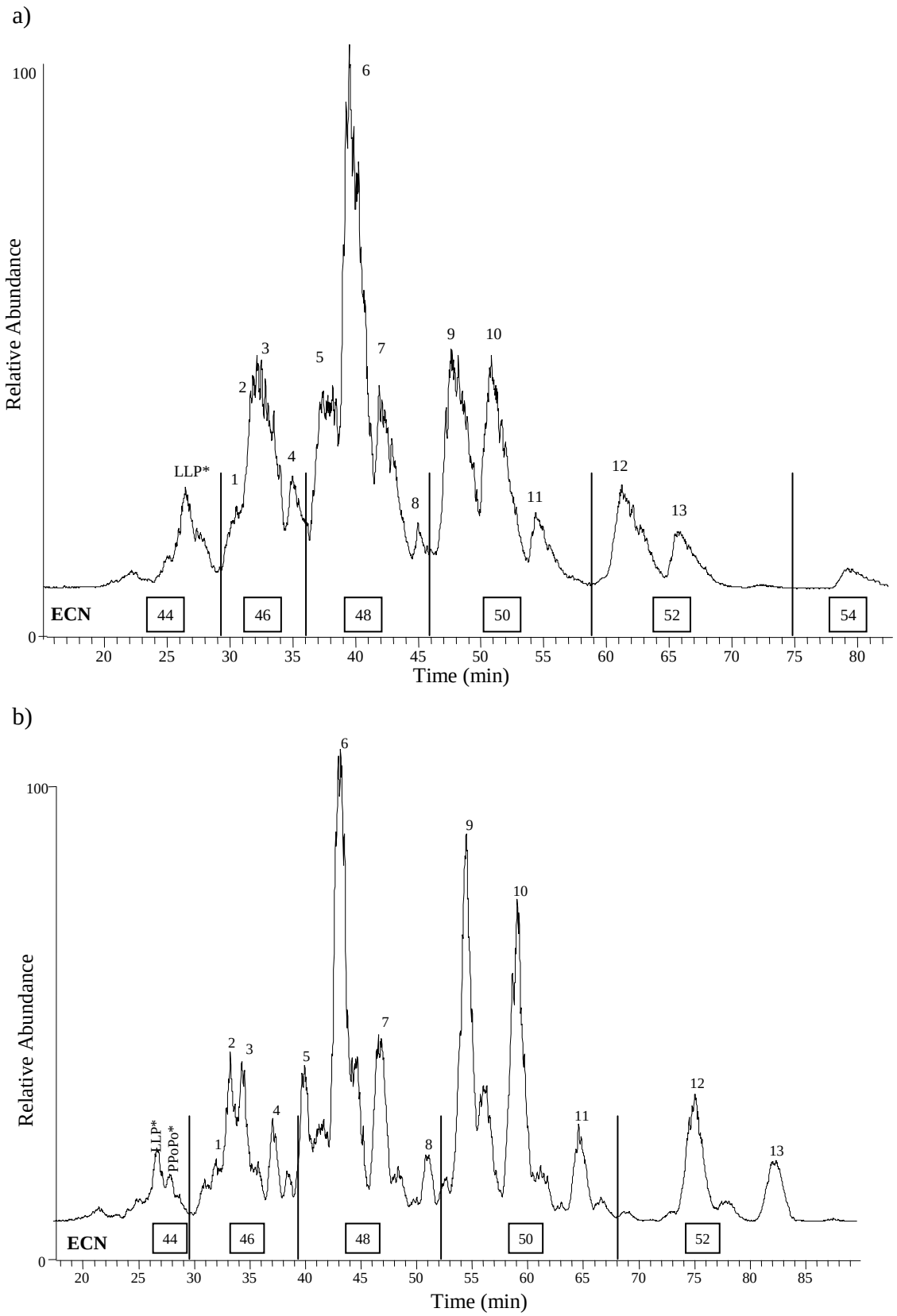

Figure 2.10: RP HPLC-APCI MS chromatogram of TAGs from beef fat a) on the Apex ODS column eluted with the mobile phase in Method E (Table 2.5a), b) on the Genesis C18 column eluted with the mobile phase in Method F (Table 2.5b).

Reducing the proportion of dichloromethane to a very low percentage (less than 15%) gave much broader peaks and did not improve the resolution. This suggests that use of a longer and smaller particle size column than the Genesis C18 is required to improve the resolution while reducing the peak width. Two Waters Spherisorb ODS2 columns with double the column length and smaller particle size (3 μm) than the Genesis C18 were explored for developing the separation of TAGs with dichloromethane in the mobile phase.

The mobile phase composition of dichloromethane and acetonitrile was adjusted for the longer column length. The proportion of dichloromethane required was determined by evaluating values from 20 to 40% by volume with 1% increments. The composition that gave good separation was found starting at 24% dichloromethane and increasing to 40% by 100 min (Method G; Table 2.6a; Fig. 2.11a). The optimal composition was with the initial eluant polarity reduced to 20% to affect earlier elution of the least polar components and a very slow increment of 1% for 82 min (about 0.01% in a min). This gradient also allowed elution of highly unsaturated TAGs having ECN values below 48. The proportion of dichloromethane was increased to 35% for further 63 min to eluting the most apolar TAGs (Method H; Table 2.6b). Ammonium acetate, NH_4Ac (10 mM) was added to the mobile phase gradient to enhance ionization.

Table 2.6: Proportions of dichloromethane and acetonitrile in the mobile phase of a) Method G, b) Method H on the Waters Spherisorb ODS2 columns for separating the TAGs of beef fat.

Time (min)	Flowrate (ml/min)	Dichloromethane (%)	Acetonitrile (%)	NH_4Ac in MeOH (10 mM)
a) Method G				
0	1	24	73	3
70	1	25	72	3
100	1	40	57	3
b) Method H				
0	1	20	76	4
82	1	21	75	4
145	1	35	61	4

The chromatogram from the Waters Spherisorb ODS2 columns eluted with the mobile phase gradient of Method H (Table 2.6b) showed much better separation of TAGs with ECN below 48, including the odd ECN TAGs (Fig. 2.11b), than the mobile phase gradient of Method G (Table 2.6a; Fig. 2.11a). Better separations of LOO and peak 1 and of peaks 2 and 3 are observed (Fig. 2.11b) and better resolution of shoulder peaks 6 (*Rs* = 1.11 in Fig 2.11b and *Rs* = 0.86 in Fig. 2.11a) are evident. Better peak shapes are seen for TAGs with odd ECN of 51 and 53 than in Fig. 2.11a. The effect on resolution of variation in the mobile phase composition might reflect the effect of polarity, chiefly a result of the number of double bonds in the TAGs, as well as the effect of hydrophobicity due to the number of carbon atoms in their FAs (Barron et al., 1987). As the proportion of DCM in the mobile phase decreases, analysis times can be observed to increase (from 94 min in Fig. 2.11a to 131 min in Fig. 2.11b). The underlying increase in retention time are much more significant for TAGs with higher ECN. The longer time for chromatographic analysis of these TAGs with the lower proportion of DCM in the mobile phase is compensated by better separation of the highly unsaturated TAGs.

Notably, all the small shoulder peaks observed in the best separation obtained with the Genesis C18 column (Fig. 2.10b) were separated using the Waters Spherisorb ODS2 columns (Figs. 2.11a and b). Thus, the shoulders on the peaks 6, 7, 9, 10 and 12 were resolved. The separations of TAGs having similar ECN are considerably better using the Waters Spherisorb ODS2 columns (e.g. peaks 6, 7 and 8 for ECN 48; peaks 9, 10 and 11 for ECN 50) than with the Genesis C18 column. Furthermore, better resolution for those peaks was achieved with the Waters Spherisorb ODS2 columns than with the Genesis C18 column, *Rs* = 2.25 vs. 2.0 for peaks 6 and 7, *Rs* = 2.7 vs. 2.5 for peaks 9 and 10 and *Rs* = 5.0 vs. 2.33 for peaks 12 and 13. Consequently, many additional peaks are observed in the chromatogram obtained with the longer column (e.g. three peaks observed between peaks 4 and 5 rather than a single peak on the Genesis C18, three peaks observed between peaks 11 and 12 and two peaks between peaks 13 and SSS, which were not observed in Genesis C18).

The advantages of the chromatogram in the present study over published method include better resolution of the TAGs with similar ECN (e.g. *Rs* = 2.7 vs. 2.0 and 1.7 for peaks 9 and 10 and *Rs* = 5.0 vs. 2.0 and 2.2 for peaks 12 and 13 for comparing with Dugo et al. (2006) and Fauconnot et al. (2004), respectively and the separation and resolution of TAGs having odd ECN. This suggests that beef fat contains TAGs having both even and odd ECN, an observation that not previously been made due to the lack of separation of

odd ECN TAGs in previous analysis. The peaks that co-eluted or are observed as shoulders on peaks 6, 7, 9 and 10 in the separation of Dugo et al. (2006) are resolved in present study. An increase in the retention of non polar components was observed and significant changes in the retention of peaks in the 90 - 126 min region also occurred: peaks were resolved from a broad peak of 7, 9 and 10 (Fig. 2.11b). Additional peaks are observed, one peak between 3 and 4, 6 and 7, 8 and 9, 9 and 10, 10 and 11, 12 and 13, two additional peaks between 7 and 8. Also, there are three additional peaks between peak 11 and 12. The TAG peaks having odd ECN values of 45, 47, 49, 51 and 53 were completely resolved. The complete peak identifications for Figs. 2.11b are in Section 2.2.3.5. Even though the separation is much better in the present study, the analysis time were longer.

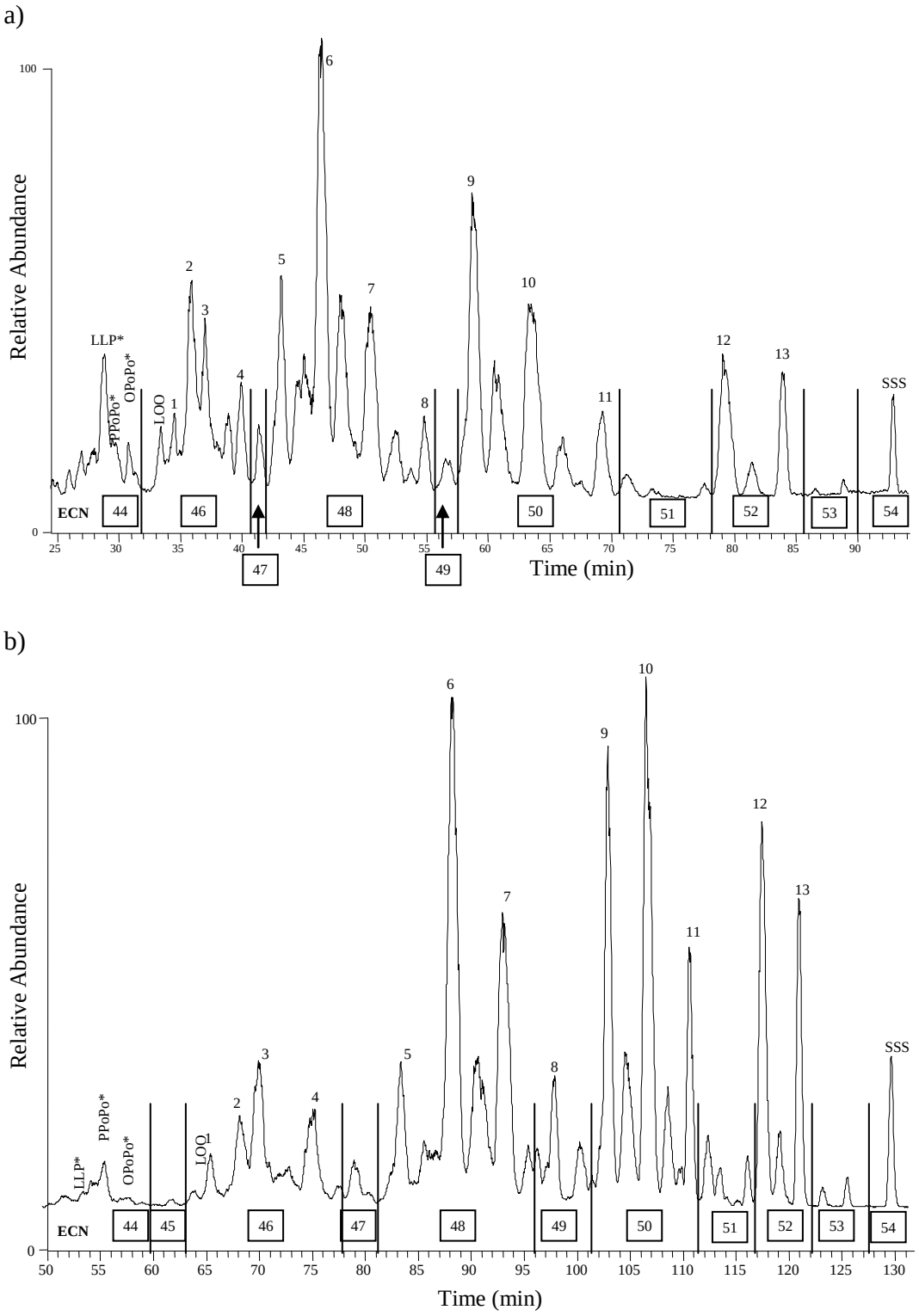

Figure 2.11: RP HPLC-APCI MS chromatogram of TAGs from beef fat on the Waters Spherisorb ODS2 column a) eluted with the mobile phase of Method G (Table 2.6a), b) eluted with the mobile phase of Method H (Table 2.6b).

The mobile phase system developed (Method H; Table 2.6b) was used for separating pork fat samples without any modification. The pork fat was extracted using the same method as employed for beef fat. Comparison of the chromatogram obtained (Fig. 2.12b) with that obtained by Dugo et al. (2006; Fig. 2.12a) reveals a number of important differences. In particular, separation of compounds coeluting with peaks 9, 15 and 18 has been achieved. The co-eluting peaks 12 and 13 are still not fully resolved but much better resolution is obtained here (Rs = 1.1) than previously (Rs = 0.8 in Dugo et al., 2006). Two peaks appeared at lower t_R than peak 11 which were not observed before. Three TAGs with odd ECN are also observed (47, 49 and 51) and the increased retention of the highly unsaturated TAGs having ECN 40 and 42 leads to them being nicely separated. The TAGs having ECN below 46 eluted closer to each other and some of them co-eluted. These TAGs are difficult to separate because they are highly unsaturated: some of them have more than five double bonds. The complete identification of peaks observed in Fig. 2.12b is given in Section 2.2.3.5.

a)

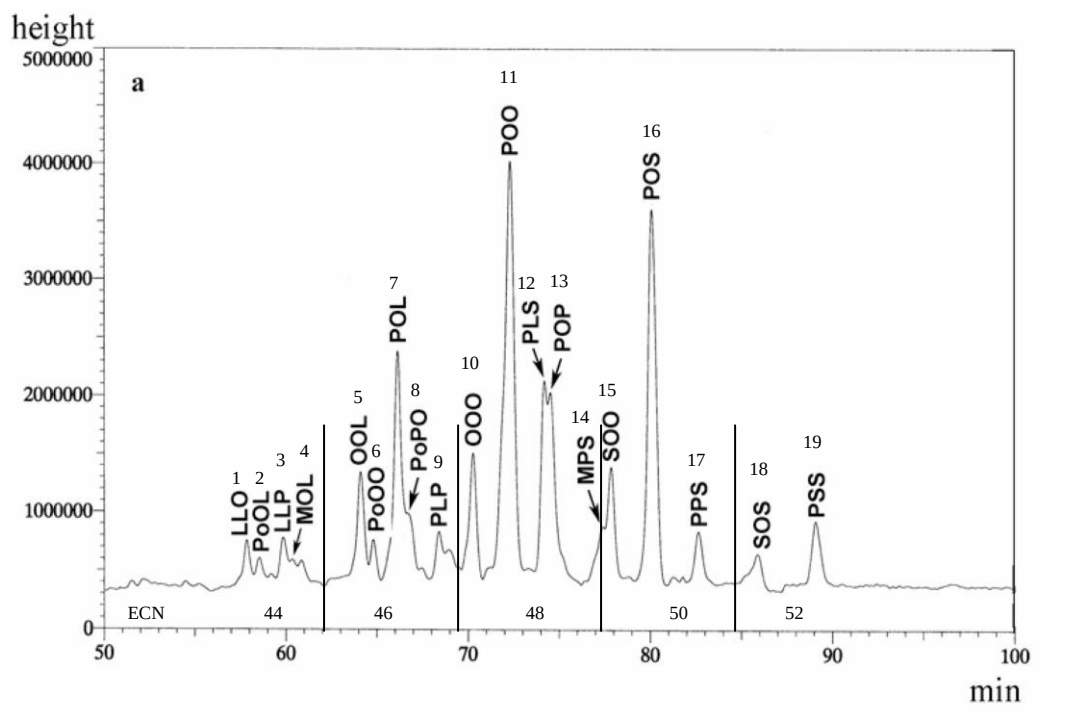

b)

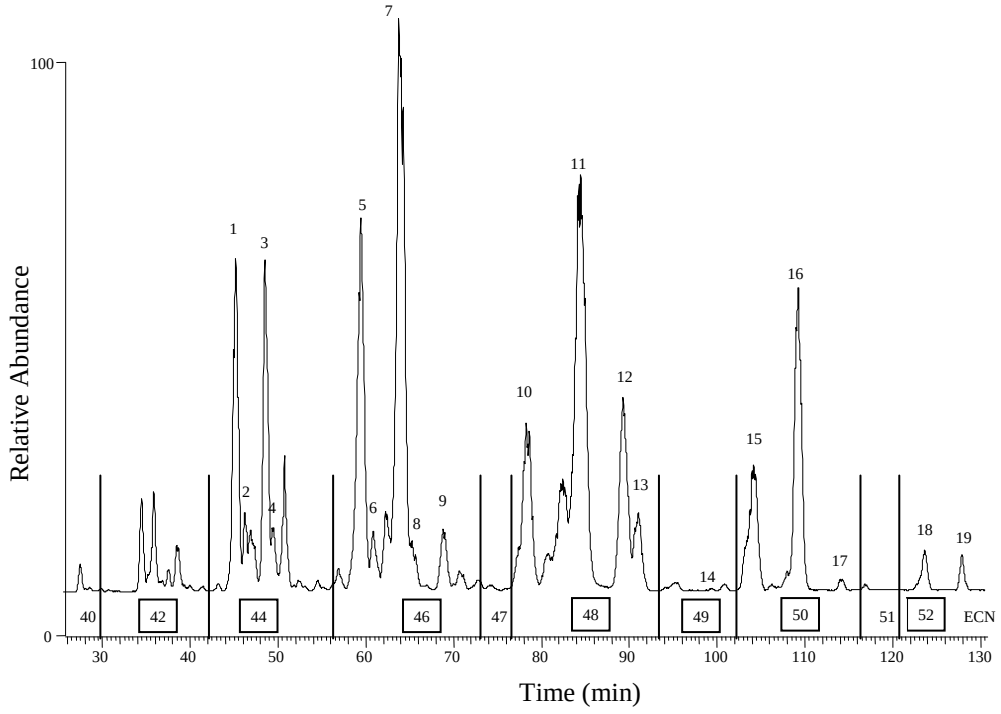

Figure 2.12: a) RP HPLC-APCI MS chromatogram of TAGs from pork fat (modified from Dugo et al., 2006). b) RP HPLC-APCI MS chromatogram of TAGs from pork fat on the Waters Spherisorb ODS2 column eluted with the mobile phase of Method H (Table 2.6b).

2.2.3.2 MS spectra of separated TAGs from RPHPLC-APCI MS.

The TAGs separated represent the compounds with ECN values between 44 and 54 for beef fat and between 40 and 52 for pork fat. A total of 28 major peaks were separated from beef fat and 33 peaks from pork fat. Only the most abundant peaks on the chromatograms of beef and pork fat are labelled with the *m/z* values for the ammoniated molecules (Figs. 2.13a and b). The TAGs exhibiting no co-elution give clean spectra, which is important in obtaining the correct DAG ion ratios for compound identification. The APCI-MS analyses of compounds separated by LC give mass spectra with abundant ammoniated and protonated molecules and DAG fragment ions depending on the TAG compound eluted. Peaks 1 to 3 can be seen to be separated completely from other components by considering the spectra over the peaks and referring particularly to the DAG the fragment ions of protonated and ammoniated TAGs (Figs. 2.14a to d). Thus, the spectra of individual ammoniated TAGs for the three most dominant peaks observed in pork fat (*m/z* 900, 874 and 876; Fig. 2.14a) show no appreciable interference from other TAG compounds. The spectrum over the peak at *m/z* 900 (Fig. 2.14a, Peak 1) has ions at *m/z* 900 and 883, representing the ammoniated and protonated molecules of the same TAG (Fig. 2.14b). Two DAG fragment ions occur at *m/z* 601.6 and 603.4. No other appreciable peaks are observed indicating the presence of one main component within the peak. Similarly, the spectrum over the peak at *m/z* 874 (Fig. 2.14a, Peak 2) show ions at *m/z* 874 and 857 corresponding to the ammoniated and protonated TAG and three DAG fragment ions at *m/z* 575.5, 577.5 and 601.5 with no other peaks detected (Fig. 2.14c). The spectrum over the peak at *m/z* 876 (Fig. 2.14a, Peak 3) has ions at *m/z* 859 and 876 (Fig. 2.14d) from the ammoniated and protonated TAG along with two abundant DAG ions at *m/z* 577.5 and 603.5. Hence, these three peaks are considered to be separated from other TAG compounds.

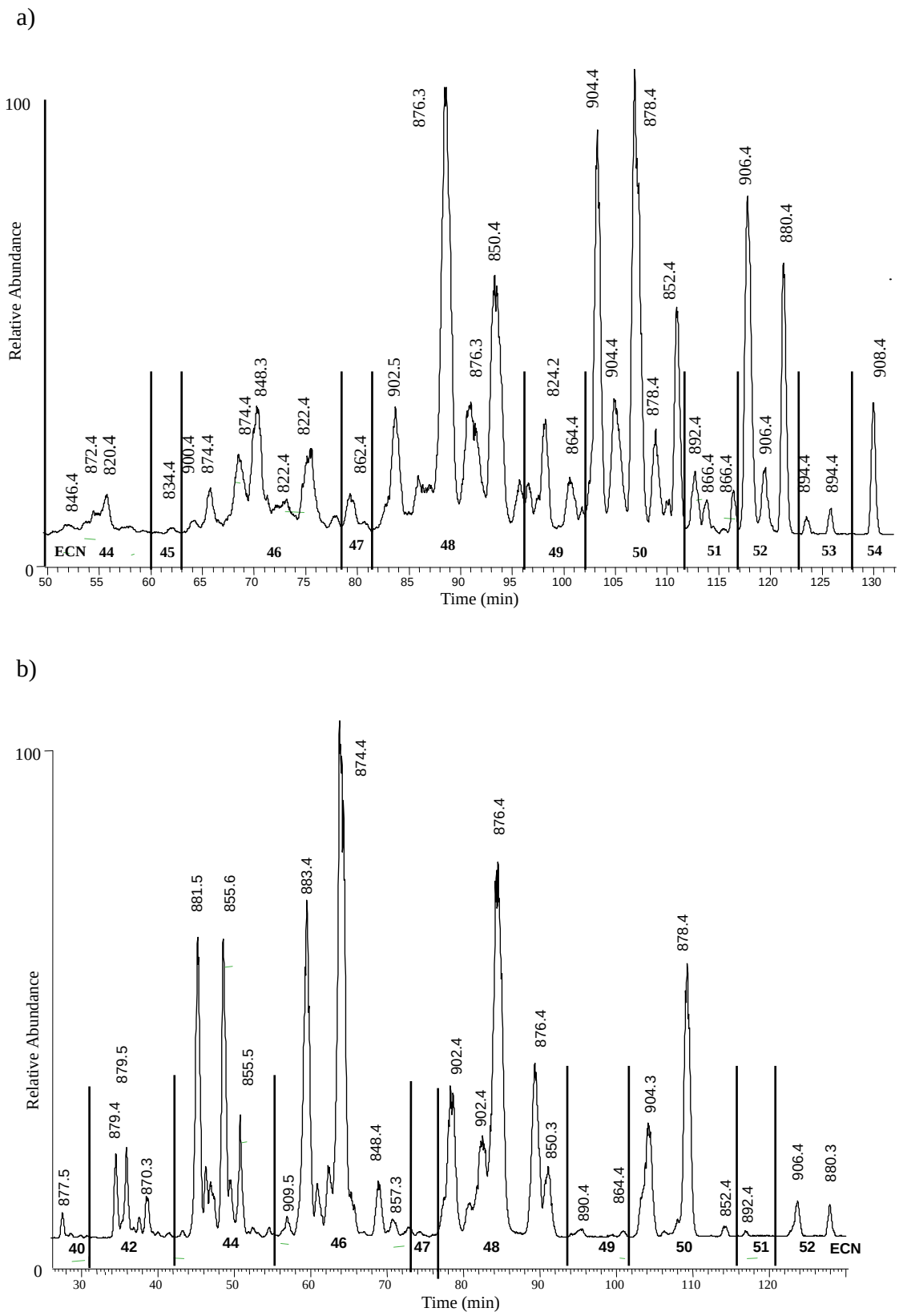

Figure 2.13: RP HPLC-APCI MS chromatograms of a) beef fat. b) pork fat.

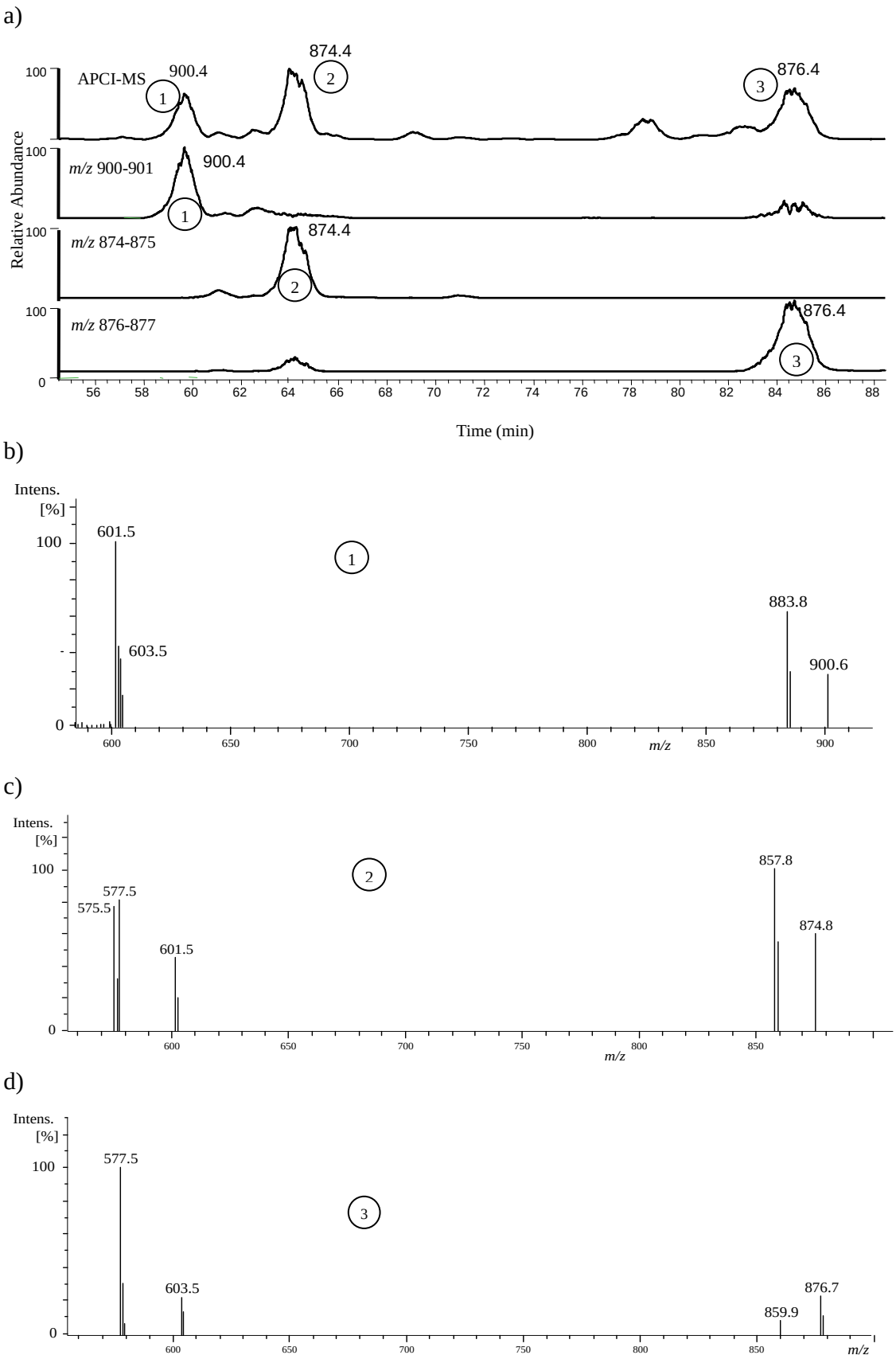

Figure 2.14: a) EIC of dominant peaks in pork fat, b) the spectrum across the peak with *m/z* 900.4, c) the spectrum across the peak with *m/z* 874.4 and d) the spectrum across the peak with *m/z* 876.4.

The region of the spectrum in which ions corresponding to the ammoniated and protonated TAGs appear (from *m/z* 803 to 908), revealed only ammoniated TAGs for peaks 1 to 6 (Fig. 2.15a; *m/z* 824, 852, 866, 880, 894 and 908). These ammoniated TAGs correspond to adduct ions of trisaturated TAG molecules. The base peak chromatogram and EICs for the trisaturated TAGs of beef fat (Figs 2.15a) are labelled: 1 (*m/z* 824), 2 (*m/z* 852), 3 (*m/z* 866), 4 (*m/z* 880), 5 (*m/z* 894) and 6 (*m/z* 908). The spectra over the peaks for the trisaturated TAGs at *m/z* 824, 852 and 880 show DAG fragment ions as the most abundant ions (Figs. 2.15b to d). The spectrum over the peak at *m/z* 824 gave dominant DAG fragment ions at *m/z* 551.5, 523.4 and 579.5 (Fig 2.15b). Similarly, there are two dominant DAG fragment ions in the spectra of each of the trisaturated TAGs at *m/z* 852 and 880 (Figs. 2.15c and d). Thus, the spectra indicate contributions from only one main component in each of the chromatographic peaks.

Absence of ammonium acetate in the mobile phase strongly affected the signal intensity of the TAG ions in MS, and also DAG ions in MS^2. Protonated TAGs are absent in the CID spectra of TAGs containing 3 saturated FAs, suggesting that the presence of double bonds fosters the formation of $[M + H]^+$. This can be attributed to the polarity of the TAGs. Abundances of the protonated TAGs are strongly dependent on the polarity of the TAGs: the abundances of the protonated TAG increases with increasing polarity (Jakab et al., 2002). The TAGs with fewer than three sites of unsaturation show one of the DAG ions as the base peak and TAGs that have more than four sites of unsaturation have the protonated TAGs as the base peak (Byrdwell, 2005). The percentage of ammonium acetate in the mobile phase can, nevertheless, be reduced to as low as 4% (from the total mobile phase percentage) without affecting the signal intensity. Reducing the percentage of 10mM ammonium acetate in mobile phase to less than 4% affects the ionization of saturated TAGs, especially for the very highly saturated species. On the other hand, increasing the amount of ammonium acetate did not have any effect on the signal intensity. Thus, the optimum percentage of ammonium acetate to facilitate TAG ionization by APCI, especially for trisaturated TAGs, with a combination of acetonitrile and dichloromethane as mobile phase is 4% (from the total mobile phase percentage). Other than trisaturated TAGs, the spectra of TAGs show both ammoniated and protonated molecules.

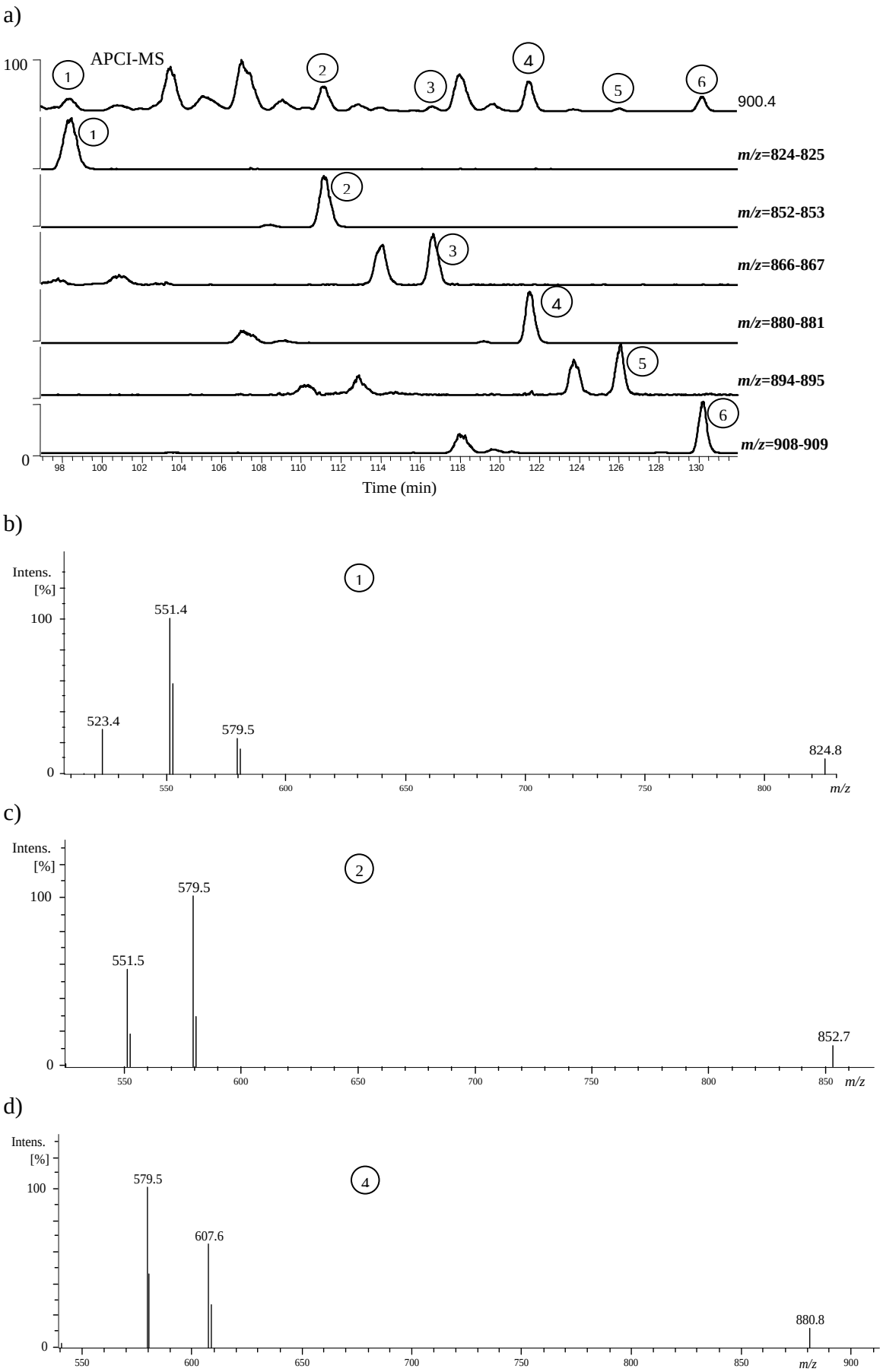

Figure 2.15: a) EIC of trisaturated TAGs in beef fat, and APCI-MS spectra for b) peak 1; *m/z* 824 to 825, c) peak 2; *m/z* 852 to 853, d) peak 4; *m/z* 880 to 881.

2.2.3.3 CID of ammoniated TAG ions in MS^2 of beef and pork fat.

The MS^2 spectrum of the direct infusion sample (Section 2.2.2) did not provide diagnostic information on the TAG assignments of compounds with the same molecular mass as these were not separated and hence were fragmented at the same time, producing common DAG product ions. For this reason on-line spectra were obtained using the RP HPLC method developed to separate the TAGs of beef and pork fat.

In APCI, TAGs were identified from the ammoniated molecules and their DAG ions in MS^2. The FA positions were identified from the presence and relative intensities of the DAG product ions in MS^2. The relative intensities of DAG product ions in the MS^2 spectra of the ammoniated TAG ions depend on FA position along the glycerol backbone (Byrdwell, 2005). No distinction can be made between *sn*-1 and *sn*-3 positions (compare well with Section 2.2.1.2).

The RP HPLC-APCI mass spectra of beef and pork fat allow three different categories of TAGs to distinguished:

AAA TAGs

Homogenous TAGs containing three identical FAs are defined as AAA. These TAGs were identified based on the protonated molecule, $[M + H]^+$ in MS^2 after loss of NH_3 (17 Da) from the ammoniated TAG and produced a single DAG ion. Peaks 1 and 2 represent AAA type TAGs (Fig. 2.16a). For example, the compound giving rise to $[M + NH_4]^+$ at *m/z* 902 (peak 1 in Fig 2.16a) was present in beef and pork fat and produced $[M + H]^+$ in MS^2 at *m/z* 885 and a single DAG ion at *m/z* 603 (Fig 2.16b). The possible TAG compounds having $[M + H]^+$ = *m/z* 885, are OOO, SLO* and GLP. Given that the TAG only produces a single DAG ion, the identity must be OOO. Similarly, the compound at $[M + NH_4]^+$ = *m/z* 908 (peak 2 in Fig 2.16a), produced a single DAG ion at *m/z* 607, corresponding to either $[SS]^+$ or $[PA]^+$. The only TAG isobar that fits this dissociation is SSS because no other peak is observed in the spectrum (Fig 2.16c). For the $[PA]^+$ ion to be formed, there would be at least two ions present in the MS^2 spectrum as a consequence of the presence of the two FAs, P and A. The assignment as SSS is confirmed by the absence of the protonated TAG molecule in the MS and MS^2 spectra for peak 2, indicates it to represent a trisaturated TAG. Another homogenous TAGs detected in pork fat is LLL. The EIC of beef fat over the ranges *m/z* 603-604 and *m/z* 607 to 608 from MS^2 (Fig. 2.16a) show that several peaks produce the same DAG ions at

different retention times. These ions arise from other TAGs that contain the same constituent FAs.

a)

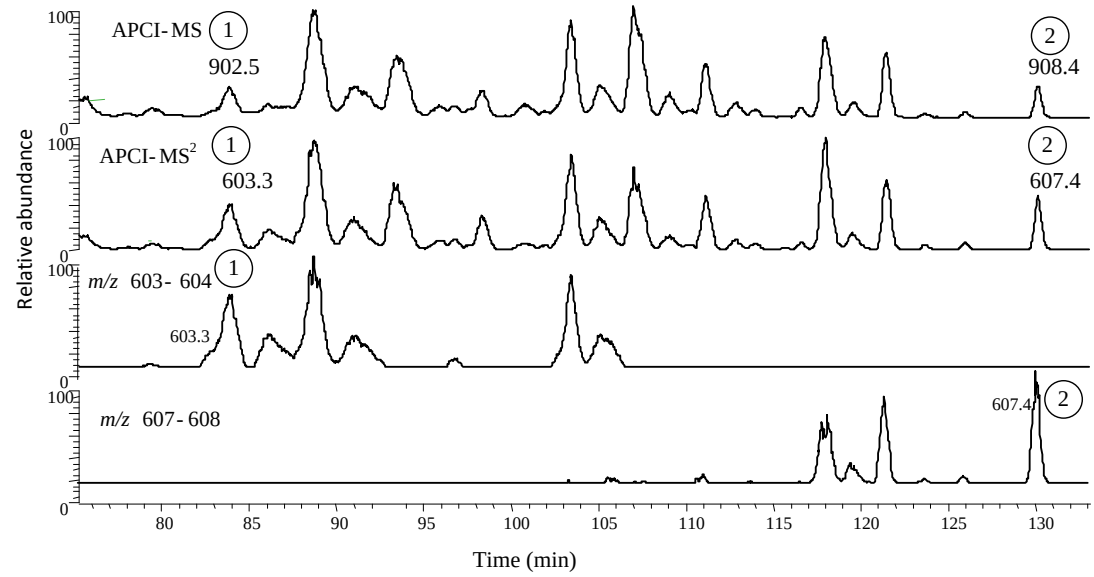

b)

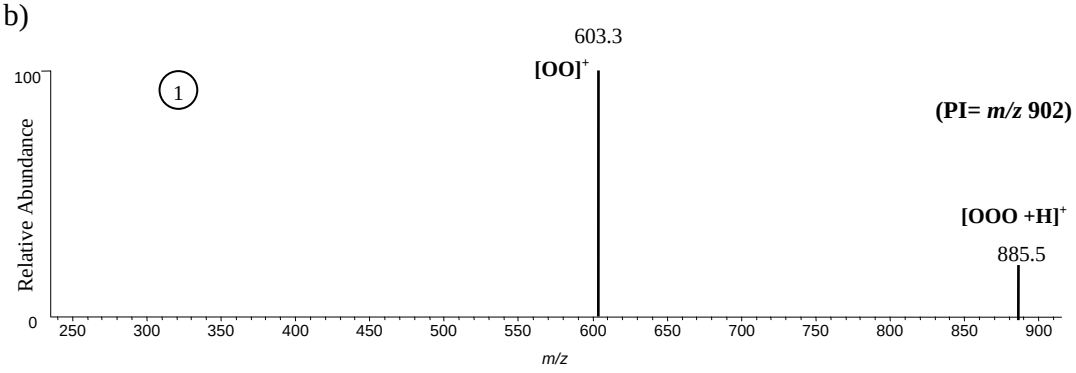

c)

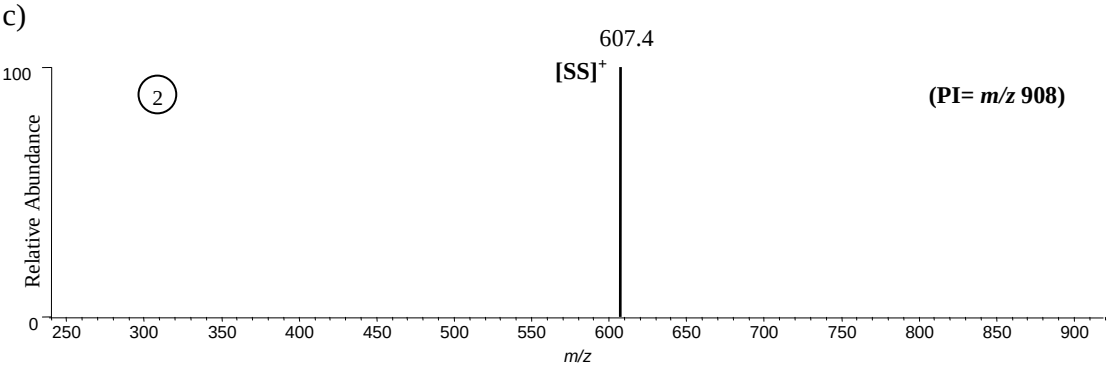

Figure 2.16: a) EIC from MS, MS^2 and mass range chromatograms of beef fat, AAA type TAGs are labelled b) MS^2 spectrum from ammoniated TAG at *m/z* 902 and c) MS^2 spectrum from ammoniated TAG at *m/z* 908 (PI=precursor ion).

ABA and AAB TAGs

Symmetric and asymmetric TAGs containing two different FAs are designated ABA and AAB. These types produce at least 2 different DAG product ions in the MS^2 spectrum. The MS and MS^2 chromatogram for pork fat reveals four ABA TAG types (Fig. 2.17a; Peaks 1 to 4). The identification of the TAG giving the peak at *m/z* 876 (2 in Fig 2.17a) was based on the protonated molecule, $[M + H]^+$ at *m/z* 859 in MS^2, formed by loss of NH_3 (17 Da) from the ammoniated TAG. Three TAGs have the same mass: OPO, PLS and GOM. Besides the protonated molecule at *m/z* 859, the dissociation of ammoniated TAG at *m/z* 876 produced DAG ions at *m/z* 577 and *m/z* 603 in MS^2 (Fig 2.17c). These ions result from the loss of NH_3 and the carboxylic acid RCOOH of the oleic and palmitic moieties, respectively; $[M + NH_4 – NH_3 - RCOOH]^+$. Although DAG ions for OP, SPo and GM have the same *m/z* (577), as do those for OO, SL and GPo (*m/z* 603), the only TAGs that fit the dissociation are OPO and OOP*, these being the only two of the possibilities that give two DAG product ions. The ratio of $[OP]^+$:$[OO]^+$ will be higher for the OPO isomer since formation of the 1,2 –isomer of the $[OP]^+$ ion from OPO requires less energy than generating the 1,3-isomer from OOP*. Thus, OPO can be identified as the TAG in the pork fat due to the DAG ion ratios for $[OP]^+$:$[OO]^+$ being about 4:1 (Fig 2.17c).

The dissociation of ammoniated SPS* at *m/z* 880 was similar to ammoniated OPO, producing two DAG ions at *m/z* 579, $[PS]^+$ and 607, $[SS]^+$ due to loss of the stearic and palmitic acid moieties, respectively. The protonated molecule was not observed in the MS^2 spectrum. Dissociation of *m/z* 880 from the pork fat sample produced a ratio for $[PS]^+$ to $[SS]^+$ of about 4:1 (Fig 2.17e), confirming SPS* as the TAG isomer in pork fat. Other mixed symmetric TAGs containing only two different FAs are OLnO*, OLO*, OPO, OMaO* in pork fat and POP, OSO and SOS in beef fat.

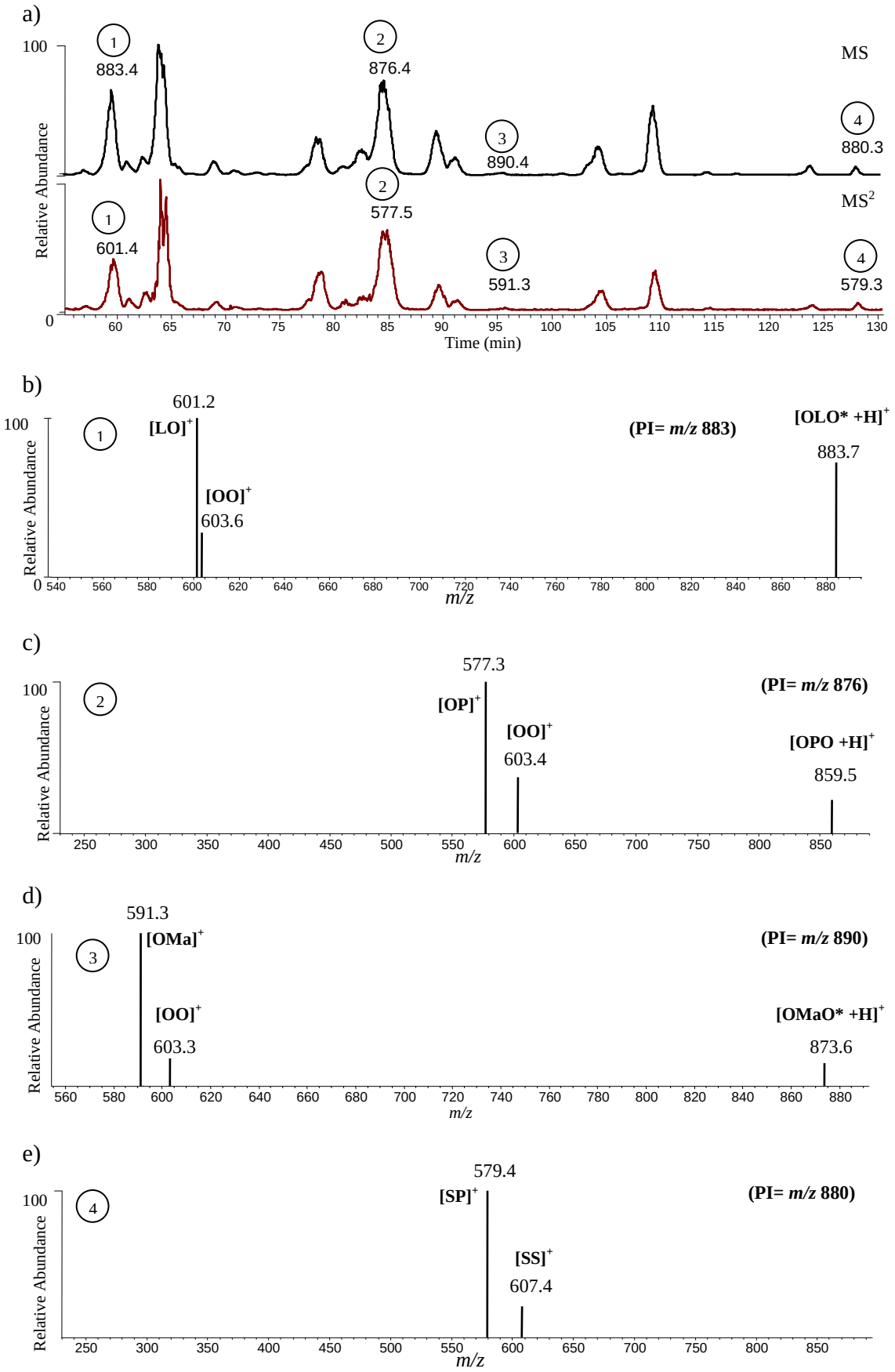

Figure 2.17: a) EIC from MS and MS^2 of pork fat labelled with ABA type TAGs and MS^2 spectra from ammoniated TAGs at b) *m/z* 883, c) *m/z* 876, d) *m/z* 890 and e) *m/z* 880 (PI=precursor ion).

The MS and MS^2 chromatograms for beef fat reveal AAB type TAGs (Peaks 1 to 5, Fig. 2.18a). The spectrum of OOP* shows a ratio for $[OP]^+$:$[OO]^+$ of about 1.6:1, confirming that it is OOP* (Fig. 2.18b). The DAG ion ratio for $[OS]^+$:$[SS]^+$ for peak 4 is about 1.2:1, indicating that the compound is SSO* (Fig. 2.18e).

One TAG in beef fat (peak 3) exhibits an ammoniated molecule at *m/z* 852 and DAG ions at *m/z* 579 ($[SP]^+$) and *m/z* 551 ($[PP]^+$) in the ratio 1.2:1 (Fig 2.18d). The TAG PPS* fits this dissociation pattern. Pork fat gave the same ratio for $[SP]^+$:$[PP]^+$ indicating the FA positions within the compounds in beef and pork fat are the same. Other asymmetric TAGs identified were LnLnO*, LLLn*, LLO*, LLS*, and PPO* in pork fat and OPoPo*, LLP*, PPoPo*, OOPo*, PPL*, OOP* and SSO* in beef fat (Table 2.7).

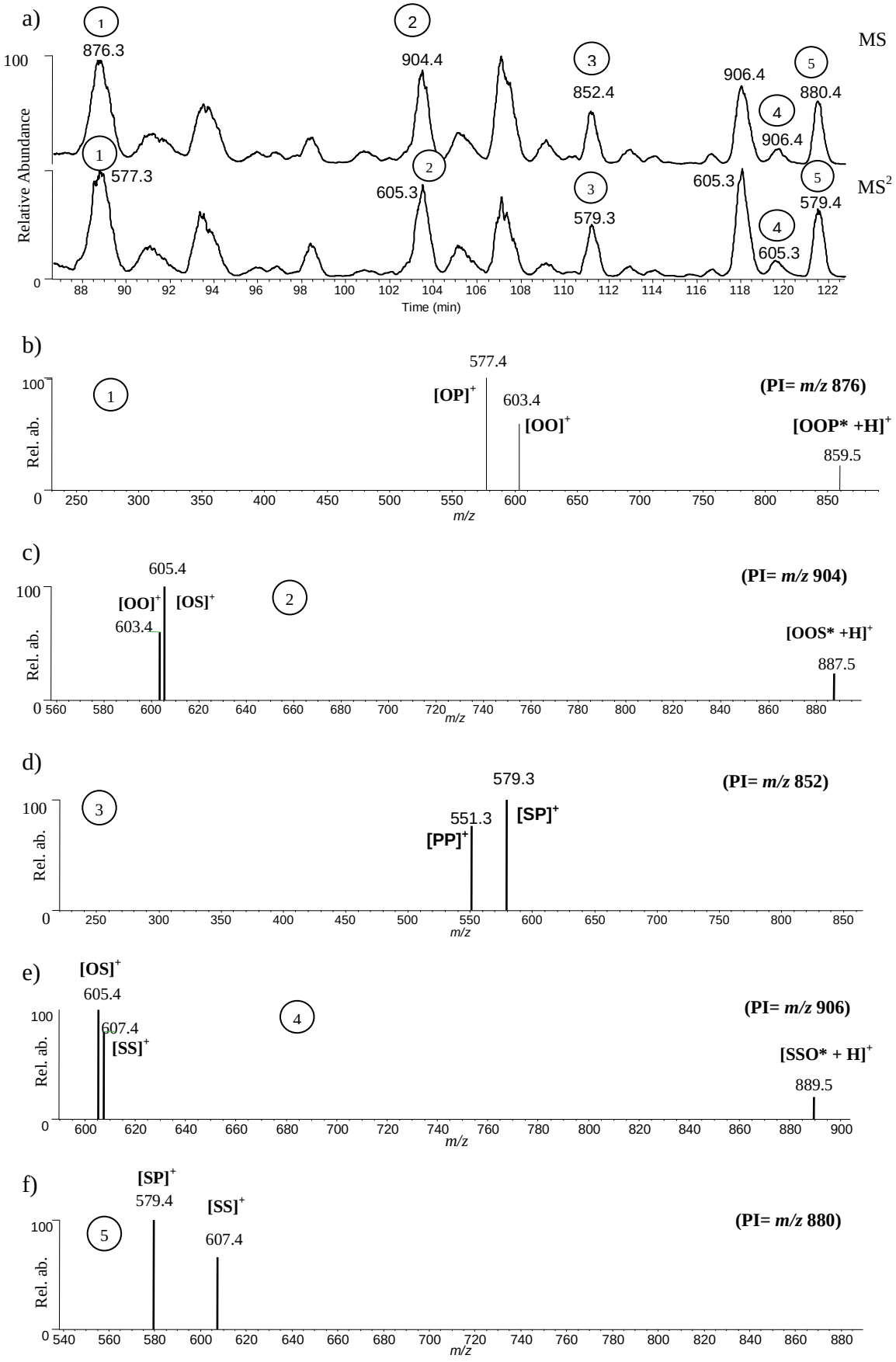

Figure 2.18: a) EIC from MS and MS^2 of beef fat labelled with AAB type TAGs and MS^2 spectra from ammoniated TAGs at b) *m/z* 876.3, c) *m/z* 904.4, d) *m/z* 852.4, e) *m/z* 906.4 and f) *m/z* 880.4 (PI=precursor ion; Rel. ab. = relative abundance).

ABC TAGs

ABC type TAGs contain 3 different FAs. The analysis of ABC-type TAGs is based on the presence in MS^2 of at least three different DAG product ions. The relative intensities of these ions are important in providing information on the positions of the fatty acids within the compound. The least abundant DAG ion in MS^2 corresponds to the loss of the FA from the *sn-2* position, since formation of this ion is energetically less favourable than that arising from loss of a fatty acid from the *sn*-1 or *sn*-3 position.

The peaks in the MS and MS^2 chromatograms for pork fat show ABC type TAGs (Peaks 1 to 3, Fig 2.19a). For example, the MS^2 spectrum from the most dominant ammoniated TAG ion at *m/z* 874 (peak 1 in Fig 2.19a) in pork fat produced the protonated TAG ion at *m/z* 857 after loss of NH_3 (17 Da) and ions at *m/z* 575, 577 and 601 corresponding to losses of oleic acid to give $[PL]^+$, linoleic acid to give $[PO]^+$ and palmitic acid to give $[LO]^+$ (Fig 2.19b). The spectrum shows that the least abundant DAG ion is formed by the loss of palmitic acid from the *sn*-2 position, generating the product ion $[LO]^+$ confirming the compound as LPO*. The unsaturated FA is usually in the *sn*-2 position, especially for linoleoyl, as reported by Holcapek et al. (2003). The relative intensities of the DAG ions might also be influenced by resonance structures of product ions which involve formation of a stable six membered ring transition state for $[PO]^+$and $[PL]^+$ ions following loss of linoleic (*sn*-1(3)) and oleic acids (*sn*-1(3); Fig. 2.20). Such a stable transition state would increasing the relative abundances of these ions with respect to $[LO]^+$. The latter would form by loss of palmitic acid from the *sn*-2 position via production of a less stable five-membered ring (Holcapek et al., 2003).

Another example of an ABC type TAG from the same sample is the component exhibiting the ammoniated molecule at *m/z* 878 (peak 2 in Fig. 2.19a). The MS^2 spectrum contains the protonated TAG at *m/z* 861, arising from loss of NH_3 (17 Da), and product ions at *m/z* 577, 579 and 605 corresponding to losses of stearic acid to give $[PO]^+$, oleic acid to give $[PS]^+$, and palmitic acid to give $[SO]^+$. The least abundant DAG ion is formed by the loss of palmitic acid from the *sn*-2 position, leaving $[SO]^+$ at *m/z* 605 (Fig 2.19c). The dissociations show that the compound is SPO*.

The TAG with ammoniated molecules at *m/z* 892 (peak 3 in Fig 2.19a), produced the protonated molecule at *m/z* 875 after a loss of NH_3 (17 Da) and DAG ions at *m/z* 591, 593 and 605 in the MS^2 spectrum, corresponding to losses of stearic acid to give $[MaO]^+$,

oleic acid to give $[SMa]^+$, and margaric acid to give $[SO]^+$. There were differences in the DAG ion intensities between the different fat samples. Specifically, in the MS^2 spectrum of pork fat the least abundant DAG ion was formed by the loss of margaric acid from the *sn*-2 position, leaving $[SO]^+$ at *m/z* 605 (Fig 2.19d). Thus, the TAG in pork fat is SMaO*. Other TAGs identified as containing three different FAs are OLnL*, PLLn*, LMO*, LPO*, PLnO, OPoM, OLnG*, MoMO*, PPoMo*, SPLn*, OPPo*, PMO*, LMaO*, OPMo*, SLO*, LPS*, SMP*, OPMa*, and SPO* (Table 2.7).

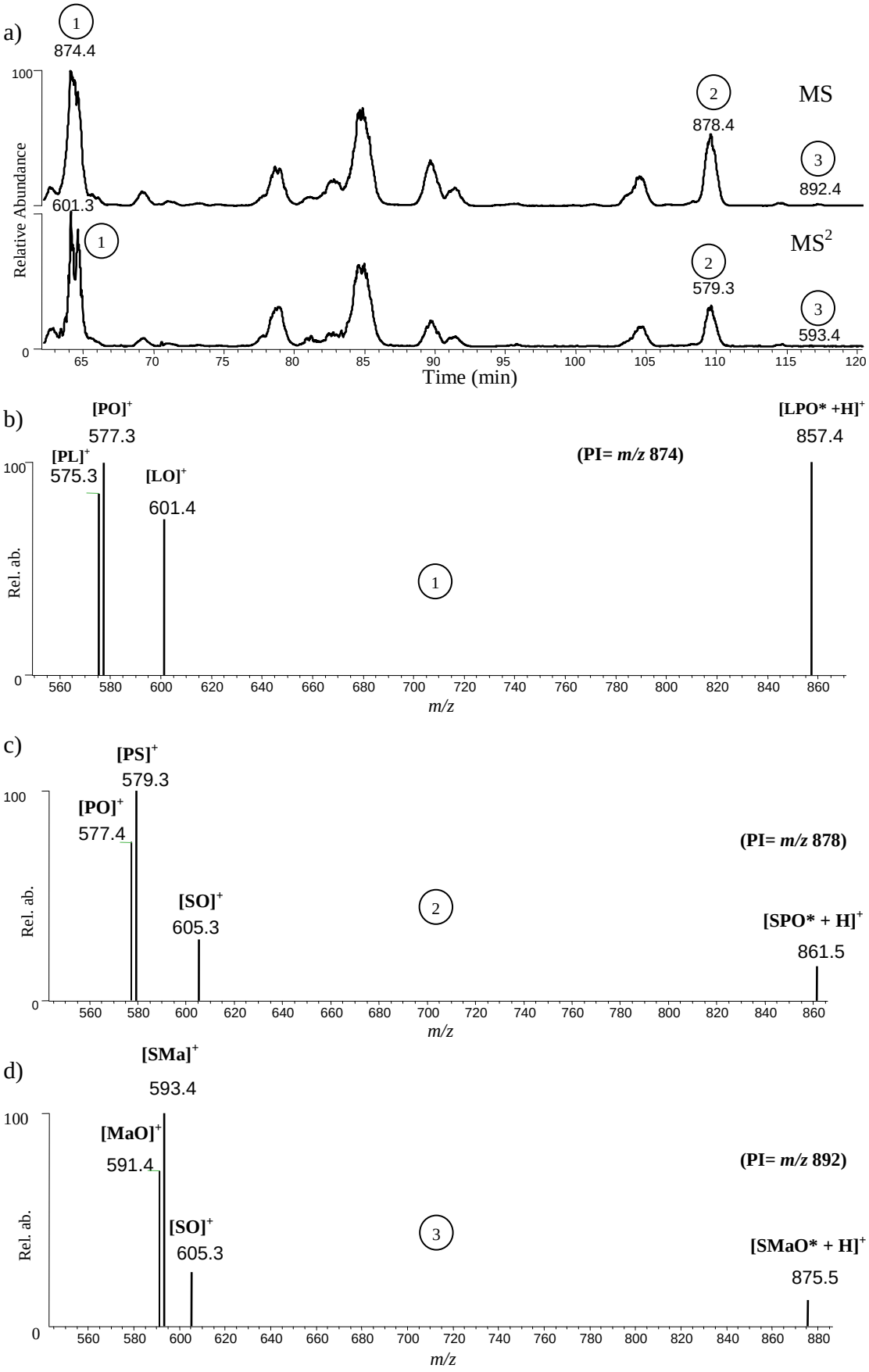

Figure 2.19: a) EIC from MS and MS^2 of pork fat labelled with ABC type TAGs and MS^2 spectra from ammoniated TAGs at b) *m/z* 874.4, c) *m/z* 878.4 and d) *m/z* 892.4 (PI=precursor ion; Rel. ab. = relative abundance).

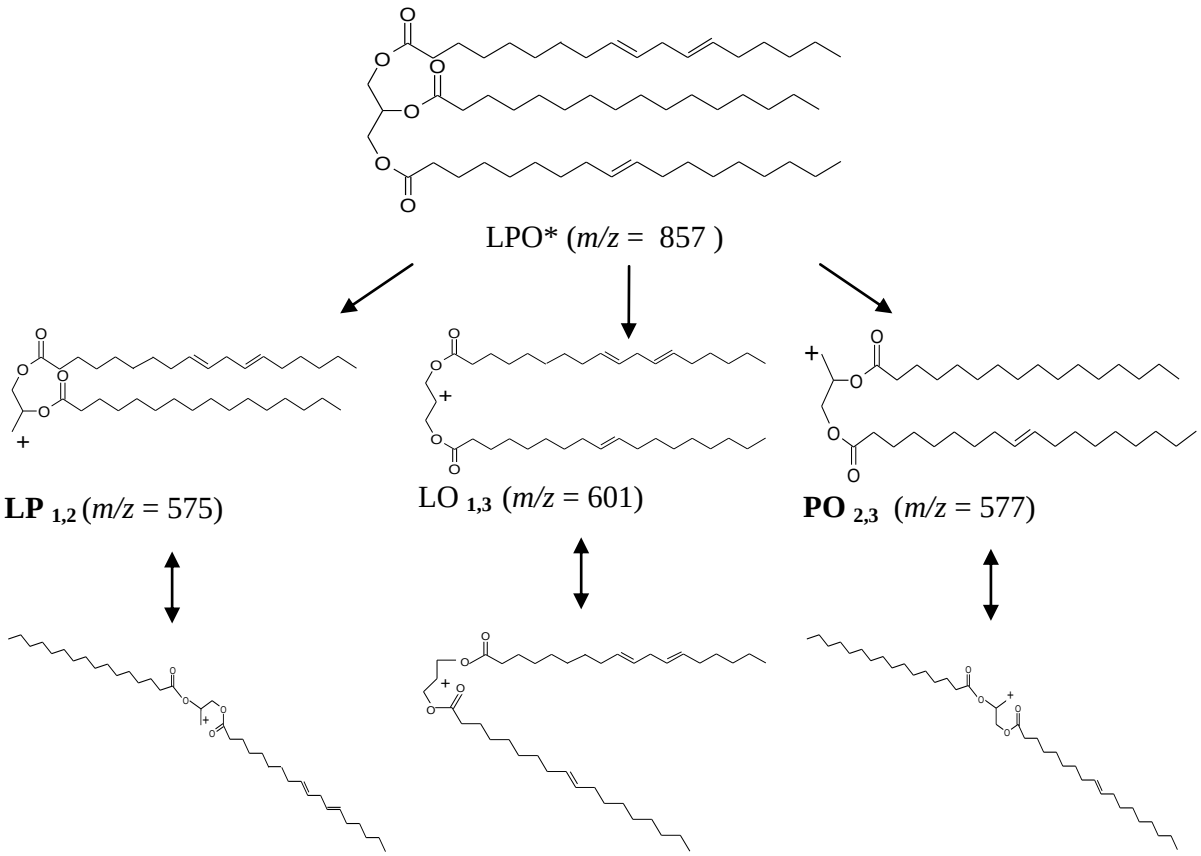

Figure 2.20: Structures of LPO* and DAG product ions including possible resonance structures (modification from Holcapek et al., 2003).

Table 2.7: TAG identifications from ammoniated molecules, $[M+NH_4]^+$, protonated molecules, $[M + H]^+$, and DAG product ions, $[M\text{-}RCO_2]^+$ of beef and pork fats analysed by RP HPLC-APCI MS/MS using the method developed in Section 2.2.3.1 (Method H).

$[M + NH_4]^+$	$[M + H]^+$	DAG ions in MS^2		TAGs		ECN
		m/z	$[M\text{-}RCO_2]^+$	Pork fat	Beef fat	
894	877	595 597 599	LnLn LLn LL, LnO	LLLn* + LnLnO*		40
896	879	597 599 601	LLn LL,OLn OL	LLL OLnL*		42
844	827	547 599	LM LL	LLM*	LLM*	
870	853	573 575 597	PLn PL LLn	PLLn*		
898	881	599 601 603	LL, LnO LO OO	LLO* OLnO*		44
846	829	547 549 575 601	LM, PoPo OM OPo OL	LMO*	OPoPo*	
872	855	573 575 577 599 601	LPo, LnP LP, OPo OP LL, LnO OL	LPoO* LLP* LnOP*	LLP*	
820	803	521 547 549 575	PoM PoPo OM, PPo OPo		PPoPo*	
834	817	535 549 561 589 563	MoM PPo PoMo MoO PMo		MoMO* PPoMo*	45
926	909	599 627 631	Oln LnG OG	OLnG*		46
900	883	599 601 603	LL LO OO, LS	OLO* LLS*	OOL*	
874	857	573 575 577 579 601 603	PLn LP, OPo OP PS OL,SLn OO	OOPo* LPO* SPLn*	OOPo* LPO*	
848	831	549 551 575 577	PPo, OM PP LP, OPo OP	OPPo* (tail to 874) PPL*	OPPo*	
822	805	523 549 577	PM MO OP		POM* PMO*	

Table 2.7: (continued)

$[M + NH_4]^+$	$[M + H]^+$	DAG ions in MS^2		TAGs		ECN
		m/z	$[M\text{-}RCO_2]^+$	Pork fat	Beef fat	
888	871	589 591 601	MaL MaO OL	LMaO*		47
862	845	563 577 589	PMo OP MoO	OPMo*	OPMo*	
902	885	601 603 605	OL LS,OO OS	OOO SLO*	OOO SLO*	48
876	859	575 577 579 603	LP OP SP OO, LS	OPO LPS*	OOP* OPO	
850	833	551 577	PP OP	PPO*	POP PPO*	
824	807	551 579 523	SM SP PM		SMP*	
890	873	591 603	OMa OO	OMaO*	OMaO*	49
864	847	565 577 591	PMa OP OMa	OPMa*	OPMa*	
838	821	551 565	PP PMa		PMaP*	
904	887	603 605	OO OS	OOS*	OOS* OSO	50
878	861	577 579 605	PO SP SO	SPO*	SOP* SPO*	
852	835	551 579	PP SP	PPS*	PPS*	
892	875	605 591 593	SO MaO SMa	SMaO*	SMaO*	51
866	849	565 579 593	PMa SP SMa		SMaP* SPMa*	
906	889	605 607	OS SS	SSO*	SOS SSO*	52
880	863	579 607	SP SS	SPS*	SPS*	
894	877	593 607	MaS SS		SSMa* SMaS	53
908	891	607	SS		SSS	54

2.2.3.4 CID of DAG product ions in MS^3

Examination of MS^3 spectra is a valuable tool to help identify the type of TAG. The key MS^3 product ions were the acylium ions (RCO^+). These ions reveal the identities of individual FA chains (Byrdwell and Neff, 2002), each FAs giving a characteristic product ion (Table 2.8). For this approach, MS^2 DAG product ions of a selected *m/z* were isolated in the ion trap and subjected to another CID event. For example, for LPO*, the most intense ion in the MS^2 spectrum from *m/z* 874 corresponds to the DAG product ion $[PL]^+$ (*m/z* 575). The DAG ion at *m/z* 575 was isolated for MS^3. The major ions in the MS^3 spectrum are due to linoleic (*m/z* 263) and palmitic (*m/z* 239) acids, indicating that the remaining acyl side-chain must be oleic acid (*m/z* 265). Closer inspection of the MS^3 spectrum from *m/z* 575 revealed ions at *m/z* 245 and *m/z* 221, which correspond to $[RCO\text{-}H_2O]^+$ ions from linoleic and palmitic acid formed after liberation of the acid. This confirms that linoleic and palmitic acid occur in the product ion *m/z* 575 which arises from the ammoniated molecule, *m/z* 874. In addition, the loss of FAs from *m/z* 577 $[PO]^+$ and *m/z* 601 $[LO]^+$ in the MS^3 spectra are consistent with losses of linoleic and palmitic acids attached to the glycerol backbone. Thus, the MS^3 data uniquely identify the LPO* TAG.

Table 2.8: RCO^+ ions observed in the mass spectra of beef and pork fat.

Fatty acids	CN: degree of unsaturation	$[RCO]^+$ *m/z*
Palmitic	16:0	239
Palmitoleic	16:1	237
Margaric	17:0	253
Heptadecenoic	17:1	251
Stearic	18:0	267
Oleic	18:1	265
Linoleic	18:2	263
Linolenic	18:3	261

2.2.3.5 TAG profiles of beef and pork fat.

The following section focuses on the investigation of TAGs for which only one distinct regioisomer is apparent from the MS/MS data. These TAGs relate to structures in which the *sn*-1 and *sn*-3 acyl groups could be interchanged. The mobile phase system developed in Section 2.2.3.1 (Method H) not only improved the resolution for TAGs with the same ECN, especially for TAGs with lower ECN, but also improved separation for TAGs with odd ECN, such as those Ma or Mo containing one moiety. Comparison of the TAGs separated and identified with those previously reported from animal fats reveals complete coverage in this study along with identification of several additional components (e.g. OPMo*, OMaO*, PMaP* and SMaO* in beef fat).

The MS and MS^2 characteristics ammoniated and protonated molecules and DAG ions of the TAGs present in the beef and pork fat are summarised in Table 2.7. The peaks identified are in order of retention time from lowest to highest. The TAGs identified in beef and pork fats are labelled in the chromatograms (Figs. 2.21a and b).

The TAG molecules that possess three saturated FAs will only produce ammoniated molecules in the APCI MS spectra: no protonated molecule is observed. The compounds identified were SMP* (*m/z* 824), PPS* (*m/z* 852), SMaP* (*m/z* 866), SPS* *(m/z* 880), SSMa* (*m/z* 894) and SSS (*m/z* 908). The rest of the TAGs gave both ammoniated and protonated molecules but with different abundances depending on the unsaturation of FAs in TAGs.

TAGs having identical masses, the same ECN value, and the same double bond numbers but different distributions, comprise critical pairs. An example of a critical pair is OPO and LPS*, both of which have an ECN of 48 and molecular mass 858. These TAGs could not be differentiated based on the ammoniated molecule peaks. Thus, the DAG product ions are crucial to differentiating these molecules. If these two TAGs were not separated, the relative intensities of the DAG ions that have the same *m/z* ($[OO]^+$ from OPO and $[LS]^+$ from LPS* are not reliable for distinguishing FA positions. Another example is OOO and SLO* where both have identical mass (884), ECN (48) and number of double bonds (3). Both TAGs give a product ion at *m/z* 603 ($[OO]^+$ and $[LS]^+$ from OOO and SLO*, respectively). There were more critical pairs in pork than in beef fat, which makes the chromatographic separation of this fat challenging.

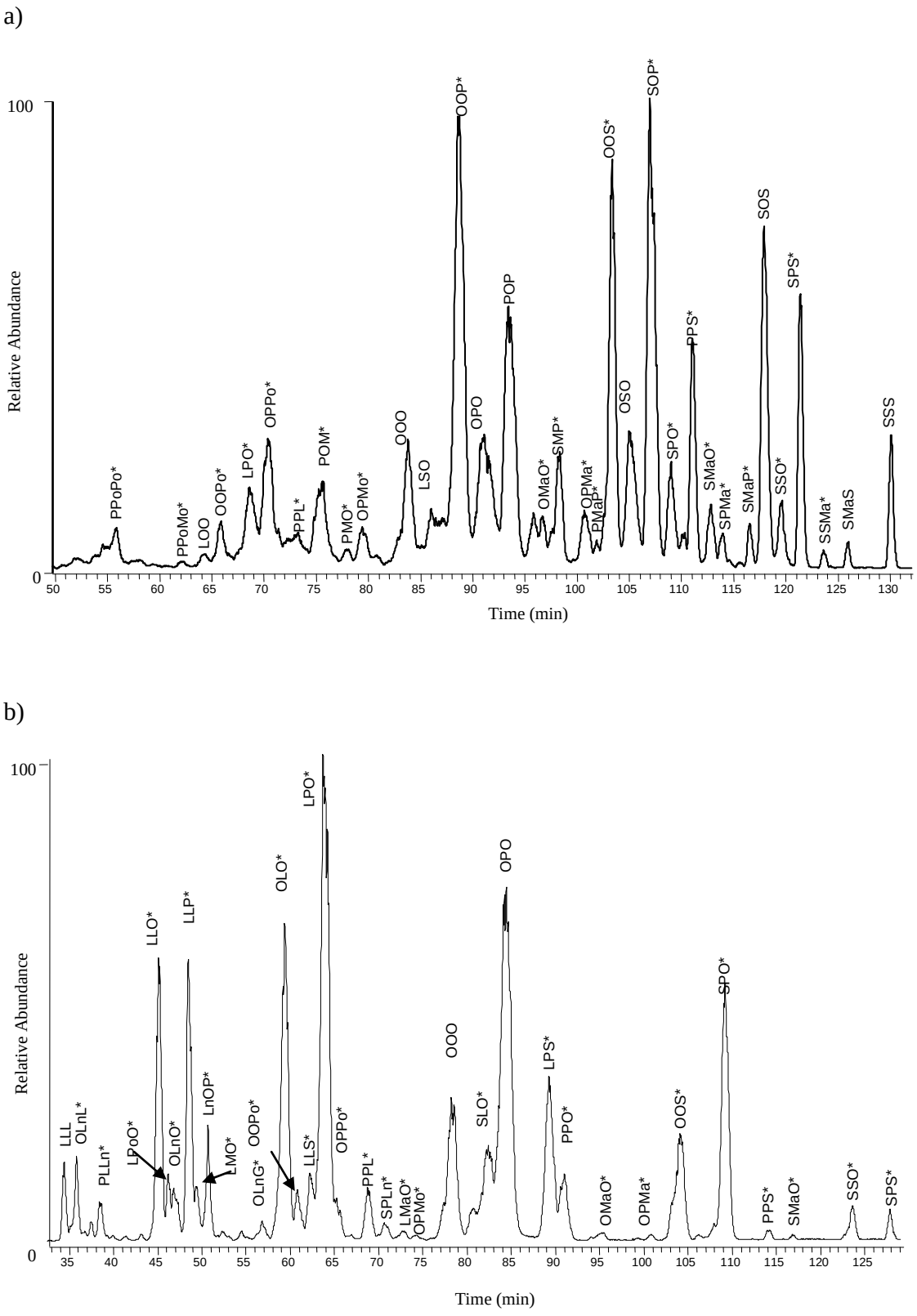

Figure 2.21: RP HPLC-APCI MS chromatograms of a) beef fat and b) pork fat labelled with identified TAG peaks on the Waters Spherisorb ODS2 column eluted with the mobile phase of Method H (Section 2.2.3.1; Table 2.6b).

Several TAGs with equal ECNs and having identical masses or critical pairs are clearly separated, whereas only partial resolution was achieved in previous work for animal fats. Exceptions were for highly unsaturated TAGs and those with the lowest ECN value of 40, which were only detected in pork fat and correspond to LLLn* and LnLnO*. This critical pair was not separated and was detected as a single or co-eluting peak. Both TAGs have identical mass and are highly unsaturated, each having seven double bonds. Critical pairs become more difficult to resolve when the DB value exceeds three (e.g. LLS* from LPO* and LMO* from LLP* in pork fat). Highly unsaturated TAGs make the separation difficult even with the very slow gradient employed. The co-eluting TAGs give DAG ions at *m/z* 595 $[LnLn]^+$ from LnLnO* and *m/z* 597 $[LLn]^+$ from LLLn* (Fig 2.22). Both DAG product ions appear at the same retention time, confirming that the TAGs were not separated. The DAG ions at *m/z* 599, $[LL]^+$ and $[LnO]^+$ from LLLn* and LnLnO*, respectively were observed as a single peak resulting in no discrimination of LLLn* and LnLnO* being achieved.

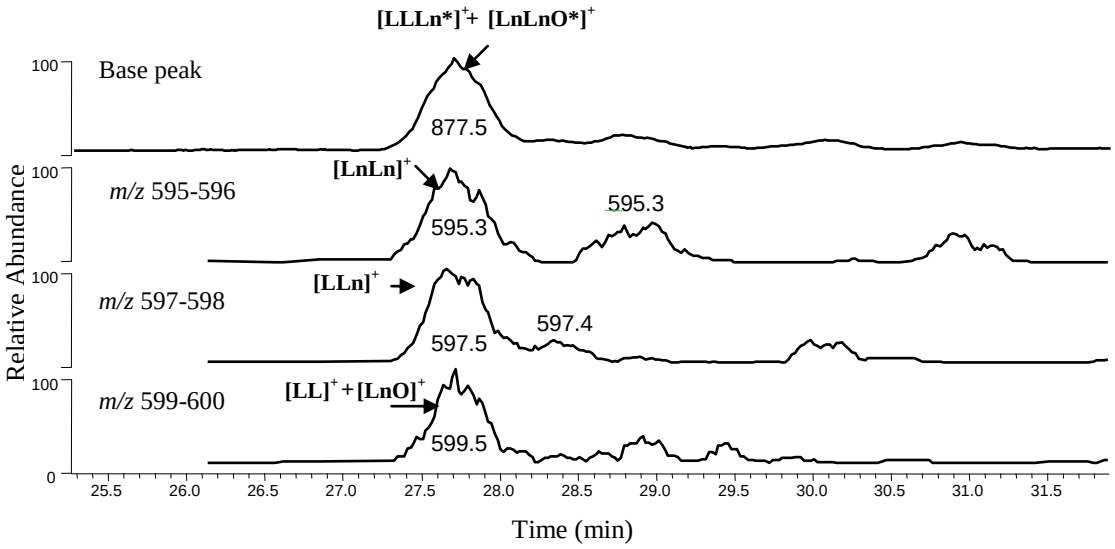

Figure 2.22: Base peak at *m/z* 877.5 for coeluted LLLn* and LnLnO* compound in pork fat and EICs for mass ranges corresponding to the DAG product ions.

The TAGs in pork fat with ECN value of 42 were all fully separated: LLL, OLnL*, LLM* and PLLn*. LLM* is the only TAG in beef fat having an ECN value of 42. The TAG compounds detected in pork fat with an ECN value of 44 were different to those in beef fat. In pork fat, LLO*, LLP* and LnOP* were clearly resolved, LMO* was present in the tail of LLP*, and LPoO* and OLnO* were not fully separated. In beef fat, OPoPo* and PPoPo* were nicely separated but with LLP* as a shoulder on the large peak of PPoPo*.

The major TAGs with an ECN value of 46: OLnG*, OLO*, OOPo*, LPO*, SPLn*, OPPo*, PPL* and PMO* were clearly separated in this work. LLS* is only detected in pork fat and it has an identical mass to OLO*. It was, however, fully separated from OLO* but was only partially resolved or on the shoulder of the larger peak of LPO*. The same situation occurred for the critical pairs of PPL* and OPPo* which were fully separated in pork and beef fat. By contrast, OPPo* in pork fat was not fully resolved from LPO*, which might be due to a very low concentration of OPPo* in the sample whilst LPO* was very concentrated. The OPPo* peak in the pork fat chromatogram is barely visible. The EIC for the range *m/z* 848 to *m/z* 849 clearly shows the peak (Fig 2.23). The chromatogram shows two peaks at *m/z* 848; the first is OPPo* and the second is PPL*. The critical pairs of OOPo*, LPO* and SPLn* were clearly separated from each other in pork and beef fat.

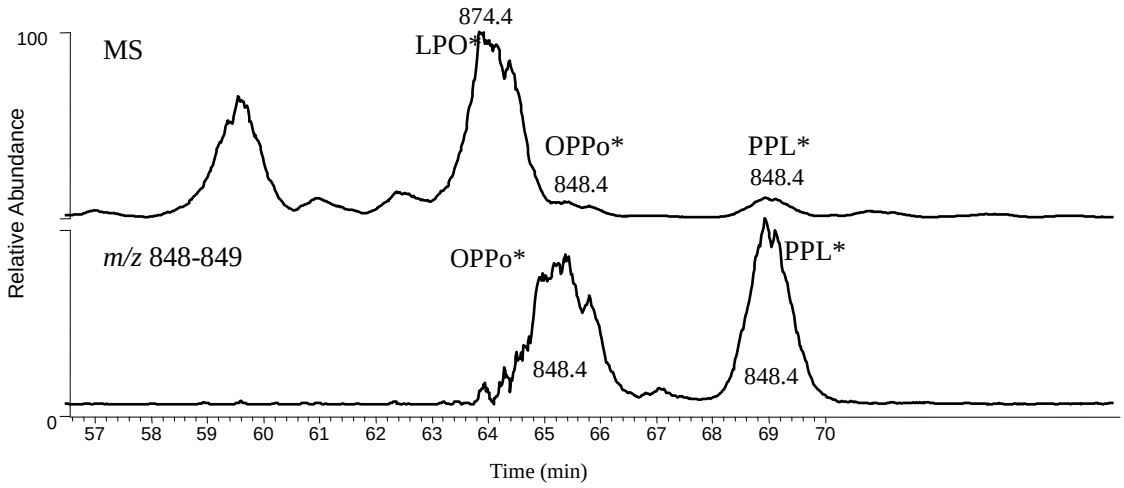

Figure 2.23: Base peak chromatogram and EIC at *m/z* 848 to *m/z* 849 for OPPo* which partially coeluted with LPO*.

For the separation of TAGs with an ECN value of 48, the retention order was OOO< SLO*< OPO< LPS* < PPO* < SMP*. Apart from SLO* and LPS* in pork fat, which were not fully resolved from OPO and PPO*, respectively, the separations were good. The SMP* was separated and detected in beef fat and was fully resolved from SOO. Notably, two other peaks eluted between SMP* and SOO. SMP* has not been reported in most literature and, where present, it was not clearly resolved from SOO. Thus, its complete separation from SOO in this work is notable. PPP forms a critical pair with SMP* ($[M + NH_4]^+$ = *m/z* 824 and $[M + H]^+$ = *m/z* 807) and these two components were not separated. The MS^2 of *m/z* 824 produced the protonated molecule at *m/z* 807 after loss of NH_3 (17 Da) and ions at *m/z* 551, 579 and 523, corresponding to $[PP]^+$ or $[SM]^+$,

$[SP]^+$ and $[PM]^+$. The greater relative abundance of *m/z* 551 suggests that, in addition to $[SM]^+$, a $[PP]^+$ ion was present. This was confirmed in the MS^3 spectrum from *m/z* 551 where product ions at *m/z* 267 ($[S]^+$) from $[SM]^+$ and *m/z* 239 ($[P]^+$) from $[PP]^+$ are apparent.

SOO, SPO* and SPP have an ECN of 50 and were completely separated from each other in pork and beef fat as were SOS and SPS* which have an ECN value of 52. SSS was the only peak detected with an ECN value of 54 and it was fully resolved from other TAGs.

Overall, a better resolution of the critical pairs of TAGs was achieved in this work. Furthermore, the groups of TAGs with different ECNs are very well separated from each other, so that there is sufficient capacity for complete separation and identification of TAGs with odd ECNs (45, 47, 49, 51 and 53). These components consist of one acyl with odd number of carbon atoms (C17:0 or C17:1). In the earlier work on animal fats the odd ECN TAG peaks were not clearly resolved from other TAGs and their identification was not represented in the spectra or peaks in the chromatogram. MoMO* and PPoMo* (ECN value of 45) can not be separated and were detected in beef fat as a single sharp peak. These compounds were not reported in any published work for animal fat and no comparison can be made. For an ECN value of 47, LMaO* was fully separated from OPMo* in pork fat. These two compounds were also not reported before in animal fats.

Three TAG compounds with an ECN value of 49 were detected: OMaO*, OPMa* and PMaP*. The poor peak shape of OMaO* in pork fat might be due to its very low concentration and it was not fully resolved in beef fat. OPMa* and PMaP* were baseline separated. PMaO was reported by Mottram et al. (2001) as a shoulder on the SOO peak but OMaO* and PMaP* were not reported. The TAGs with an ECN value of 51 are SMaO* and SMaP*, and that with an ECN of 53 is SSMa*. All showed very good peak shape and were baseline separated. SMaP* and SSMa* were only separated and detected in beef fat. SMaO* was the only TAGs with an ECN value of 51 in pork and beef fat.

It is noted in this study that the same mobile phase gradient which gave the best TAG separations for beef fat was not the best mobile phase gradient to separate the TAGs in pork fat. This might be due to different concentrations of each TAG in each fat sample. Thus, a generic method for separating TAGs from animal fats was developed for use in

this study. It started with a very slow addition of dichloromethane, at about 1% for 82 mins allowing all the highly unsaturated TAGs to be eluted from the column slowly. Then, the dichloromethane was increased to 35% to make sure that all of the TAGs were eluted, especially the apolar trisaturated TAGs (e.g. SSS). The TAGs identified in pork and beef fat are denoted in Table 2.7. They reveal highly complete distributions and illustrate that the method developed has the ability to reveal the most comprehensive inventory of TAGs in fats.

2.2.4 RP HPLC-APCI MS/MS separation of regioisomers of TAGs from beef, pork, chicken and lamb fat.

2.2.4.1 Chromatographic separation of TAG isomers from beef, pork, chicken and lamb fat.

The mobile phase system developed in Section 2.2.3.1 (Method H, Table 2.6b) not only gave better resolution of the TAGs with similar ECN and separated TAGs with odd ECN, but also made the separations of regioisomer of TAGs possible. The separation of animal fat TAG regioisomers in a one dimensional HPLC system has not been reported before except for partial separation of POS/PSO and SOS/SSO* from beef and lamb fat (Mottram et al., 2001).

Samples from different animal species (beef, pork, chicken and lamb) were examined with the mobile phase system developed to observe the separation of TAG isomers. All the fats were extracted using the same method as employed for beef fat: extraction with chloroform methanol followed by reduction to dryness. APCI MS/MS was used for determining the positional distributions of FAs in the TAGs. The TAG isomers produce identical ammoniated and protonated molecules and the dissociation of ammoniated TAG isomers produce the same DAGs product ion in MS^2 but in differing relative intensities. The DAG product ion abundances are very important for distinguishing between isomers. For example, OOP* and OPO isomers produce a protonated molecule at *m/z* 859.5; in MS^2, DAG product ions occur in the ratio of $[OP]^+$: $[OO]^+$ about 3:1 for OPO and about 1:1 for OOP*.

The prevalence of regioisomers in the beef and lamb fat is obvious due to one isomer being more abundant than the other. The peaks observed eluting after PMO*, OOP*, POP, OOS*, SOP*, SMaP*, SOS and SSMa* in beef fat are identified in MS^2 to their regioisomers (Fig. 2.24). Thus, eight groups of TAG regioisomers were resolved from beef fat: POM*/PMO*, OOP*/OPO, POP/PPO*, OOS*/OSO, SOP*/SPO*, SOS/SSO* including 2 groups having odd ECN: SPMa*/SMaP* and SSMa*/SMaS.

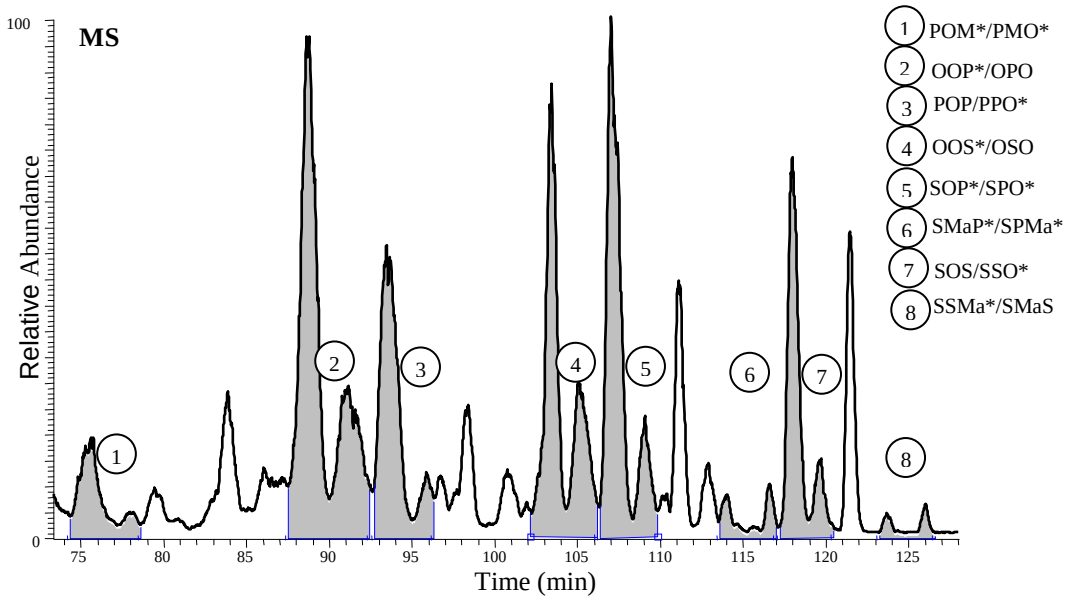

Figure 2.24: RP HPLC-APCI MS chromatogram of beef fat labelled with 8 groups of separated regioisomers of TAGs eluted with the mobile phase of Method H (Section 2.2.3.1; Table 2.6b).

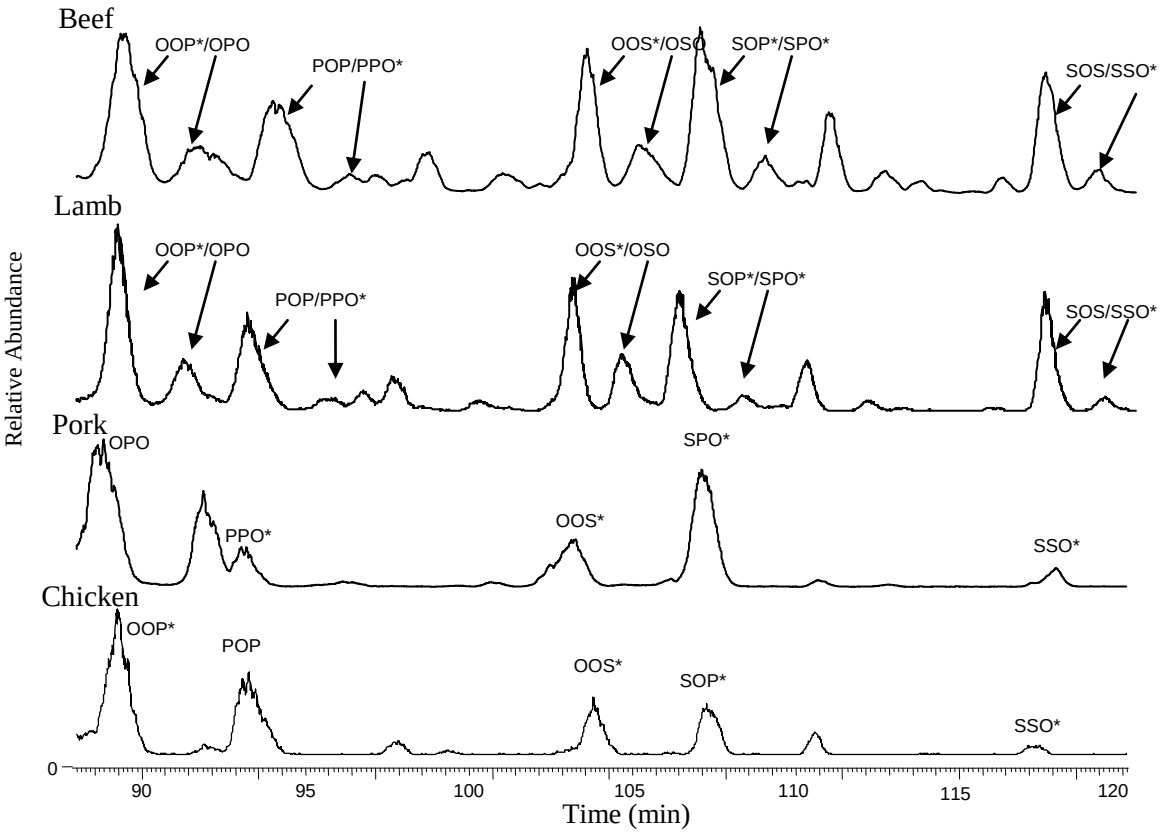

Figure 2.25: RP HPLC-APCI MS chromatograms of TAG isomers from beef, lamb, chicken and pork fat eluted with the mobile phase of Method H (Section 2.2.3.1; Table 2.6b).

The most important influence on the elution order of the regioisomers is the position of the unsaturated FA in the TAG molecules. In all cases, the isomer with the unsaturated FA in either the *sn*-1 or *sn*-3 position is retained more strongly than the isomer with the unsaturated FA in the *sn*-2 position. This is due to the polarity of the stationary phase, which can interact more strongly with the more polar unsaturated FA when it is located in the more accessible position of the TAG molecule (Momchilova et al., 2004).

In the case of TAGs containing both saturated and unsaturated FAs, the regioisomer with the unsaturated FA in the *sn*-2 position is always the most abundant in animal fats. The TAG isomer separation for the four different animal species examined shows that TAG isomers are prevalent in beef and lamb but not in pork and chicken in which only the most abundant isomers are observed (Fig 2.25).

2.2.4.2 Mass spectra of separated TAG isomers from beef fat.

The first TAG isomer pair to elute in beef fat has an ECN of 46, corresponding to POM* and PMO* (1 in Fig. 2.24). Both isomers produce identical ammoniated and protonated molecules at different retention times, and the dissociation of these ammoniated POM* and PMO* isomers produce the same DAGs product ions: $[PM]^+$, $[PO]^+$ and $[MO]^+$ in MS^2 but in differing relative intensities (Fig 2.26). The POM* isomer elutes first; the unsaturated FA being located in the *sn*-2 position. The MS^2 spectrum shows the least abundant DAG ion $[PM]^+$, formed by loss of oleic acid from the *sn*-2 position, at *m/z* 523. The later eluting and minor isomer, PMO*, shows loss of margaric acid from the *sn*-2 position to produce the least abundant $[PO]^+$ ion at *m/z* 577. A peak corresponding to MPO was not detected, though it is not possible to rule out its presence as a minor constituent. The separation of this isomer pair is completed by 79 min for this particular run and the resolution of the peaks, *Rs* is about 1.2.

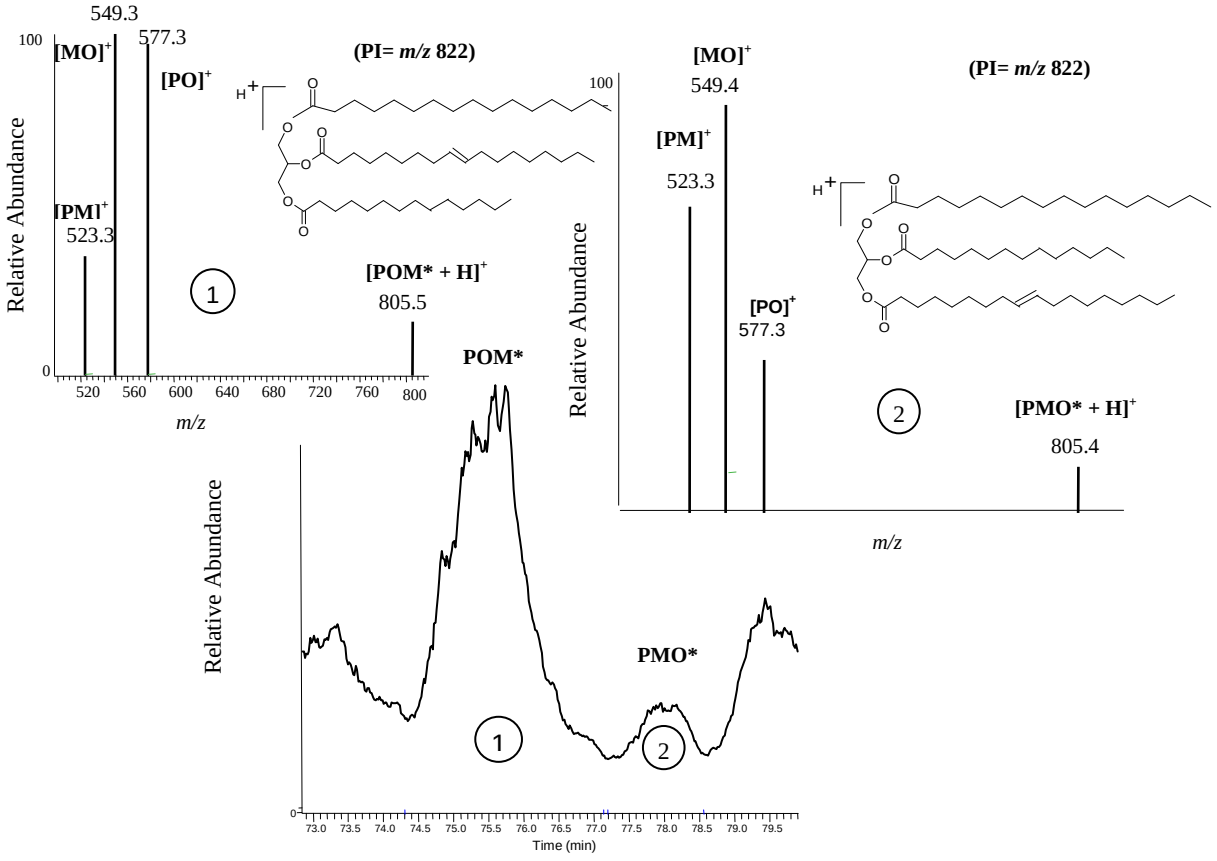

Figure 2.26: RP HPLC-APCI MS chromatogram of POM*/PMO* isomers in beef fat and MS^2 spectra (PI = precursor ion).

Within the OOP* group (2 in Fig. 2.24) the isomer can either be symmetric or asymmetric. The OOP* isomer elutes first due to one of the unsaturated oleic acids being located in the *sn*-1/3 position. The OPO isomer in which oleic acid occupies both the *sn*-1 and *sn*-3 positions, exhibits greater retention. OPO and OOP* have the same ammoniated and protonated molecules at *m/z* 876 and 859, respectively, and give the same DAG product ions in MS^2: $[OP]^+$ (*m/z* 577) and $[OO]^+$ (*m/z* 603) but in differing relative intensities. The ratio of $[OP]^+$:$[OO]^+$ is higher for OPO (about 3:1) than for OOP* where it is 1:1 (Fig 2.27). The resolution (*Rs* = 1.83) is slightly better than in the previous published method (*Rs* = 1.11; Dugo et al., 2004); where regioisomers of rice oil TAGs were separated by off-line coupling of reversed-phase and silver ion HPLC-MS. Here, slightly better resolution of the OOP*/OPO isomers has been achieved by using a one dimension system. The separation of this isomer pair was completed within 93 min for this particular separation.

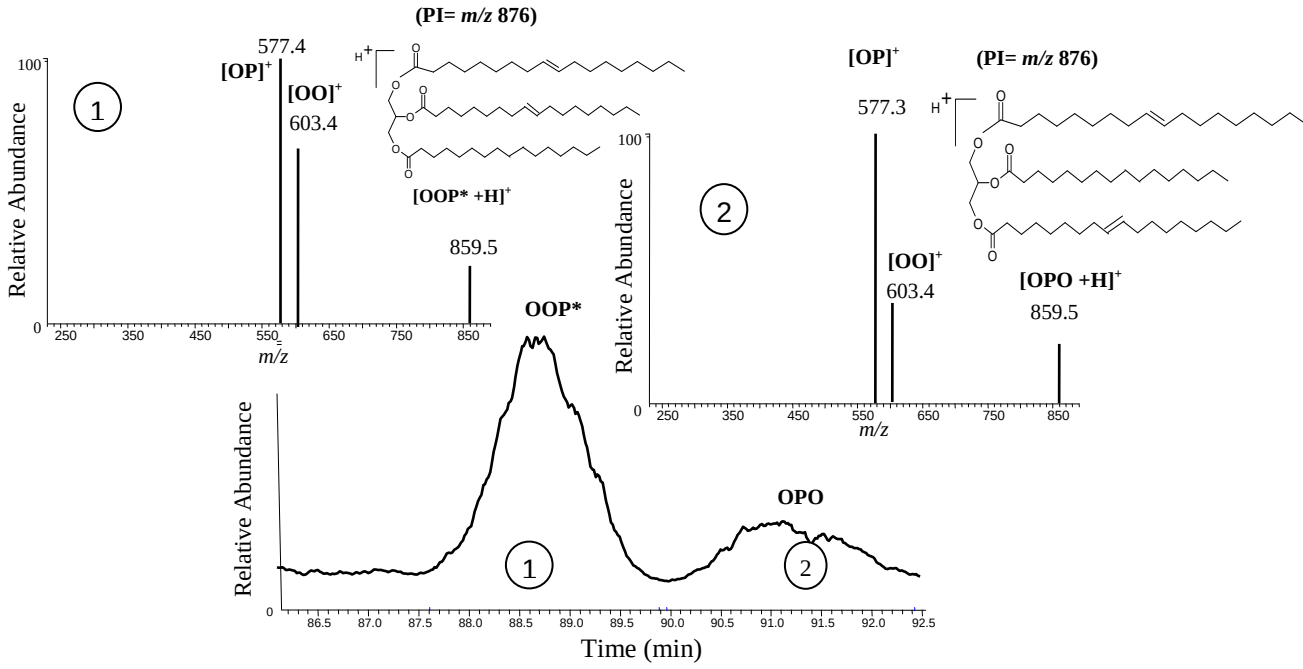

Figure 2.27: RP HPLC-APCI MS chromatogram of OOP*/OPO isomers from beef fat and insert MS^2 spectra (PI = precursor ion).

For the POP/PPO* isomer pair (3 in Fig 2.24), POP is the most abundant isomer in the samples and is the first to elute. The unsaturated FA, being located in the *sn*-2 position, gives the shorter t_R and the MS^2 spectrum shows a DAG product ion ratio of $[OP]^+$ to $[PP]^+$ of about 3:1 for POP and about 1:1 for PPO* (Fig 2.28). The POP/PPO* isomers were fully separated within 93 to 96 min in this particular separation of beef fat, yielding a much shorter analysis time than a published method (Momchilova et al., 2004). Those authors separated laboratory prepared POP and PPO within 216 min with a single column of LiChroCART^{TM} RP-18 (250 x 4 mm ID and 4 μm particle size) and 530 min with two of the same columns in series. The resolution for POP/PPO* isomers in the present work is much better (*Rs* = 1.41) compared with that obtained by Momchilova et al., 2004 (*Rs* = 0.80 on the single column) and about the same as that obtained with two connected columns (*Rs* = 1.43).

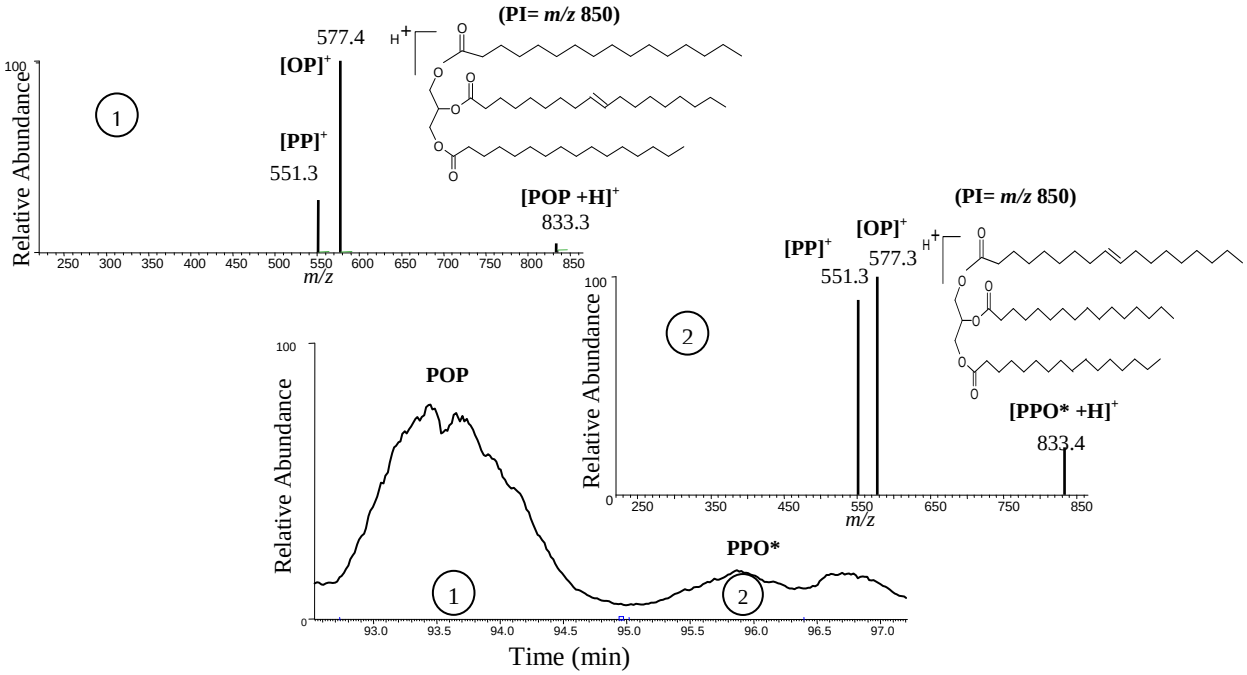

Figure 2.28: RP HPLC-APCI MS chromatogram of POP/OPP* isomers in beef fat and insert MS^2 spectra (PI = precursor ion).

For the OOS* and OSO isomer pair (4 in Fig. 2.24), OOS* elutes first: the unsaturated oleic acid occupies the *sn*-1 and *sn*-3 positions in OSO, hence the isomer is retained preferentially. OOS* is the most abundant isomer in beef fat (Fig 2.29). The structure was confirmed from the MS^2 spectrum by consideration of the DAG product ions: the ratio of $[OS]^+$ to $[OO]^+$ is about 2:1 for OOS* and 3:1 for the OSO isomer. The separation of this isomer pair was completed within 106.1 min for this particular run. The resolution (*Rs* = 1.13) is about the same as that obtained in the published method for the separation of rice oil TAGs (*Rs* = 1.10; Dugo et al., 2004).

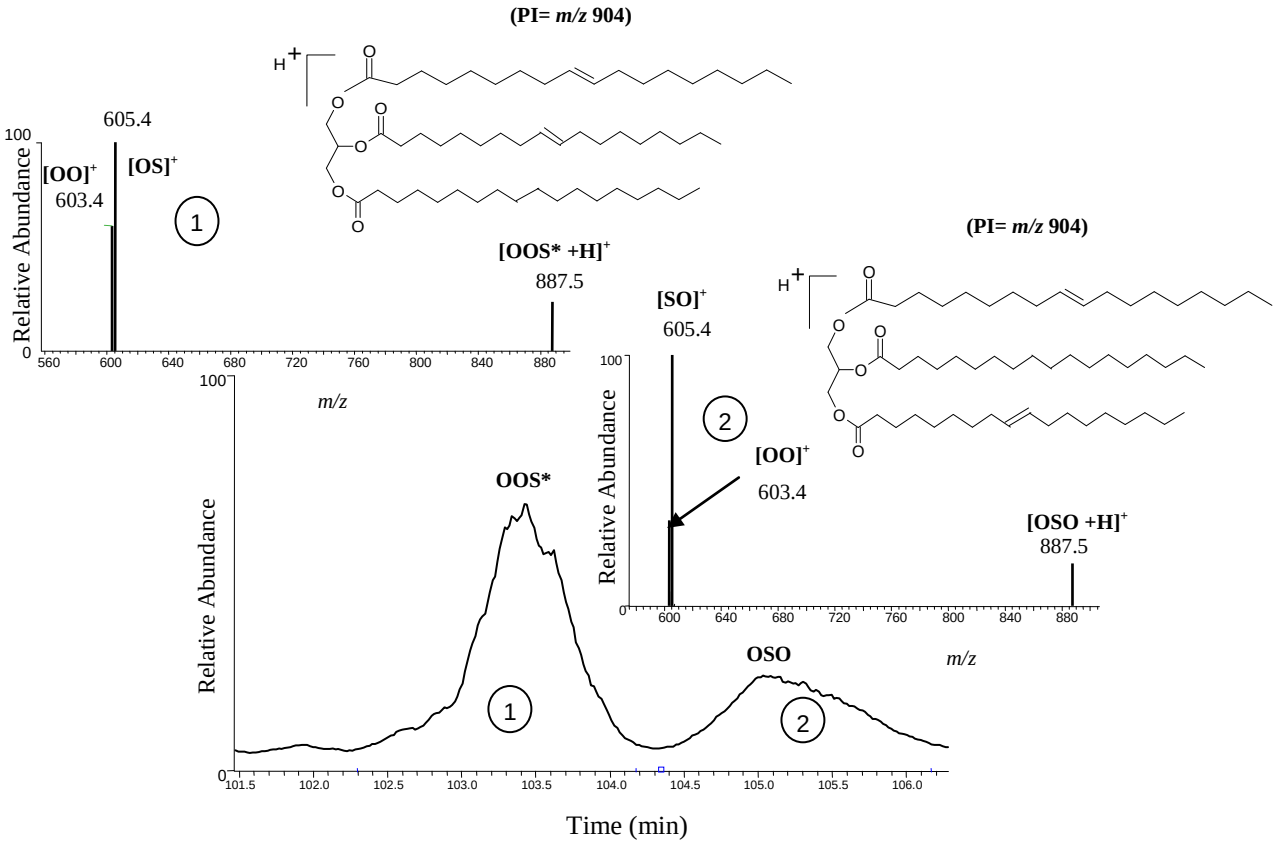

Figure 2.29: RP HPLC-APCI MS chromatogram of OOS*/OSO isomers in beef fat and insert MS^2 spectra (PI = precursor ion).

Within the SOP*/SPO* isomer group (5 in Fig 2.24), SOP* was first to elute as the unsaturated FA is located in the *sn*-2 position. The DAG ions in the MS^2 spectra are $[PO]^+$ (*m/z* 577), $[PS]^+$ (*m/z* 579) and $[SO]^+$ (*m/z* 605). The SOP* isomer MS^2 spectrum shows the least abundant DAG ion to be $[PS]^+$ which results from loss of oleic acid from the *sn*-2 position showing that the compound is SOP*. The later eluting isomer shows $[SO]^+$ as the least abundant DAG ion due to loss of palmitic acid from *sn*-2 position. This dissociation confirms that the compound is SPO* (Figure 2.30). The PSO isomer was not detected; this could be connected to a very low concentration or co-elution with SPO*. The separation of this isomer pair was completed within 109.8 min for this particular run, and better resolution (*Rs* = 1.31) was obtained than in the previous published method (*Rs* = 0.90; Dugo et al., 2004).

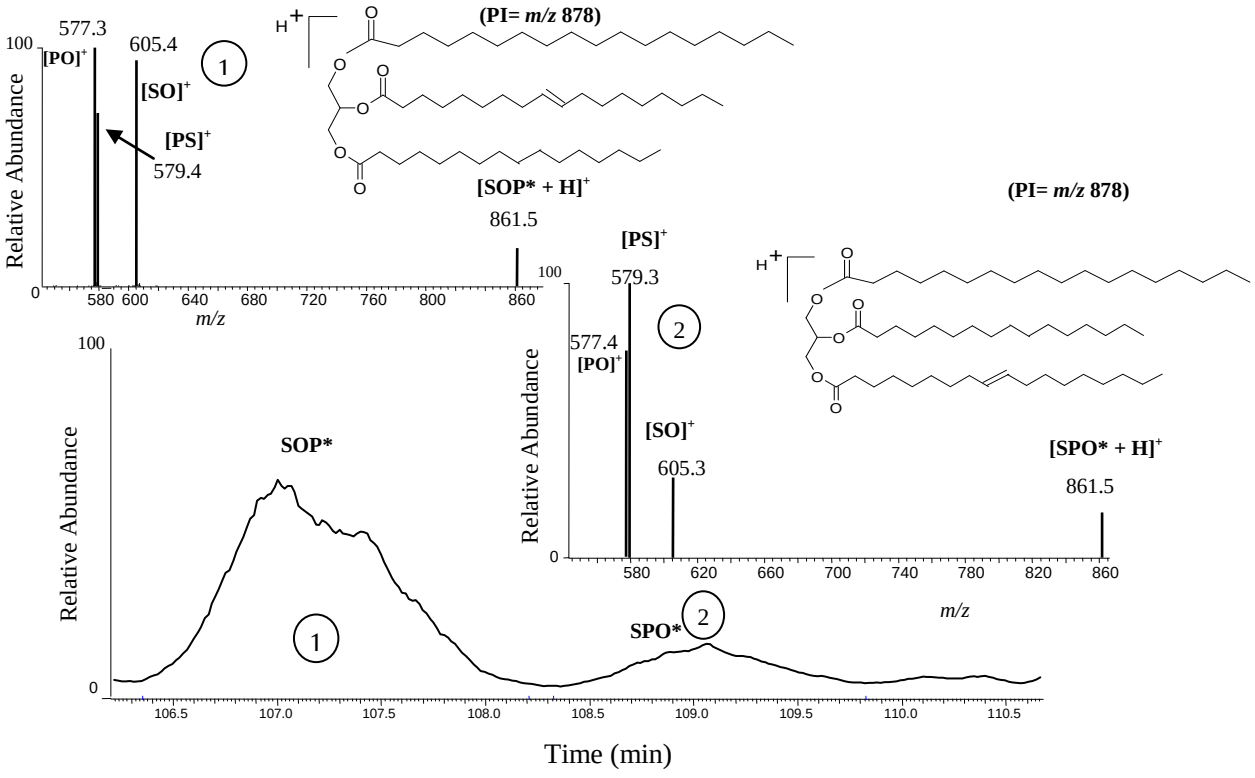

Figure 2.30: RP HPLC-APCI MS chromatogram of SOP*/SPO* isomers from beef fat and insert MS^2 spectra (PI = precursor ion).

The isomers with odd ECN and containing margaric acid, SPMa* and SMaP* were only detected in beef fat and were separated within 113.5 to 117 min (6 in Fig. 2.24). SPMa* elutes before SMaP* and both produce three similar DAG ions at *m/z* 565 ($[PMa]^+$), *m/z* 579 ($[SP]^+$) and *m/z* 593 ($[SMa]^+$). The first isomer has the $[SMa]^+$ ion as the least abundant DAG product ion and the later eluting isomer has $[SP]^+$ as the least abundant DAG ion (Fig. 2.31). There was no indication of the PSMa isomer present. The resolution of these two peaks is very good (*Rs* = 3.06).

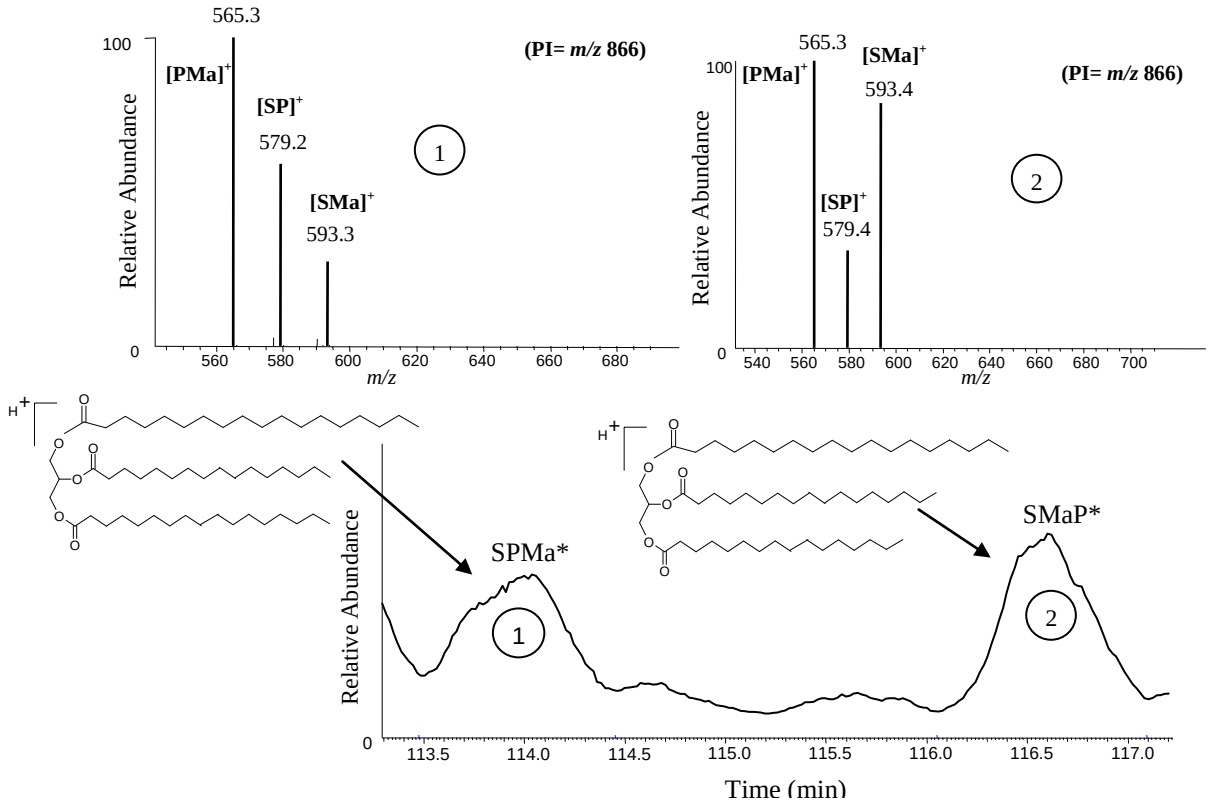

Figure 2.31: RP HPLC-APCI MS chromatogram of SPMa*/SMaP* isomers from beef fat and insert MS^2 spectra (PI = precursor ion).

For the isomer pair SOS/SSO*, SOS was first to elute as the unsaturated FA is located in the *sn*-2 position and SSO*, which has the unsaturated FA in the *sn*-1/3 position, is retained preferentially (7 in Fig 2.24). Both isomers undergo dissociation to produce two DAG ions at *m/z* 605 ($[OS]^+$) and *m/z* 607 ($[SS]^+$) in MS^2 due to loss of stearic and oleic acids, respectively (Fig 2.32). The spectrum of the first eluting isomer shows a ratio for $[OS]^+$ to $[SS]^+$ of about 4:1, confirming that it is SOS. The later eluting isomer dissociated to produce the same product ions in a 1:1 ratio, corresponding to the SSO* isomer. The elution of the SOS and SSO* isomer pair occurred by 121 min for this particular run, and with a resolution of about 1.36.

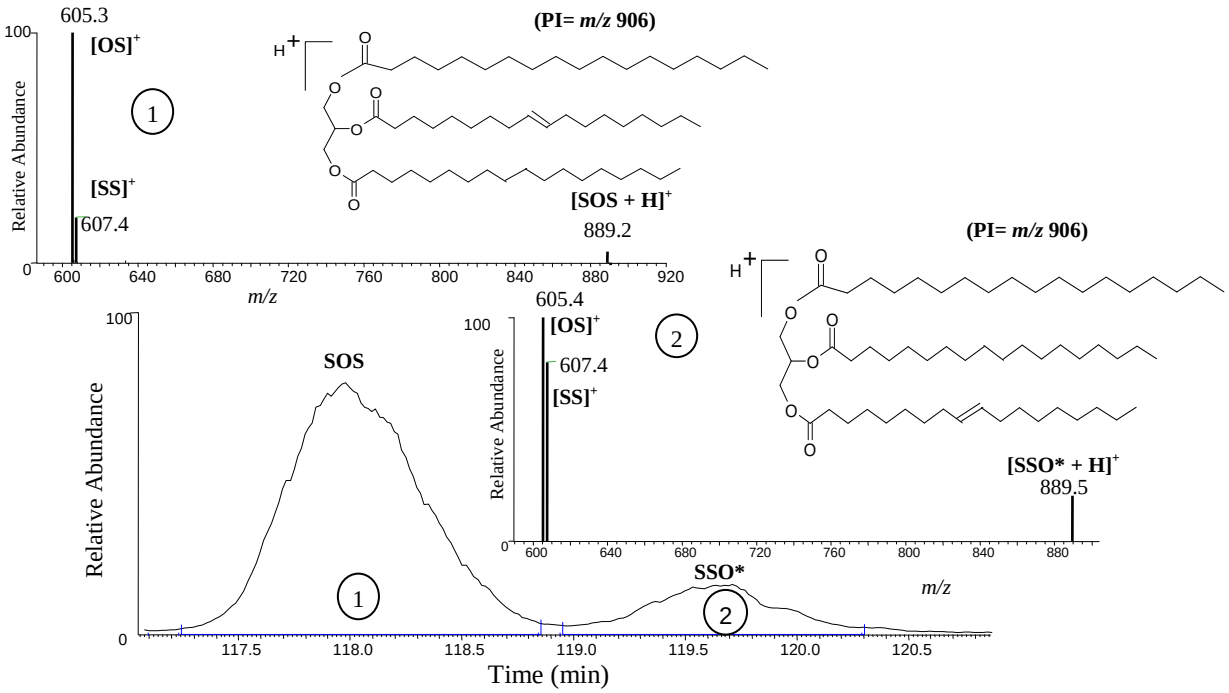

Figure 2.32: RP HPLC-APCI MS chromatogram of SOS/SSO* isomers from beef fat and insert MS^2 spectra (PI = precursor ion).

For the SSMa* and SMaS isomer pair, SSMa* eluted before SMaS (8 in Fig 2.24). Both isomers undergo dissociation to produce DAG ions at *m/z* 593 ($[MaS]^+$) and *m/z* 607 ($[SS]^+$). The SSMa* isomer shows a ratio of about 2:1 for $[MaS]^+$: $[SS]^+$ and SMaS gave a 4:1 ratio and eluted later (Fig 2.33). For these TAGs the less abundant isomer eluted first.

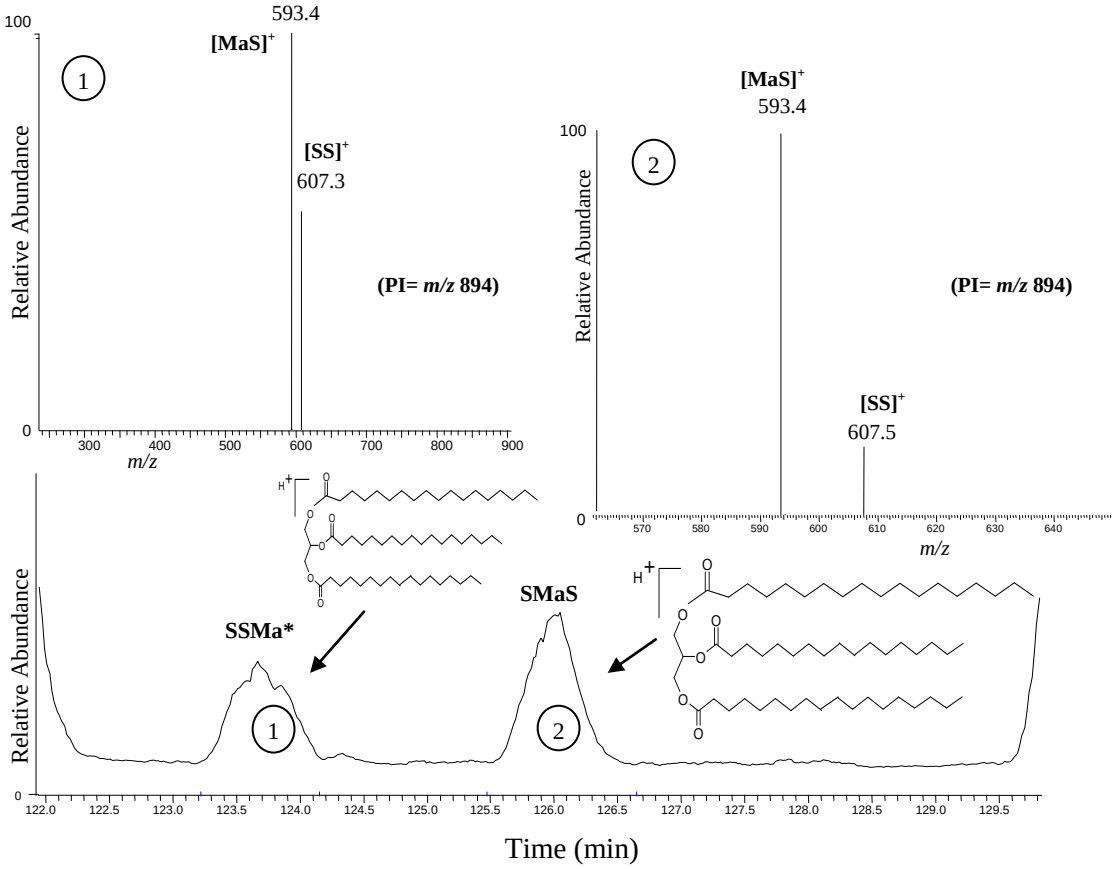

Figure 2.33: RP HPLC-APCI MS chromatogram of SSMa*/SMaS isomers from beef fat and insert MS^2 spectra (PI = precursor ion).

In the SLO*/SOL*/LSO* isomer group, retention time increases as the degree of unsaturation on the external FAs increases, due to greater interaction with the stationary phase. SLO* was first to elute followed by SOL* and then LSO*; both unsaturated FAs being present on the external positions (*sn*-1 and *sn*-3) in LSO*. The three isomers were not fully separated in any of the samples, giving a very broad peak (Fig. 2.34). Nevertheless, from the MS^2 spectrum the dominant isomer at particular t_R can still be determined; SLO* MS^2 spectrum shows the least abundant DAG ion of $[SO]^+$ at *m/z* 605 formed by loss of linoleic acid from the *sn*-2 position. The later eluting and major isomer is SOL*, showing loss of oleic acid from the *sn*-2 position to produce the least abundant $[SL]^+$ ion at *m/z* 603. The next eluting isomer is LSO*, showing loss of stearic acid from the *sn*-2 position to produce the least abundant $[LO]^+$ ion at *m/z* 601.

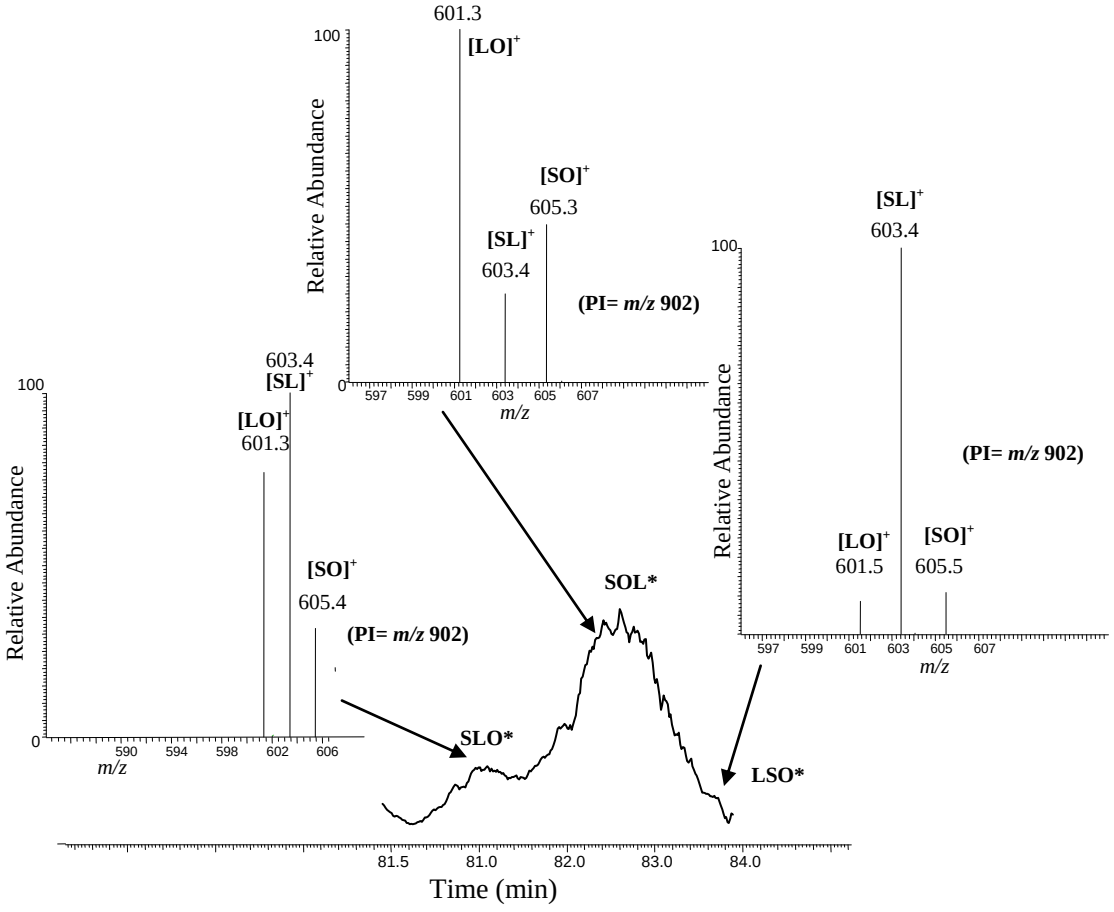

Figure 2.34: RP HPLC-APCI MS chromatogram and insert MS^2 spectra of SLO* isomers; SLO*, SOL* and LSO* from pork fat (PI = precursor ion).

2.2.4.3 Regioisomer compositions of TAGs of beef, lamb, pork and chicken fats.

The area percent for each isomer in beef, lamb, chicken and pork fat was obtained by the summation of the area under the peaks in EIC corresponding to the ammoniated and protonated molecules, and DAG fragment ions. For example, the area percent of the OOS*/OSO isomer pair in lamb fat was obtained by the summation of the area under the peaks in the EIC for ammoniated OOS*/OSO at *m/z* 904, protonated OOS*/OSO at *m/z* 887 and DAG fragment ions of $[OO]^+$ at *m/z* 603 and $[SO]^+$ at *m/z* 605 (Fig 2.35a). The histogram for the area percent or ratio of OOS* and OSO shows that lamb fat contained 64% OOS* and 36% OSO (Fig 2.35b). Thus, the percentage of SFA in the *sn*-2 position for OOS*/OSO isomer pair is 36%. The percentages of each isomer present in beef, lamb, chicken and pork fats were calculated (Table 2.9).

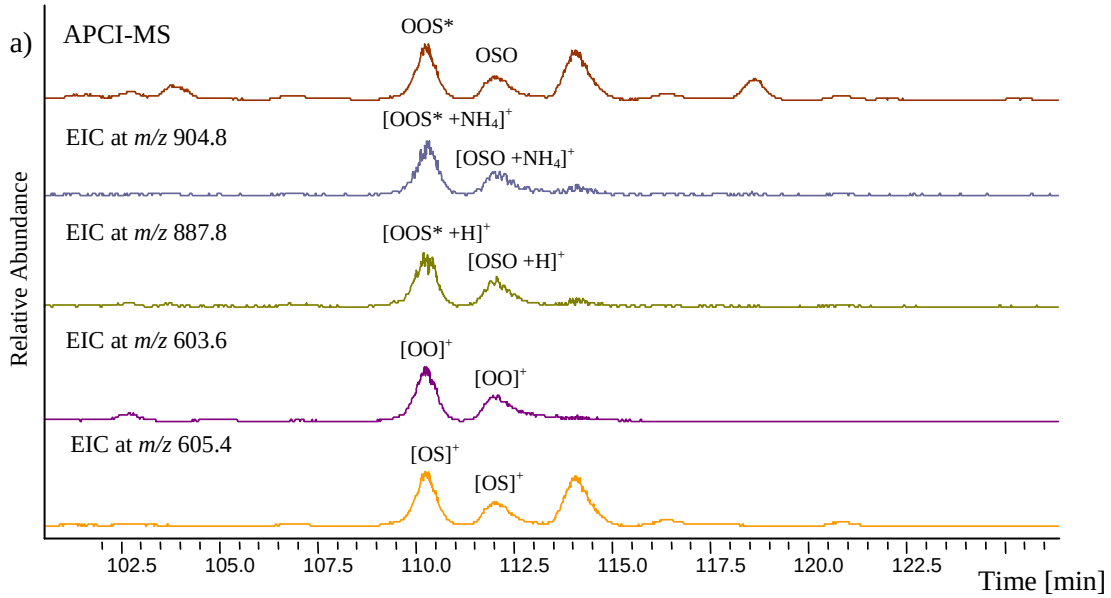

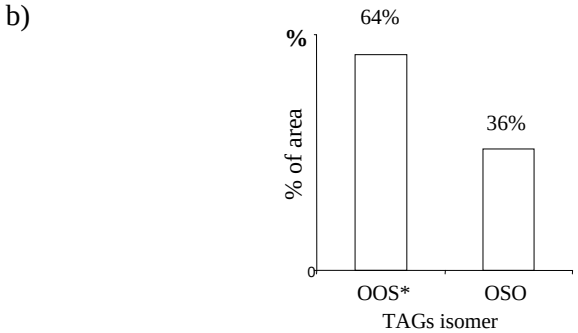

Figure 2.35: a) RP HPLC-APCI MS chromatogram and EIC for all ions present for OOS*/OSO isomers of lamb fat and b) the histogram of area percent for OOS* and OSO isomers.

Table 2.9: Percentages of TAG isomers resolved from beef, lamb, chicken and pork fat.

TAGs	Isomers	Beef	Lamb	Chicken	Pork
POM*	POM*	95	84	-	-
	PMO*	5	16		
OOP*	OOP*	91	74	100	-
	OPO	9	26	-	100
POP	POP	96	86	100	-
	PPO*	4	14	-	100
OOS*	OOS*	86	64	100	100
	OSO	14	36	-	-
SOP*	SOP*	95	87	100	-
	SPO*	5	13	-	100
	PSO*	-	-	-	-
SOS	SOS	95	85	-	-
	SSO*	5	15	100	100

Only separated TAG isomers of POM*/PMO*, OOP*/OPO, POP/PPO*, OOS*/OSO, SOP*/SPO* and SOS/SSO* are shown and discussed. Notably, the proportions of isomer differ for different animals. The area percent of TAG isomers observed in beef and lamb fat varies according to the degree of unsaturation of the TAGs. Thus the separated TAG isomers can be divided into three groups; a) TAG having one monounsaturated FA and two saturated FAs (POM*/PMO*, POP/PPO*, SOP*/SPO* and SOS/SSO*). For these TAGs, the average ratio of about 95:5 is observed for beef fat and about 86:14 for lamb fat. The isomers with the saturated FA in the *sn*-2 position represent about 4 to 5% for beef fat and 13 to 16% for lamb fat (Table 2.9). Notably, the percentage of PPO and SSO isomers with the SFA in the *sn*-2 position was much higher for lamb fat in a previous study (32%; PPO and 33%; SSO; Mottram et al., 2001). The differences observed might be explained by the differences in ionization efficiency and better separation of TAGs and isomers in the present study. The percentage of PPO isomer in beef fat (4%) is also much lower than in previous published work (40%; Dugo et al., 2006). A published report on the regioisomers of TAGs in rice oil showed that the isomer with the SFA in the *sn*-2 position ranged from 14 to 17% (Dugo et el., 2004) close to the values observed here for lamb fat but much higher than those observed for beef fat. This difference might be a consequence of animal fat having a constraint/limitation with TAGs being mostly sourced from their diet.

The next TAG group is; b) TAG with two monounsaturated FAs and one saturated FA: OOP*/OPO and OOS*/OSO. For these TAGs, a much higher ratio was observed for the isomer with the SFA in the *sn*-2 position than for the isomers having an unsaturated FA in the same position: 9 to 14% for beef fat and 26 to 36% for lamb fat. This difference is a result of lamb having a stronger tendency to produce TAGs with unsaturated FAs on the *sn*-1/3 position. Notably, OPO is the only isomer that was detected from beef and lamb fat in the previous published study (Mottram et al., 2001). Also, OSO was more abundant in beef fat (about 68%) and lamb fat (about 77%) in their study than in the present study (14%; beef fat and 36%; lamb fat). These differences might also be explained by the lack of separation of these isomers in the earlier study.

The third TAG group; c) only detected in beef fat, comprises TAGs having odd ECN (SPMa*/SMaP* and SSMa*/SMaS) and containing all saturated FAs. The later eluting TAGs are more abundant than the earlier eluting TAGs for both isomer groups.

The TAG isomers of beef and lamb fat having both saturated and unsaturated FAs, all show the regioisomer with the unsaturated FA in the *sn*-2 position as the most abundant component. This is not the case for OPO, PPO*, SPO* and SSO* in pork fat and SSO* in chicken.

For the OOP*/OPO isomer pair, OPO is the only isomer in pork fat, consistent with the published reports (Fauconnot et al., 2004 and Mottram et al., 2001). Also, within the POP/PPO* isomer pair, PPO* is the only isomer in pork fat, also in line with a published study (Dugo et al., 2006). Those authors determined the proportions of the regioisomers in lard and tallow without separation, and confirmed that lard contains only the PPO isomer while tallow contained 60.3% POP and 39.7% PPO (Dugo et al., 2006). However, the percentages ratio of OOP*/OPO and POP/PPO* for lard are 6.3/93.7 and 9.4/90.6 by UPLC/ESI-MS/MS in previous work (Leskinen et al., 2007). The differences observed might be explained by the isomer ratio being determined by analyzing linear calibration plots of fractional DAG fragment intensities vs. the fractional composition of binary mixture of standard in the previous study instead of by the separation of the isomers as in the present study.

Chicken has similar TAG isomer abundances of OOS* and SSO* to pork fat. There are, however, differences in the OOP*/OPO, POP/PPO* and SOP*/SPO* isomer profiles with OOP*, POP and SOP* being the only isomers present in chicken and OPO, PPO* and SPO* the only isomers in pork fat. POP and SOP* were also the only isomers reported in chicken fat (Mottram et al., 2001).

In the case of OOL* (one diunsaturated FA, two monounsaturated FAs), the regioisomer ratio of OLO/OOL is 40:60 in the work on rice oil (Dugo et al., 2004). In the present study OLO* is the only isomer present in pork fat: the OOL* concentration was either too low to be observed or the isomer co-eluted with OLO*. OOL* is the only isomer that was observed in beef fat for this particular sample, in agreement with its previous detection in beef fat at a very low abundance, about 0.15% (Mottram et al., 2001). It is difficult to resolve the isomers of TAGs such as OOL* having three or more double bonds. When the difference in the number of double bonds in the unsaturated FAs is only one (e.g. oleic and linoleic acids) resolution is difficult. Thus, the separation of OLO*/LOO which have 4 double bonds is challenging. The TAG combinations with two saturated FAs and a diunsaturated FA isomer, for example, PLP and PLS were not separated in this study. Also, no TAGs having all three saturated FAs were separated into their constituent isomers, except for the odd ECN TAGs SMaP*/SPMa* and SSMa*/SMaS.

2.2.5 UHPLC vs. HPLC for separating TAGs of beef fat sample.

Toward the end of the study, UHPLC equipment became available and the opportunity was taken to develop an improved UHPLC method. Owing the timing of the execution of the work in this section, it was not possible for the method that was developed to be applied in the analyses detailed in the next two chapters in this thesis.

Although good separation of TAGs and their isomers were achieved with the mobile phase system developed on the conventional HPLC (Method H; Section 2.2.3.1), analysis times are long. Thus, rapid separation by ultra-performance LC was explored to reduce analysis times and improve resolution. For the rapid separation of TAGs, a Dionex UHPLC instrument (Ultimate 3000 RS) was equipped with two RSLC Acclaim 120 C18 2.2 um (2.1 x 100 mm, 2.2 μm) columns. The mobile phase gradients for separation of TAGs by UHPLC contained dichloromethane, acetonitrile and 10 mM of ammonium acetate (NH_4Ac) in methanol. The proportion of dichloromethane required was determined by evaluating values from 20 to 40% by volume in 1% increments. The optimum composition that gave good separation was found starting at 20% dichloromethane and maintaining a constant level for 50 min followed by an increase linearly to 40% by 90 min (Table 2.10). The same fat sample of beef was used in both separation methods to compare conventional HPLC and UHPLC. Hexane:acetonitrile:2-propanol (1:1:1,v/v/v) was used as sample solvent.

Table 2.10: The mobile phase gradient for separation of TAGs on the Ultimate 3000 RS (Dionex) UHPLC system with two RSLC Acclaim 120 C18 2.2 um (2.1 x 100 mm, 2.2 μm) columns (Method I).

Method I:

Time (min)	Flow rate (ml/min)	Dichloromethane (%)	Acetonitrile (%)	NH_4Ac in methanol (%)
0	0.7	20	76	4
50	0.7	20	76	4
90	0.7	40	56	4

The chromatogram of TAGs produced from the optimum mobile phase gradient on the UHPLC system (Fig. 2.36) shows the separations achieved were comparable to those of conventional HPLC (Fig. 2.37) using the mobile phase system developed in Section 2.2.3.1 (Method H). The comparison of those chromatograms indicates the run time is reduced to almost half for UHPLC: analysis times being 74 min for UHPLC, and 123 min for HPLC. The run time of 74 min for UHPLC in the present study is still much higher than for a previous published report for reference TAGs, lard, sunflower and rapeseed oil separation by UHPLC with an Acquity UPLC^{TM} BEH C18 (100 x 2.1 mm i.d., 1.7 μm) column (Leskinen et al., 2007). Those authors separated lard within 24 min, however only four TAG were separated (PLO, OOP, PLS and POS). Five important TAGs in pork fat, which are present at high relative abundance levels, were not observed in their separation (LLO*, LLP* and OLO* which elute before PLO and OOO and OOS* which should separate between PLO and POS).

The UHPLC system improved the resolution and response for the TAGs by producing narrower peaks, thus increasing the signal-to-noise ratio. Slightly better resolution was achieved in the UHPLC with a column length 2/3 that in HPLC; the resolution for peaks SPS* and SOS is about 2.59 for HPLC and 2.88 for UHPLC. Also, the resolution for peaks SPO* and PPS* was slightly better for UHPLC (*Rs* = 2.4) than HPLC (*Rs* = 1.7). However, the separations for OPO and POP and OSO and SOP* were better with HPLC than UHPLC. The peak widths for some of the separated TAGs in UHPLC were almost half those in HPLC. For example, the peak widths of SOS are reduced to about half (1.6 min in HPLC of 0.9 min in UHPLC). The improvement of the peak shape is also observed for PPS*, SOS and SPS* with the UHPLC system. Furthermore, the acclaim 120 C18 UHPLC column exhibited better retention time stability than the conventional system, which might be due to the higher dichloromethane proportion at the end of the run time (40% on the acclaim 120 C18 column and 35% on the Waters Spherisorb ODS2), leading to removal of retained compounds more efficiently.

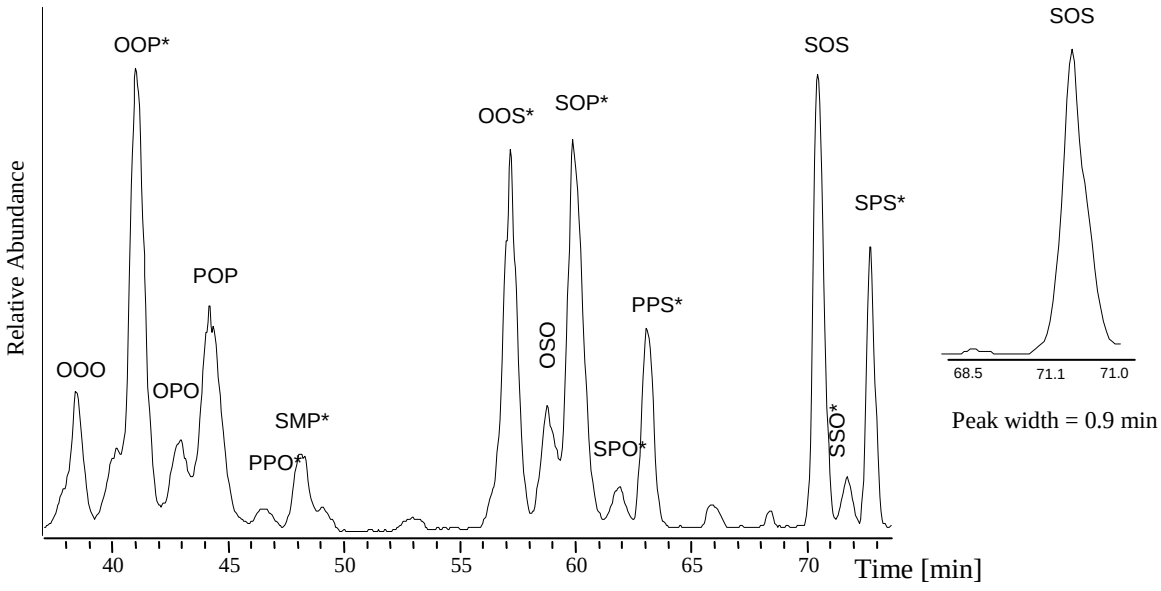

Figure 2.36: UHPLC-APCI MS chromatogram of TAGs from beef fat sample on the two RSLC acclaim 120 C18 (2.1x100mm, 2.2µm) columns with the mobile phase of Method I (Table 2.10).

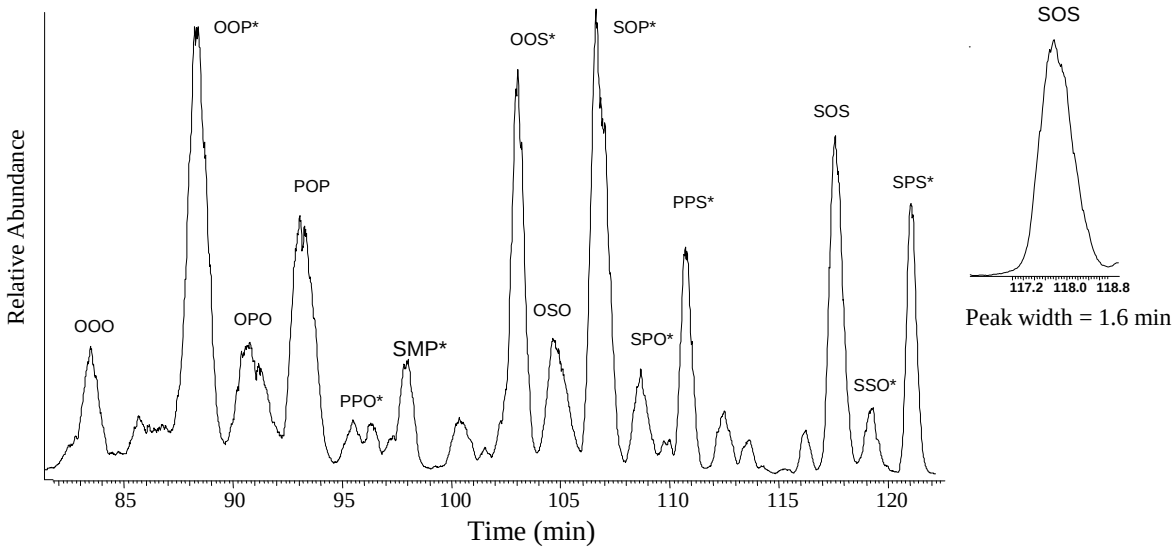

Figure 2.37: HPLC-APCI MS chromatogram of TAGs from beef fat sample on the two Waters Spherisorb ODS2 (4.6x150mm, 3µm) columns with the mobile phase of Method H (Section 2.2.3.1).

2.3 Conclusions

The dissociation behaviour of OOP* and OPO standards is very similar under APCI and ESI conditions with ammonium acetate present in the solvent. The APCI and ESI precursor ions of ammoniated TAGs give similar dissociation products in MS^2 and MS^3. The presence of ammonium ions is important for both ionization techniques in order to give rise to constant dissociation in MS^2. Thus, the intensities of DAG product ions in the MS^2 spectra formed are sufficient to differentiate the positional isomers of TAGs. The APCI source with ammonia in the mobile phase provides an alternative to ESI for MS/MS analysis of FA positional isomers in TAGs with lower noise levels and free from sodium adduct ions.

Two Waters Spherisorb 3 µm ODS2 columns connected in series and eluted with a very slow gradient of dichloromethane and acetonitrile improved the resolution for TAGs with the same ECN (e.g. for peaks OOS* and SOP*, peaks SOS and SPS*) and critical pairs. Ammonium acetate was added to facilitate ionization and hexane:acetonitrile:2-propanol (1:1:1,v/v/v) was used to dissolve the samples for injection onto the column. The separation is significantly better than in earlier reported HPLC analyses, especially for TAGs with lower ECN, including the TAGs containing odd number of carbon atoms such as Ma (C17:0) and Mo (C17:1). The odd ECN TAG peaks of animal fats were not clearly resolved from other TAGs and their identification was not represented in the spectra or peaks in the chromatogram in the earlier work (e.g. OPMo*, OMaO*, PMaP* and SMaO* in beef fat). The separations were only possible with analysis times that are long.

The mobile phase system developed not only gave better resolution of the TAGs with similar ECN and separated TAGs with odd ECN, but also made the separations of positional isomer of TAGs possible. The prevalence of isomers in the beef and lamb fat is obvious due to one isomer being more abundant than the other. Eight groups of TAG positional isomer were resolved from beef fats: POM*/PMO*, OOP*/OPO, POP/PPO*, OOS*/OSO, SOP*/SPO*, SOS/SSO* including 2 groups having odd ECN: SPMa*/SMaP* and SSMa*/SMaS. In all cases, the isomer with the unsaturated FA in either the *sn*-1 or *sn*-3 position is retained more strongly than the isomer with the unsaturated FA in the *sn*-2 position. In the case of TAGs containing both saturated and unsaturated FAs, the positional isomer with the unsaturated FA in the *sn*-2 position is always the most abundant in animal fats. The TAG isomer separation for the four

different animal species examined shows that TAG isomers are prevalent in beef and lamb but not in pork and chicken in which only the most abundant isomers are observed. The area percent of TAG isomers observed in beef and lamb fat varies according to the degree of unsaturation of the TAGs. Notably, the proportions of isomer differ for different animals. For the TAG having a monounsaturated FA and two saturated FAs (POM*/PMO*, POP/PPO*, SOP*/SPO* and SOS/SSO*), the average ratio of about 95:5 is observed for beef fat and about 86:14 for lamb fat. For the TAGs with two monounsaturated FAs and one saturated FA: OOP*/OPO and OOS*/OSO, a much higher ratio was observed for the isomer with the SFA in the *sn*-2 position than for the isomers having an unsaturated FA in the same position: 9 to 14% for beef fat and 26 to 36% for lamb fat. The distributions of TAG isomers for animal fats show good potential for discriminating fats of different animal species.

Converting the method from HPLC to UHPLC has advantages of improved speed and resolution. The analysis times are reduced to almost half. In general, UHPLC improved the resolution slightly by improving peak width and peak shape. The peak widths for some of the separated TAGs were almost half in UHPLC compared with HPLC. Furthermore, the column used in UHPLC exhibited better retention time stability than the conventional system.

CHAPTER 3

FA and TAG variations in different anatomical location of pigs and different animal species

3.1 Introduction and aims

Introduction

FA and TAG profiles of animal fats vary widely with species, tissue, diet and environment and the distribution of FAs in animal fat tissues differs appreciably according to animal species and the location of the adipose tissue in the body (Gutierrez and Barron, 1995). Effects of anatomical locations on the FA compositions of pork have been reported (Timon et al., 2001; Bragagnolo and Rodriguez-Amaya, 2002; Suzuki et al., 2006; Franco et al., 2006; and Monziols et al., 2007). FA compositions were shown to differ between anatomical locations for subcutaneous and intermuscular adipose tissue of ham, shoulder, belly and loin in pork fat (Monziols et al., 2007). A study on subcutaneous adipose tissue and muscle from loin chops and steaks from pigs, sheep and cattle shows that adipose tissue has a much higher FA content than muscle but the FA composition of the two tissues is broadly similar. There are, however, differences between species (Enser et al., 1996). Pigs have much higher proportions of Ln in both subcutaneous adipose tissue and muscle than do cattle and sheep.

The effect of genetic differences on FA composition was studied and the FA profiles were shown to be significantly different for four types of beef (Belgian Blue double-muscled, Limousin, Irish and Argentine, Raes et al., 2003). By contrast, the study of the pork muscle showed that the FA composition was little affected by genetic differences (Armero et al., 2002).

The effects of breed and diet on the FA composition of beef were compared and it was found that diet had the largest effect on FA composition in all age groups (Warren et al., 2008). The FA compositions of intramuscular fat in beef from different breeds and diet also show that diet is more important than breed (Garcia et al., 2008). The combination of breed and diet was also the main factor in variation of FA profiles for fat tissues in lamb (Juarez et al., 2008).

The changes of FA and TAG compositions during fattening of beef have been reported (Suzuki et al., 2007). Those authors found that POO showed the highest concentration during the fattening period and that the level of POLn increased, while the levels of PPP, PPS*, PSS and PSO decreased, with growth. Also, it has been found that as calves age, MUFA and PUFA levels increase and saturated FA levels decrease by about 10%

(Huerta-Leidenz et al., 1996). Significant sex differences in individual FAs were detected for pigs, with barrows having greater concentrations of SFA and MUFA but lower PUFA than gilts (Zhang et al., 2007).

The instrumental techniques used for analysis of FA and TAG profiles are frequently paired with the use of chemometrics such as PCA and PLS for data analysis to examine similarities or differences among the subjects. Chemometric analysis of FT-Raman spectroscopic data for different animal species showed that PCA and PLS separated the different classes of animal fats (Abbas et al., 2009). The muscle samples of beef, pork, sheep and chicken were analysed in the UV-VIS and NIR regions (400-2100 nm) and PCA scores plots showed clusters of samples according to the different meat species (Cozzolino and Murray, 2004).

Aims

The aims of the work described in this chapter were to examine:

a) the extent to which the improved characterization of TAG profiles (using the method reported in Chapter 2) improves discrimination within and between animal species.
b) the extent of variation in FA and TAG profiles in four different animal species (beef, lamb, chicken and pork) and to compare the discriminating power of the two methods.
c) the variation of FA and TAG profiles from subcutaneous and intermuscular fat of four different anatomical locations (belly, ham, loin and shoulder) of pigs to assess natural variability within a subject.
d) the extent to which FA and TAG profiles in different animal species and anatomical locations of pigs are differentiated by the application of PCA.

3.2 Results and discussion

The three letter code of TAGs includes the suffix * where more than one regioisomer can exist in a form that can, potentially, be separated chromatographically.

3.2.1 FA profiles of beef, lamb, chicken and pork fats.

The FAME analyses were performed for ruminants (beef and lamb) and non ruminants (pig and chicken). Samples of beef sirloin steaks, lamb chops, chicken and pork (ham intermuscular fat) purchased in retail outlets were homogenised and extracted with chloroform methanol (2:1) and replicate analysis (≥ 5) was performed. Fatty acid methyl esters were prepared with methanolic sulphuric acid (Section 6.1.4) and FAMEs were analysed using GC with FID detection (Table 6.2, Section 6.2.1, Chapter 6). A FAME standard mix (C14 to C22) was used for peak identification. The peaks observed were identified by comparing the retention times with the FAME standard mixture.

The most abundant FAMEs identified for all samples are: C16:0, and C18:1*cis* which dominate the chromatograms (Figs. 3.1a to d). C18:0 and C18:2*cis* show a high degree of variation, maximising in lamb and chicken, respectively. C14:0, C16:1, C17:0, C17:1, C18:1*trans* and C18:3 were present in low relative abundance. C14:1, C15:0 and C15:1 were only observed in beef and lamb and contribute very little to the total FAs.

The individual FAME peak areas of all ten identified compounds for pork and chicken and all thirteen for beef and lamb are expressed relative to the total peak area. The variations in the proportions of FAMEs between different species were examined taking account of the Y-error bar at the 95% confidence level (two standard deviations) of the mean percentage of FAMEs (Fig. 3.2a). For the low relative abundance FAMES the histogram was rescaled (Fig. 3.2b).

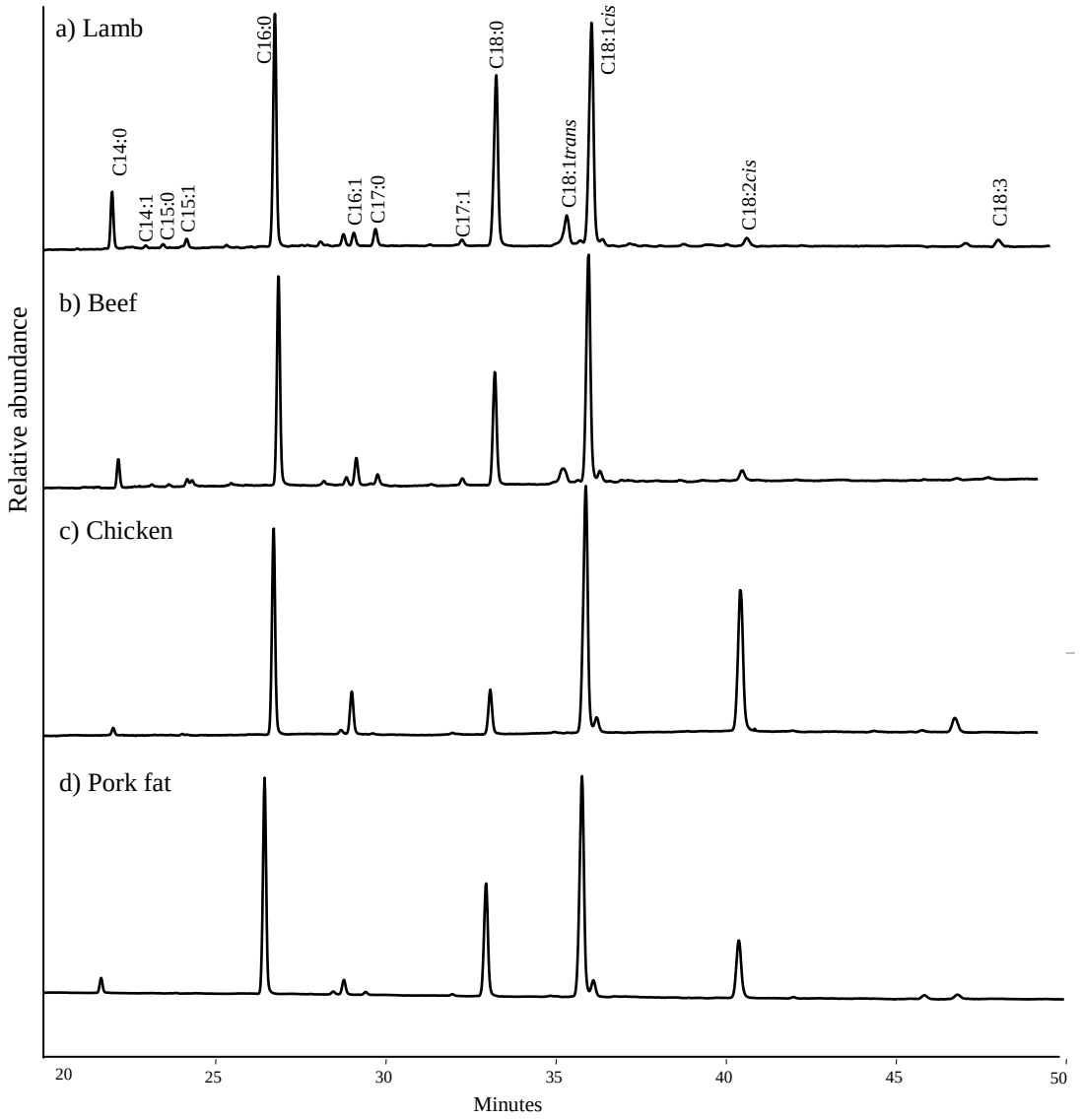

Figure 3.1: GC chromatograms of FAMEs for a) lamb b) beef c) chicken and d) pork fat.

a)

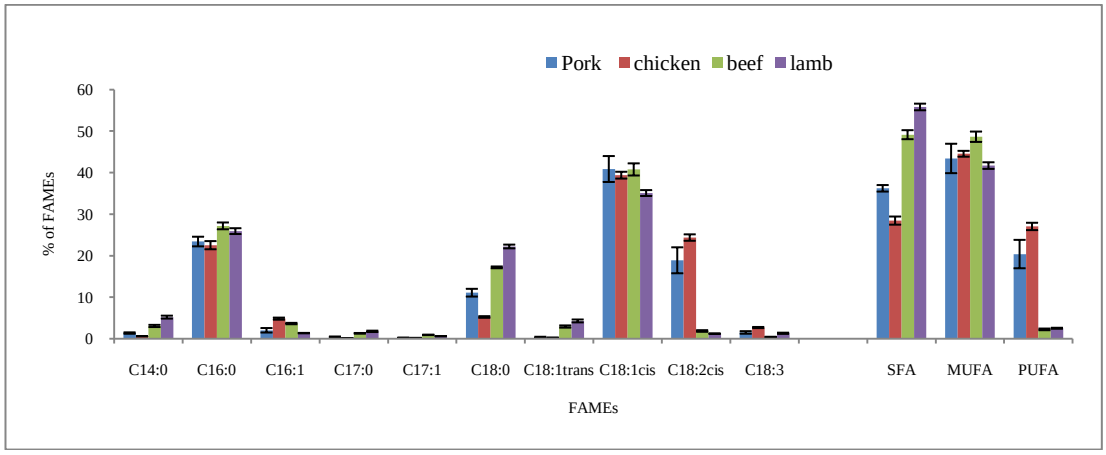

b)

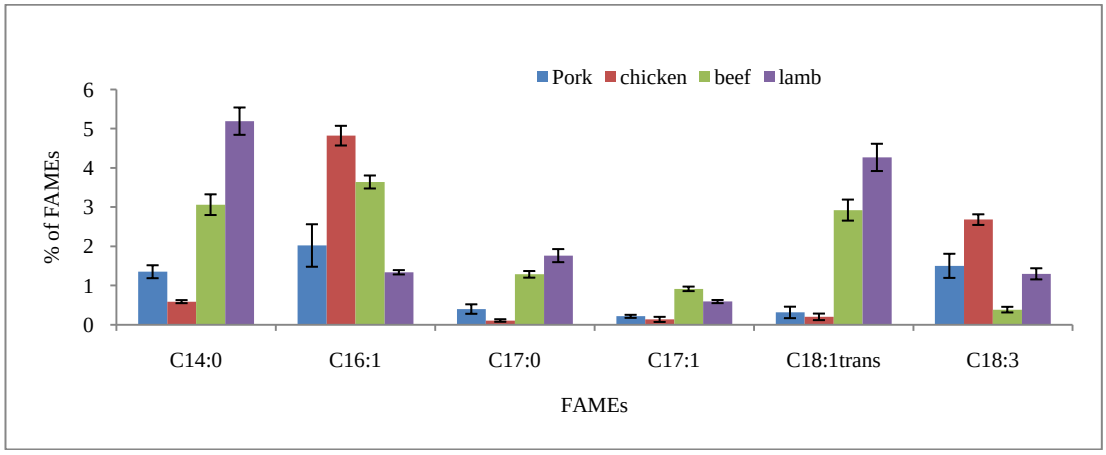

Figure 3.2: a) Percentages of FAMEs for beef, lamb, chicken and pork. b) Percentages of FAMEs for beef, lamb, chicken and pork (rescale to low relative abundance FAMEs).

For SFA, all the samples are significantly different with beef and lamb having much higher levels than pork and chicken. Chicken has the lowest content of SFA. By contrast, the proportion of MUFA for pork is similar to chicken and lamb. For beef, the MUFA is of a significantly higher level than the rest of the samples. The relative abundance of this group is significantly different for chicken, beef and lamb. Beef and lamb have similar levels of PUFA which are significantly lower than pork and chicken (representing about 20 to 30% of the PUFA).

The most abundant FAMEs in all the samples are C18:1*cis*, C16:0, C18:0 and C18:2*cis*; with the quantitative order being dependant on the animal type. For all species, the proportion of C18:1*cis* is highest, contributing about 35 to 40% of the total FA. Pork,

chicken and beef have similar proportions of this acid whereas lamb has a significantly lower proportion. The proportion of this acid for beef, about 41%, is higher than that reported by Enser et al. (1996; 36%); Woods et al. (2008; 35%) and Garcia et al. (2008; 31%) but lower than that observed by Suzuki et al. (2007; 48%). C16:0 is the next most abundant FA for pork, beef and lamb (about 23 to 27%). Pork and chicken have similar levels of this acid which are significantly lower than beef and lamb. Overall the fatty acid compositions of chicken in the current study are very close to those reported for chicken skin by Van Heerden et al. (2002).

C18:2*cis* is the next most abundant FA for chicken and the level is significantly higher than the rest of the species. C18:2*cis* is the major contributor to PUFA abundances in chicken and pork fat. All species have a significantly different level of this acid with beef and lamb having much lower levels ($\leq$ 2%) than chicken and pork.

Lamb has a significantly higher level of C18:0 than the other samples and chicken has the lowest proportion. Consequently, chicken has a significantly lower proportion of SFA than the rest of the species. All species have a significantly different level of this acid. The proportion of C18:0 for lamb in the current work is particularly high (about 4 to 9% higher than in the previous published work; Angood et al., 2008; Woods et al., 2008; Juarez et al., 2008 and Velasco et al., 2001). The value is, however, comparable to those reported by Enser et al. (1996). The higher value is probably due to the presence of IM fat in the samples, this fat contains more saturated FAs than the subcutaneous fat (Enser et al., 1996).

The percentages of C14:0, C17:0 and C18:0 were significantly different in all species, resulting in differences in their SFA contents. Chicken has the lowest proportion while lamb has significantly higher levels of those acids. C14:0 and C17:0 are present in higher amounts in lamb and beef than in chicken and pork and the differences are significant.

Chicken and pork fat contains very small levels of the *trans* isomer of C18:1 (less than 0.5%) whereas beef and lamb contain about 3 and 5%. This reflects rumen microbial biohydrogenation of C18:2 to produce either saturated FA C18:0 or C18:1 with the double bond *trans* (Woods et al., 2008). The rumen microbial biohydrogenation process also explains the lower abundance levels of C18:2 in beef and lamb than in chicken and pork. In addition, the essential FAs C18:2 and C18:3 cannot be synthesized in animals

due to mammals lacking the enzyme to form double bonds beyond the 9th carbon. This explains the significantly higher proportion of C18:2*cis*, C18:3 and PUFA for chicken than for beef and lamb, and the similarity to pork. C18:2*cis* in chicken and pig is unchanged from the stomach to tissues due to the absence of biohydrogenation processes within the gut, explaining the high contents in pork and chicken. For ruminants, only about 10% of C18:2 goes into tissues due to microbial biohydrogenation which transforms this acid into monounsaturated and saturated FA (Wood et al., 2008). The high proportion of C18:2 in pork in the current study is similar to that in published work in which pigs fed with high levels of C18:2 (grains and oil-seed) were found to have much higher proportions of C18:2 in both tissue (adipose and muscle) than cattle and sheep (Wood et al., 2008).

The relationship between SFA and PUFA shows discrimination of the samples into two classes: ruminant (beef and lamb which have high levels SFA and low levels of PUFA) and non-ruminat (chicken and pork) which have high levels of PUFA and low proportions of SFA (Fig. 3.3). This is because the monogastric animals, pig and chicken, incorporate substantial proportions of dietary plant acids such as C18:2 and C18:3 directly into their adipose tissue, resulting in much higher PUFA levels than in beef and lamb. By contrast, beef and lamb have similar levels of the most abundant SFA which is C16:0 and the levels are significantly higher than in chicken and pork. Furthermore, beef and lamb have significantly higher levels of C18:0 than chicken and pork, explaining the differences in their SFA contents.

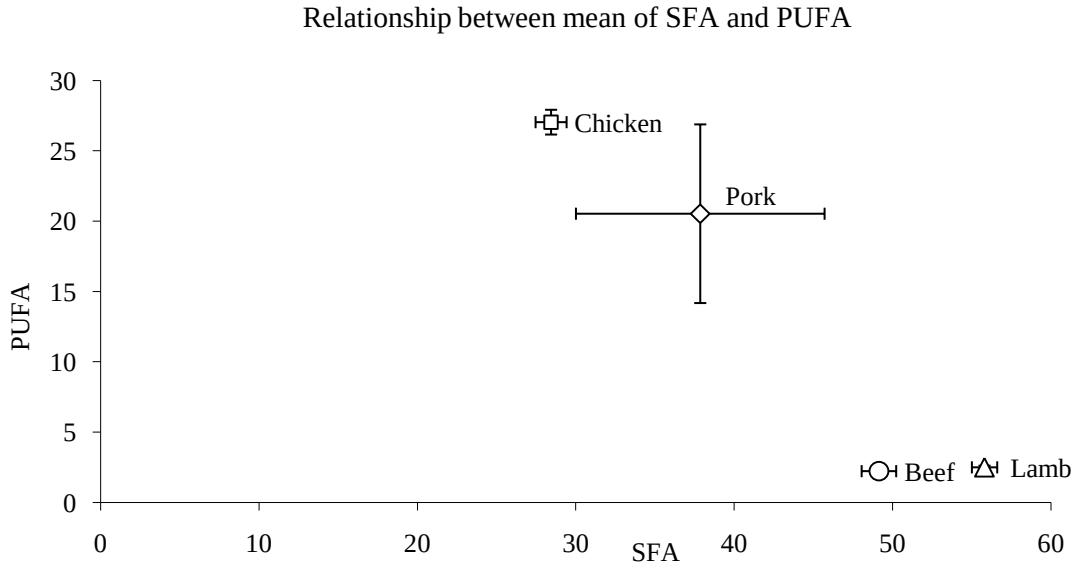

Figure 3.3: Relationships between mean of SFA and PUFA in animal fats.

3.2.2 FA profiles from different anatomical locations of pork adipose tissues

A total of twenty four samples of adipose tissue were taken from subcutaneous (SC) and intermuscular (IM) regions of three different pigs. The samples were from four different anatomical locations; ham, shoulder, loin and belly. The pigs were of the same breed (Tamworth), age (about 10 months) and gender (male) without controlled diet. Each sample was extracted with chloroform methanol (2:1) and triplicate analysis was performed. The FAMEs were analysed and identified as described in Section 3.2.1. The abbreviations used for different anatomical locations of pork fat are HIM (ham intermuscular), BIM (belly intermuscular), SIM (shoulder intermuscular), LIM (loin intermuscular), HSC (ham subcutaneous), BSC (belly subcutaneous), SSC (shoulder subcutaneous) and LSC (loin subcutaneous).

The most abundant FA peaks for the pork fat are: C16:0, C18:0, C18:1*cis* and C18:2*cis* (Fig. 3.1d). The individual FA peak areas are expressed relative to the total for all ten identified compounds, peak areas being the average of triplicate analysis from each of three different pigs. Total saturated FAs (SFAs) were calculated from a summation of C14:0, C16:0, C17:0 and C18:0, total monounsaturated FAs (MUFAs) from the total percentage of C16:1, C17:1, C18:1*trans* and C18:1*cis*, and polyunsaturated FAs (PUFAs) from the total of C18:2*cis* and C18:3 (Table 3.1).

The variations in the proportions of FAMEs between different anatomical locations were examined taking account of the Y-error bar at the 95% confidence level (two standard deviations) of the mean percentage of FAMEs (Fig. 3.4a). For low relative abundance FAMEs the histogram was rescaled (Fig. 3.4b).

Four compounds dominate the profile, being present in high relative abundance (C16:0, C18:0, C18:1*cis* and C18:2*cis*). By contrast, all the other compounds occur in very low levels ($\leq$ 2.5%). For all locations, the C18:1*cis* is the most abundant FA, followed by C16:0, C18:2*cis* and C18:0 each of which occur in high relative abundance. The relative abundance order is similar to the published report for hairless Mexican pig ham (Delgado et al., 2002) and also for muscle and subcutaneous adipose tissue from loin chops of pig purchased from various retail outlets (Enser et al., 1996). Notably, however, C18:0 occurred in higher relative abundance than C18:2*cis* in Iberian pigs (Timon et al., 2001), Celta pigs (Franco et al., 2006) and Duroc pigs (Suzuki et al., 2006).

Table 3.1: Mean percentages of FAMEs for different anatomical locations of pork adipose tissues.

FAMEs	Ham		Belly		Shoulder		Loin	
	IM	SC	IM	SC	IM	SC	IM	SC
C14:0	1.35	1.28	1.59	1.51	1.31	1.28	1.41	1.30
C16:0	23.39	22.26	27.55	25.15	24.48	25.17	23.55	22.34
C16:1	2.02	2.10	1.34	2.44	1.92	1.91	1.71	1.73
C17:0	0.40	0.33	0.34	0.27	0.41	0.39	0.36	0.43
C17:1	0.21	0.22	0.14	0.21	0.28	0.26	0.18	0.22
C18:0	11.07	11.13	14.91	10.55	12.95	13.18	11.41	9.81
C18:1t	0.31	0.31	0.17	0.14	0.22	0.22	0.18	0.27
C18:1c	40.86	44.47	31.73	39.29	40.33	39.74	39.03	38.63
C18:2c	18.88	16.59	20.37	18.84	16.79	16.53	20.34	23.17
C18:3	1.50	1.31	1.84	1.60	1.30	1.24	1.83	2.10
SFA	36.22	35.01	44.41	37.47	39.15	40.02	36.73	33.89
MUFA	43.41	47.10	33.38	42.09	42.76	42.08	41.10	40.84
PUFA	20.38	17.90	22.21	20.44	18.09	17.76	22.17	25.27

BIM has a significantly lower level of C18:1*cis* than BSC, ham (IM and SC) and SIM. Consequently, BIM has a significantly lower proportion of MUFA than BSC, ham (IM and SC) and SIM. Other locations have similar levels of C18:1*cis*. The percentage of C18:2*cis* for SIM is significantly lower than LSC and the proportions are similar in the rest of the samples. BIM has a significantly higher level of C18:0 and C16:0 than BSC and Ham (IM and SC). Consequently, BIM has a significantly higher proportion of SFA than BSC and ham (IM and SC).

The proportions of FAMEs in different anatomical locations were compared for subcutaneous and intermuscular (SC vs. IM), subcutaneous and subcutaneous (SC vs. SC) and intermuscular and intermuscular (IM vs. IM). Slightly different percentages of FAMEs were observed between different anatomical locations, the greatest differences being observed for SC vs. IM for belly and IM vs. IM for belly and ham samples.

Only belly shows significant differences between the SC and IM adipose tissues with significantly higher relative abundances of C18:1*cis* and C16:1 and significantly lower relative abundance of C18:0 in SC than IM. On average belly IM had about 4.4% more C18:0 and about 1.1 and 7.6% less C16:1 and C18:1*cis* than belly SC. This results in a significantly higher SFA content (about 6.9%) and a significantly lower MUFA content (about 8.7%) for the IM fat in the belly region. Although the proportions of individual FA in SC and IM were not significantly different for shoulder, loin and ham, the IM fat

contains more saturated FAs than SC fat: C14:0, C16:0 and C18:0 were higher in IM fat in all locations. In addition, MUFA levels were higher in SC fats than in IM fats in shoulder, loin and ham, consistent with the previous published report (Monziols et al., 2007).

a)

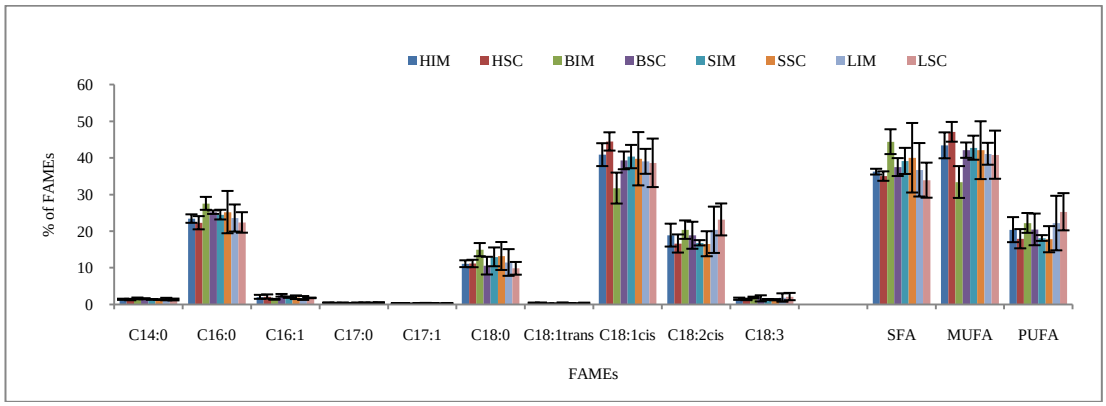

b)

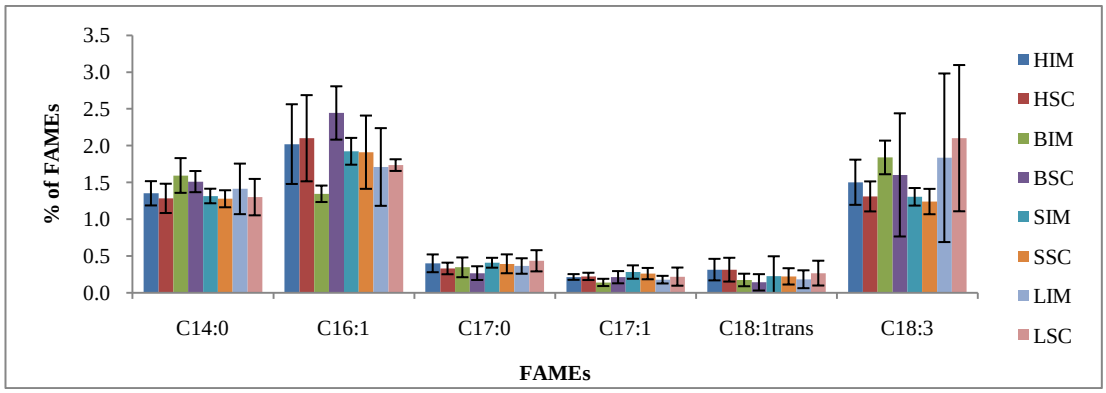

Figure 3.4: a) Percentages of FAMEs for different anatomical location of pork b) Percentages of FAMEs for different anatomical location of pork rescaled to low percentage of FAMEs).

The relative abundance of the C18:1*cis* FA for belly IM in the present study is much lower (about 10%) than in the published work on belly IM fat (Monziols et al., 2007). By contrast, the C18:2*cis* is much higher (about 10%) in the current work (compares well with Monziols et al., 2007). The differences in C18:1*cis* in the SC and IM fat layers for belly could be due to differences in the activity of the stearoyl Co-A desaturase enzyme in the various adipose tissues. A previous published study showed that the

activity of stearoyl Co-A desaturase enzyme was higher in the SC adipose tissue than in perirenal fat, explaining the difference in the monounsaturated FA content of different fat layers (Thompson et al., 1969). A study found that lipogenic enzyme activities were higher in the adipose tissue of pigs fed a diet containing 4% maize oil than pigs fed a diet containing 4% tallow. Notably, however, diet has no effect on lipogenesis in the muscle (Kouba and Mourot, 1999).

Comparison between SC fat from different locations (SC vs. SC) shows that belly has a significantly higher proportion of C16:1 (about 0.7% higher) than loin. Also, belly contain significantly higher levels of C16:0 (about 2.9%) and lower levels of C18:1*cis* (about 5.0%) than ham (Fig. 3.5a). These differences result in MUFA being statistically lower in belly (about 5.2%) than in ham. No other locations show significant differences of FAs of SC fats.

The IM fats of different locations (IM vs. IM) show that belly has statistically different relative abundances of C16:1, C18:1*cis*, C18:2*cis*, C18:3, MUFA and PUFA from shoulder (Fig. 3.5b). The PUFA content of belly IM is significantly higher (about 4.0%) than shoulder IM, resulting mainly from the significantly higher levels of C18:3 (about 0.5%) and C18:2*cis* (about 3.6%) in belly. MUFA levels are, however, significantly higher (about 9.4%) in shoulder than in belly due to significantly higher levels of C18:1*cis* (about 8.6%) and C16:1 (about 0.6%).

Belly IM fat also has significantly higher relative abundances of C16:0 (about 4.2%) and C18:0 (about 3.8%) than ham IM fat, giving a significantly higher SFA content (about 8.2%). By contrast, the proportions of C18:1*cis* and C16:1 were significantly higher (about 9.1% and 0.7%) for ham than for belly, leading to the percentage of MUFA for ham being significantly higher (about 10.0%) than for belly. BIM has a significantly lower level of C18:1*cis* than other fat locations. Consequently, BIM has a significantly lower proportion of MUFA than the rest of the samples. The results show that differences in the proportions of FAs occur not only within different fat layers but also in different locations.

a)

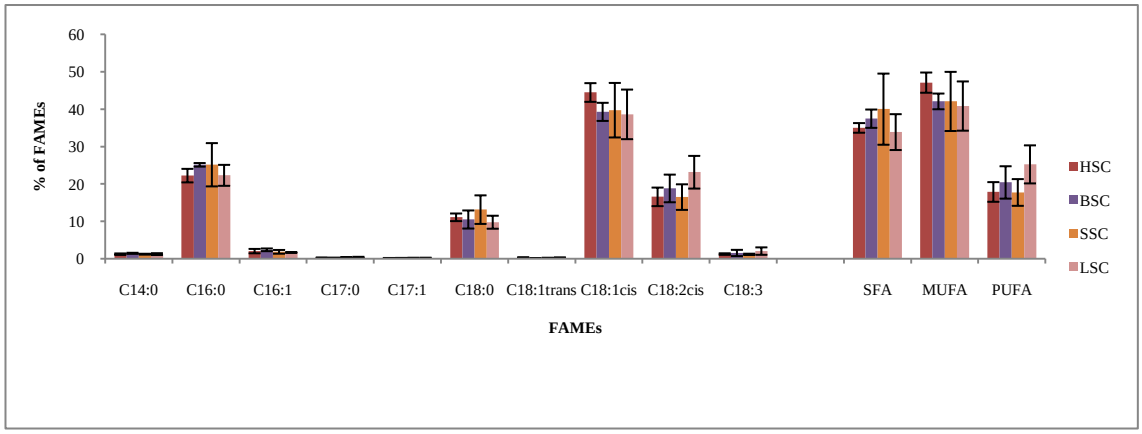

b)

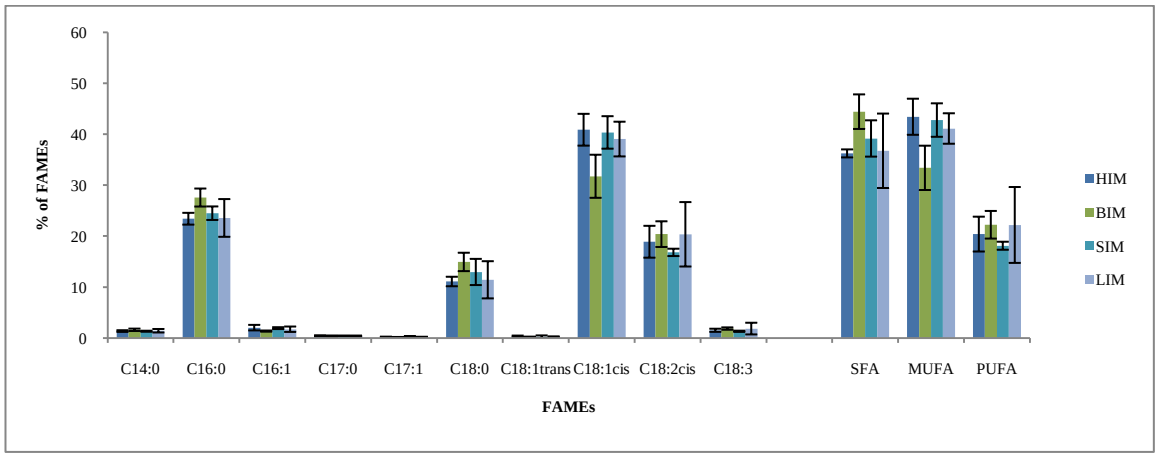

Figure 3.5: a) Percentages of FAMEs for SC fats of pork b) Percentages of FAMEs for IM fats of pork.

Each location studied show a discrimination between belly IM fat and other fat locations (Fig 3.6). Belly IM fats have much higher SFAs than ham IM and much lower MUFAs for IM than other locations. The proportion of SFAs for belly IM fats in the present study is similar to the published report, but the proportion of MUFA is much lower (about 11%) in the present work (Monziols et al., 2007). The proportion of MUFAs for Ham SC fats in the current work is about the same as for ham in the published works (Monziols et al., 2007 and Delgado et al., 2002), though the proportion of SFAs in the present study is slightly lower (about 5% lower compared with Monziols et al., 2007 and about 2% lower than Delgado et al., 2002).

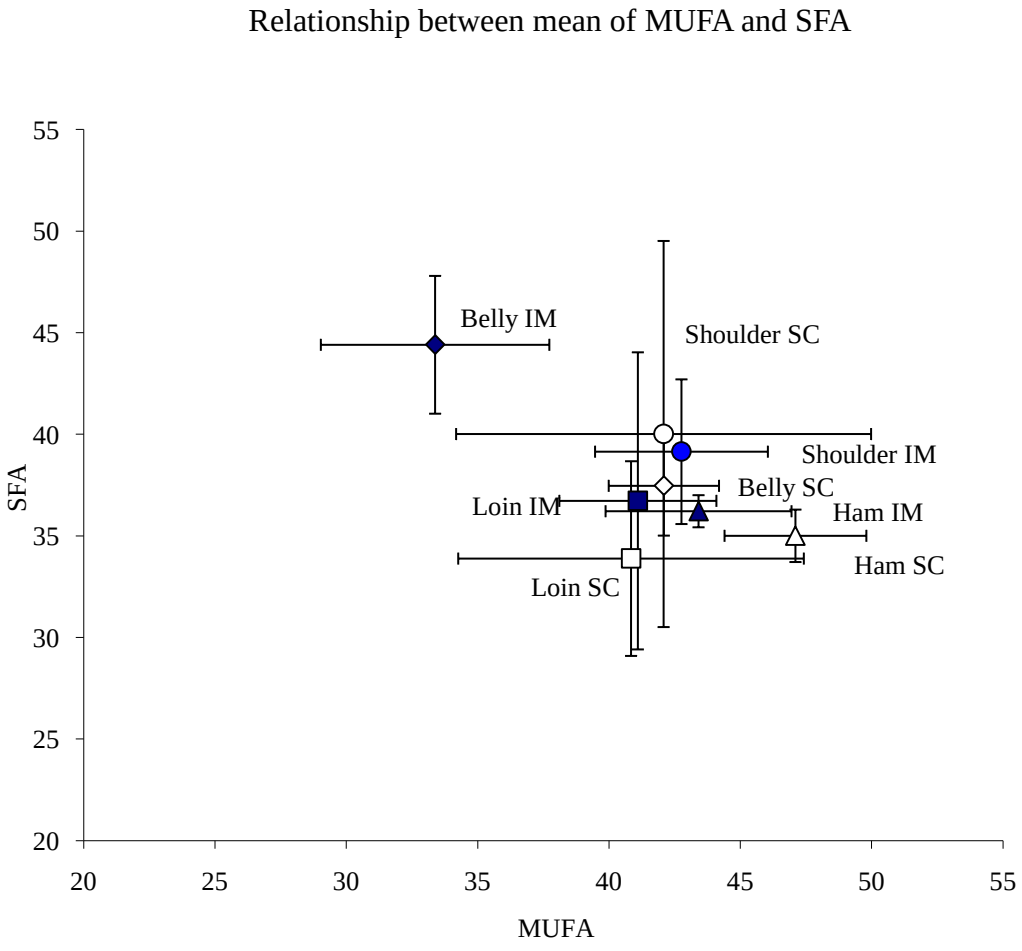

Figure 3.6: Relationships between mean of MUFA and SFA from different anatomical locations of pork adipose tissues.

The PUFA contents show considerably spread for different locations (about 17% in shoulder SC to 25% in loin SC; Fig 3.7). The study on the fat compositions of different locations in Iberian pig carcasses found that IM fat of *biceps femoris* had the highest percentage of MUFA and the lowest percentage of PUFA (Vazquez et al., 1996). Overall, PUFA contents for all the fat locations in the present study are much higher than in the previous work (Enser et al., 1996; Delgado et al., 2002; Franco et al., 2006; and Monziols et al., 2007). This could be due to the diet of the pigs used in the present study, which might contain higher levels of linoleic acid (C18:2) which contributes about 93% of the PUFA content in the fat samples. This acid cannot be synthesized and comes entirely from the diet. The previous published study on pigs fed with various dietary levels of sunflower seed found that, for pig muscle, deposition of linoleic acid is proportional to the level in the feed (Marchello et al., 1983).

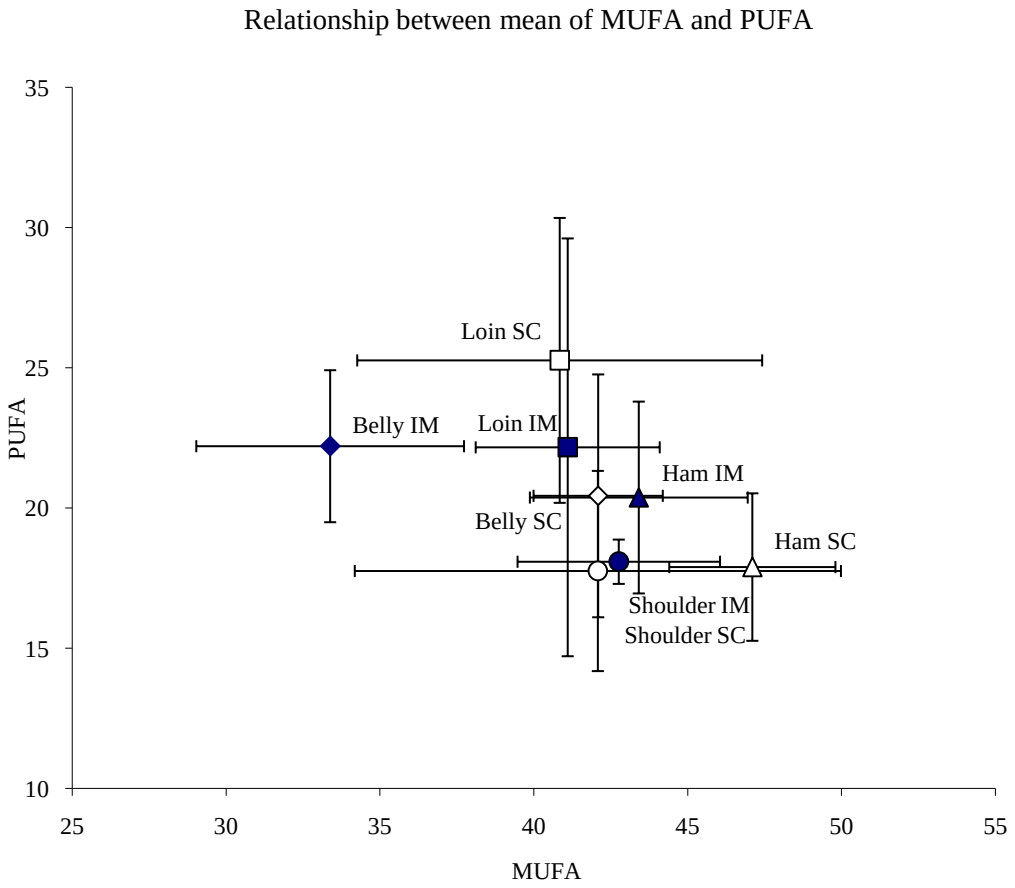

Figure 3.7: Relationships between mean of MUFA and PUFA from different anatomical locations of pork adipose tissues.

.

3.2.3 TAG profiles of beef, lamb, chicken and pork.

The TAGs analyses were performed for samples of beef sirloin steak, lamb chop, chicken and pork (ham intermuscular fat) from the same samples as were used for FAME analysis in Section 3.2.1. Each sample was analysed in replicate (≥ 5). The TAGs were separated by An Ultimate 3000 (Dionex) HPLC coupled to ion trap MS with APCI ionization using the mobile phase combination of acetonitrile and dichloromethane system developed in Section 2.2.3.1 with slight modification (Method J; Chapter 6; Section 6.2.4). The TAG profiles were identified following the detailed in Section 2.2.3.3.

Eighteen abundant TAGs were identified in beef, seventeen in lamb, twenty four in chicken and twenty one in pork (Figs. 3.8a to d; Table 3.2). Apart from the slight differences in the relative abundances of some of the compounds, the TAG profiles of beef/lamb and chicken/pork were most similar to each other. The TAGs containing O, P and S dominate the chromatograms of beef and lamb (OOP*, POP, SOP*, OOS* and SOP*). By contrast, relatively high proportions of L, Ln and O are present in pork and chicken fat, reflected by the shorter retention times of TAGs such as LLLn*, LLL, OLnL*, PLLn*, LLO*, LLP*, LnOP*, OLO*, LPO* and OOP*/OPO.

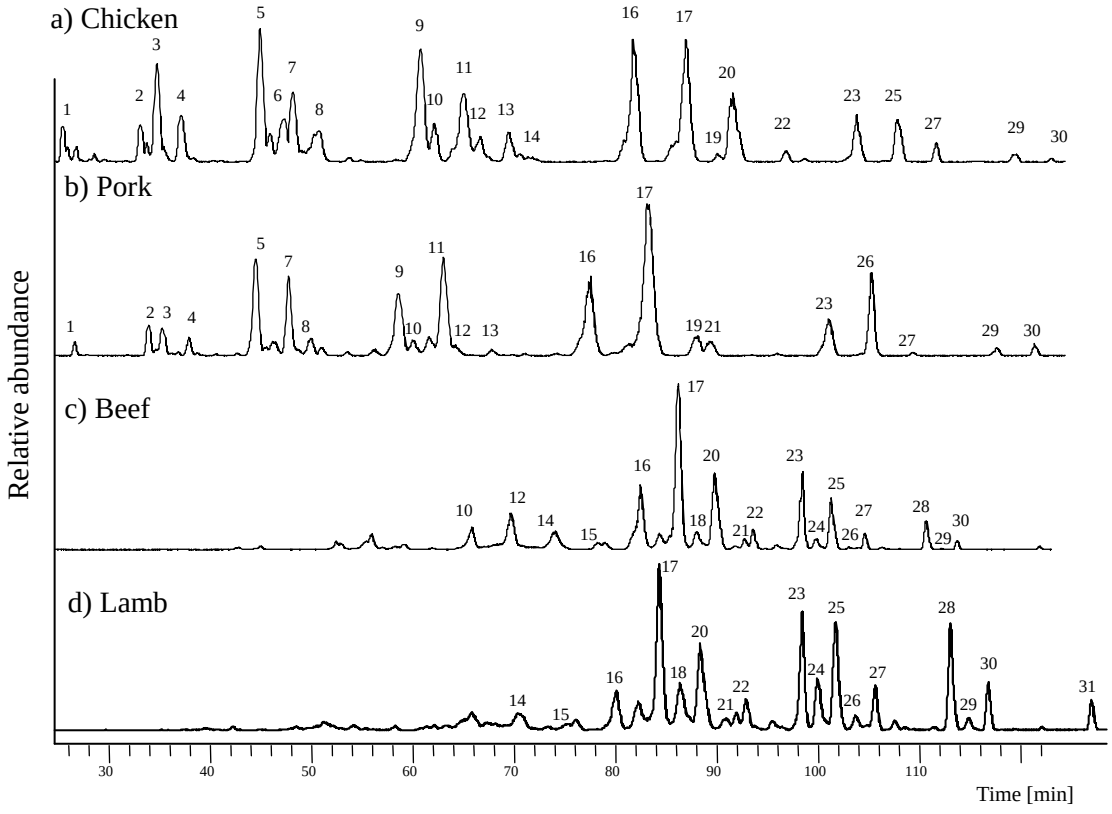

Figure 3.8: Chromatograms of TAGs for a) Chicken, b) Pork, c) Beef and d) Lamb.

The individual TAG peak areas of all eighteen identified compounds for beef, all seventeen for lamb, all twenty four for chicken and all twenty one for pork are expressed relative to the total peak area (Table 3.2). Three compounds dominate each profile, being present at high relative abundance in pork (LPO*, OPO and SPO*), chicken (OLO*, LPO* and OOP*), beef (OOP*, POP and OPPo*) and lamb (OOP*, SOP* and OOS*). OOO, OOS*, PPS*, SSO* and SPS* are the TAGs present in all the samples analysed.

Table 3.2: Mean percentages of TAGs for different animal species analysed by RP HPLC-APCI MS/MS (Method J; Chapter 6; Section 6.2.4).

TAGs	Peak No.	Chicken	Pork	Beef	Lamb
LLLn*	1	1.73	0.68	-	-
LLL	2	2.19	1.95	-	-
OLnL*	3	5.90	1.72	-	-
PLLn*	4	3.25	1.38	-	-
LLO*	5	8.63	6.75	-	-
OLnO*	6	3.53	-	-	-
LLP*	7	4.14	7.05	-	-
LnOP*	8	3.49	1.98	-	-
OLO*	9	13.61	9.03	-	-
OOPo*	10	2.97	0.10	3.66	-
LPO*	11	11.43	18.84	-	-
OPPo*	12	2.72	0.21	10.06	-
PPL*	13	1.61	1.48	-	-
POM*	14	0.67	-	5.00	3.50
PMO*	15	-	-	0.26	0.66
OOO	16	7.19	5.62	7.02	3.32
OOP*	17	11.54	-	30.49	20.11
OPO	18	-	17.73	3.02	7.07
LPS*	19	0.70	5.82	-	-
POP	20	5.53	-	10.43	7.77
PPO*	21	-	3.03	0.43	1.27
SMP*	22	0.60	-	2.26	3.22
OOS*	23	3.04	3.82	9.19	10.12
OSO	24	-	-	1.49	5.70
SOP*	25	3.67	-	9.73	16.29
SPO*	26	-	11.08	0.51	2.43
PPS*	27	0.82	0.53	2.00	3.98
SOS	28	-	-	3.14	8.16
SSO*	29	0.76	0.23	0.17	1.44
SPS*	30	0.28	0.80	1.08	3.66
SSS	31	-	-	-	1.52

- Not considered due to the low relative abundances (≤ 0.1%).

The variations in the proportions of TAGs between different species were examined taking account of the Y-error bar at the 95% confidence level (two standard deviations) of the mean percentage of TAGs (Fig. 3.9). The proportion of OOP* for beef dominates the histogram and is significantly higher than for lamb and chicken. All species show significant differences in the relative abundance of OOP*. LPO* is the most abundant TAG in pork and the level is significantly higher than in chicken. This TAG was not identified in beef and lamb. The relative abundances of OPO, SPO* and PPO* are significantly different for pork, beef and lamb. Pork has the highest levels of OPO, SPO* and PPO*, and lamb the next highest.

Lamb has significantly higher levels of PPS*, SSO* and SPS* than the rest of the samples. The proportion of SPS* in the current study is lower than previous report (about 4.5% lower, Mottram et al., 2001). Beef and lamb have similar levels of OOS*, these being significantly higher than for chicken and pork. The proportion of OOO for lamb is significantly lower than for beef and chicken. Pork, chicken and beef have similar levels of this TAG.

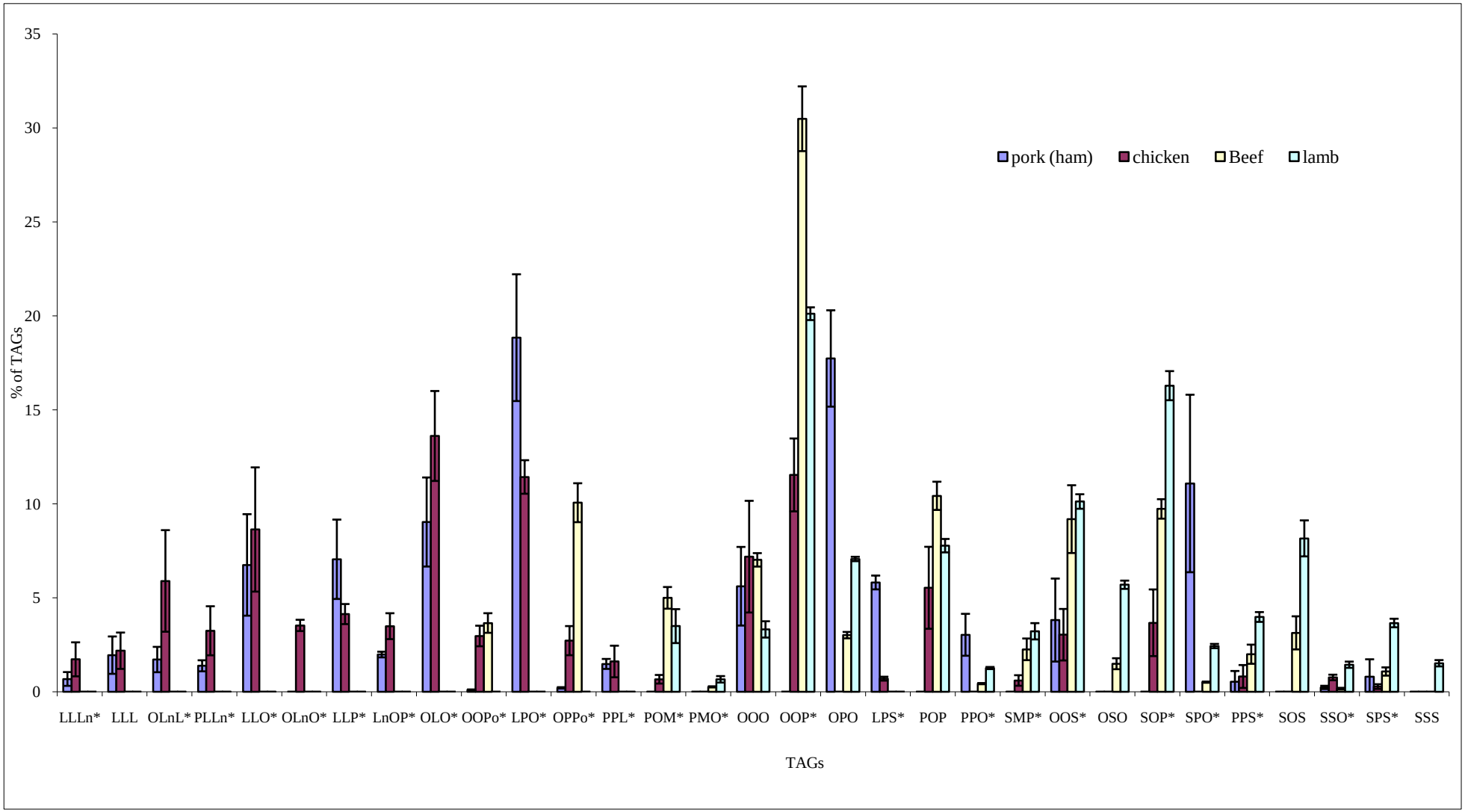

Figure 3.9: Histograms for the proportions of TAGs for pork, chicken, beef and lamb.

Comparison between pork and chicken shows that for LLLn*, LLL, LLO*, OLO*, PPL*, OOO, OOS*, PPS* and SPS*, the TAGs contents for pork and chicken are not significantly different (Fig.3.10a). OLnL*, PLLn*, LnOP*, OOPo*, OPPo* and SSO* have significantly higher levels in chicken than in pork whereas pork has significantly higher levels of LLP*, LPO* and LPS* than chicken. OLnO* is only observed in chicken.

Although beef and lamb are both ruminants, the TAG profiles show that lamb has statistically higher relative abundances of PMO*, OPO, PPO*, SMP*, SOS, SOP*, SPO*, PPS*, SOS, SSO* and SPS* than beef, whereas beef contains significantly higher levels of OOO, OOP* and POP than lamb (Fig. 3.10b). Only the proportions of POM* and OOS* in beef are similar to lamb. Even though SSS is detected in the beef fat (Fig. 2.21a in Section 2.2.3.5) and in the previous work (about 3.44% of SSS in beef fat; Mottram et al., 2001) there were no sign of SSS observed in the beef sirloin steak. This could be due to the very low proportion of this TAG in beef meat compared with their fat.

Comparison between pork and beef shows considerable difference in the TAG profiles (Fig. 3.10c). Beef contains significantly higher levels of OOPo*, OPPo*, SMP*, OOS*, PPS* and SOS and lower levels of OPO and SPO* than pork. Only the proportions of SPS* and OOO are similar in beef and pork. The TAGs containing L are only observed in pork and not in beef.

Comparison between chicken and lamb shows similarities exist that only the proportion of POP (Fig. 3.10d). The TAGs containing L were observed in chicken but not in lamb. For the TAGs containing S, the levels are significantly higher in lamb than in chicken (e.g. OOS*, SOP*, PPS*, SSO* and SPS*).

a)

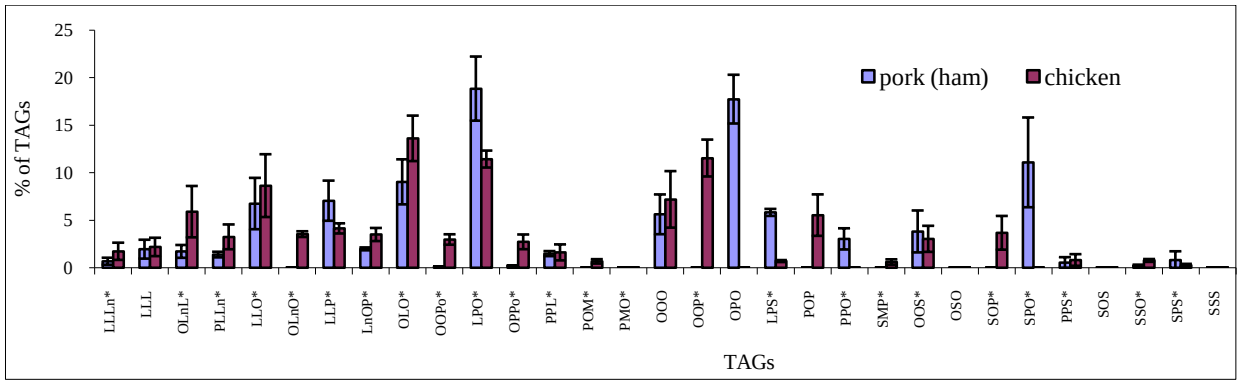

b)

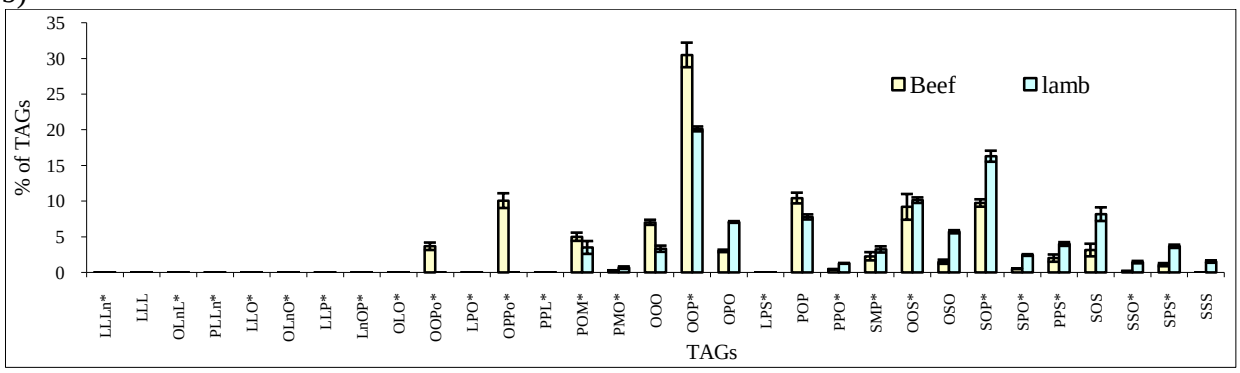

c)

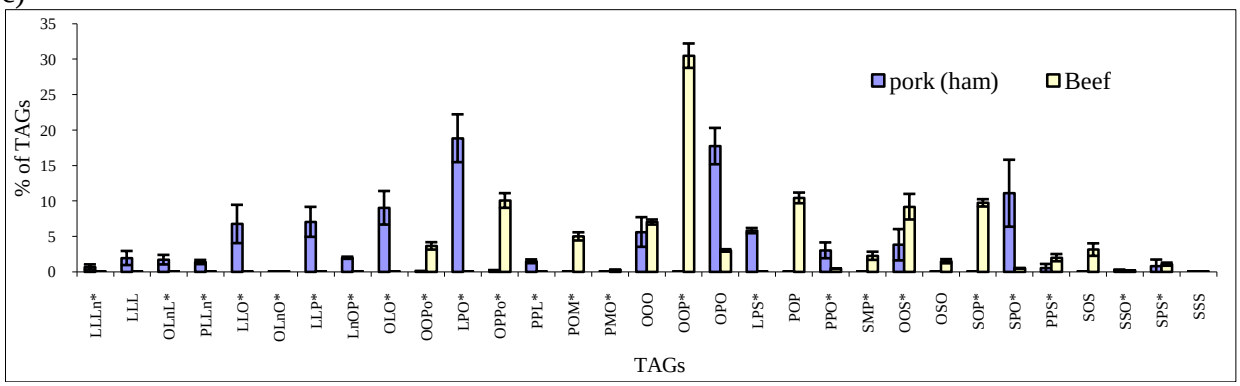

d)

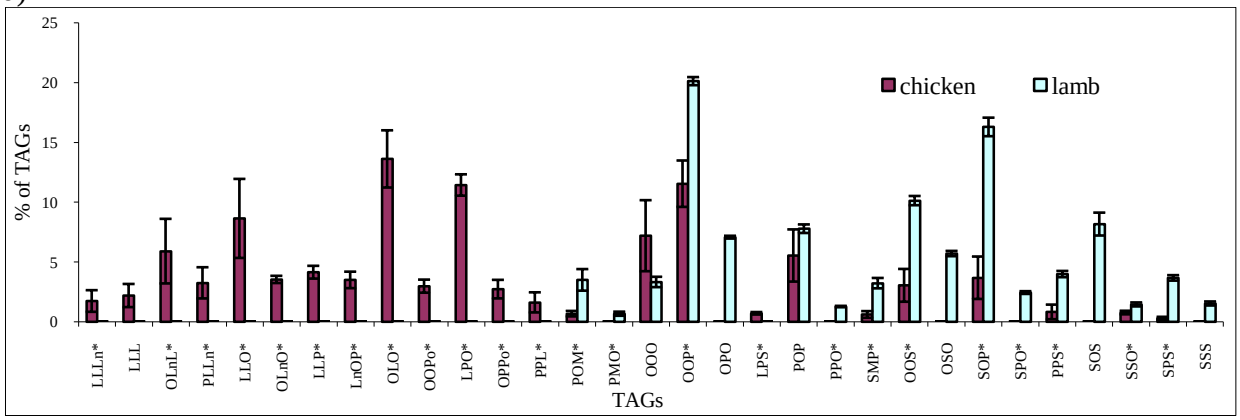

Figure 3.10: Histograms for the proportions of TAGs of a) pork and chicken b) beef and lamb c) pork (ham) and beef and d) chicken and lamb.

The TAG profiles of fats reflect their FA compositions, showing a high proportion of unsaturated FAs for chicken and pork, the major TAGs detected being LPO*, OPO, LLP*, LLO* and OLO* in which the acids (O, L and P) represent about 88% (about 64% from O and L, and 24% from P) of the total FA in GC. In beef and lamb, saturated FAs are dominant in the major TAGs detected: SOP*, SOO, SPP, SSP and SOS; and these acids (O, P and S) represent about 85% (about 40% from O and 45% from P and S) of the total FAs in GC.

The comparison of the FA and TAG contents in samples is somewhat affected by trace FAs not being identified in HPLC/APCI-MS: one FA may be distributed among many different combinations in TAGs which results in TAG concentrations that are below the detection limit. Furthermore, the co-elution of trace TAGs with more abundant TAGs may prevent the identification of constituent trace FAs. In this study all the FAs identified in the samples detected by GC were observed in the TAG compounds analysed by HPLC/APCI-MS. The odd carbon numbered FAs, for example C15:0 and margaric acid, are also resolved in TAGs during separation by HPLC-MS. One advantage of TAG analysis is that it is not necessary to saponify the fat extract to obtain methyl ester of FAs, simplifying the analytical procedure and avoiding the production of artefacts and sample alteration. Furthermore, the TAG compositions of pig tissues show higher sensitivity than FA compositions in assessing the influence of the diet, since the rates of increase of some TAG markers are higher than for the corresponding FA markers (Pascual et al., 2007b).

3.2.4 TAG profiles of adipose tissue for different anatomical locations of pork.

The TAGs analyses were performed for twenty four samples of subcutaneous (SC) and intermuscular (IM) regions from ham, shoulder, loin and belly of pigs. The samples used were the same as for the FAMEs analysis reported in Section 3.2.2. The TAGs were analysed and identified as described in Section 3.2.3. The abbreviations used for different anatomical locations of pork fat were given previously (Section 3.2.2).

Twenty one peaks in the chromatograms of pork fat from different anatomical locations were identified as TAGs (Figs. 3.11a to d; Table 3.3). Apart from the slight differences in the relative abundances of some of the compounds, the TAG profiles from different anatomical locations are very similar.

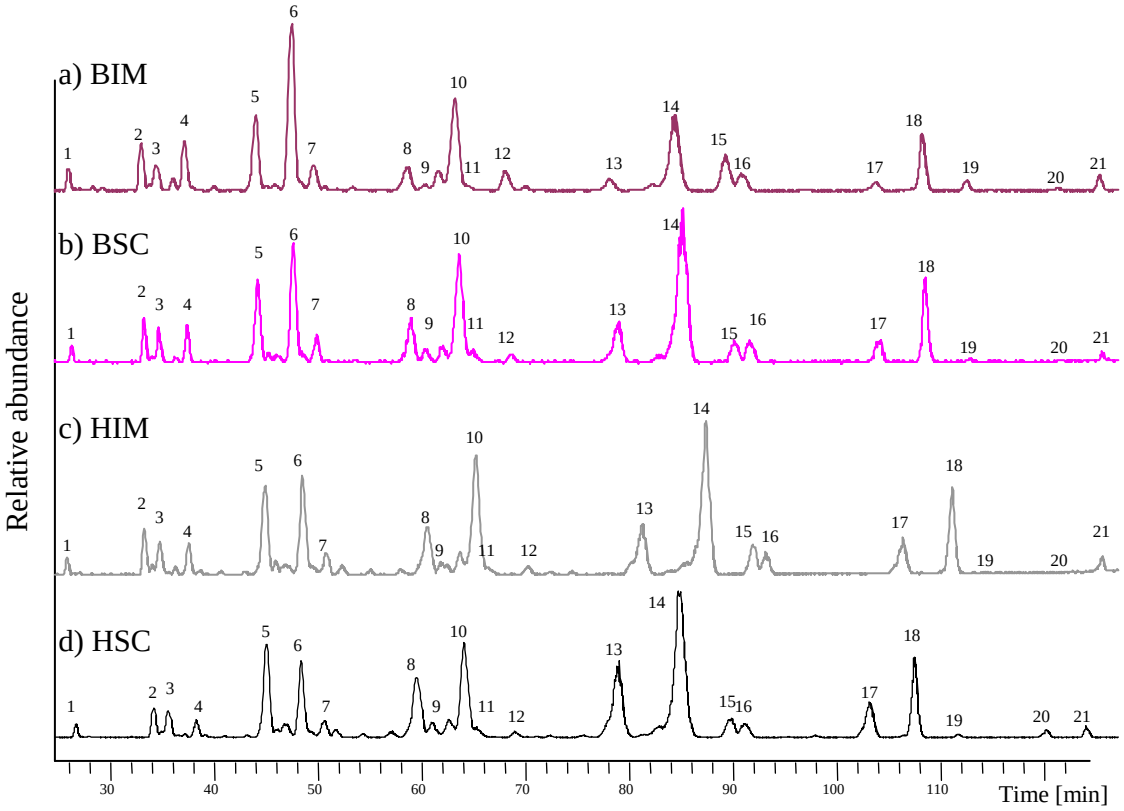

Figure 3.11: Chromatograms of TAGs for a) BIM, b) BSC, c) HIM and d) HSC (Refer to Table 3.3 for identification of TAGs peak).

The individual TAG peak areas are expressed relative to the total for all twenty one identified compounds, peak areas being the average of duplicate analysis from each of three different pigs (Table 3.3).

Table 3.3: The mean percentage of TAGs for different anatomical locations of pork fat (Method J; Chapter 6; Section 6.2.4).

TAGs	Peak No.	Ham		Belly		Shoulder		Loin	
		IM	SC	IM	SC	IM	SC	IM	SC
LLLn*	1	0.68	0.50	0.72	0.83	0.48	0.30	0.53	0.83
LLL	2	1.95	1.40	1.72	2.17	1.12	1.07	1.38	2.28
OLnL*	3	1.72	1.48	1.38	1.85	1.12	1.12	1.52	2.20
PLLn*	4	1.38	1.10	2.08	1.92	1.05	0.98	1.35	1.78
LLO*	5	6.75	5.97	4.83	6.62	4.53	5.00	5.52	7.50
LLP*	6	7.05	5.42	9.23	8.60	4.83	5.32	7.08	8.62
LnOP*	7	1.98	1.88	2.13	2.35	1.78	1.75	2.18	2.40
OLO*	8	9.03	9.32	4.28	6.62	8.28	7.82	7.97	9.42
OOPo*	9	0.10	0.10	0.05	0.07	0.09	0.09	0.09	0.10
LPO*	10	18.84	17.36	20.49	20.80	16.60	18.94	21.68	20.80
OPPo*	11	0.21	0.19	0.23	0.23	0.18	0.21	0.24	0.23
PPL*	12	1.48	1.33	2.30	1.53	2.08	1.60	1.72	1.63
OOO	13	5.62	6.94	1.90	3.39	5.92	5.49	4.58	4.42
OPO	14	17.73	20.03	16.35	20.1	18.37	21.33	18.52	15.28
LPS*	15	5.82	4.87	10.08	4.77	7.60	6.33	6.78	5.98
PPO*	16	3.03	3.05	3.67	3.12	4.42	3.73	3.90	2.63
OOS*	17	3.82	4.97	2.15	2.73	4.97	3.75	3.47	3.08
SPO*	18	11.08	12.27	13.93	11.20	13.80	13.35	10.60	9.35
PPS*	19	0.53	0.63	1.18	0.45	1.15	0.75	0.42	0.55
SSO*	20	0.23	0.29	0.08	0.14	0.25	0.23	0.19	0.18
SPS*	21	0.80	1.00	1.25	0.50	1.52	0.88	0.37	0.85

Three compounds dominate the profile, being present in high relative abundance (LPO*, OPO and SPO*). By contrast, several compounds occur in very low level ($\leq 0.5\%$), such as OOPo*, OPPo* and SSO*. The variations in the proportions of TAGs between different anatomical locations were examined taking account of the Y-error bars at the 95% confidence level (two standard deviations) of the mean percentage of TAGs (Fig. 3.12a and b).

For all locations, LPO*, OPO and SPO* are the three most abundant TAGs; LPO* being the most abundant except for shoulder and HSC where OPO is the most abundant TAG. These TAGs accounted for about 45 to 54% of the total TAGs and contain O, P, L and S, the major FAs in pork fat. It is shown in previous studies that the two most abundant TAGs of pork are OPO and SPO (Mottram et al., 2001; Dugo et al., 2006; Fauconnot et

al., 2004 and Viera Alcaida et al., 2007). The slight differences in the result obtained here could be due to differences in the diet of the animal studied. The effect of diet on the TAG profiles of Iberian pigs were examined and samples from the *montanera* (acorn and pasture) type yielded higher levels of OOO and OOL, while for the *cebo* (commercial feed, combination of acorn and grain) PSO was the most abundant TAG (Viera Alcaida et al., 2007). Acorn is high in oleic (60%) and linoleic (27%) acids, which together constituted more than 80% of the total FA (Leon-Camacho et al., 2004).

Comparison between SC fat from different locations (SC vs. SC) shows no significant differences were observed for TAG profiles in all the fat locations. The IM fats of different locations (IM vs. IM) show that belly has statistically higher relative abundances of LLP* and lower levels of OLO*, OOO and OOS* than shoulder, resulting mainly from the significantly higher level of C18:2*cis* in belly. Also, belly contains significantly higher levels of LPS* and lower levels of OLO* than ham, resulting from higher levels of C16:0 and lower levels of C18:1*cis* in belly than in ham. The OOS* content of shoulder IM fat is significantly higher than loin IM fat. No other locations show significant differences of TAGs in IM fats. Comparison between SC and IM fats for each location (SC vs. IM) shows that belly IM fat contains significantly higher levels of LPS* than belly SC. No significant differences were observed for other locations.

The relative abundance of LPO* is much higher than in the previous work (Diaz et al., 1996). The proportions of LPO* show that SIM has a significantly lower level than BSC, LIM and LSC. Furthermore, the percentage of LPO* for all SC fats are similar to the corresponding IM fats in the current study whereas the previous study found that IM fat had higher percentages of LPO* than SC for Iberian pigs fed with acorns (Diaz et al., 1996). For all locations, the proportion of OPO is similar, ranging from 15.3 to 21.3%. This range is about the same as found by Dugo et al., 2006 but is much lower than found for Iberian pigs by Viera-Alcaide et al., 2007 (≈ 32%) and Diaz et al., 1996 (32 to 35%).

No significant differences were observed for SPO*, LLO*, PPO*, SPS*, PPS*, LnOP*, OLnL*, LLL and LLLn* among all of the fat locations. The relative abundance of OOO is similar in IM and SC fat for all locations. By contrast, the SC fat had lower levels of OOO than IM fat in the previous study (Diaz et al., 1996). BIM has a significantly lower level of OOO than IM and SC fat of shoulder and HSC. The average percentage of OOO (≈ 5.2%, not including the percentage of BIM) compares reasonably well with levels

determined by Mottram et al., 2001(≈6.8%) and Dugo et al., 2006 (5.6%) but is much lower than the value reported by Viera-Alcaide et al., 2007 (11.8%) and Diaz et al., 1996 (≈12%). OOO is among the most promising TAG along with PSO, to discriminate Iberian Pigs raised on the two different feeding systems of *montanera* and *cebo* (Viera-Alcaide et al., 2007) and also to act as markers of the activation/inhibition of monounsaturated TAG synthesis (Pascual et al., 2007).

SIM is the only location which has significantly higher levels of OOS* than belly (IM and SC fat) and LIM. For LPS*, the only significant difference observed is for BIM, which has a higher content of this TAG than their SC fats and ham (IM and SC). By contrast, BIM has a significantly lower level of OLO* than ham and shoulder (IM and SC). This work represents the first detailed comparison of the TAG profiles for different anatomical locations of pig and reveals important differences between belly IM fat and other locations.

a)

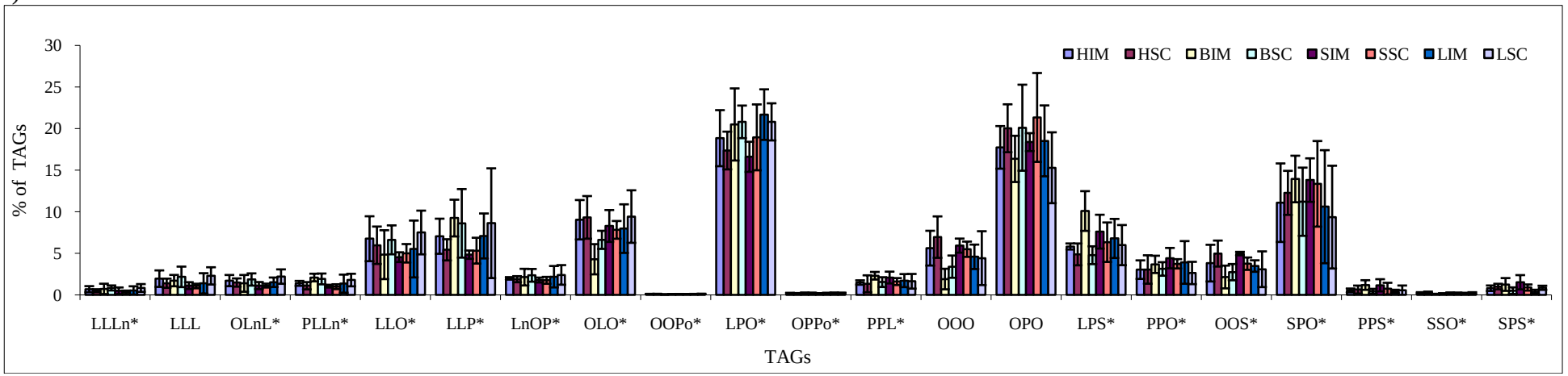

b)

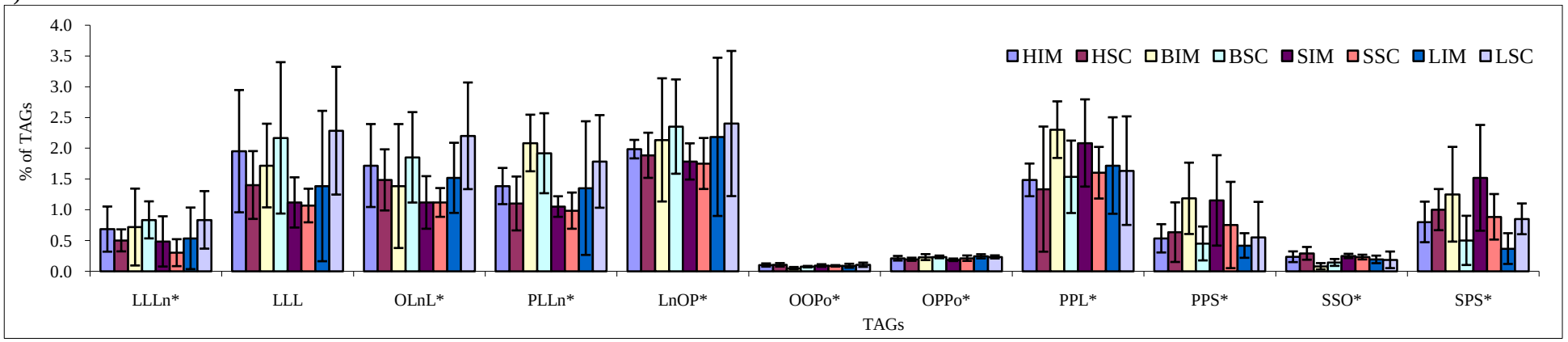

Figure 3.12: Histograms of the percentages of TAGs for a) different location of pork b) different location of pork (rescaled to low relative abundance of TAGs).

3.2.5 PCA of FAME and TAG profiles for different animal species.

3.2.5.1 PCA of FAMEs for beef, lamb, chicken and pork.

The FAME profiles of beef, lamb, chicken and pork were analysed by application of PCA to explore the extent of variation between different animal species. All the FAMEs identified in the samples were analysed. The SFA, MUFA and PUFA levels were analysed separately. The first two principal components in the PCA scores plot show the distribution of different animal species according to their FAMEs and with 85% of the variance being explained; 66% from the first component (PC1) and 19% from the second one (PC2, Fig. 3.13). No overlap occurs between different animal species though chicken plots very close to the pork fat, particularly the ham and loin. Their proximity indicates similarity in their FAME profiles. Beef and lamb are separated well and no overlap is observed between them and they are also isolated from pork fat.

Species are divided into two classes in PC1: beef/lamb and chicken/pork as shown in the scores plot. The loadings plot for PC1 reveals the FAMEs that discriminate these groups as those having high positive and high negative loadings values (Fig. 3.14a). The positive loadings are consistent with beef/lamb having significantly higher levels of SFA reflected in the higher proportions of C14:0, C17:0, C16:0, C18:0 and C18:1*trans* than in chicken/pork. The negative loadings values represent the significantly higher levels of C18:2*cis* in chicken/pork than in beef/lamb a consequence that is also reflected in the differences in their PUFA contents. Thus, the differences in the SFA and PUFA levels of beef/lamb and chicken/pork contribute much to the discrimination on PC1. Even though the C14:1, C15:0 and C15:1 occurred only in low levels in beef and lamb, the PCA shows them to be important in the discrimination. Only C18:1*cis* and C16:1 stand out as contributing very little to PC1, both have negative loadings values. Also, C18:3 do not contribute as much to the discrimination on PC1.

Beef and lamb are separated well in PC2. Beef plots close to pork ham and lamb plots close to the pork shoulder and loin. C18:1*cis* is the most important descriptor having the highest negative loading, followed by C16:1 and C16:0 (Fig. 3.14b). The substantial variations of C18:1*cis* and C16:0 for different locations of pork cause chicken and beef to plot close to pork ham. The proportion of C16:1 for chicken is significantly higher than for other samples, making chicken plot separately.

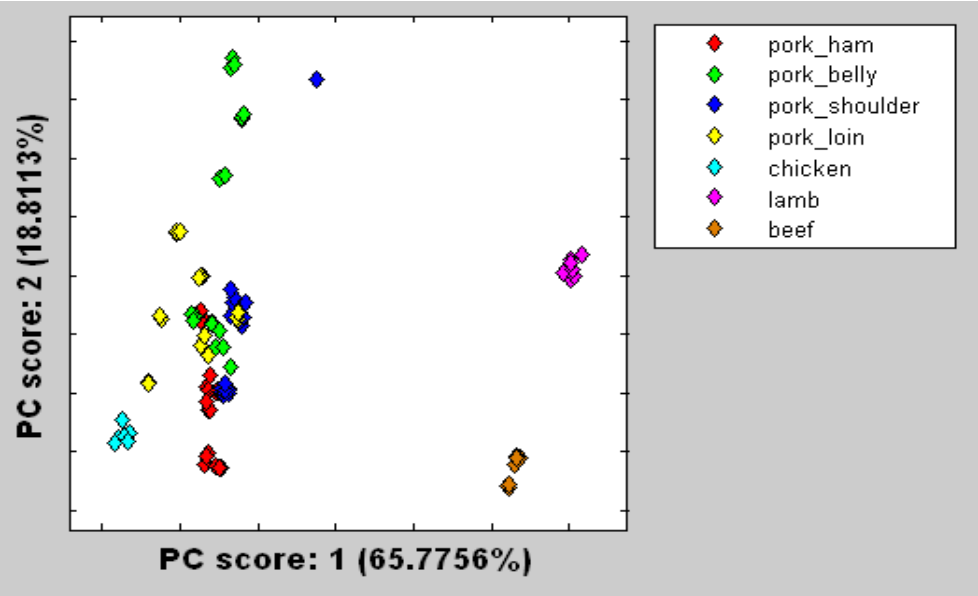

Figure 3.13: PCA scores plot of FAMEs in different animal species.

a)

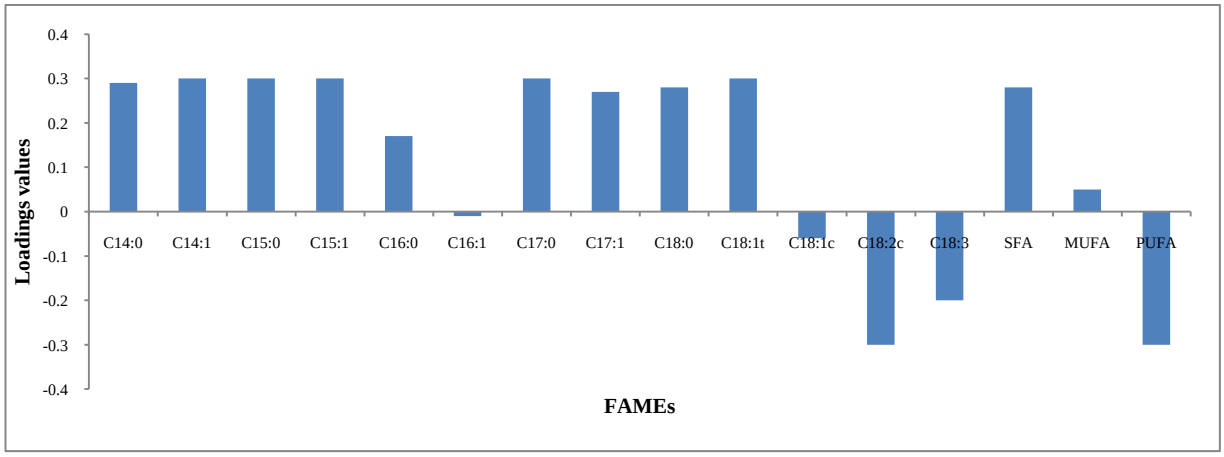

b)

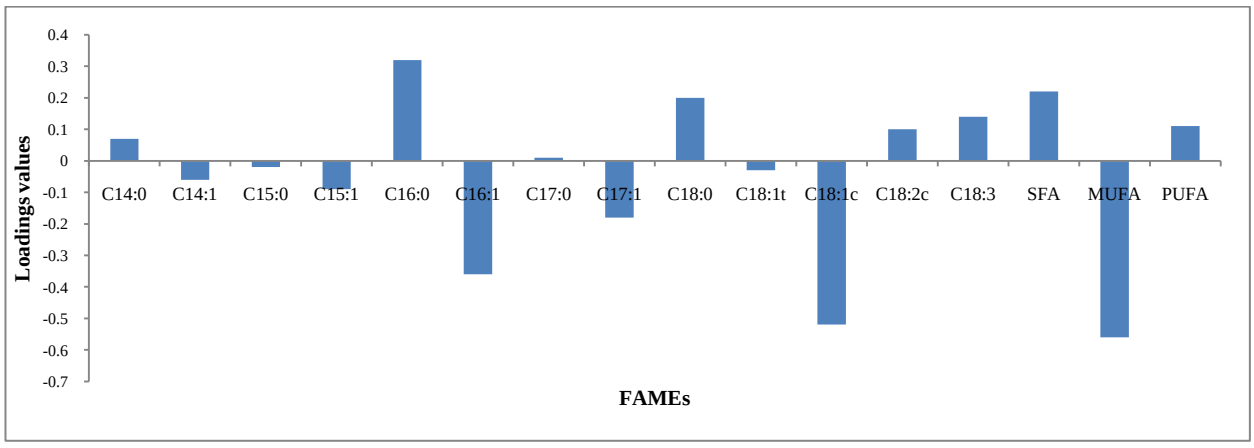

Figure 3.14: a) Loadings plot for PC1 of FAMEs for different animal species b) Loadings plot for PC2 of FAMEs for different animal species

The PCA scores plot of FAME profiles managed to discriminate beef, lamb and pork very clearly but do not distinguished chicken clearly from pork fat. The TAG profiles were explored by PCA for better discrimination of different animal species, particularly chicken and pork fat.

3.2.5.2 PCA of TAGs for beef, lamb, chicken and pork.

The TAG profiles of beef, lamb, chicken and pork were analysed by application of PCA to explore the extent of variation between different animal species. All of the TAGs identified in the samples were analysed. The first two principal components in the PCA scores plot show the distribution of different animal species according to their TAGs and with 79% of the variance being explained; 58% from the first component (PC1) and 21% from the second one (PC2, Fig. 3.15a). All animal species are separated well and no overlap is observed between them despite the substantial variation in the pork fat samples.

PC1 divided the different animal species into two classes: chicken/pork and beef/lamb as shown in the scores plot for PC1. The loadings plot reveals TAGs with high positive and high negative loadings values (Fig. 3.15b). Those with positive loadings values (e.g. LLLn*, LLL, LLO*, OLO*, LPO*, LPS* and SPO*) are significantly higher in chicken/pork than in beef/lamb. By contrast, the TAGs with negative loadings values (e.g. OOP*, OOS*, SOP* and SOS*) are significantly higher in beef/lamb than in chicken/pork. The highly unsaturated FAs L and Ln being prominent for chicken/pork while beef/lamb have similar profiles of TAGs containing highly saturated FAs S and P. The loadings plot for PC1 reveals that LPO*, SMP* and SOP* have slightly higher magnitude and contribute most to the discrimination on PC1. This is due to the proportion of LPO* for pork fat being significantly higher than for chicken and this TAG not being observed in beef and chicken. In addition, the levels of SMP* and SOP* for chicken are significantly lower than for beef and lamb, while those TAGs are not detected in pork. Those influences cause all the different animal species being isolated in the score plot. The next important descriptors include LLO*, LLP*, POM*, PMO*, OOP*, OOS* and SOS, having about the same magnitude, indicating that those TAGs contribute fairly equal to PC1. LLO* and LLP* are only observed in chicken and pork while SOS and PMO* are only detected in beef and lamb, this causes those variables to be important descriptors for PC1. OLnO* contributes very little to the discrimination on PC1 due to it only being detected in chicken.

Chicken and beef are separated well in PC2, whereas lamb is similar to pork belly. OLnO* is the most important descriptor having the highest positive loading (Fig. 3.15c). This TAG is only detected in chicken and cause the chicken samples to plot separate from the other samples. The next most important loadings include OLnL*, OOPo*,

LLLn*, OPO and PPO*, have about the same influence on the PC2 plot. Chicken has significantly higher levels of OLnL* than pork and this TAG was not observed in beef and lamb. In addition, OPO and PPO* were not detected in chicken, resulting in chicken plotting separately to the rest of the samples. Overall, almost all important descriptors having negative loadings values on PC2 (OPO, LPS, PPO and SPO) in pork have significantly higher levels than in chicken, accounting for the discrimination in PC2. By contrast, the important descriptors having positive loadings values on the PC2 (OLnL, PLLn, OLnO and LnOP) are significantly higher in chicken than in other species, causing the chicken samples to plot separately to the other samples.

Some of the FAs are not important for species discrimination but are present in TAGs that are important for species discrimination in the PCA plot. The discrimination of animal species based on the FAME profiles in PC1 is not influenced strongly O, P and L, but those acids are important for discriminating between species in the combinations of LPO*, SMP* and SOP*. Overall, the TAG profiles give much better discrimination of different animal species than FA profiles, particularly for chicken and pork.

a)

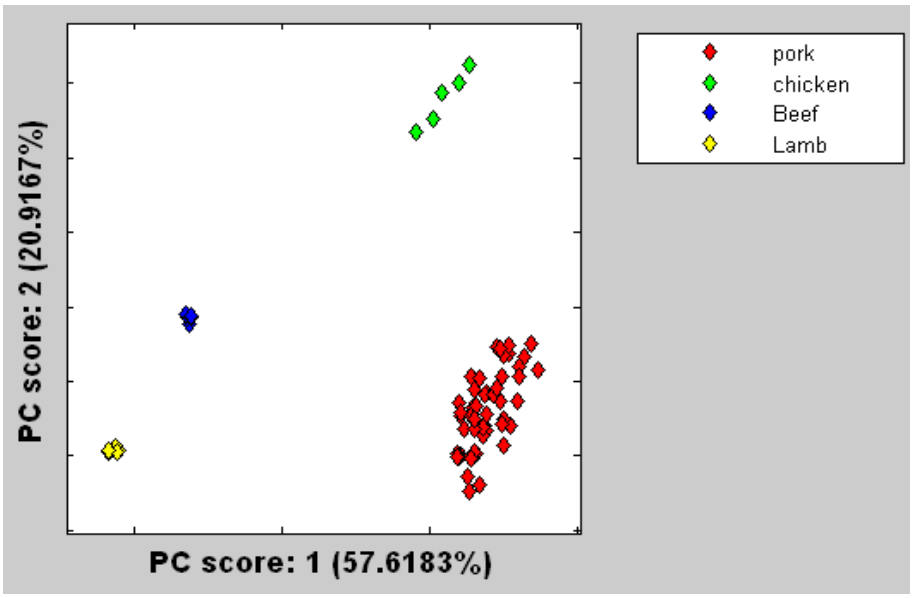

b)

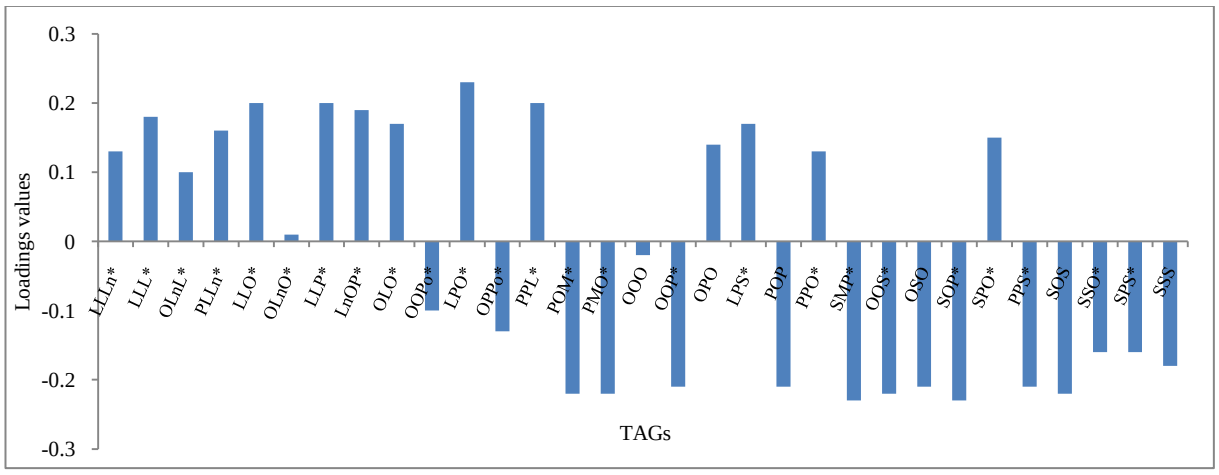

c)

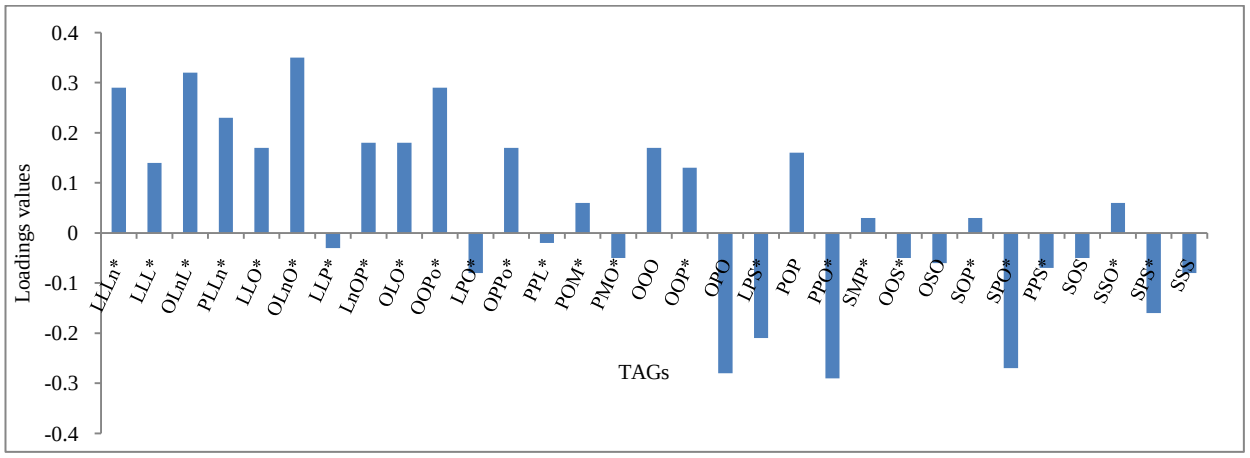

Figure 3.15: a) PCA scores plot of TAGs in different animal species, b) Loadings plot for PC1 of TAGs for different animal species, c) Loadings plot for PC2 of TAGs for different animal species.

The inspection of the profiles of TAGs in animal species highlighted a number of components that are important for species discrimination. A plot of PC1 vs. PC2 loadings values from for TAGs from different animal species reveal the TAGs that are important for species discrimination by the similarities in their coordinate values to the regions of the scores plot in which the species are located (compare Figs. 3.16 and 3.15a). POP, OOP* and OPPo* are identifiable as the important TAGs for recognition of beef. This coincides with the significantly higher levels of those TAGs in beef than in other species (Region A, Fig. 3.16). Seven TAGs are important in discriminating lamb from other species (PMO*, SOS, OOS*, PPS*, OSO, SPS* and SSS; Region B, Fig. 3.16). Only two TAGs are important for discrimination of chicken: OLnO* and OLnL* (Region C, Fig 3.16). Four TAGs, OPO, PPO*, SPO* and LPS* are important descriptors for discriminating pork (Region D, Fig. 3.16).

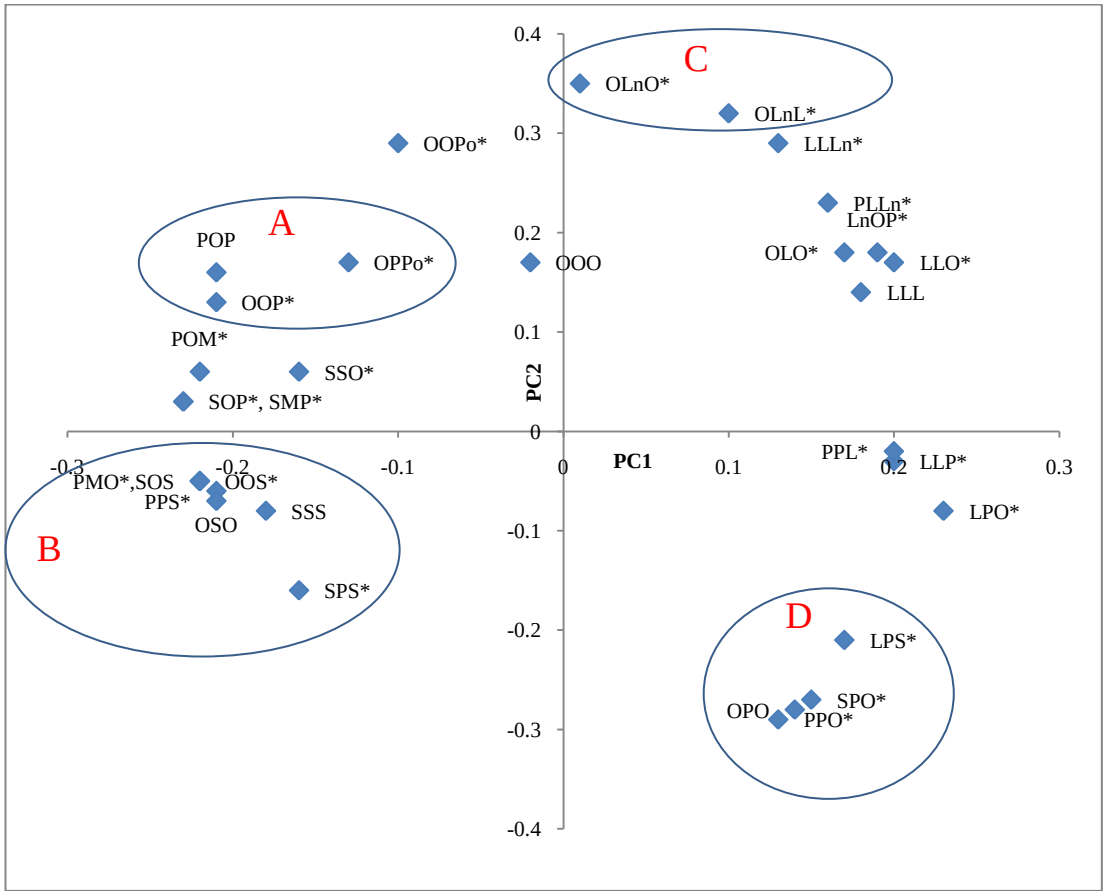

Figure 3.16: Plots of PC1 vs. PC2 loadings values from PCA scores plot of TAGs from different animal species.

Improved separation of TAGs in this study gives much better discrimination between animal species. In particular, the regioisomers PPO*/POP and SPO*/SOP* discriminate pork from beef and lamb. Good separation of TAGs containing highly unsaturated FAs (e.g. OLnL and PLLn) result in effective discrimination of chicken from pork.

3.2.6 PCA of FAME and TAG profiles of adipose tissue from different anatomical locations of pork.

3.2.6.1 PCA of FAMEs of adipose tissue from different anatomical locations of pork.

The FAME profiles of different anatomical locations of pork fat were analysed by application of PCA to explore the extent of variation between different locations. All of the FAMEs identified were included in the analysis. The abbreviations used for different anatomical locations of pork fat are as described in Section 3.2.2. The first two principal components in the PCA scores plot show the distribution of different anatomical locations of pork according to their FAMEs and with 61% of the variance being explained; 35% from the first component (PC1) and 26% from the second one (PC2, Fig. 3.17). The fats from belly; IM and SC are separated well and no overlap is observed between BIM and the rest of the fats. HIM is also separated from HSC but to a much lesser extent. There are some overlap between IM and SC fat for loin and shoulder, indicating similarity in their FAME profiles. Overlaps are also observed between different locations (e.g. SSC overlaps with SIM, BSC and HIM).

PC1 segregated the BIM from the rest of the fats. The loadings plot for PC1 shows that C18:1*cis* is the most important descriptor, having the highest negative loading, followed by C16:0, C18:0 with positive loading, and C16:1 with negative loading (Fig. 3.18a). This is a result of the significantly lower level of C18:1*cis* in belly IM than in other IM fats. The C16:1 level in BIM is also significantly lower than in HIM and SIM, whereas the proportions of C16:0 and C18:0 in BIM are higher than in HIM. Low proportions of C18:1*cis* and C16:1 in BIM results in MUFA being the most important descriptor on the PC1. The C18:0 and C16:1 variables have essentially the same magnitude, meaning they contribute equally to PC1 but C18:0 has a positive loading value while it is negative for C16:1. C14:0 and C18:1*trans* stand out as contributing very little due to the relative abundance of those acids being similar for all locations.

PC2 shows the separation of LSC and LIM from other fats and also a much greater spread for the fats of the same location. C18:2*cis* and C18:3 are the most important descriptors having about the same magnitude for their negative loadings (Fig. 3.18b). The next most important variable is C18:0 followed by C16:0, and both of which have positive loading values. PUFA is the most important descriptor for PC2 result from the C18:2*cis* and C18:3 being the most important descriptors on the PC2.

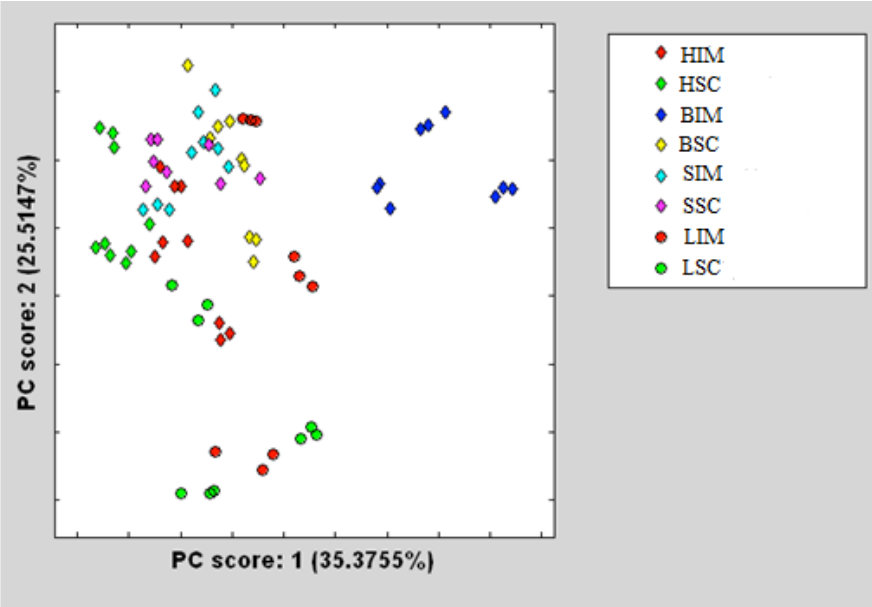

Figure 3.17: PCA scores plot of FAMEs for different anatomical locations of pork fats (*n* = 9 for each location).

a)

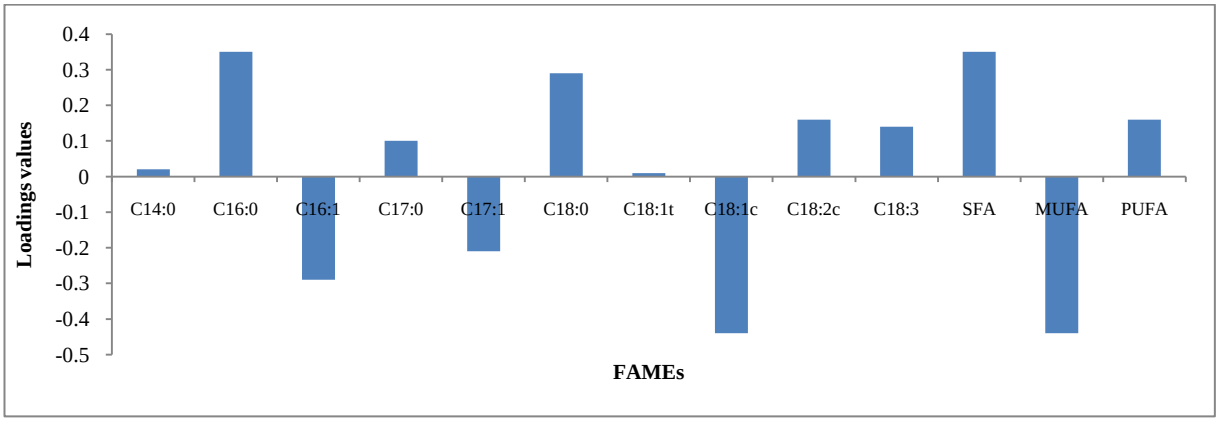

b)

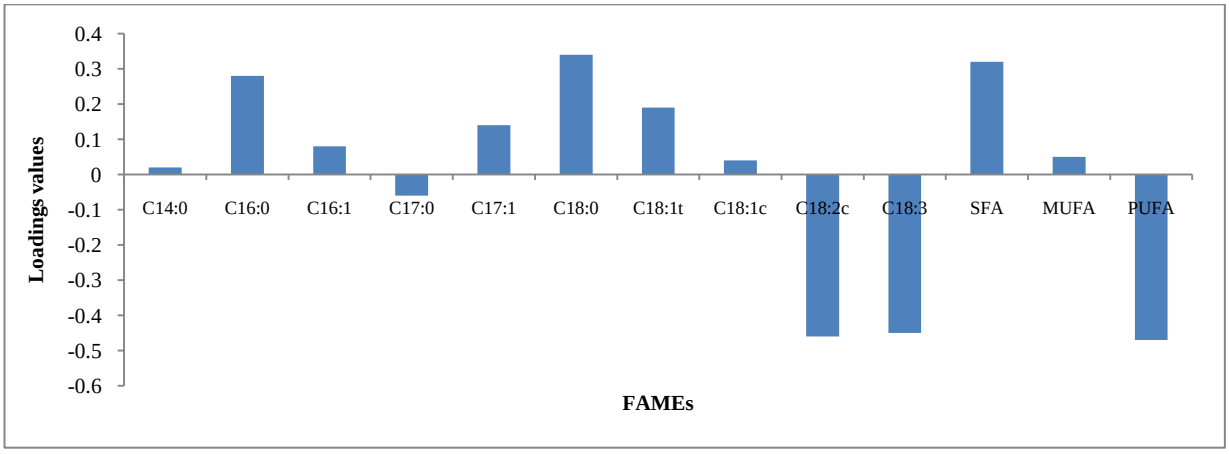

Figure 3.18: a) Loadings plot for PC1 of FAMEs for different locations of pork. b) Loadings plot for PC2 of FAMEs for different locations of pork.

Analysing the variation of FAME profiles of different anatomical locations for three different pigs (A, B and C) in the PCA scores plot shows there is no obvious discrimination between different animals (Fig 3.19). This indicates that all three animals have quite similar proportions of FAMEs and this might be explained by the similarities in age, breed and diet of the subjects.

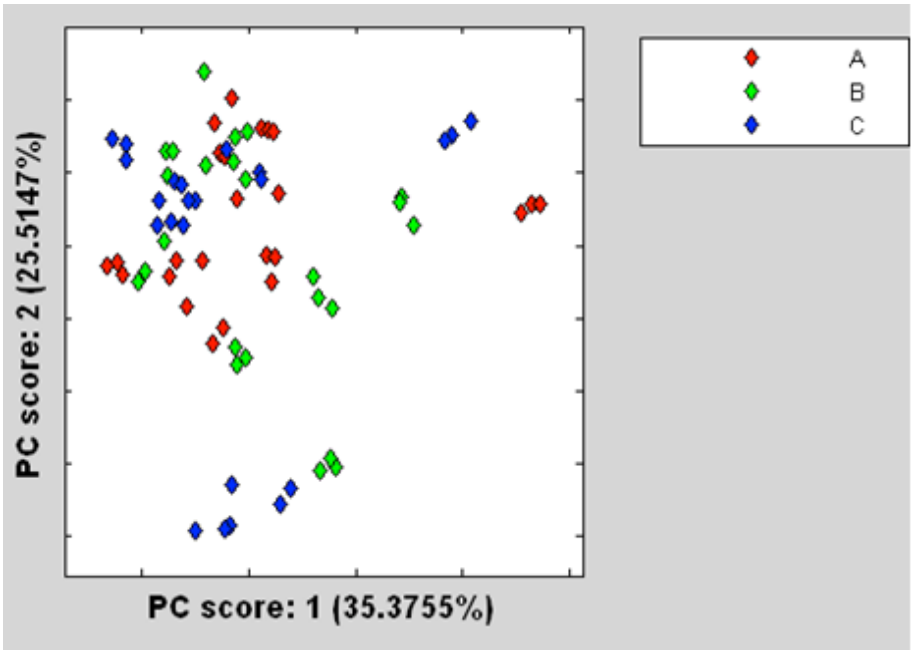

Figure 3.19: The PCA scores plot of FAMEs for three different pigs (A, B and C). (*n*=24 for each animal).

3.2.6.2 PCA of TAGs of adipose tissue from different anatomical locations of pork.

The TAG profiles of different anatomical locations of pork fat were analysed by application of PCA to explore the extent of variation between different locations. All twenty one TAGs identified were analysed. The first two principal components in the PCA scores plot show the distribution of different anatomical locations of pork according to their TAGs and with 73% of the variance being explained; 48% from the first component (PC1) and 25% from the second (PC2, Fig. 3.20). There is no distinction observed between different anatomical locations, except for BIM which is separated well from BSC and other fats. Analysing the SC separately from IM fat, shows that ham and shoulder are different to belly and loin. Even though fats from different locations are not well separated, IM and SC fat of shoulder and belly samples are different and there is no overlap between them. Overall, IM fat of all locations has similar TAG percentages except for belly.

There is no separation of different locations in PC1 and the loadings show that LLLn*, LLL, PLLn* and LLP* as have about equal influence, indicating these variables contribute equally to PC1 (Fig. 3.21a). They are followed closely by LnOP*, LPO*, OPPo* and OOS*. All of the most important descriptors have positive loadings values except for OOS*.

PC2 discriminated BIM from the rest of the fats and the loadings plot shows OLO*, OOPo* and LPS* are the most important variables for the discrimination (Fig. 3.21b). This is due to lower levels of those TAGs in BIM than in ham and shoulder for both SC and IM fat. Also, the relative abundance of LPS* for BIM is higher than for BSC and ham (IM and SC fat). Also, these TAGs containing O, P and S reflect the segregation of BIM from other samples on the PCA score plot of FAMEs for PC1.

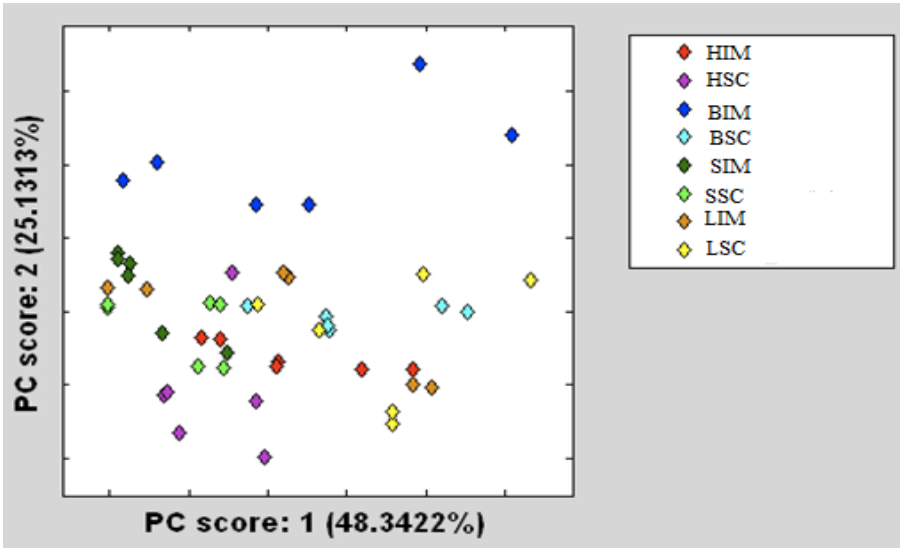

Figure 3.20: PCA scores plot for TAGs of different pork fat locations (*n*=6 for each location).

a)

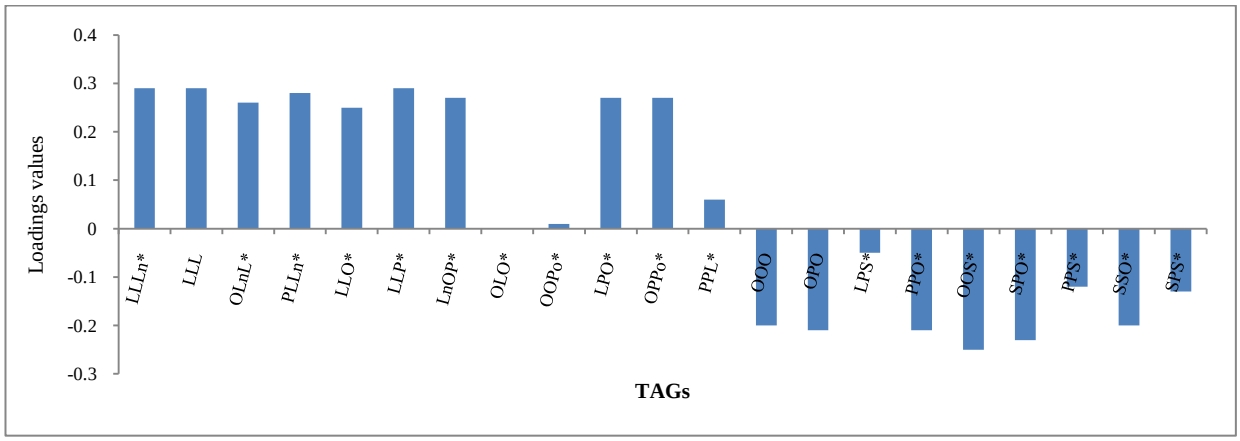

b)

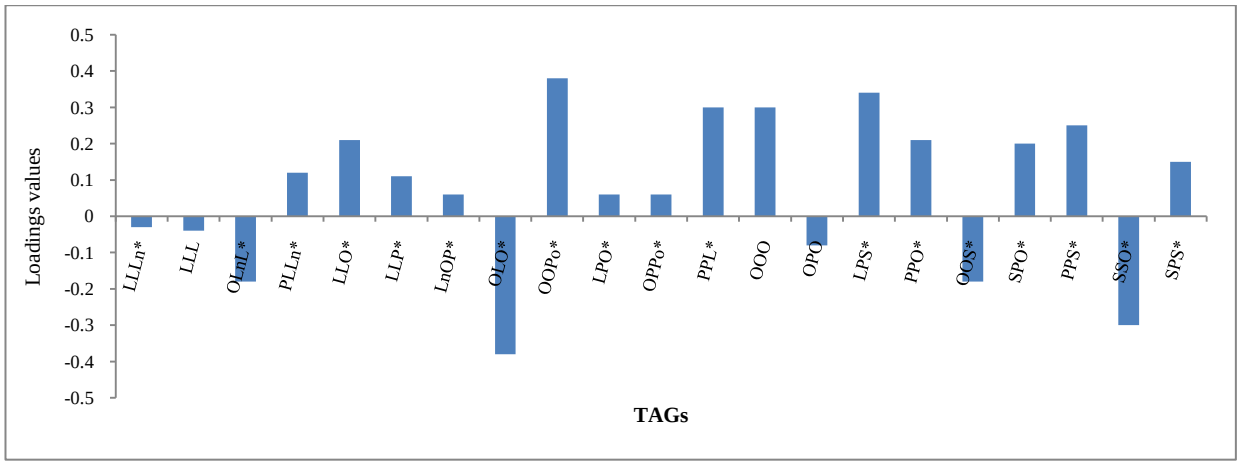

Figure 3.21: a) Loadings plot for PC1 of TAGs for different locations of pork. b) Loadings plot for PC2 of TAGs for different locations of pork.

Analysing the variation in the TAG profiles of different anatomical locations for three different pigs (A, B and C) in the PCA scores plot shows there is no obvious discrimination between different animals (Fig 3.22). This indicates that all animals have quite similar proportions of TAGs as might be explained by their similarities in age, breed and diet, and is in agreement with the results for the FAME profiles.

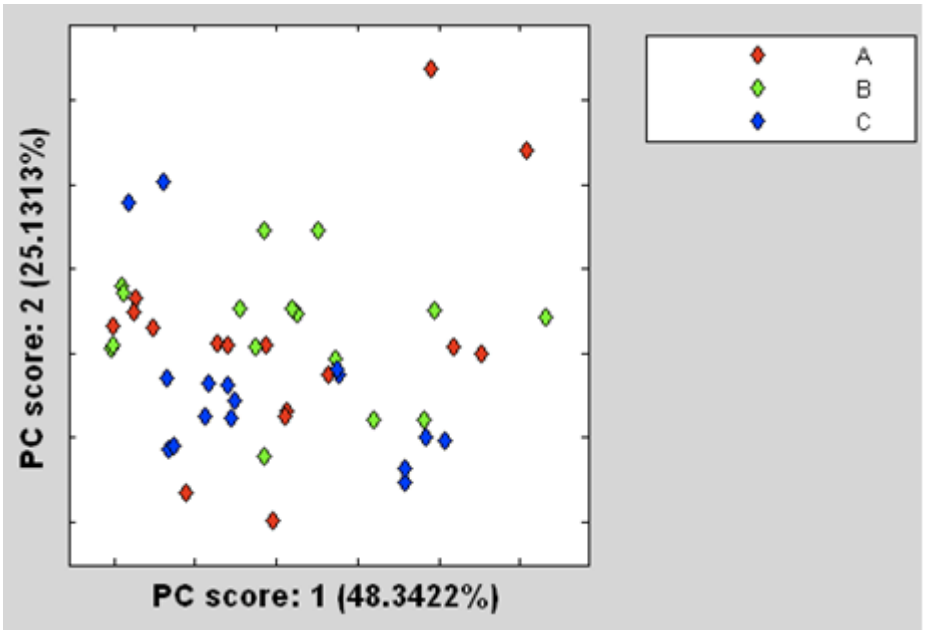

Figure 3.22: PCA scores plot of TAGs for three different pigs (A, B and C). (*n*=16 for each animal).

3.3 Conclusions

The most abundant FAMEs identified for all samples (beef, lamb, chicken and pork) are C16:0, and C18:1*cis* with the proportion of C18:1*cis* being highest, contributing about 35 to 40% of the total FA. C18:0 and C18:2*cis* show a high degree of variation among species, maximising in lamb and chicken, respectively. Chicken has a significantly higher proportion of C18:2*cis*, C18:3 and PUFA than beef and lamb, and is similar to pork, explained by the absence of biohydrogenation processes in pig and chicken digestive system.

For all locations of pork fat, the C18:1*cis* is the most abundant FA, followed by C16:0, C18:2*cis* and C18:0 each of which occur in high relative abundance. Only belly shows significant differences between the SC and IM fats with significantly higher relative abundances of C18:1*cis* and C16:1 and significantly lower relative abundance of C18:0 in SC than IM fat. Comparison between SC fat from different locations (SC vs. SC) shows that only belly has a significant difference to loin (C16:1) and ham (C16:0 and C18:1c). The IM fats of different locations (IM vs. IM) show that belly has statistically different from shoulder (C16:1, C18:1*cis*, C18:2*cis*, C18:3, MUFA and PUFA) and ham (C16:0, C16:1, C18:0, C18:1*cis*, SFA and MUFA). Furthermore, BIM has a significantly lower level of C18:1*cis* than other IM fat locations. Consequently, BIM has a significantly lower proportion of MUFA than the rest of the IM fat samples. The results show that differences in the proportions of FAs occur not only within different fat layers but also in different locations of pork.

The TAG profiles of fats reflect their FA compositions, showing a high proportion of unsaturated FAs for chicken and pork, the major TAGs detected being LPO*, OPO, LLP*, LLO* and OLO* in which the acids (O, L and P) represent about 88% (about 64% from O and L, and 24% from P) of the total FA in GC. In beef and lamb, saturated FAs are dominant in the major TAGs detected: SOP*, SOO, SPP, SSP and SOS; and these acids (O, P and S) represent about 85% (about 40% from O and 45% from P and S) of the total FAs in GC.

For all locations of pork, LPO, OPO and SPO are the three most abundant TAGs in all fat locations; accounting for about 45 to 54% of the total TAGs and containing O, P, L and S, the major FAs in pork fat. Comparison between SC and IM fats for each location (SC vs. IM) shows only belly IM fat being significantly different from belly SC fat

(LPS). Comparison between SC fat from different locations (SC vs. SC) shows no significant differences were observed for TAG profiles in all the fat locations. The IM fats of different locations (IM vs. IM) show that belly is statistically different to shoulder (LLP, OLO, OOO and OOS), ham (OLO) and loin (OOS). No other locations show significant differences in the TAG profiles of IM fats of pork.

The PCA scores plot for FAME of different animal species show no overlap between animal species. Chicken plots very close to pork fat, particularly ham and loin. Species are divided into beef/lamb and chicken/pork on PC1 and almost all variables have about the same influence. Beef and lamb are separated well between them in PC2, with C18:1*cis* as the most important descriptor. Notably, however, chicken and beef plot close to pork ham and lamb plot close to pork shoulder and loin.

All animal species are separated very well in the PCA scores plot of TAG profiles and no overlap is observed between them despite the substantial variation in pork fat. PC1 divided the different animal species into chicken/pork and beef/lamb. Chicken and beef are separated well in PC2, whereas lamb is similar to pork belly. Some of the FAs are not important for species discrimination but are present in TAGs that are important for species discrimination in the PCA plot. The discrimination of animal species based on the FAME profiles in PC1 does not take into account O, P and L, but those acids have strong contributions to the discrimination between species in the TAG combinations LPO, SMP and SOP.

The improved RP HPLC separation of TAGs developed in this study has been shown to give more reliable discrimination of different animal species than previous methods. Improved separation of important TAGs leads to improved PCA scores for different animal species. The important TAGs for discriminating different animal species are: POP, OOP* and OPPo* for beef, PMO*, SOS, OOS*, PPS*, OSO, SPS* and SSS for lamb, OLnO* and OLnL* for chicken and OPO, PPO*, SPO* and LPS* for pork fat. The important TAGs for discrimination of beef and pork (POP and PPO, OOP and OPO) were not separated in the previous study but separated here and lead to better discrimination on PCA. Hence, it is suggested that the improved method has greater potential for separating different species effectively.

PCA of FAMEs for different anatomical locations of pork show that the fats from belly (IM and SC) are separated well and no overlap is observed between BIM and the rest of the fats. HIM is also separated from HSC but at a much lesser extent. There is some overlap between IM and SC fat for loin and shoulder and overlaps are also observed between different locations (e.g. SSC overlaps with SIM, BSC and HIM). PC1 segregated the BIM from the rest of the fats and the loadings plot for PC1 shows that C18:1*cis* is the most important descriptor followed by C16:0, C18:0 and C16:1. PC2 shows the separation of LSC and LIM from other fats and also a much greater spread for the fats of the same location. C18:2*cis* and C18:3 are the most important descriptors for PC2 and have about the same magnitude.

There is no distinction observed between different anatomical locations, except for BIM which is separated well from BSC and other fats in PCA scores plot of TAGs for different locations of pork. No separation of different locations is observed in PC1 and the loadings show LLLn, LLL, PLLn and LLP as having about the same influence. PC2 discriminated BIM from the rest of the fats and the loadings plot shows OLO, OOPo and LPS are the most important variables for the BIM discrimination. The discrimination results from lower levels of those TAGs in BIM than in ham and shoulder for both SC and IM fat.

Overall, the TAG profiles give much better discrimination of different animal species than FA profiles, particularly for chicken and pork.

CHAPTER 4

Analysis of TAGs for discrimination of cooked meat products

4.1 Introduction and aims

Introduction

Most food consumed in the developed world has been subjected to varying degrees of heat treatment at one stage or another, through cooking, baking, broiling, toasting, roasting, canning, concentrating, pasteurizing, drying or frying to modify its flavour or texture and to improve its ability to be stored (Nawar, 1984). Meat usually has to be cooked before being consumed. Cooking causes several positive effects on meat such as texture and flavour enhancement, destruction of microorganisms, increase in shelf life and improved digestibility. Cooking also produces some negative effects such as the formation of polycyclic aromatic hydrocarbons (PAHs) and nutritional losses (Broncano et al., 2009). Lipid oxidation in meat is an important source of taste and odour compounds and is the main reason for the deterioration of meat products, giving undesirable odours, rancidity, texture modification, nutritional losses or production of toxic compounds. The development of oxidation reactions in meat depends on the method, temperature and time of cooking (Broncano et al., 2009). When heated, the chemical and physical changes that occur in meat products depend on the composition (i.e., balance of lipids, proteins and carbohydrates) and the conditions of treatment. In the presence of air, the deterioration of TAGs in meat during deep frying is caused by high temperature thermal oxidation of FA chains and a variety of compounds are generated such as polar compounds, polymerized glycerides and oxidised FAs (Shimizu et al., 2004). Studies of the influence of different cooking methods (grilling, frying, microwave and roasting) on meat from Iberian pigs showed that the grilled meat was the least affected by lipid oxidation (tested by the standard reaction by thiobarbituric acid-reactive substances, TBARs; Broncano et al., 2009).

A variety of studies on thermal decomposition of TAGs covering different substrates, different conditions of heating and different techniques of analysis gave varied results. A study of lipid compositions of raw and microwaved roasted walnut, hazelnut and almond shows no changes in kernel lipid after microwave roasting at full power for 3 min (Momchilova et al., 2007). Roasting of hazelnuts showed minor changes in the FA and TAG compositions (Amaral et al., 2006). Those authors found that increases in temperature and roasting led to a modest increase of the proportions of oleic and saturated FAs and a decrease of linoleic acid. Similarly, an increase of TAGs containing oleic acid and decrease of those containing linoleic acid was observed in roasted

samples. Although there were some minor changes, the corresponding profiles remained essentially identical to those of raw hazelnuts and the relative proportions were not altered significantly in the roasted samples (Amaral et al., 2006). There was no difference in thermal deterioration between DAG oil (prepared from soybean and rapeseed FA) and TAG oil (prepared from rapeseed, perilla and safflower) during deep-frying (Shimizu et al., 2004). The major decomposition products from TAGs containing even-numbered saturated FA chains C6 to C18 after heating in air for 1 h at 180 and 250°C were alkanes, methyl ketones, alkanals, and γ- and δ-lactones (Crnjar et al., 1981).

Changes in the fatty acid profiles of pork loin chops fried in different culinary fats (olive oil, sunflower oil, butter and pig lard) and during 10 days of refrigerated storage were studied. Neutral lipids and free fatty acids from pork loin chops fried in olive and sunflower oils, butter and pig lard showed different fatty acid profiles as a result of the exchange between the culinary fat and the meat (Ramirez et al., 2005). A more recent study on the effect of pan-frying, either with or without culinary fats, employed pork from pigs fed various dietary fat sources. The FA composition of the fried meat tended to be similar to that of the culinary fat that was used (Haak et al., 2007). Pan-frying altered the FA content and composition of the culinary fats and those were dependent on the absorption of oil into the meat, together with oxidation of the FA during pan frying, and release of water from the meat during frying.

The effect of grill cooking on the FA compositions of beef steaks from different locations of crossbred steers showed that the levels of SFA and PUFA both increased slightly after cooking, but not significantly (Jiang et al., 2010). A previous study on ground beef patties from Brown Swiss bulls fed different diets found that cooking decreased the proportions of SFA (C14:0, C16:0, C18:0) and C18:1 *trans* while increasing the proportion of PUFA (Scheeder et al., 2001). The authors suggested that the proportional change in SFA and PUFA during grilling may result from drip loss, which is dominated by triglycerides from adipose tissue.

Studies on another type of heat treatment, broiling, have been done on neutral, polar and total lipid fractions of beef intramuscular tissue to an internal temperature of 70°C. Broiling reduced the percentages of oleic, linoleic, and linolenic acids and increased the percentage of stearic acid (Duckett and Wagner, 1998). The published work on lean tissue of longissimus steaks, which were broiled on four degrees of doneness - raw, rare

(55°C), medium (70°C) and well (80°C), and external fat treatments indicated that external trim level and degree of doneness influenced the amount of fat in steaks, but did not alter the fatty acid composition of cooked steaks (Harris et al., 1992).

The effects of roasting and currying on the TAGs profiles of pork, chicken, lamb or beef has not been reported.

Aims

The aims of this chapter were to examine:

a) the extent of variation in TAG profiles of meat products cooked by microwave, roasting and currying for discriminating meat of different species (beef, pork, chicken and lamb) in cooked food products.
b) the extent to which the improved characterization of TAG profiles (using method reported in Chapter 2) improves discrimination between raw (uncooked) and cooked meat products. Compounds other than TAGs that are generated from heat treatment of meat were not assessed.
c) the extent to which TAG profiles in different cooking methods from different animal species are differentiated by the application of PCA.

4.2 Results and discussion

The three letter code of TAGs includes the suffix * where more than one regioisomer can exist in a form that can, potentially, be separated chromatographically.

4.2.1 RP HPLC-APCI MS/MS separation of TAGS from cooked meat products of beef, lamb, chicken and pork.

Cooked meat products of pork (roasted and microwaved), chicken (roasted, microwaved and curried), beef (roasted, microwaved and curried) and lamb (roasted, microwaved and hotpot) were obtained to determine the TAG distributions after different cooking methods applied to the different meats. The roasted, curry and hotpot samples were purchased from a local supermarket and were homogenised and extracted on the day of purchase. The raw meat of beef, chicken, lamb and pork (ham intermuscular fat) were from the same samples as were used in Chapter 3, Section 3.2.3 (Table 3.7) and were extracted with chloroform methanol (2:1). For the microwave cooking, raw sirloin beef steak, lamb chop, chicken and pork (ham) were cooked in a 700 W microwave oven at full power for 4 min. All the cooked meat samples were extracted by ASE 350 accelerated solvent extractor (DIONEX) and replicates (≥ 2) were performed. The TAGs were separated following Section 3.2.3 using an Ultimate 3000 (Dionex) HPLC coupled to a Brucker HCT ultra ETD II ion trap.

The retention times observed for each chromatogram produced were fairly consistent, except for one batch/lot of samples where the retention times decreased (e.g. Fig 4.3 batch run of microwave samples of chicken gave reduced retention times for TAGs such as OOO, OPO, PPO* and OOS*). This is attributed to very late eluting compounds, either TAGs or components derived from TAGs, being retained on the column and not being removed efficiently. This indicates that the HPLC column required an additional final wash or flush regularly.

With the exception of curried beef and chicken and apart from slight differences in the relative proportions of some of the compounds, the TAG profiles from cooked beef, lamb, chicken and pork were identical to those of the corresponding raw material. The chromatogram of beef curry shows the unsaturated TAGs having low ECN (peaks eluting before OOPo*:10) are prominent (Fig. 4.1). This part of chromatogram labelled

as ‘vegetable oil’ in Fig 4.1, is very similar to the chromatogram of TAGs for rapeseed oil in a published report (Holcapek et al., 2003). This is due to the addition of rapeseed oil during cooking and this oil is listed as a ingredient on the product's label. There are no obvious differences observed for the chromatograms of TAGs from roasted and microwave beef compared with raw beef, except for slightly higher PPS* and SPS* peaks for roasted beef. The chromatograms for lamb samples show reduced levels of OOO, OPO and PPO* but for microwave more prominent peak for SOS than for the raw meat (Fig. 4.2). Also, the chromatogram of slow cooked lamb hotpot shows slightly higher relative abundances of peaks for OOS*, SOP* and SOS than for the raw lamb.

The TAGs for the chicken samples show an obvious increase in the proportion of the lower ECN TAG peaks LLLn* to OLO* for chicken curry with consequent reduction in the peaks for OPO to SPS*. The increased peaks look identical to those observed for beef curry, suggesting that rapeseed oil was used for cooking (Fig 4.3). Vegetable oil is mentioned on the product label of chicken curry but the type of oil was not specified. In addition, the relative proportion of OOO from chicken curry is much higher than for raw chicken. The chromatograms of roasted and microwave chicken look similar to those for the raw meat. The TAGs from microwave pork do not differ much from the raw meat. The OPO peak for roasted pork is much more abundant than in raw pork, resulting in reduction in the relative abundances of other peaks, particularly those eluting before OPO (Fig. 4.4).

The individual TAG peak areas of all eighteen identified compounds for beef, all seventeen for lamb, all twenty four for chicken and all twenty one for pork are expressed relative to the total peak area (Table 4.1).

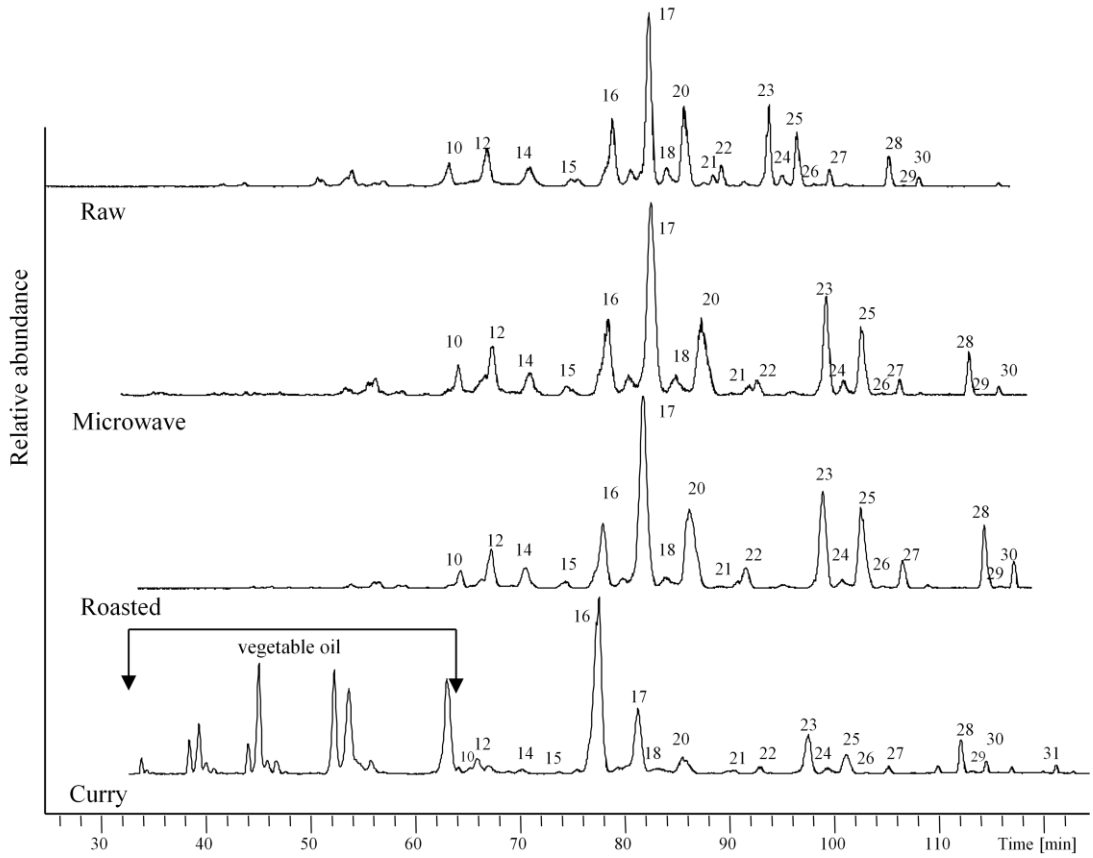

Figure 4.1: Chromatograms of TAGs from raw and cooked beef products. (Refer Table 4.1 for peak identifications).

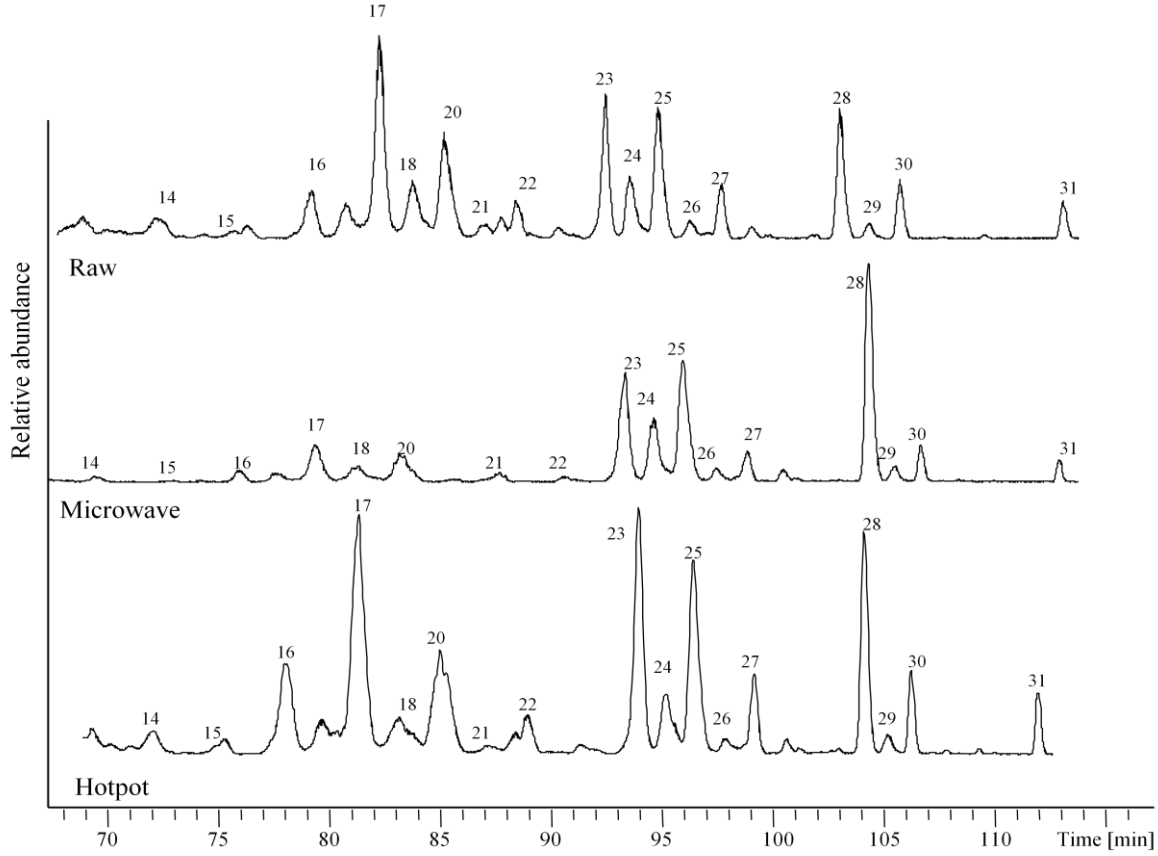

Figure 4.2: Chromatograms of TAGs from raw and cooked lamb products. (Refer Table 4.1 for peak identifications).

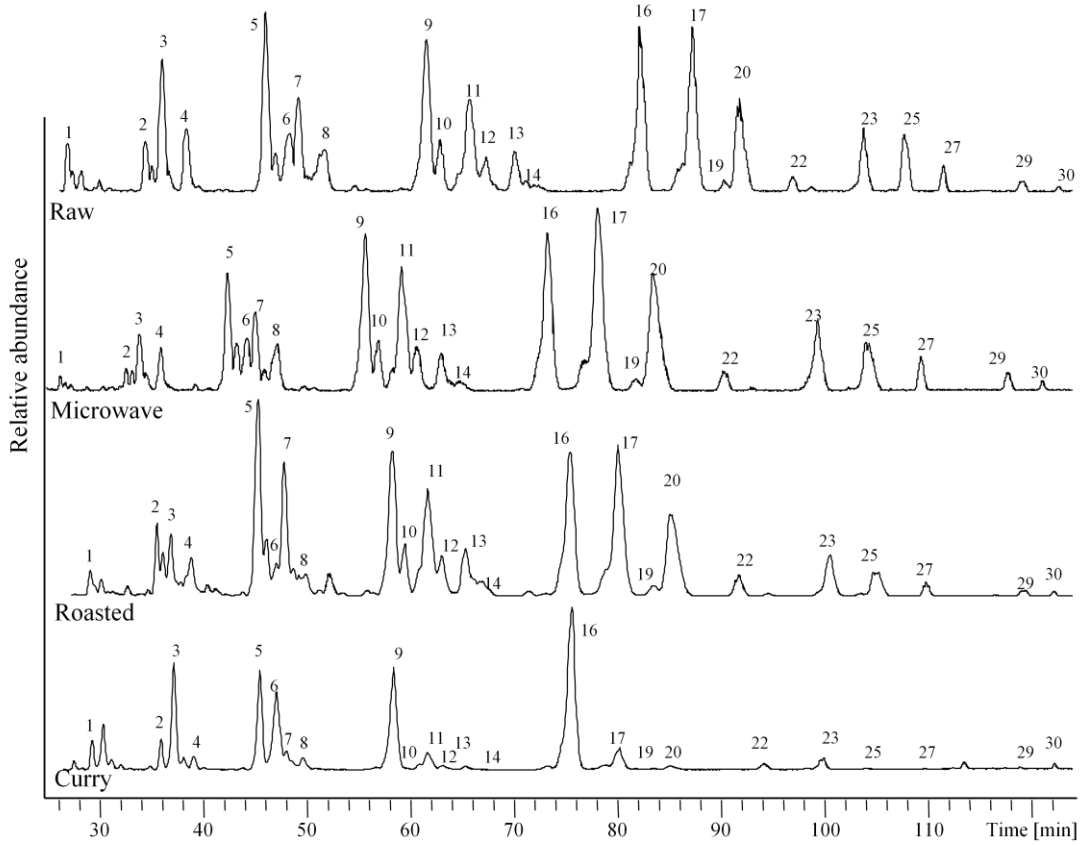

Figure 4.3: Chromatograms of TAGs from raw and cooked chicken products. (Refer Table 4.1 for peak identifications).

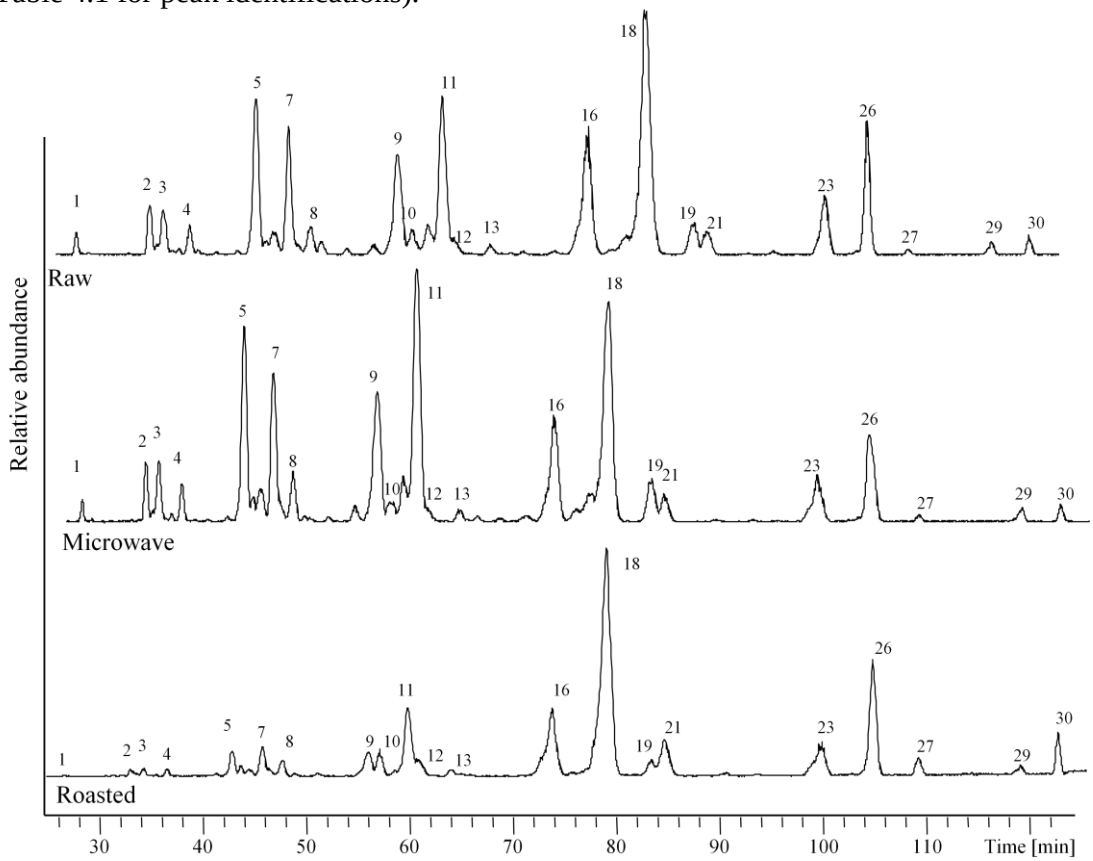

Figure 4.4: Chromatograms of TAGs from raw and cooked pork products. (Refer Table 4.1 for peak identifications).

Table 4.1: Mean percentages of TAGs from raw and cooked meat products of pork, chicken, beef and lamb.

TAGs	Peak No.	Pork			Chicken				Beef				Lamb		
		Raw	Microwave	Roasted	Raw	Microwave	Roasted	Curry	Raw	Microwave	Roasted	Curry	Raw	Microwave	Hotpot
LLLn*	1	0.68	0.35	0.11	1.73	0.28	0.54	1.48	-	-	-	-	-	-	-
LLL	2	1.95	1.33	0.32	2.19	0.47	1.61	1.81	-	-	-	-	-	-	-
OLnL*	3	1.72	1.51	0.51	5.90	1.63	1.70	7.89	-	-	-	-	-	-	-
PLLn*	4	1.38	1.05	0.41	3.25	1.24	1.34	1.20	-	-	-	-	-	-	-
LLO*	5	6.75	7.10	1.80	8.63	3.79	7.68	10.10	-	-	-	-	-	-	-
OLnO*	6	-	-	-	3.53	2.12	1.38	10.71	-	-	-	-	-	-	-
LLP*	7	7.05	5.77	2.06	4.14	2.71	4.83	2.11	-	-	-	-	-	-	-
LnOP*	8	1.98	1.86	1.43	3.49	2.90	2.04	1.83	-	-	-	-	-	-	-
OLO*	9	9.03	11.06	4.63	13.61	10.59	13.39	23.55	-	-	-	-	-	-	-
OOPo*	10	0.10	0.12	0.05	2.97	3.42	2.95	0.36	3.66	4.01	2.24	1.45	-	-	-
LPO*	11	18.84	18.85	11.61	11.43	10.94	13.52	5.30	-	-	-	-	-	-	-
OPPo*	12	0.21	0.21	0.13	2.72	3.88	3.58	0.27	10.06	10.14	7.35	3.26	-	-	-
PPL*	13	1.48	1.04	1.07	1.61	2.35	3.42	0.47	-	-	-	-	-	-	-
POM*	14	-	-	-	0.67	0.98	1.88	0.13	5.00	4.22	3.83	1.68	3.50	1.28	2.79
PMO*	15	-	-	-	-	-	-	-	0.26	0.32	0.14	0.15	0.66	0.34	0.30
OOO	16	5.62	6.74	6.82	7.19	10.12	8.73	23.36	7.02	8.31	6.11	37.06	3.32	1.80	5.31
OOP*	17	-	-	-	11.54	17.03	13.48	5.24	30.49	31.60	28.37	20.06	20.11	8.31	19.24
OPO	18	17.73	18.18	30.89	-	-	-	-	3.02	3.32	1.65	2.40	7.07	4.38	3.93
LPS*	19	5.82	4.38	3.60	0.70	1.21	1.23	0.28	-	-	-	-	-	-	-
POP	20	-	-	-	5.53	8.93	6.97	0.79	10.43	9.68	11.88	4.92	7.77	5.67	6.97
PPO*	21	3.03	2.51	5.47	-	-	-	-	0.43	0.40	0.30	0.35	1.27	0.92	0.61
SMP*	22	-	-	-	0.60	0.99	1.04	0.12	2.26	1.49	2.16	0.93	3.22	2.04	2.54
OOS*	23	3.82	5.26	5.53	3.04	5.74	3.66	2.14	9.19	10.58	11.46	10.58	10.12	13.13	12.24
OSO	24	-	-	-	-	-	-	-	1.49	1.58	1.27	1.77	5.70	9.06	4.21
SOP*	25	-	-	-	3.67	6.01	3.59	0.51	9.73	9.21	13.62	7.67	16.29	22.47	16.53
SPO*	26	11.08	11.34	19.20	-	-	-	-	0.51	0.53	0.42	0.58	2.43	2.63	1.36
PPS*	27	0.53	0.46	1.55	0.82	1.25	0.75	0.11	2.00	1.21	2.45	1.40	3.98	3.42	4.67
SOS	28	-	-	-	-	-	-	-	3.14	2.51	4.56	3.56	8.16	18.92	10.80
SSO*	29	0.23	0.28	0.28	0.76	1.03	0.50	0.18	0.17	0.22	0.19	0.35	1.44	1.64	1.15
SPS*	30	0.80	0.76	2.57	0.28	0.45	0.26	0.07	1.08	0.68	1.69	1.37	3.66	2.97	5.32
SSS	31	-	-	-	-	-	-	-	-	-	0.32	0.48	1.52	1.03	2.36

4.2.2 Evaluation of regioisomer of TAGs resolved from cooked meat products.

The ratios of resolved regioisomers were evaluated for cooked products of beef and lamb and were compared with raw meat. The area percent for each isomer was obtained by the summation of the area under the peaks in EIC corresponding to the ammoniated and protonated molecules, and DAG fragment ions present on the chromatograms of beef and lamb (Table 4.2 and 4.3).

Table 4.2: Percentages of resolved regioisomer of TAGs from raw and cooked beef

		Beef			
TAGs	Isomers	Raw	Microwave	Roast	Curry
POM^{+}	POM*	95	94	96	92
	PMO*	5	6	4	8
OOP^{++}	OOP*	91	91	94	89
	OPO	9	9	6	11
POP^{+}	POP	96	96	97	93
	PPO*	4	4	3	7
OOS^{++}	OOS*	86	87	89	85
	SOS	14	13	11	15
SOP^{+}	SOP*	95	95	97	93
	SPO*	5	5	3	7
	PSO	-	-	-	-
SOS^{+}	SOS	95	92	96	91
	SSO*	5	8	4	9

$^{+}$ First group of TAGs – having one monounsaturated FA and two saturated FAs

$^{++}$ Second group – having two monounsaturated FAs and one saturated FA

Similar to raw beef, the area percent of TAG isomers observed in cooked beef also varies according to the degree of unsaturation of the TAGs. For TAGs having a monounsaturated FA and two saturated FAs (POM*/PMO*, POP/PPO*, SOP*/SPO* and SOS/SSO*; labelled $^{+}$; Table 4.2), the isomers with the saturated FA in the *sn*-2 position represent about 3 to 4% for microwave and roasted beef. This percentage is about the same as for raw meat. Notably, the percentage is slightly higher for beef curry (7 to 9%). This might be due to interference from the TAGs of rapeseed oil which affect the percentages of isomers for beef curry. For the TAG with two monounsaturated FAs and one saturated FA (OOP*/OPO and OOS*/SOS; labelled $^{++}$; Table 4.2), the isomer

with the saturated FA in the *sn*-2 position for cooked beef is about the same as for raw beef with a slightly lower OPO ratio for roasted pork (6%).

Overall, the area percent of TAG isomers for cooked beef is similar to raw beef, except for beef curry which showed interference from rapeseed oil. Notably, however, the percentage of isomers with saturated FAs in the *sn*-2 position for the first group of TAGs is lower than the next group for any cooked products. This observation shows that the isomer distribution for beef was not affected by cooking.

By contrast, the area percent of TAG isomers observed in cooked lamb differ from the raw meat. Similar to raw lamb, the first group of TAGs (having a monounsaturated FA and two saturated FAs: POM*/PMO*, POP/PPO*, SOP*/SPO* and SOS/SSO*; labelled $^{+}$; Table 4.3) have a lower percentage of TAG isomers with saturated FAs in the *sn*-2 position than the next group (TAG with two monounsaturated FAs and one saturated FAs: OOP*/OPO and OOS*/SOS; labelled $^{++}$; Table 4.3) for both cooked lamb dishes.

Table 4.3: The percentages of separated TAG isomers from raw and cooked lamb

		Lamb		
TAGs	Isomers	Raw	Microwave	Hotpot
POM^{+}	POM*	84	82	90
	PMO*	16	18	10
OOP^{++}	OOP*	74	66	82
	OPO	26	34	18
POP^{+}	POP	86	86	92
	PPO*	14	14	8
OOS^{++}	OOS*	64	62	76
	SOS	36	38	24
SOP^{+}	SOP*	87	89	92
	SPO*	13	11	8
	PSO	-	-	-
SOS^{+}	SOS	85	92	89
	SSO*	15	8	11

$^{+}$ First group of TAGs – having one monounsaturated FA and two saturated FAs

$^{++}$ Second group – having two monounsaturated FAs and one saturated FA

For hotpot lamb, the abundances of the TAG isomers with saturated FAs in the *sn*-2 position was slightly lower than the raw lamb for all such TAGs. The abundances of PMO*, OPO and SOS were slightly higher for microwave lamb. This shows that microwave and hotpot cooking does affect the isomer distribution for lamb. Even though the abundances of TAG isomers for cooked lamb differ to that of raw meat, the isomers with saturated FAs in the *sn*-2 position were much higher relative abundance than for beef.

4.2.3 TAG variations of raw and cooked meat products.

The variation in the TAG profiles between raw and cooked beef, lamb, chicken and pork were explored by plotting histograms with the Y-error bars. Bar-overlaps were compared at the 95% confidence level (two standard deviations) for the mean percentage of TAGs.

The histograms for raw and cooked beef reveal that OOS*, OSO and PPO* are the only TAGs showing no significant abundance differences in any of the beef samples (Fig. 4.5a), indicating that the various different cooking methods do not change the proportions of OOS*, OSO and PPO* from those raw meat. By contrast, OOO is much higher in curry, about 28% greater than any of the other samples of cooked meat. This excessive proportion of OOO for beef curry is attributed to rapeseed oil used for cooking, which contains about 17% and 19% of OOO as reported in published work (Holcapek et al., 2003 and Marikkar et al., 2005). The oxidation of rapeseed oil TAGs containing the di and tri unsaturated FAs linoleic and linolenic acids could also reduce the levels of those acid and consequently increase the proportions of TAGs containing oleic acid, OOO in particular. It was shown that Ln is susceptible to oxidation during frying and the oxidation level was significantly different with different levels of Ln in rapeseed oil (Eskin et al., 1989). Furthermore, the high proportion of OOO makes OOP*, POM*, POP, SMP*, SOP*, OPPo* and OOPo* significantly lower for curry by comparison with the other cooked meat samples. Except for OOO, SMP*, PPS* and SPS*, all other TAGs for microwave cooked beef have identical proportions to those of raw beef. The proportions of OOO, OOP*, SMP*, OOS*, OSO, PPO* and PPS* for roasted beef are very similar to those of raw beef. Although curry has much higher proportion of OOO than raw beef, the levels of PMO*, PPO*, OOS*, OSO, SPO*, PPS* and SOS for curry cooked beef are similar to the raw meat.

The histogram of raw beef, curry (including TAGs rapeseed oil) and rapeseed oil (Holcapek et al., 2003) show that all the TAGs present in rapeseed oil were observed in the curry (Fig. 4.5b). The TAG profiles of curry show high proportions of unsaturated FAs as seen in rapeseed oil. The proportions of LLL, OLnL*, PLLn*, LLP* and LnOP* for curry are close to those of rapeseed oil. None of those TAGs were observed in raw beef.

Due to the very high proportion of OOO for curry, the histogram plot was normalised to OOP* in order to subtract any possible TAGs added during cooking. The normalised abundances of OOO for curry were fixed to those of raw beef (20%; Fig. 4.5c) assuming the balance/excess was from rapeseed oil. Following the adjustment, the relative abundances of all other TAGs in curry were reassessed and scaled to the new OOO value of curry (about 7%). The histogram was reproduced from the reassessed TAG percentages after subtracting possible TAGs from rapeseed oil (Fig. 4.5d). This approach, to take out, as much as possible, the effect of added TAGs from rapeseed oil, is important to reveal the underlying TAG profile that results purely from beef. The histogram with reassessed beef curry shows increasing proportions of OOP*, OOS*, SOP* and SOS for curry. Reassessed curry has statistically higher proportions of OOS* and SOP* than for raw beef, whereas the proportions of OOPo*, OPPo*, POM* and POP are significantly higher in raw beef. However, the levels of OOP*, SOS, SPS*, PPS*, OPO, PMO*, PPO* and SPO* for reassessed curry are the same as for raw beef. The results suggest that the cooking procedure for curried beef, like those for roasted and microwave cooking, does not impart much difference in the TAG profile relative to the raw meat.

a)

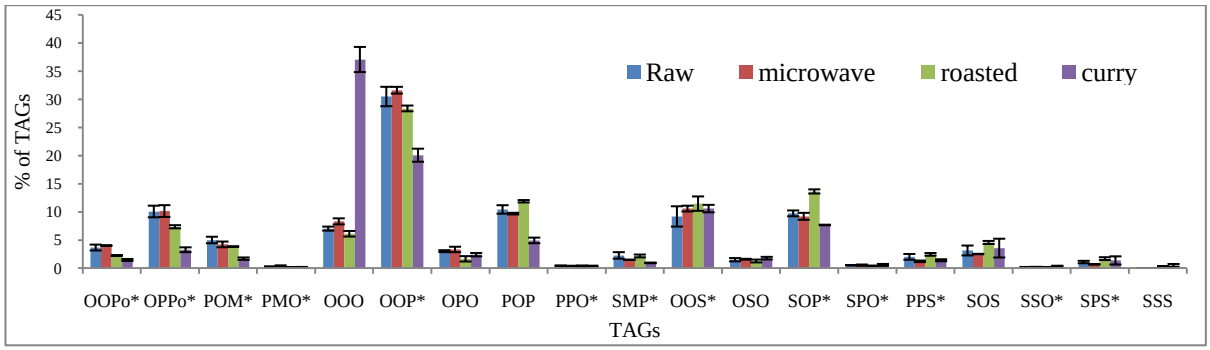

b)

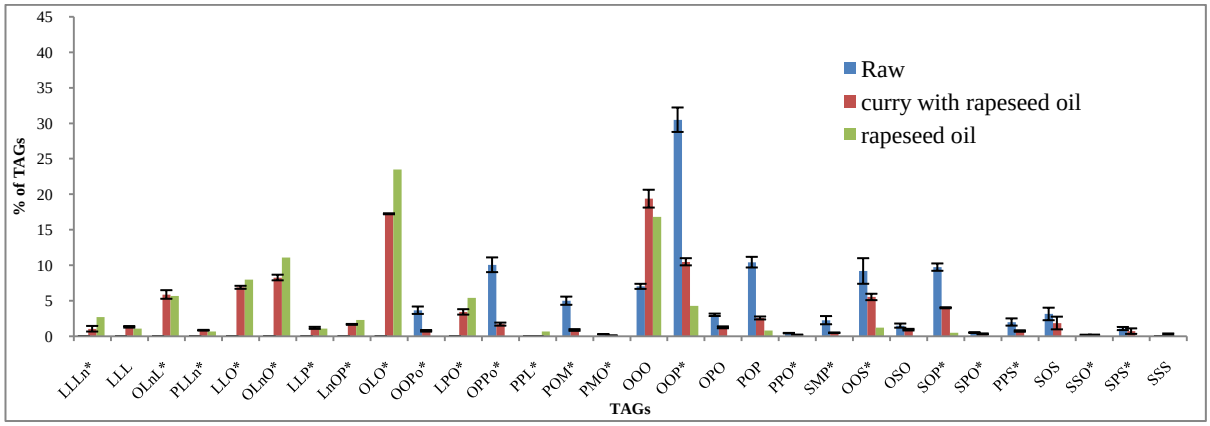

c)

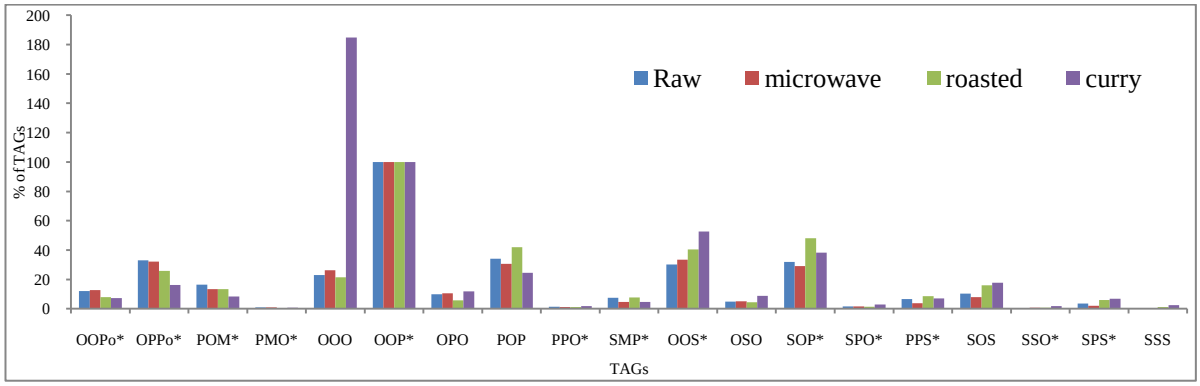

d)

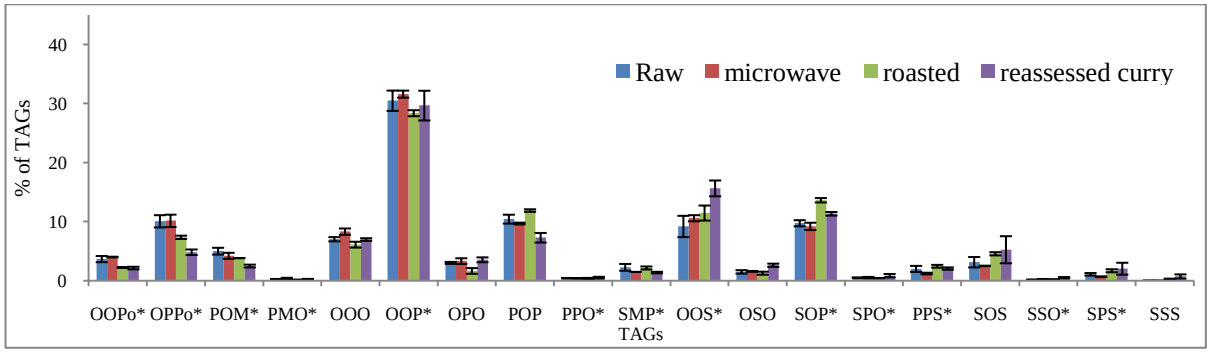

Figure 4.5: Percentage of TAGs for a) raw and cooked beef, b) beef curry with rapeseed oil c) raw and cooked beef normalised to OOP* and d) the reproduced histogram of TAGs proportion for raw and cooked beef with reassessed beef curry.

The histograms for raw and cooked lamb reveal that OOS* is the only TAG showing no significant abundance differences in any of the lamb samples (Fig. 4.6a), indicating that microwave and hotpot cooking do not change the proportions of OOS* from those in raw meat. The TAG profile of lamb hotpot is quite similar to that of the raw meat except for OOO, SPS*, PPS* and SSS which are significantly higher for hotpot, whereas the levels of OPO, OSO, PMO*, PPO*, SMP* and SPO* are significantly higher in raw lamb. Butter has been added during hotpot cooking as listed in the ingredients and this is presumably from cow's milk. Cow milk butter contains high concentrations of OOP* and OOS* (Frede and Thiele, 1987) and the TAG profiles of lamb hotpot does not show evidence that butter contributes much to the TAG profiles relative to the raw lamb.

The proportions of OSO, SOP* and SOS are very much higher for microwave than for raw lamb and hotpot and the differences are significant. The higher proportions of these TAGs make the proportions of POM*, PMO*, OOO, OOP*, OPO, POP, PPO*, SMP*, SPS* and SSS significantly lower in microwave lamb than in the raw meat. The much higher proportion of SOP* after microwave cooking is attributed to oxidation of TAGs containing O, consequently reducing the proportion of OOP* and increased the level of SOP*. This strongly suggest that microwave cooking of lamb does vary the relative proportions of TAGs slightly, different to hotpot even with the addition of butter. It is also clear that different meat behaves differently during microwave cooking; it does not impart much difference in the TAG profile for beef but varies the relative proportions of TAGs for lamb. The TAG profiles for all lamb samples were normalised to SOP* and no subtraction was done due to no obvious sign of added oil/fat observed (Fig. 4.6b).

a)

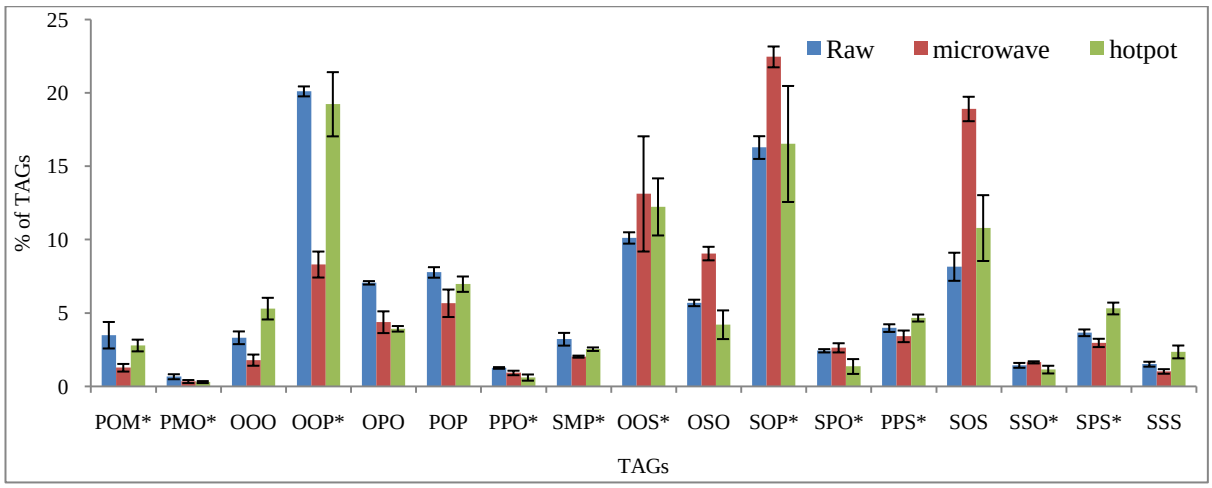

b)

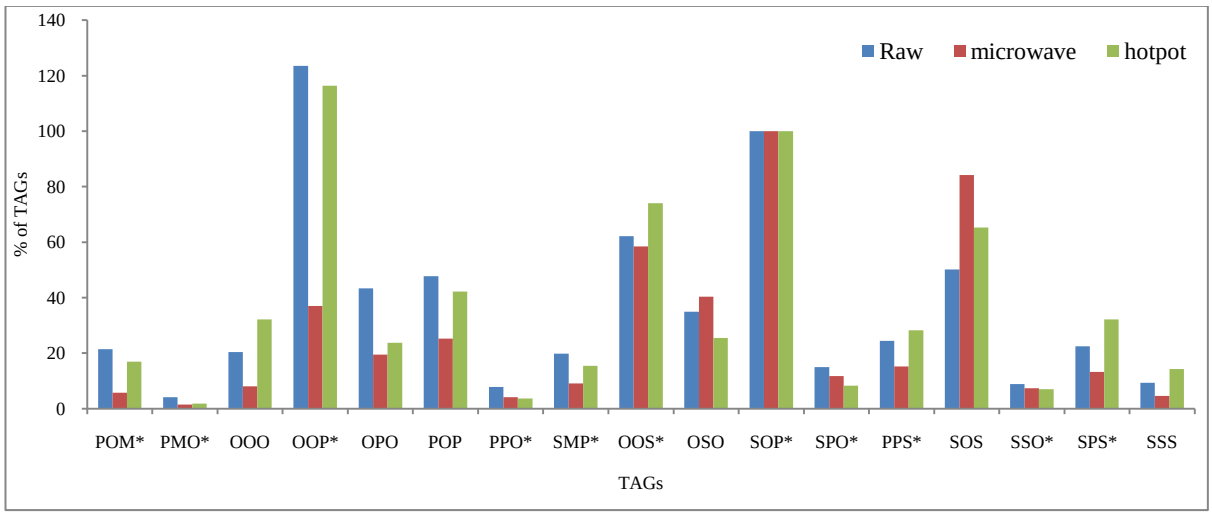

Figure 4.6: Percentages of TAGs for a) raw and cooked lamb, b) raw and cooked lamb normalised to SOP*.

The TAG profiles for different methods of cooking chicken vary from that of the raw meat (Fig. 4.7a). The Y-error bars for twenty four TAGs show that no TAG has similar proportions for all of the samples. TAGs containing L and Ln were significantly higher for raw chicken than for microwave cooking and roasting (e.g. LLLn*, OLnL*, PLLn* and OLnO*), whereas chicken curry has the highest OLnO* proportions and also very high proportions of OLO* and OOO. The increased proportion of OOO for chicken curry is similar to that observed for beef. This is due to the addition of vegetable oil as listed on the product label, presumably rapeseed oil based on the proportions of TAGs for chicken curry compared with rapeseed oil (Fig. 4.7b). Chicken curry and rapeseed oil have similar levels of OLnO* and OLO*, but chicken curry has much a higher level of OOO than rapeseed oil and raw chicken. Apart from vegetable oil, coconut has been added to the chicken curry as listed on the product label. However, the major TAGs obtained for coconut oils were LaLaLa, LaLaM and CLaLa (Marina et al., 2009) and hence there is no evidence that coconut contributes much to the proportions of TAGs for chicken curry.

The relative proportions of TAGs from roasted chicken are essentially identical to those of the raw meat, except for significantly lower abundances of OLnL*, OLnO* and LnOP* and higher abundances of LPO*, PPL* and POM*. The lower proportions of TAGs containing L and Ln for roasted and microwave chicken coincide with increases in the proportions of TAGs containing saturated FAs (e.g. S and P). This might be due to the oxidation of L and Ln during cooking. The differences resulting from microwave cooking, with significantly higher levels of OOP*, POP, OOS* and SOP* are most pronounced, and are observed for roasting at a lower impact level. Overall, the TAG proportions for microwave cooking and curry vary significantly from that of raw meat, suggesting that the high temperatures for microwave cooking and addition of vegetable oils in curry are responsible for changes in the TAGs of cooked chicken.

The histogram plots for chicken were normalised to LPO*. The normalisation was performed to determine if correction for TAGs added during cooking should be applied. Five TAGs of curry were dominant (OLnL*, LLO*, OLnO*, OLO* and OOO), hence it was assumed that the excess of these TAGs arise from rapeseed oil added to the curry (Fig. 4.7c).

Two procedures have been applied for reassessment of chicken curry:

a) After normalisation, the abundances of OLnL*, LLO*, OLnO*, OLO* and OOO for curry were fixed to those of raw chicken which are 52% (OLnL*), 76% (LLO*), 31% (OLnO*), 120% (OLO*) and 63% (OOO) assuming the balance/excess was from rapeseed oil. Following the adjustment of OLnL*, LLO*, OLnO*, OLO* and OOO, the relative abundances of all other TAGs in curry were reassessed and scaled to the new value of curry (1st procedure; Table 4.4). The histogram was reproduced from the reassessed TAGs and this approach is important to take out, as much as is possible, the effect of added TAGs from rapeseed oil in order to reveal the underlying TAG profile that results purely from chicken.

b) After normalisation to LPO*, the normalised abundances of OOO for curry were fixed to those of raw chicken (63%; Fig. 4.7c). Following the adjustment, the relative abundances of all other TAGs in curry were reassessed and scaled to the new OOO value of curry. The reassessed TAGs percentages were adjusted by subtraction of their relative proportions in rapeseed oil (5.7% of OLnL*, 8% of LLO*, 11.1% of OLnO* and 23.5% of OLO*). The proportions of TAGs for rapeseed oil were obtained from the previous study (Holcapek et al., 2003). The relative abundances of all TAGs in chicken curry following the reassessment and subtraction are comparable with the 1st procedure (2nd procedure; Table 4.4) and the histograms of TAG profiles for chicken curry from the 1st procedure were reproduced (Fig. 4.7d).

Table 4.4: Reassessed proportions of TAGs for chicken curry after subtracting possible TAGs from rapeseed oil.

TAGs	Chicken curry	Reassessed chicken curry	
		1st procedure	2nd procedure
LLLn*	1.48	3.48	3.58
LLL	1.81	4.26	4.38
OLnL*	7.89	6.43	8.05
PLLn*	1.20	2.80	2.88
LLO*	10.10	9.49	8.86
OLnO*	10.71	3.85	4.63
LLP*	2.11	4.95	5.08
LnOP*	1.83	4.30	4.42
OLO*	23.55	15.08	11.56
OOPo*	0.36	0.82	0.84
LPO*	5.30	12.48	12.82
OPPo*	0.27	0.64	0.66
PPL*	0.47	1.09	1.12
POM*	0.13	0.30	0.31
PMO*	-	-	-
OOO	23.36	7.85	8.06
OOP*	5.24	12.32	12.65
OPO	-	-	-
LPS*	0.28	0.65	0.67
POP	0.79	1.85	1.90
PPO*	-	-	-
SMP*	0.12	0.27	0.28
OOS*	2.14	5.03	5.17
OSO	-	-	-
SOP*	0.51	1.21	1.24
SPO*	-	-	-
PPS*	0.11	0.26	0.26
SOS	-	-	-
SSO*	0.18	0.41	0.42
SPS*	0.07	0.16	0.16

The corrected histogram shows increases of PLLn*, LLP*, LnOP*, LPO*, OOP* and OOS* for curry. The proportion of TAGs are almost identical to the raw meat, except for significantly higher levels of LLL and OOS*, and lower levels of OOPo*, OPPo*, POP and SOP* (Fig. 4.7d). As observed for beef, this suggests that curry cooking does not have much effect on the TAG profile of chicken.

a)

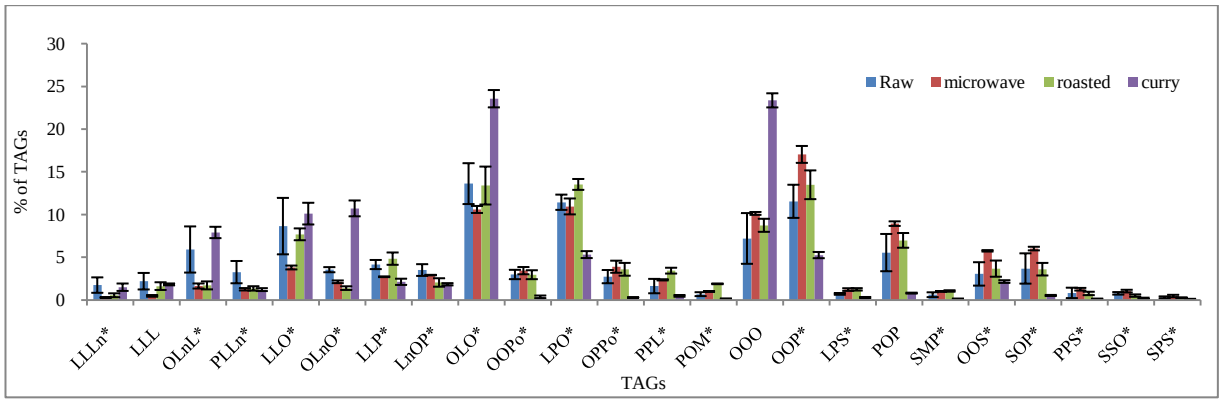

b)

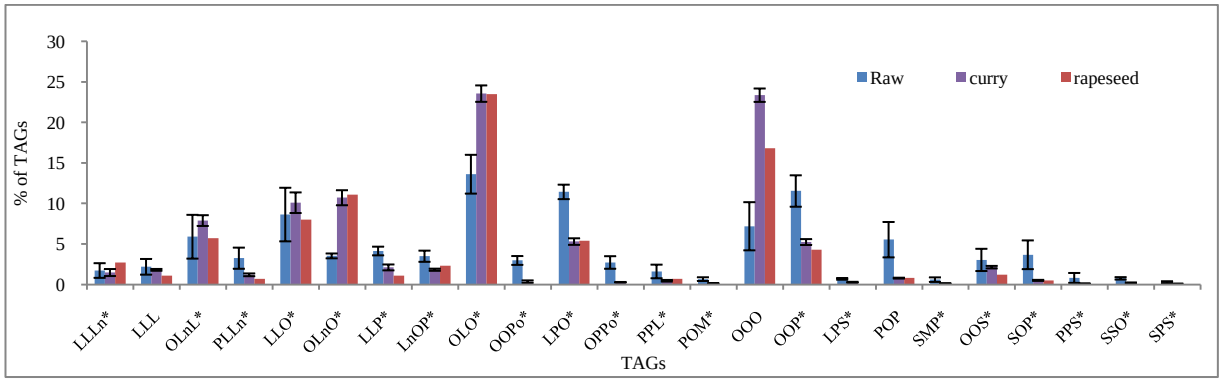

c)

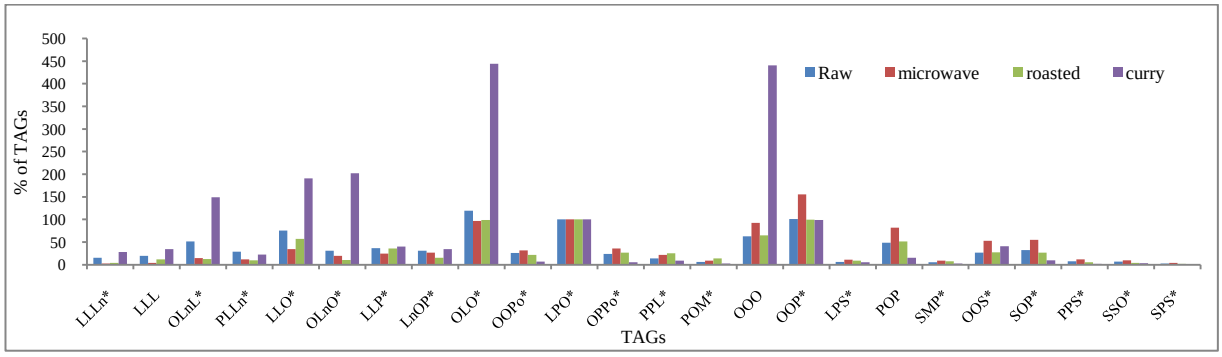

d)

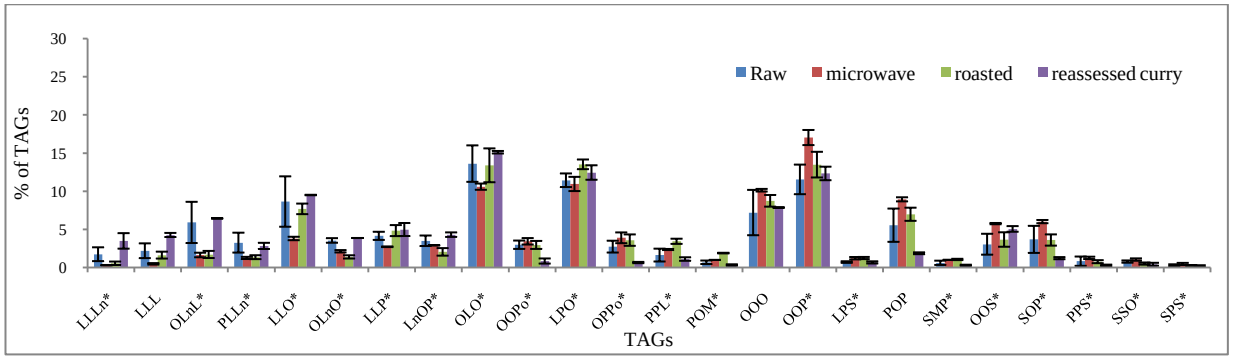

Figure 4.7: Percentage of TAGs for a) raw and cooked chicken, b) chicken curry and rapeseed oil c) raw and cooked chicken normalised to LPO* and d) reproduced histogram of TAGs proportion for raw and cooked chicken with reassessed chicken curry.

The TAG proportions for raw pork were examined from ham in order to make a fair comparison with the microwave pork which was from the ham. The histogram shows that the profile after microwave was identical to that for the raw meat. By contrast, roasted pork shows obvious differences in the levels of OPO and SPO* which are significantly higher for the roasted meat (Fig. 4.8a). Also, the proportion of TAGs containing the highly unsaturated FAs L and Ln are low for roasted pork (e.g. OLnL*, PLLn*, LLP*, LnOP*, OLO* and LPO*). This suggests the oxidation of L and Ln occurred during roasting and consequently increasing the relative abundance of the TAGs containing O, in particular OPO and SPO*. Notably no addition of fat/oil was listed among the roasted pork ingredients. The pork sample shows that roasting does change the TAG proportions but that microwave does not. Although there were differences in the TAG proportions for roasting, the basic profile remains quite similar to that of the raw meat. The normalisation to LPO* was performed on samples and reveals that the abundances of OPO and SPO* for roasted pork were almost double those for the raw meat (Fig. 4.8b). No correction was performed for roast pork, assuming that the excess proportions of OPO and SPO* are from the oxidation of TAGs containing the highly unsaturated FAs L and Ln, consistent with the decreasing levels of these TAGs. The TAG profiles for raw pork from different locations (ham, belly, shoulder and loin) were examined (Fig. 4.8c) and show no differences in the TAG profiles by comparison with those for ham (Fig. 4.8a), except for LPO* which is slightly lower for microwave than raw pork. This indicates that the TAG profiles are similarly affected by the cooking method regardless of the location within the animal.

Overall, microwave cooking of chicken and lamb give similar changes in the TAG profiles, attributed to oxidation of TAGs containing the highly unsaturated FAs L and Ln. Thus, reduced levels of the low ECN unsaturated TAGs and increased levels of the highly saturated TAGs are apparent. By contrast, microwave cooking for beef and pork give similar profiles to the raw meat. Whereas, the TAG profiles of roast chicken and beef are very similar to the raw meat, pork shows considerable higher proportions of OPO and SPO* and lower proportions of TAGs having highly unsaturated FAs. The correction of curry cooking for beef and chicken revealed the underlying profiles relating to the meat, indicating there is merit in this approach for meat that has been cooked.

a)

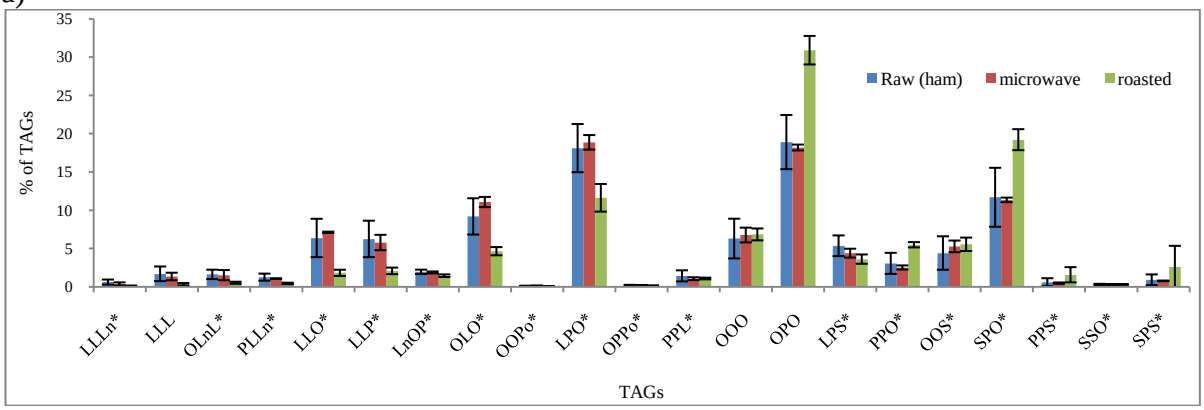

b)

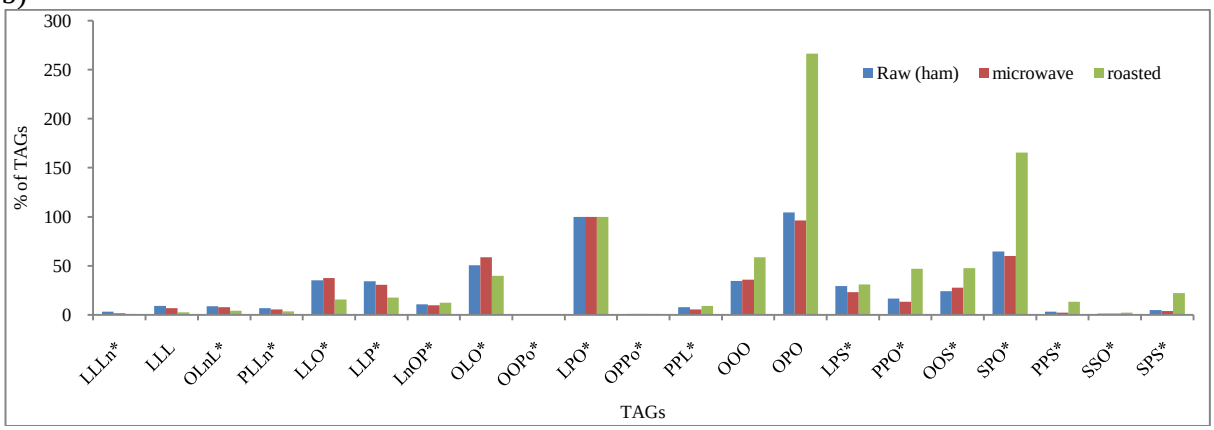

c)

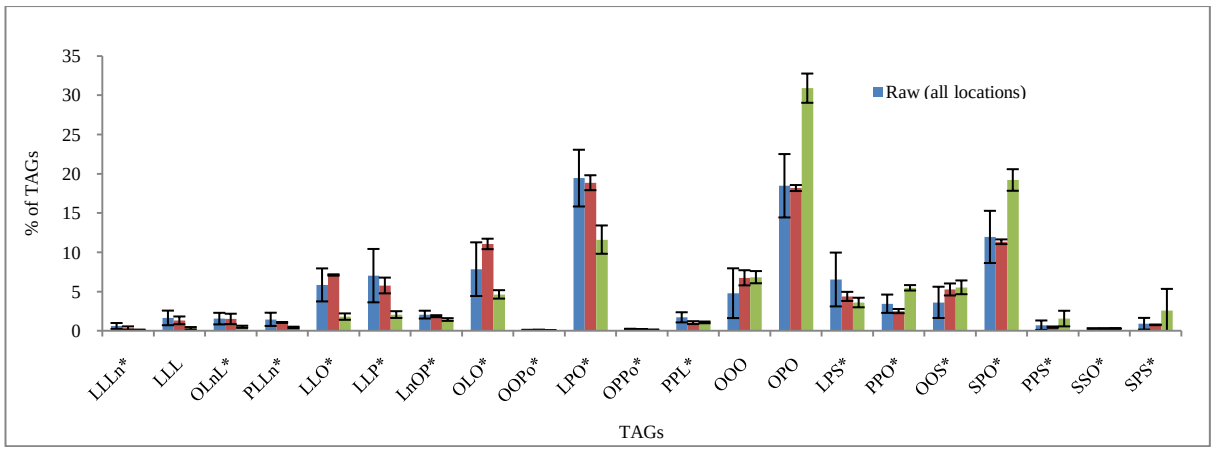

Figure 4.8: Percentage of TAGs for a) raw and cooked pork, b) raw and cooked pork normalised to LPO* and c) raw and cooked pork with all pork locations of ham, belly, loin and shoulder.

4.2.4 PCA of TAG profiles for raw and different cooking methods of beef, lamb, chicken and pork.

The PCA scores plots for different species were explored to reveal the variations between the raw meat and different cooking methods.

4.2.4.1 PCA of TAGs for raw and cooked beef.

PCA was performed for raw and cooked beef samples excluding the TAGs labelled with 'vegetable oil' in Fig. 4.1 from the profile for beef curry. No overlap is observed, with microwave cooked beef being much closer to the raw meat than with roasted and curried beef (Fig. 4.9a).

PC1 shows the separation of two classes: curry and raw/microwave/roasted beef. The loadings plot reveals the important descriptors as OOO, OOP*, OPPo* and PMO*, with all having about the same magnitude, followed by OOPo*, POP and SMP* (Fig. 4.9b). The TAG OOO being much higher in curry, about five times higher than other TAG in raw/microwave/roasted beef indicates it to be a significant factor discriminating the curry. By contrast, the relative abundances of OOP*, OPPo* and PMO* were much lower in curry as a consequence of high level of OOO. In addition, OOP* contribute much less in curry than other classes of beef. Also, the proportion of POP in curry is about half that of the other classes of beef examined. These differences result in curry cooking being clearly distinguished from other beef samples in PC1.

PC2 shows the separation between roasted and raw/microwave/curry beef. The variables mainly responsible for the differences are SOP* which is higher in roasted beef than in the other class of raw/microwave/curry beef. The next important loadings, PPS*, SOS, SPS*, OPO and SPO*, contribute fairly equal to PC2 (Fig. 4.9c). The microwave samples were also slightly separated in PC2 due to the lower levels of SPS*, SOS and PPS* than for the raw meat.

a)

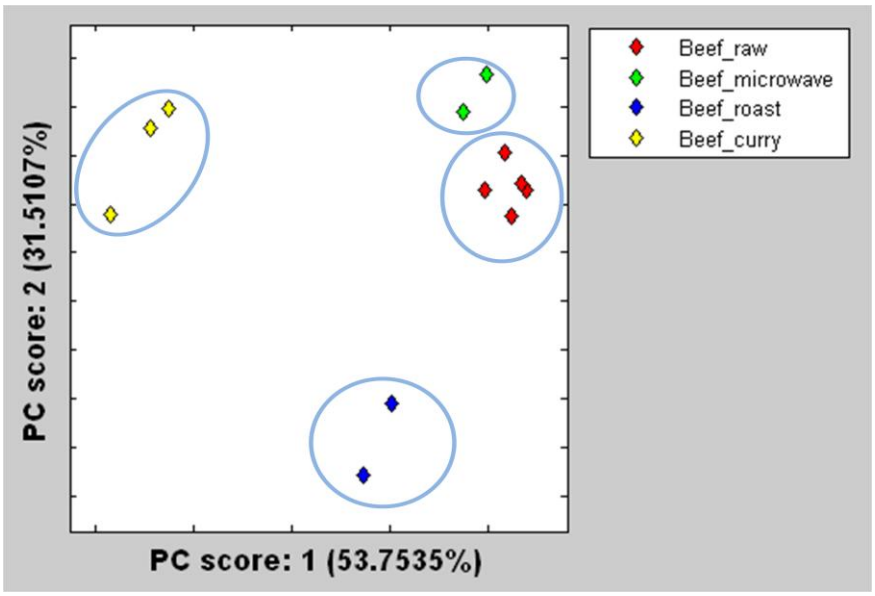

b)

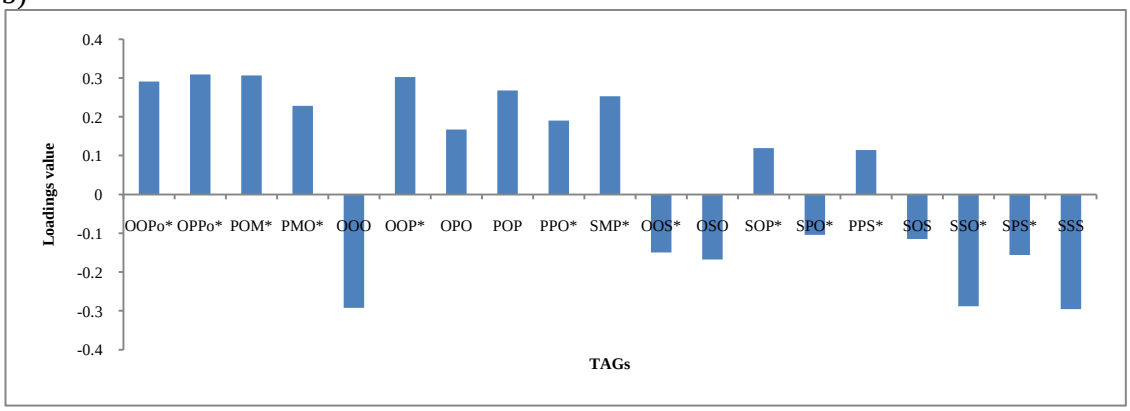

c)

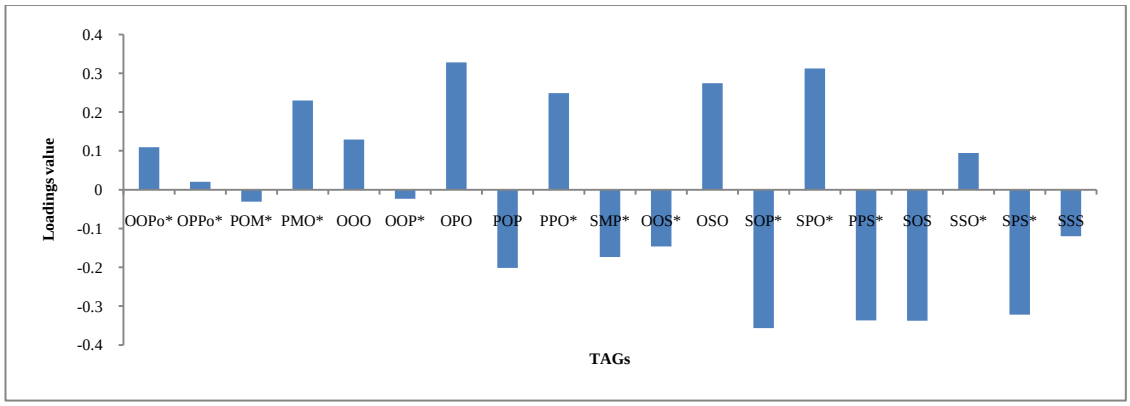

Figure 4.9: a) PCA scores plot of TAGs for raw and cooked beef (excluding the vegetable oil for curry samples, b) loadings plot for PC1, c) loadings plot for PC2.

The PCA scores plot for the TAG profiles for reassessed beef curry** (Section 4.2.3) following the subtraction of OOO shows that beef curry** is separated from raw/microwave/roasted beef as before, but is shifted slightly to lower PC1 score (PC1, Fig. 4.10). Roasted beef is slightly closer to curry than before. The loadings plot shows that the important descriptors are different to those for the previous plot, OOS*, SSS and OPPo* being most important for PC1. Reassessed curry has significantly higher levels of those TAGs than for raw meat, microwave and roasted cooking. OOS* has a much higher proportion (about 8% higher) for curry than raw meat but the value is closer to roasted beef (OOS* 5% lower). The proportion of OPPo* for curry shows a similar trend being about half the amount in raw meat. For PC2, roasted beef was separated from raw/microwave/curry beef and OPO being the most important descriptor followed by OOO. Roasted beef has significantly lower levels of OPO and OOO than raw meat and other cooking method. The results show that the PCA discrimination is fairly insensitive to variation in OOO, indicating that OOO is not one of the most important TAGs for discriminating beef from other species.

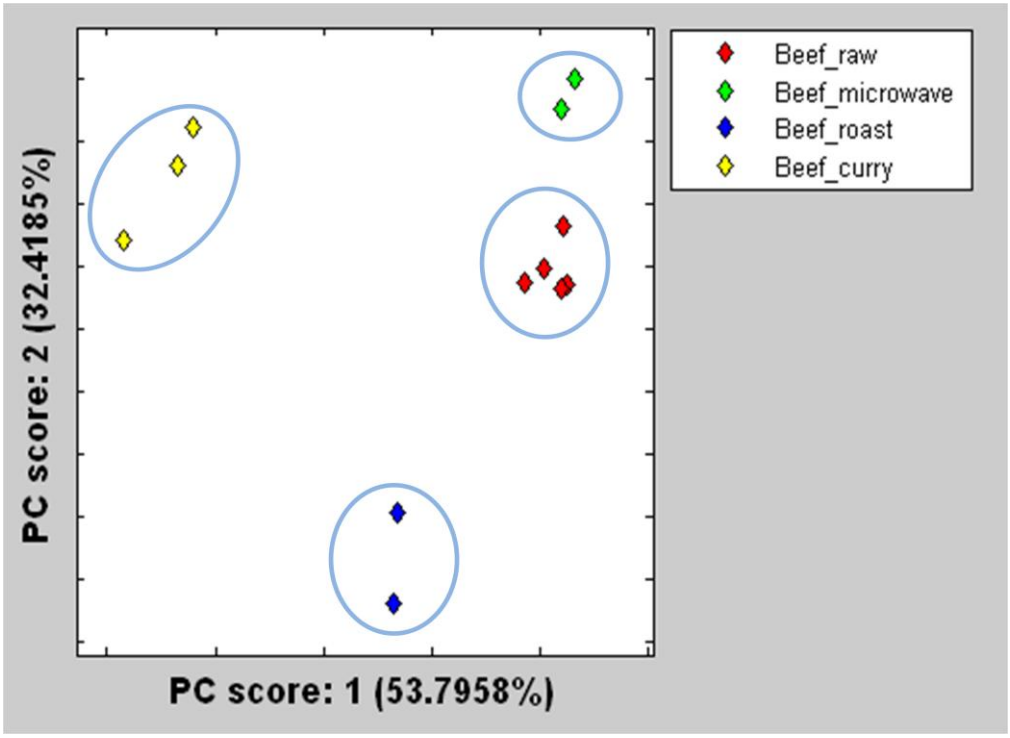

Figure 4.10: PCA scores plot of TAGs for raw and cooked beef with reassessed beef curry.

4.2.4.2 PCA of TAGs for raw and cooked lamb.

The PCA scores plot for raw and cooked lamb differentiates between microwave and raw/hotpot cooking in PC1 (Fig. 4.11a). The loadings plot shows OOP*, SOP* and OSO as having about the same influence, indicating these variables contribute equally to PC1 (Fig. 4.11b). The hotpot cooking has a similar proportion of these TAGs to raw meat, except for OOP* which is higher in raw meat than in hotpot. This is reflected in the lack of no differentiation in PC1. The proportions of SOP* and OSO are significantly higher in microwave cooked than in hotpot and raw lamb and OOP* is significantly lower for microwave than for the other samples, explaining the separation of microwave lamb in PC1. The next important loadings are SOS and POM*.

PC2 segregated all of the lamb samples with microwave cooking being closer to hotpot than raw meat. PPO* is the most important variable for this PC, having the highest positive loading, followed by OPO and PMO* (Fig. 4.11c). The proportion of these TAGs in microwave cooking is closer to hotpot than raw meat, explaining the closer proximity to hotpot in PC2.

a)

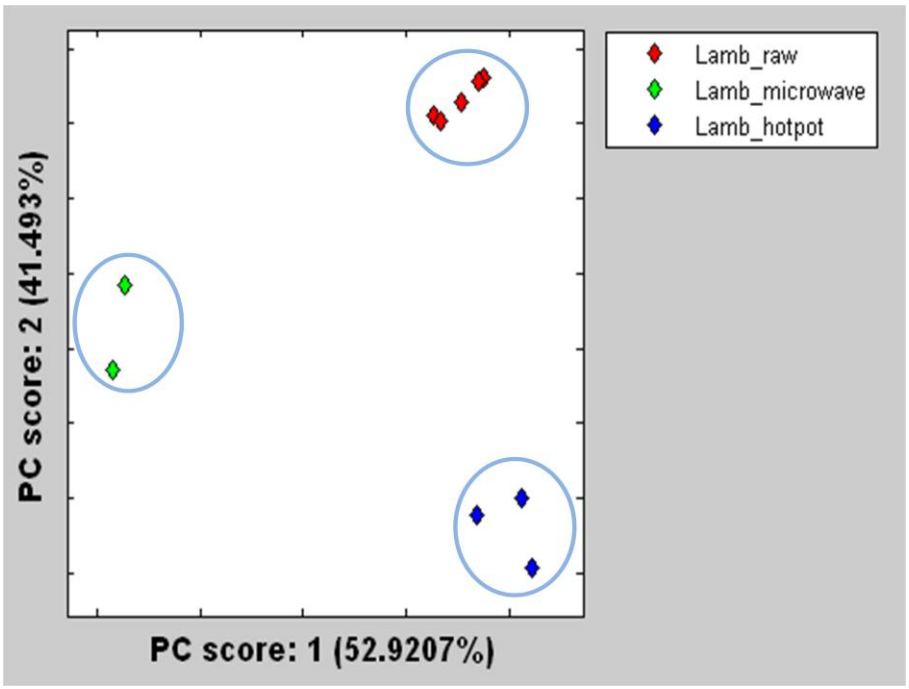

b)

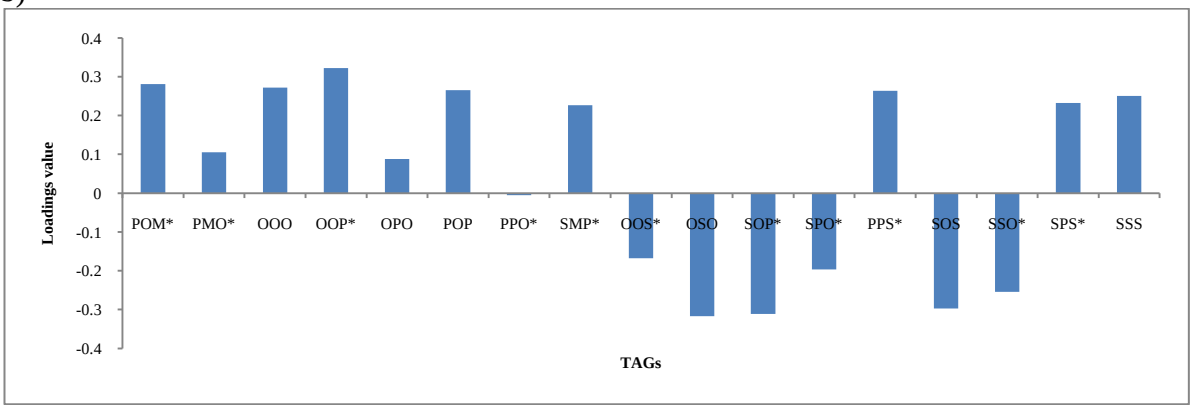

c)

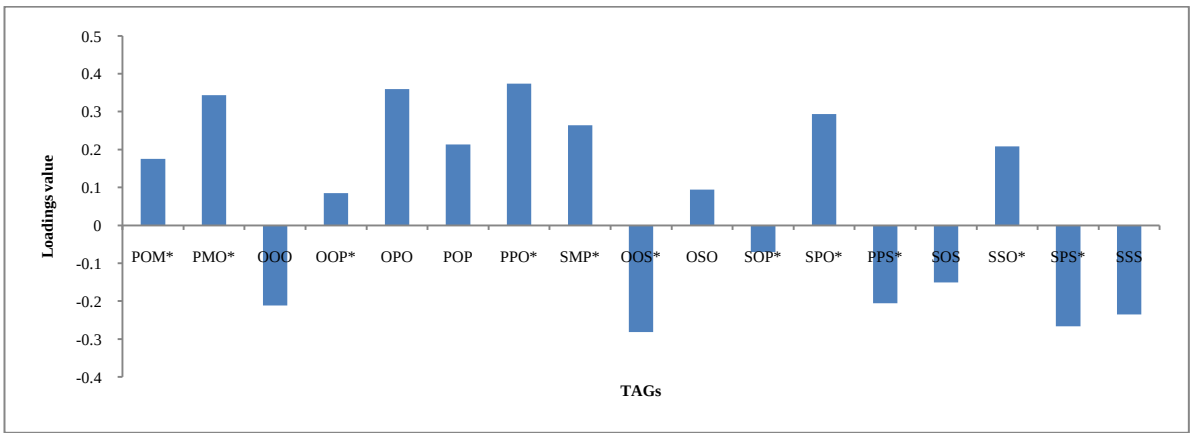

Figure 4.11: a) PCA scores plot of TAGs for raw and cooked lamb, b) loadings plot for PC1, c) loadings plot for PC2.

4.2.4.3 PCA of TAGs for raw and cooked chicken.

The PCA scores plot for raw and cooked chicken shows roasted chicken is closer to raw meat than microwave and curry. The differences between curry and raw/roasted/microwave cooking are obvious in the first component (PC1, Fig. 4.12a). The most important variables are OOP* and POP which have about the same loadings values (Fig. 4.12b). Chicken curry has significantly lower proportions of OOP* and POP, about three times less for OOP* and seven times less for POP than the raw meat. Microwave cooking has a significantly higher proportion of those TAGs, almost double that for raw chicken, accounting for the microwave samples being the most separated from curry. Other important descriptors are OLO*, OLnO*, OOPo*, SMP* and SOP*. OLO* and OLnO* are higher for curry than for raw chicken and the other cooked chicken samples whereas OOPo*, SMP* and SOP* are lower in curry than in the other chicken samples.

There is a clear separation between raw, roast/curry and microwave cooked chicken for PC2. The most important descriptor is PLLn* having the highest positive loadings value (Fig. 4.12c). The proportion of PLLn* in raw meat is about three times higher than in the cooked chicken samples. The next important descriptor is LLL, which is significantly lower in microwave chicken than in the other chicken samples, explaining why microwave chicken plots slightly separate in PC2. Lower proportions of TAGs containing L and Ln, particularly PLLn* and LLL in cooked meat than in the raw chicken show that cooking reduces the levels of PUFAs. Overall, roasted chicken is much closer to raw chicken for both PC1 and PC2 than microwave and curry, suggesting that high localised temperature for microwave and the addition of rapeseed oil in curry have a effect on the profiles of TAGs for chicken.

a)

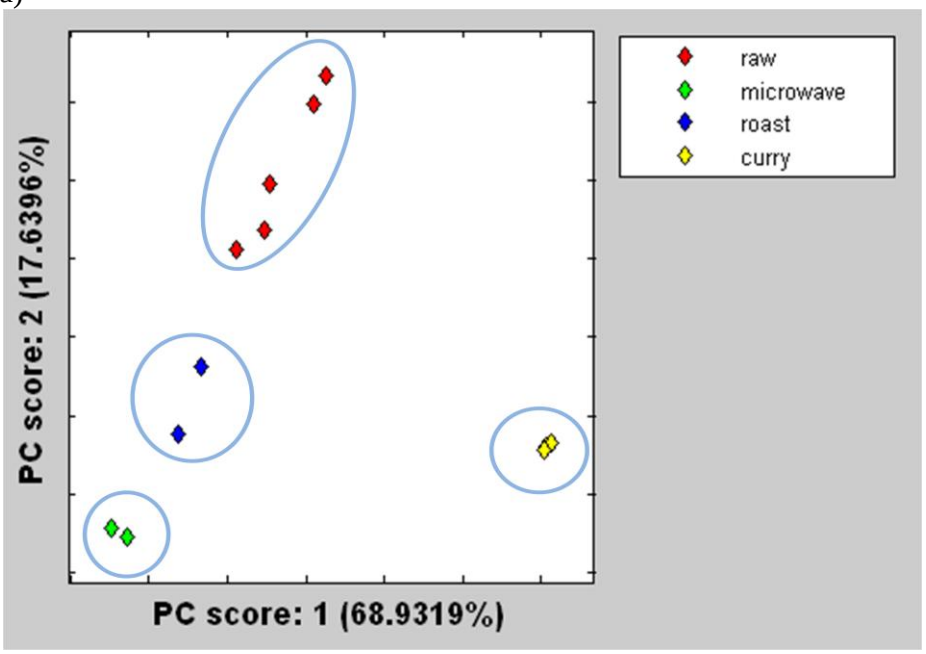

b)

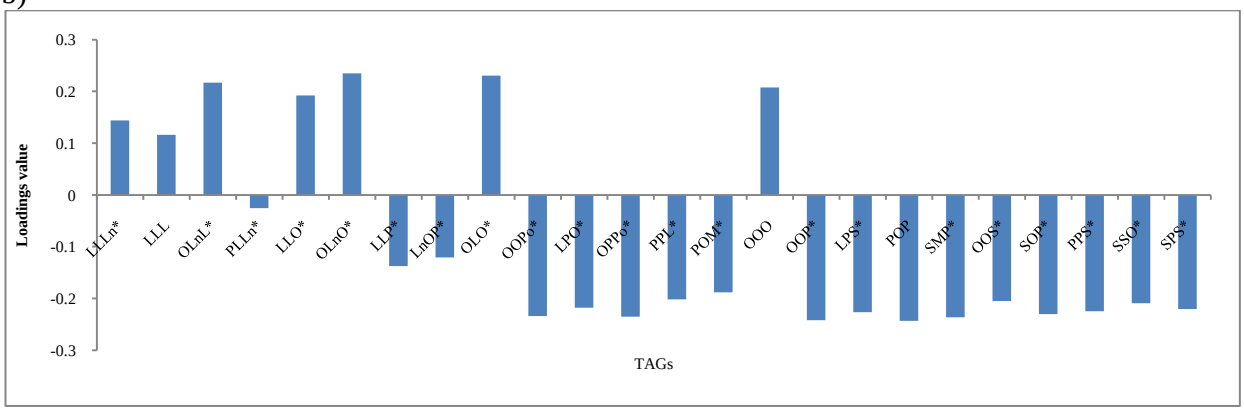

c)

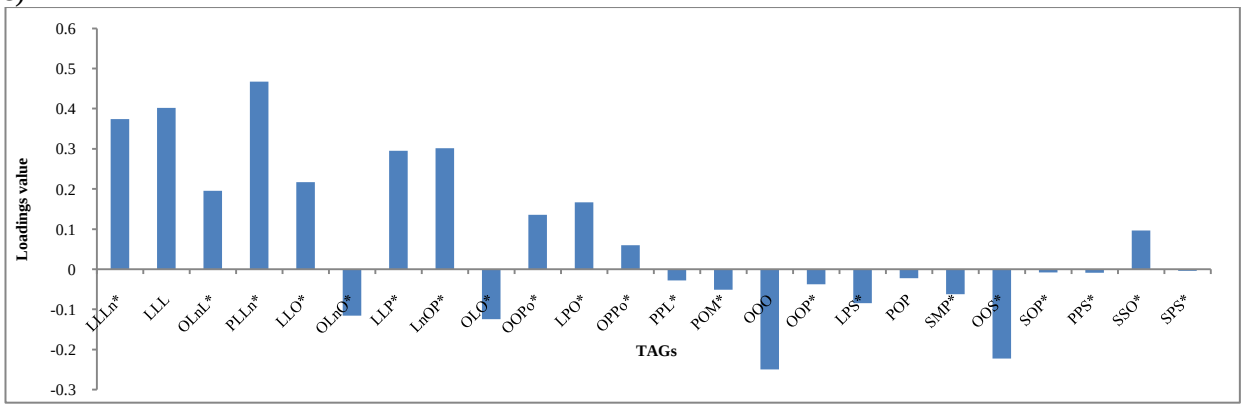

Figure 4.12: a) PCA scores plot of TAGs for raw and cooked chicken, b) loadings plot for PC1 and c) loadings plot for PC2

The PCA scores plot incorporating the reassessed TAG profile for chicken curry following the subtraction of OOO and removal of the contribution of added TAGs from rapeseed oil (OLnL*, LLO*, OLnO*, and OLO*) shows that curry is much closer to the raw meat on the PC1, with microwave being slightly more separated from raw chicken (Fig. 4.13). The loadings values (not shown) revealed show LPS*, POP and OOS* as being the most important descriptors for PC1, each having and have about the same influence. The proportion of LPS* for reassessed curry is similar to raw chicken, explaining their closeness in PC1, and is higher for microwave and roasted chicken. Microwave chicken has the highest proportion of OOS* of the chicken samples and makes the microwave quite separated from raw meat. PC2, with main descriptors being PPL* and POM* separated the roasted chicken from raw meat, microwave and curry cooking. Roasted chicken has significantly higher level of those TAGs than the other chicken samples contributing to the separation in PC2. Comparing the reassessed TAGs plot with the previous plot (Fig. 4.12a) shows that reassessment influenced the positions of the microwave and curry cooked samples, indicating the removal of TAGs, particularly OLnO* and OLnL* which are important in the discrimination of chicken.

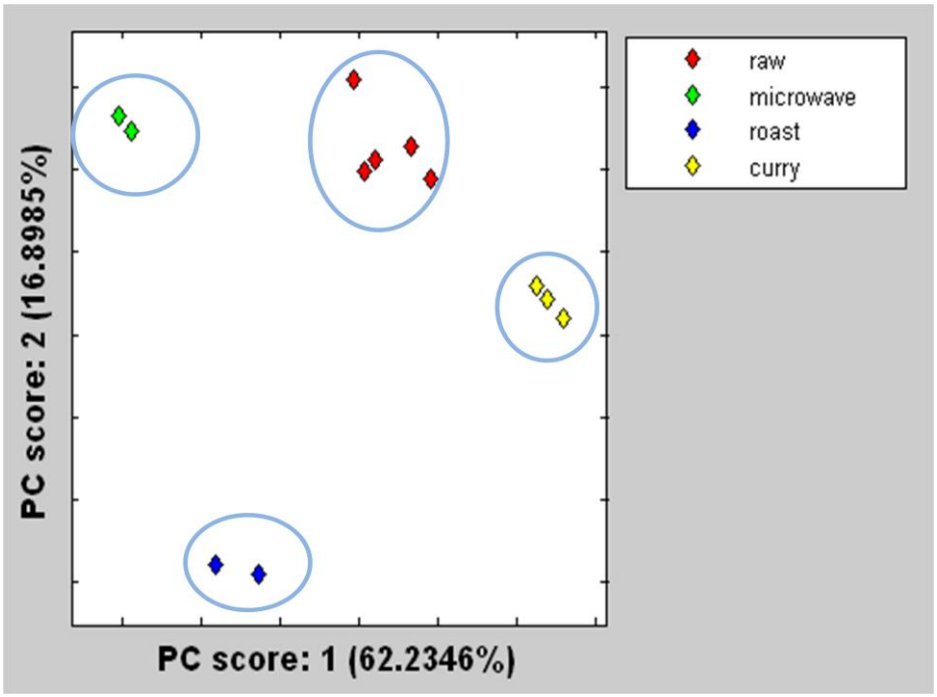

Figure 4.13: PCA scores plot of TAGs for raw and cooked chicken with reassessed chicken curry.

4.2.4.4 PCA of TAGs for raw and cooked pork.

The PCA scores plot for raw and cooked pork shows that the microwave pork samples overlap with raw pork, grouping with the ham (Fig. 4.14a). Ham was used for microwave cooking, illustrating that microwave cooking does not cause significant change in the proportions of TAGs for ham. PC1 separates the roasted pork from raw/microwave cooking. The loadings plot for PC1 reveals that almost all variables have about the same influence with slightly higher influence of LLL, LLP* and LPO*. The proportions of these TAGs for microwave cooking are similar to the raw ham, whereas they are much lower in roasted pork, causing microwave to overlap with raw ham while roasted pork plots separately to the other samples. The loadings plot reveals TAGs with high positive and high negative loadings values (Fig. 4.14b). Those with positive loadings values (e.g. LLO*, LLP*, OLO* and LPO*) are significantly lower in roasted than in raw/microwave cooking. By contrast, the TAGs with negative loadings values (e.g. OPO, PPO* and SPO*) are significantly higher in roasted than in raw/microwave cooking. OLO* and OOPo* are the most important descriptors for PC2 having the highest negative loadings, followed by OOO and SSO* (Fig. 4.14c). Pork microwave separated from roasted pork in PC2 and roasted pork overlaps with shoulder, loin and belly.

a)

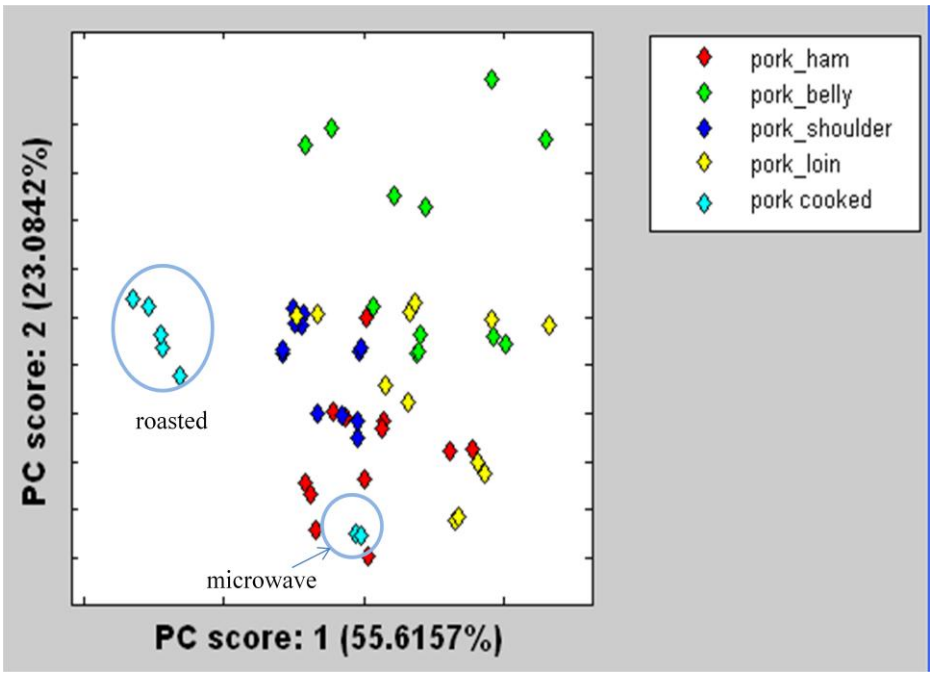

b)

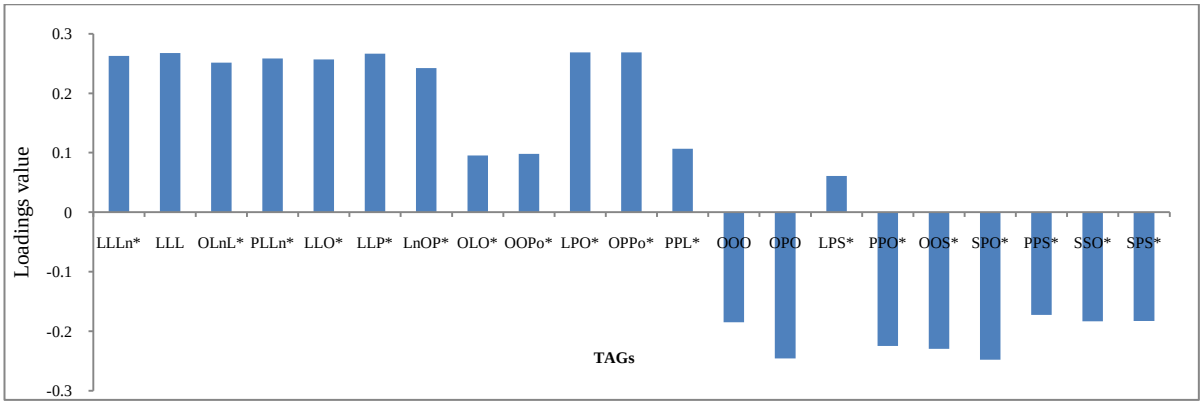

c)

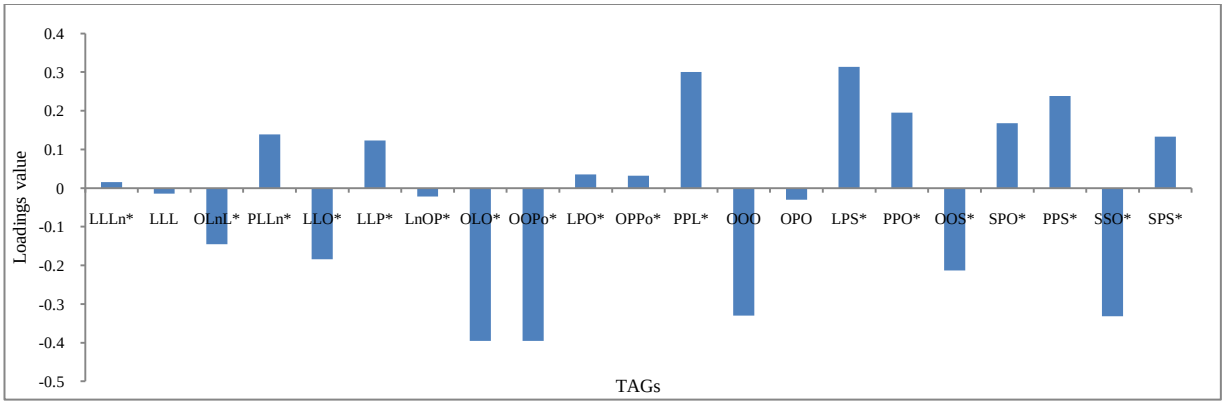

Figure 4.14: a) PCA scores plot of TAGs for raw and cooked pork, b) loadings plot for PC1 c) loadings plot for PC2.

4.2.5 PCA of TAG profiles for raw and cooked meat products.

The TAG profiles of raw and cooked beef, lamb, chicken and pork were analysed by the application of PCA to explore the extent of variation occurring with different types of cooking and different animal species. All of the TAGs observed from the raw and cooked meat samples were included in the analysis. The TAGs for beef curry was assessed by incorporating the TAGs labelled with 'vegetable oil' (Fig. 4.1). Chicken curry samples were analysed without modification, i.e. including the added vegetable oils. The PCA score plot was constructed by combining the beef curry^{+} and chicken curry which includes the TAGs from rapeseed oil added during cooking. All of the raw and cooked meat products group well by species and are separated well between species with no overlap between them. Notably, however, the beef curry^{+} samples were very close to the raw chicken and did not plot within the beef group (Fig. 4.15). This is explained by the higher proportion of TAGs containing L and Ln from rapeseed oil which are not observed for raw beef but are present in about the same abundances in raw chicken (e.g. OLnL*, LLO* and OLO*). By contrast, chicken curry overlaps with raw chicken even with the added vegetable oils being represented in the TAG profiles.

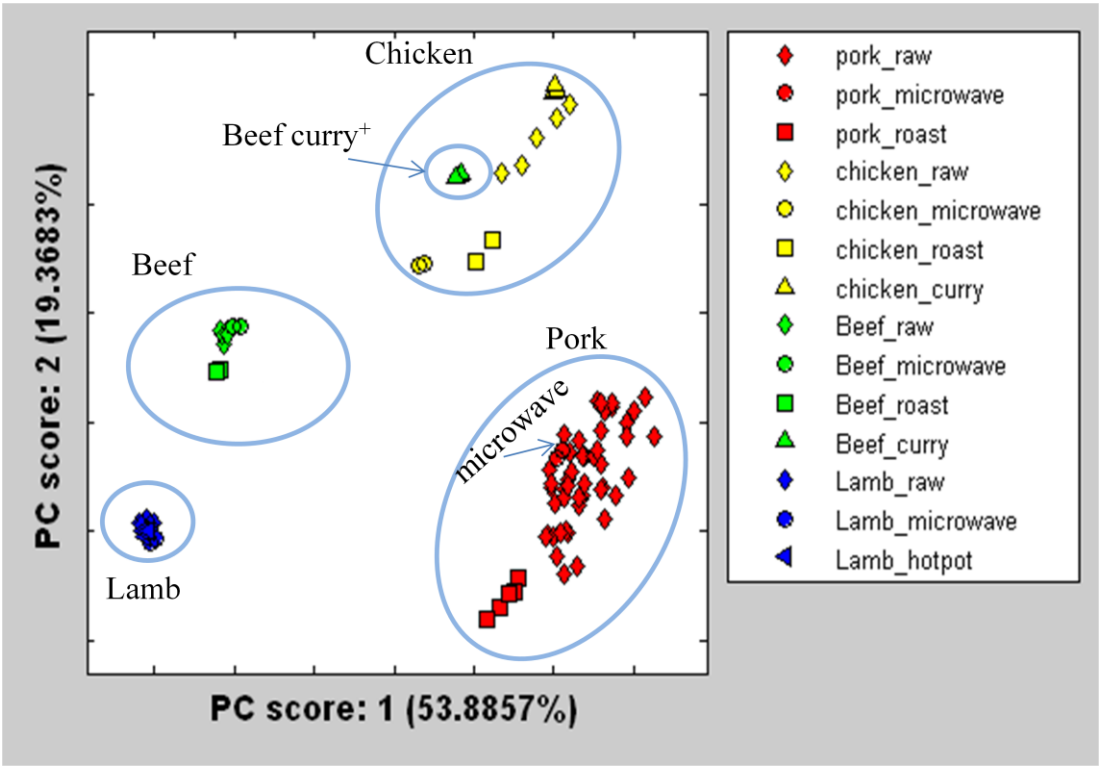

Figure 4.15: PCA scores plot of TAGs for raw and cooked meat products including the beef curry^{+} (label $^{+}$ in beef curry indicates the contribution of rapeseed oil has been incorporated in the TAG profiles)

The beef curry including the TAG attributed to rapeseed oil (labelled with $^{+}$) was compared with the distributions for rapeseed oil (Holcapek et al., 2003 and raw beef Table 4.5). The TAGs containing the highly unsaturated FAs L and Ln for beef curry^{+} are quite comparable with rapeseed oil except for LLLn*, LLO*, OLnO*, LnOP*, OLO* and LPO*. This difference is due to the high proportion of TAGs containing saturated FA for beef (e.g. POP, OOS*, SOP* and SOS), consequently reducing the proportion of TAGs containing unsaturated FAs. There is an indication of a lower level of TAGs containing Ln (LLLn*, OLnO* and LnOP*) after heating during cooking for beef curry^{+}, suggesting the oxidation of Ln. It was shown that Ln is susceptible to oxidation during frying and the oxidation level was significantly different with different levels of Ln in rapeseed oil (Eskin et al., 1989).

Table 4.5: The reassessed proportions of TAGs for beef curry[+] after considering the TAGs from rapeseed oil and TAGs for beef curry [++] after subtracting possible TAGs from rapeseed oil.

TAGs	Raw beef	Beef curry[+]	Beef curry (excludes rapeseed oil)	Reassessed beef curry[++]	Rapeseed oil (Holcapek et al., 2003)
LLLn*	-	1.05	-	NI	2.7
LLL	-	1.32	-	NI	1.1
OLnL*	-	5.88	-	NI	5.7
PLLn*	-	0.84	-	NI	0.7
LLO*	-	6.89	-	NI	8.0
OLnO*	-	8.27	-	NI	11.1
LLP*	-	1.18	-	NI	1.1
LnOP*	-	1.66	-	NI	2.3
OLO*	-	17.24	-	NI	23.5
OOPo*	3.66	0.76	1.45	2.14	-
LPO*	-	3.42	-	NI	5.4
OPPo*	10.06	1.70	3.26	4.82	-
PPL*	-	-	-	-	0.7
POM*	5.00	0.88	1.68	2.48	-
PMO*	0.26	0.08	0.15	0.23	-
OOO	7.02	19.37	37.06	6.97	16.8
OOP*	30.49	10.48	20.06	29.66	-
OPO	3.02	1.25	2.40	3.54	4.3
LPS*	-	-	-	-	-
POP	10.43	2.57	4.92	7.27	-
PPO*	0.43	0.18	0.35	0.52	0.8
SMP*	2.26	0.49	0.93	1.38	-
OOS*	9.19	5.53	10.58	15.64	1.2
OSO	1.49	0.92	1.77	2.61	-
SOP*	9.73	4.00	7.67	11.33	0.5
SPO*	0.51	0.30	0.58	0.86	-
PPS*	2.00	0.73	1.40	2.06	-
SOS	3.14	1.86	3.56	5.24	0.07
SSO*	0.17	0.18	0.35	0.51	-
SPS*	1.08	0.72	1.37	2.03	-
SSS	-	0.25	0.48	0.71	-

[+] includes the TAGs from rapeseed oil.
[++] reassessed TAGs percentage after subtracting possible TAGs from rapeseed oil and the TAGs of LLLn* to OLO* were not included.
NI – not included.

The PCA scores plot was reconstructed including only the TAGs OOPo* to SSS for beef curry, the TAGs labelled with 'vegetable oil' (Fig. 4.1) were excluded prior to PCA whereas all the TAGs identified from chicken curry were analysed. The first two principal components in the PCA scores plot show the distribution of raw and cooked meat according to their TAGs and with 74% of the variance being explained; 55% from the first component (PC1) and 19% from the second one (PC2, Fig. 4.16a). All of the raw and cooked meat products group well by species and are separated well between species with no overlap between them. Notably, all raw and cooked lamb samples overlap, the microwave pork and beef samples overlap with the corresponding raw meat and chicken curry overlaps with raw chicken. It is particularly noteworthy that the cooked meats plot close/overlap to the raw meat for each species, indicating similarity in their TAG profiles. This work show that the discrimination of different species is possible for both raw and cooked meat products, revealing that the difference between cooking methods were less than the variations between species.

PC1 clearly divided the raw and cooked meats into two classes/groups: chicken/pork and beef/lamb. This is explained by the similarities in the TAG profiles, the highly unsaturated FAs L and Ln being prominent for raw and cooked pork and chicken while beef and lamb have similar TAG profiles containing highly saturated FAs (e.g. S and P). The loadings plot for PC1 reveals that almost all variables have about the same magnitude, meaning that all TAGs contribute fairly equal to PC1 (Fig 4.16b). Notably, the loadings values of LPO*, OOS*, SOP* and SMP* are slightly higher, indicating that the variation of these TAGs for chicken/pork and beef/lamb are the most significant factor discriminating the meats. For example, the percentage of OOS* for lamb and beef is much higher (about 10% for raw lamb and 13% for microwave lamb) compared with pork and chicken (about 2% for curry and 3% for raw chicken) whereas LPO* is present only in pork and chicken samples. Only OOO and OLnO* stand out as contributing very little to the discrimination, probably due to the variation in cooked meat products of the same species especially for beef and chicken curry (e.g. the OOO for roasted beef is about 6% compared with beef curry which is 37%) whereas OLnO* is present only in chicken samples. Interestingly, the PCA scores plot shows beef curry grouped together with the raw beef even though the distribution of TAGs shows a much greater proportion of OOO than for raw beef.

PC2 shows the variation between classes of chicken, beef and lamb/pork of raw and cooked products with a much greater spread for chicken samples. OPO and PPO* are the most important descriptors having the highest negative loading followed by OLnL*, OLnO*, OOPo* and SPO* (Fig. 4.16c). The levels of OPO and PPO* vary between different animal species, pork has significantly higher levels of both TAGs than beef and lamb, whereas this TAG is not observed in chicken. The proportion of OOPo* for chicken and beef (about 0.4 to 3.5% for chicken and 1.5 to 4% for beef) is considerably higher than for lamb and pork samples (<0.1%). The great range of OOPo* relative abundance among the chicken samples (0.4% for curry and 3.5% for microwave) is responsible for the spread in the chicken data. In addition, OLnO* has a much higher proportion (11%) in chicken curry than in roasted chicken (1%). OLnO* is only dominant in chicken, particularly curry, and is present only in very low abundance for roasted chicken. The proportion of SPO* also varies between different cooking methods as well as between species. The higher proportions of OOP*, POP, OOS* and SOP* for roasted and microwave chicken than for raw chicken cause the group to plot closer to beef. Also, the TAGs containing L and Ln (LLLn*, LLL, OLnL* and PLLn*) cause roasted and microwave cooked chicken to plot closer to pork as a result of the much lower proportion of these TAGs compared with raw chicken, and their proportions are close to pork samples. For chicken curry, the addition of rapeseed oil increases the OLnO*, OLO* and OOO and partially separate the samples from raw meat. Even though some of the cooked products plot some distance from their raw meat counterparts, the PCA plot can still be used to distinguish the species origin.

a)

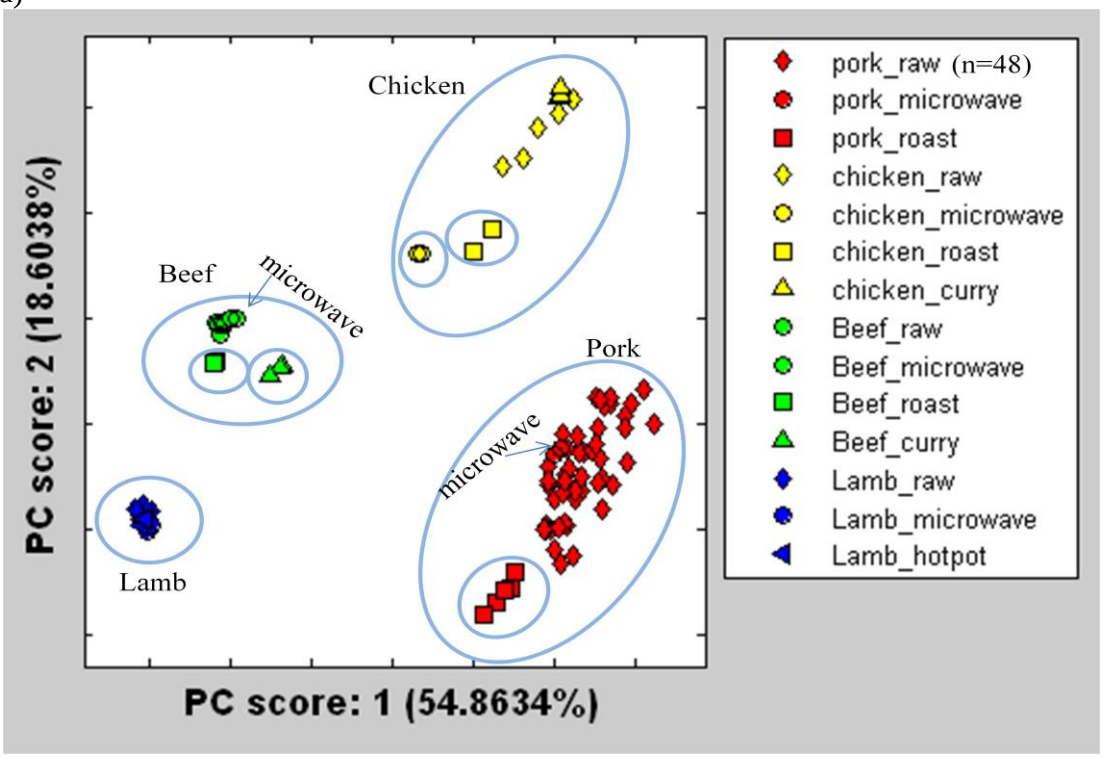

b)

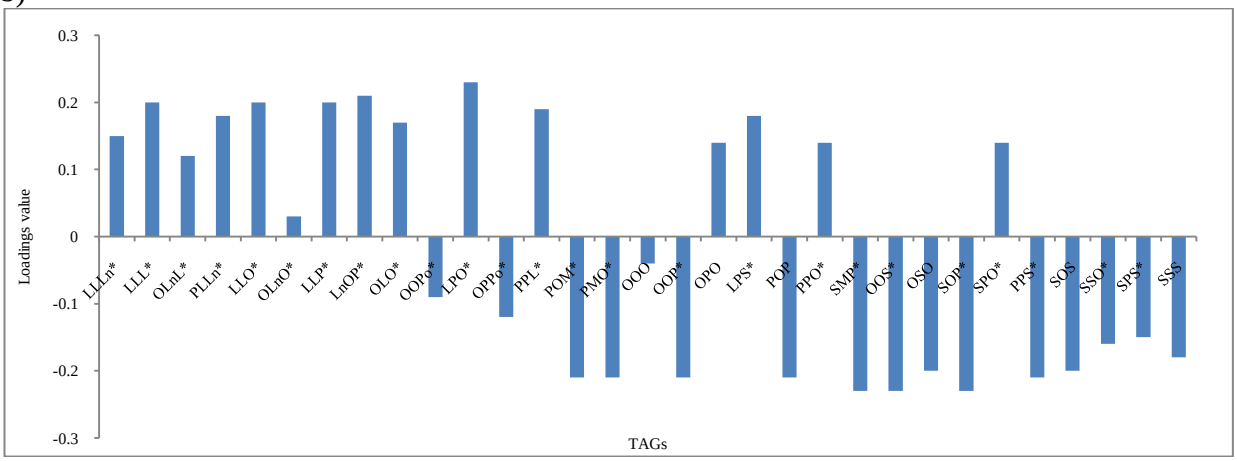

c)

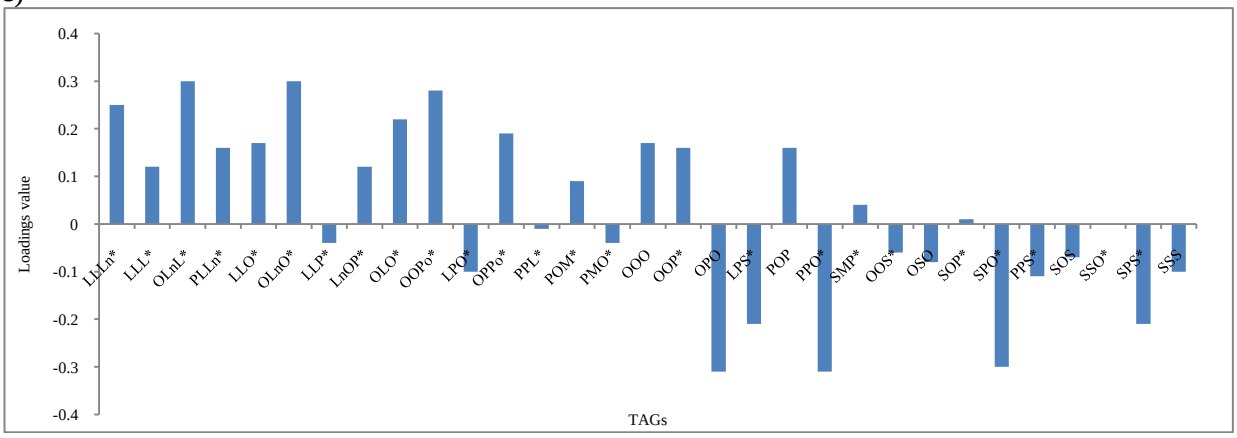

Figure 4.16: a) PCA scores plot of TAGs for raw and cooked meat products, b) loadings plot for PC1, c) loadings plot for PC2.

The loadings values of PC1 and PC2 for the scores plot of TAGs for raw and cooked meat products are similar to the raw meat in different animal species (Fig. 3.15b and c) and have the same important descriptors for discrimination. It should be recognised that the similarities in the PCA scores plots are partly a result of the weighting of sample numbers in the PCA (samples being dominated by the raw meats). PC1 divided the raw and cooked meat products into two classes: chicken/pork group and beef/lamb group as shown in the scores plot for PC1. The loadings plot reveals TAGs with high positive and high negative loadings values (Fig. 4.16b). Those with positive loadings values (e.g. LLLn*, LLL, LLO*, OLO*, LPO*, LPS* and SPO*) are significantly higher in chicken/pork group than in beef/lamb group. By contrast, the TAGs with negative loadings values (e.g. OOP*, OOS*, SOP* and SOS*) are significantly higher in beef/lamb group than in chicken/pork group.These results are similar to the raw meat in different animal species.

Overall, almost all important descriptors having negative loadings values on PC2 (OPO, LPS, PPO and SPO) in raw and cooked pork have significantly higher levels than in raw and cooked chicken, accounting for the discrimination in PC2. By contrast, the important descriptors having positive loadings values on the PC2 (OLnL, PLLn, OLnO and LnOP) are significantly higher in raw and cooked chicken than in other species, causing the chicken samples to plot separately to the other samples.

A plot of PC1 vs. PC2 loadings values for TAGs for raw and cooked meat products (Fig. 4.17) reveals the important TAGs for discrimination of raw and cooked products of different animal species. The important descriptors are the same as those identified for the raw samples alone (Section 3.2.5.2; Region A: beef, Region B: lamb, Region C: chicken and Region D: pork).

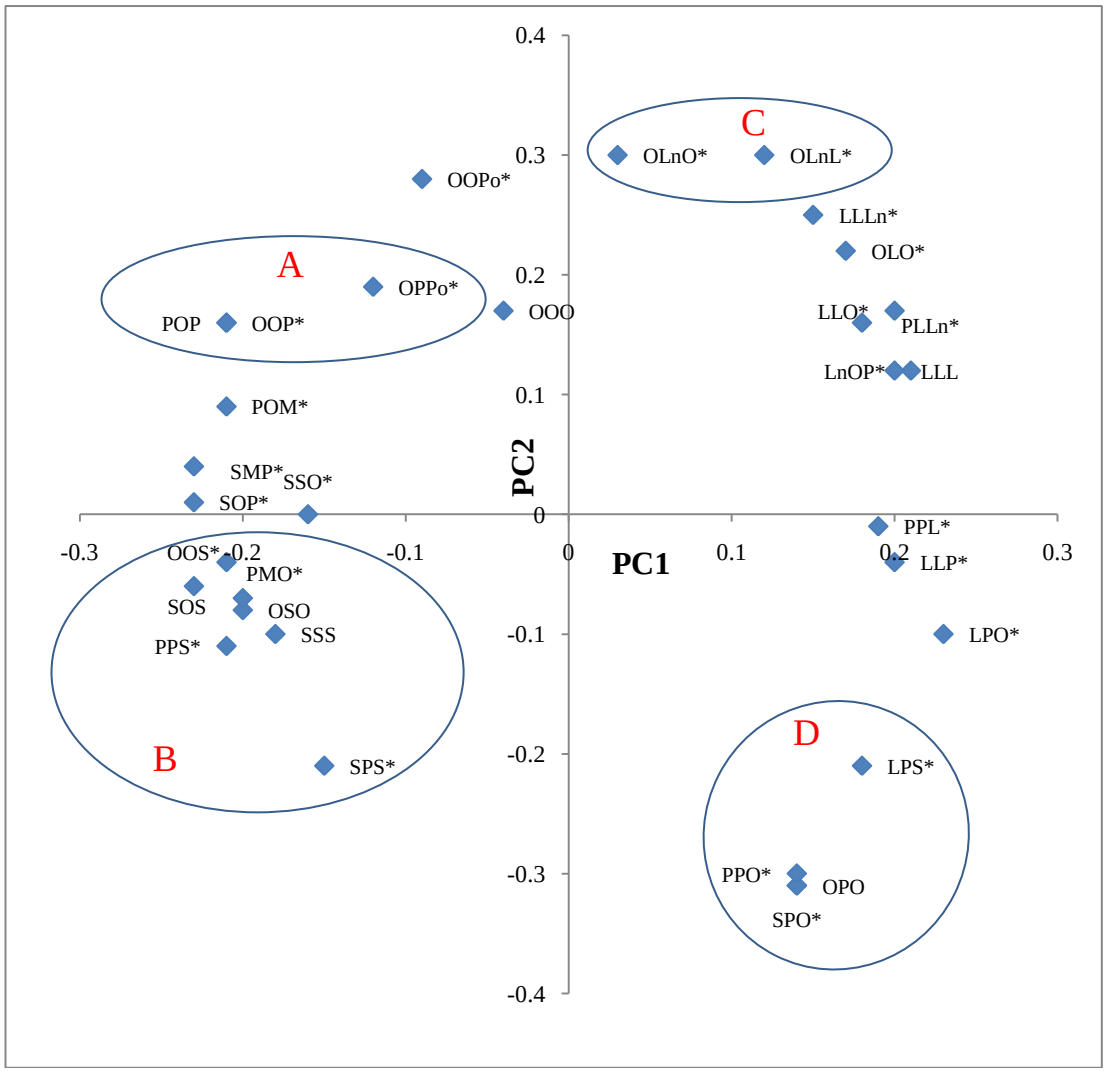

Figure 4.17: Plots of PC1 vs. PC2 loadings values from PCA scores plot of TAGs from raw and cooked meat products

Since added TAGs were also observed for beef curry, OOO in particular, reassessment of the TAG profile was performed following the subtraction of excess OOO. The reassessed TAGs profile of beef curry ($^{++}$ in Table 4.5) was closer to that for raw beef than without subtraction for added vegetable oil (i.e. excluding the TAGs profile from rapeseed oil and from OOO). Similarly, the reassessment of the TAG profile was performed for chicken curry which shows the addition of TAGs from rapeseed oil. The PCA scores plot was reconstructed from the TAGs profile of reassessed beef and chicken curry (Fig. 4.18a). The plot shows chicken curry is slightly separated from the raw chicken after reassessment but cluster well with the chicken set.

The loadings plot for PC1 and PC2 are the same as before reassessment (Fig. 4.16b and c) with LPO*, OOS*, SOP* and SMP* being the most important descriptors for PC1 (Fig. 4.18b) and OPO, PPO* and OLnO* the most important descriptors for PC2 and having the same influences (Fig. 4.18c). The slight separation of chicken curry from the raw chicken is attributed to the higher proportions of LLL and OOS*, but lower proportion of OOPo*, OPPo*, POP and SOP* after removing the contribution of added TAGs. The reassessed beef curry^{++} was closer to roasted beef than the raw meat due to the slightly higher levels of OOS*, SOP* and SOS in beef curry^{++}. Furthermore, the proportions of OOPo*, OPPo* and POM* for beef curry^{++} were also closer to roasted beef than the raw meat. The PCA plot for reassessed beef and chicken distinguished beef from other species more effectively. Notably, however, the chicken curry became slightly separated from the raw chicken, though the curry and raw chicken still plot very close and group together.

a)

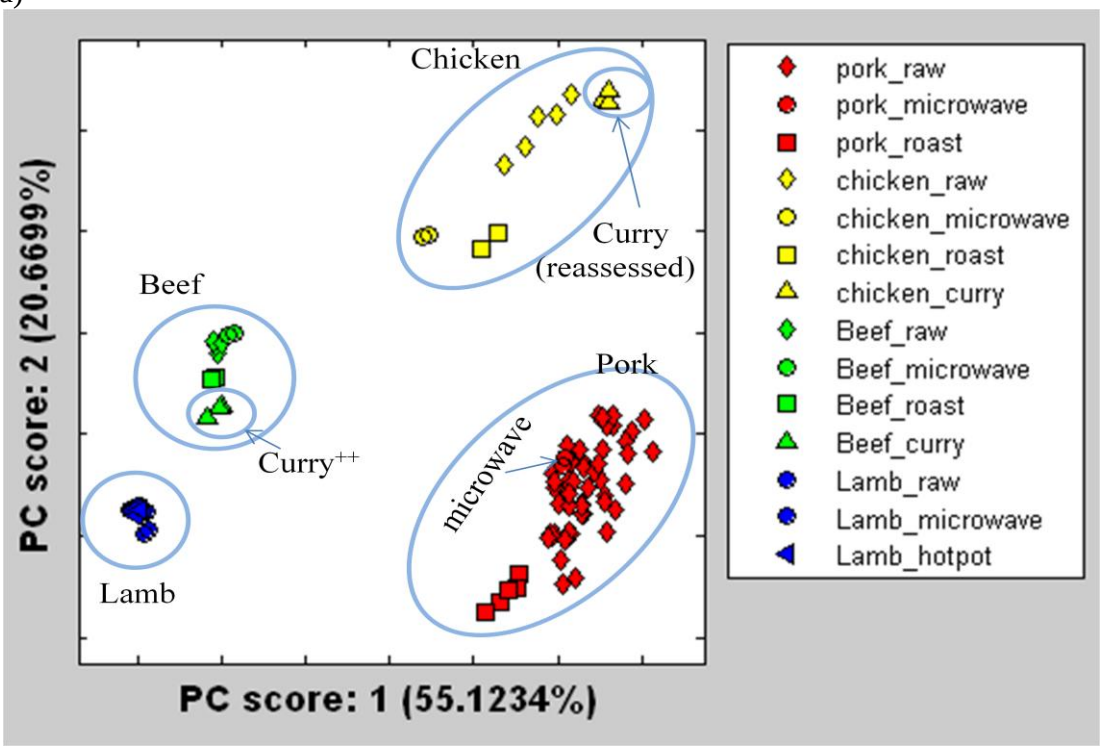

b)

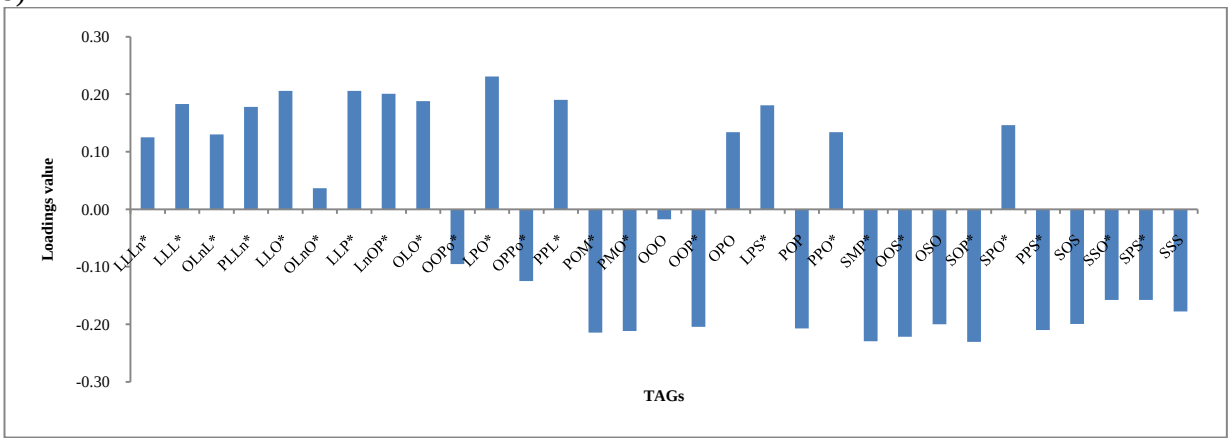

c)

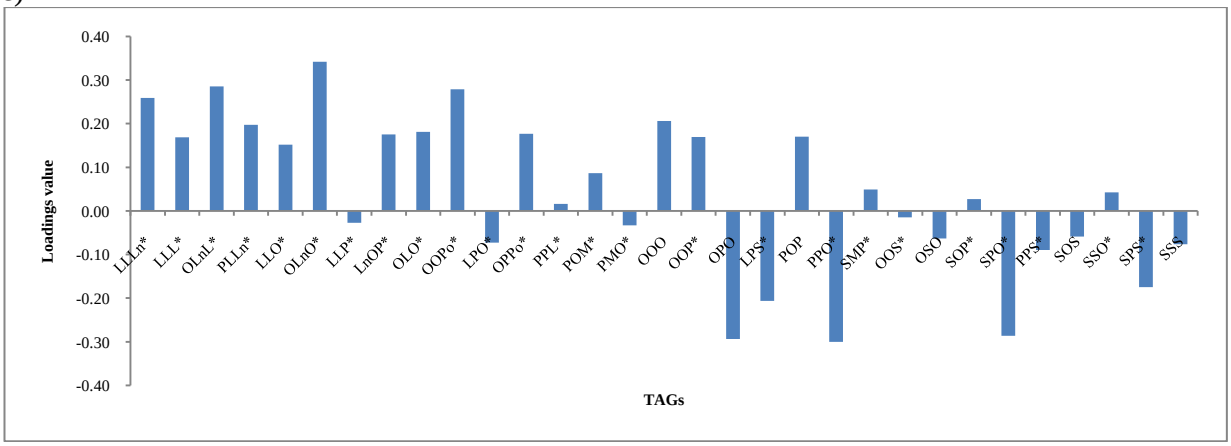

Figure 4.18: a) PCA scores plot of TAGs for raw and cooked meat products including reassessed beef^{++} and chicken curry. b) loadings plot for PC1 c) loadings plot for PC2.

4.3 Conclusions

Microwave cooking of chicken and lamb gives similar changes in the TAG profiles attributed to oxidation of TAGs containing the highly unsaturated FAs L and Ln. By contrast, microwave cooking for beef and pork give similar profiles to the raw meat. The TAG profiles of roast chicken and beef are much more similar to the raw meat whereas pork shows considerably higher proportions of OPO and SPO* and lower proportions of TAGs having highly unsaturated FAs. The correction of curry cooking for beef and chicken managed to reveal the underlying profiles relating to the meat indicating there is merit in the approach for meat that has been cooked.

PC1 of raw and cooked beef separated curry from raw/microwave/roasted beef with OOO, OOP*, OPPo* and PMO* being the important descriptors, having about the same magnitude. PC2 shows the separation between roasted and raw/microwave/curry beef with SOP* as the most important descriptor. The PCA scores plot for raw and cooked lamb differentiates between microwave and raw/hotpot cooking in PC1 with OOP*, SOP* and OSO having about the same influence. PC2 segregated all of the lamb samples with microwave cooking being closer to hotpot than raw meat and with PPO* as the most important variable. The differences between curry and raw/roasted/microwave cooking are obvious in the first component with the most important variables being OOP* and POP. PC2 separated raw from roast/curry and microwave with PLLn* being the most important descriptor. Overall, roasted chicken is much closer to raw chicken for both PC1 and PC2 than microwave and curry, suggesting that high localised temperature for microwave and the addition of rapessed oil in curry affect the profiles of TAGs for chicken. Microwave cooking does not cause significant changes in the proportions of TAGs for ham and the first component separates the roasted pork from raw/microwave cooking.

The raw and cooked meat products of different species are separated well in the PCA scores plot. It is particularly noteworthy that the cooked meats plot close/overlap to the raw meat for each species, indicating similarity in their TAG profiles. This work shows that the discrimination of different species is possible for both raw and cooked meat products, revealing that the difference between cooking methods were less than the variations between species. PC1 clearly divided the raw and cooked meat into chicken/pork and beef/lamb and almost all variables have about the same magnitude.

PC2 shows the variation between classes of chicken, beef and lamb/pork of raw and cooked products with OPO and PPO* being the most important descriptors.

The reconstructed PCA scores plot of reassessed beef curry and chicken curry distinguished beef from other species slightly more effectively. The chicken curry separated slightly from the raw chicken, though the curry and raw chicken were still very close and grouped together.

CHAPTER 5

Overall conclusions and future works

5.1 Overall conclusions

The primary aim of this study was to improve on current methods for the separation of TAGs; especially those are having identical masses or the same ECNs. The requirements of the method were that it be suitable for the analysis of complex mixtures of TAGs in animal fats and cooked meat products. Such a method would be extremely useful for detecting adulteration in cooked meat products where the thermal processing limits the use of DNA technologies to identify meat products. The development of this method will also support a wide range of studies on metabolism, biosynthesis, and degradation of individual TAG species within biological systems.

A generic method was developed for separating TAGs from animal fats and used throughout this study to separate the highly complex mixture of TAGs present in natural fats. Thus, simultaneous analysis of TAGs differing in molecular structure and with a broad range of ECN values was achieved, providing good resolution of components in a reasonable analysis time. The method developed here offers significant improvements on existing methods for TAG analysis, giving better resolution of TAGs with similar ECN, and good separation of TAGs with odd ECN and TAG regioisomers of animal fats. Although the analysis times for chromatographic analysis of these TAGs are long, this is compensated by better separation of highly unsaturated TAGs.

The techniques developed here have made important advances in the analysis of TAGs demonstrating clear improvements in their chromatographic resolution and, by utilizing APCI in combination with ammonium acetate to identify regioisomers, enabling their distributions to be characterised more accurately.

In APCI, TAGs were identified from the ammoniated molecules and their DAG ions in MS^2. The FA positions were identified from the presence and relative intensities of the DAG product ions in MS^2. The RP HPLC-APCI MS/MS of beef and pork fat allow three different categories of TAGs to be distinguished: AAA TAGs (e.g. LLL, OOO, SSS), ABA (e.g. OLO, OPO, OSO and POP) and AAB TAGs (e.g. PPS, SSO, LLP and PPL) and ABC TAGs (e.g. LPO, LPS, SPO and SMP).

Notably, the proportions of TAG isomers differ between animal species and TAG regioisomers are prevalent in beef and lamb but not in pork and chicken, in which only the most abundant isomers are observed. The distributions of TAG isomers for animal

fats show good potential for discriminating fats of different animal species. The isomers with saturated FAs in the *sn*-2 position are present in higher relative abundance in lamb than in beef. This is an entirely new observation for animal fat as previous methods are not able to separate isomers sufficiently. The differences in the relative proportions of isomers between animal species might be the result of differences in the biosynthesis of TAGs in different animals with those reactions in sheep having a stronger tendency to produce TAGs with unsaturated FAs on the *sn*-1/3 position compared with beef.

FA and TAG profiles for different animal species and different anatomical locations of pork were explored as a basis for studying discrimination between cooked meat products. In this study all the FAs detected in the samples by GC were observed in the TAG profiles analysed by LC. The TAG profiles of fats reflect their FA compositions, showing high proportions of unsaturated FAs for chicken and pork, the major TAGs detected are LPO*, OPO, LLP*, LLO* and OLO* in which the acids (O, L and P) represent about 88% (about 64% from O and L, and 24% from P) of the total FA contents in GC. In beef and lamb, saturated FAs are dominant in the major TAGs detected: SOP*, SOO, SPP, SSP and SOS; and these acids (O, P and S) represent about 85% (about 40% from O and 45% from P and S) of the total FA contents in GC.

The application of PCA to TAG profiles gives much better species discrimination than PCA of FA profiles. All animal species separated well in the PCA plot of TAG profiles, whereas in the PCA plot of FA, chicken plots very close to pork fat, particularly ham. The much better segregation of different animal species observed for TAGs most likely results from the better separation achieved for complex mixture of TAGs. Furthermore, some of the FAs are not important for species discrimination but important for TAGs containing those FAs for species discrimination in the PCA plot. In the PCA plot the lack of overlap for different animal species produces a good foundation for the discrimination of meat products prepared by different cooking methods. Despite the substantial variation in pork fat, no overlap is observed with the TAG profiles of different animal species on the PCA. PC1 divided the different animal species into two classes: chicken/pork and beef/lamb as shown in the scores plot for PC1. The loadings plot reveals TAGs with high positive and high negative loadings values. Those with positive loadings values (e.g. LLLn*, LLL, LLO*, OLO*, LPO*, LPS* and SPO*) are significantly higher in chicken/pork than in beef/lamb. By contrast, the TAGs with negative loadings values (e.g. OOP*, OOS*, SOP* and SOS*) are significantly higher in beef/lamb than in chicken/pork. Overall, almost all important descriptors having

negative loadings values on PC2 (OPO, LPS, PPO and SPO) in pork have significantly higher levels than in chicken, accounting for the discrimination in PC2. By contrast, the important descriptors having positive loadings values on PC2 (OLnL, PLLn, OLnO and LnOP) are significantly higher in chicken than in other species, causing the chicken samples to plot separately to the other samples.

The improved RP HPLC separation of TAGs developed in this study has been shown to give more reliable discrimination of different animal species than previous methods. Improved separation of important TAGs leads to improved PCA scores for different animal species. In particular, the regioisomers PPO*/POP and SPO*/SOP* discriminate pork from beef and lamb. Good separation of TAGs containing highly unsaturated FAs (e.g. OLnO, OLnL and PLLn) results in effective discrimination of chicken from pork. The inspection of the profiles of TAGs in animal species highlighted a number of components that are important for species discrimination. The important TAGs for discriminating different animal species are: POP, OOP* and OPPo* for beef, PMO*, SOS, OOS*, PPS*, OSO, SPS* and SSS for lamb, OLnO* and OLnL* for chicken and OPO, PPO*, SPO* and LPS* for pork fat.

Variations in FA and TAG profiles were explored further by considering different anatomical locations of pork. Apart from belly IM fat, no distinction could be observed between the different anatomical locations of pork based on PCA scores plots of FA and TAG profiles. Both profiles have about the same influence on their PCA scores plot. This work represents the first detailed comparison of the TAG profiles for different anatomical locations of pig and reveals important differences between belly IM fat and other locations.

The work reported in this thesis shows that variation exists in the composition of pork fat between individual species, even with pigs of the same age and sex that had been fed on a very similar diet. Notably, however, these differences are relatively small and they appear to relate more closely to differences between the different layers of adipose tissues. This might be a result of the timing of fat deposition or might relate to metabolism. Evaluation of the cause of these differences is, however, beyond the scope of this project. The discrimination between different species is very clear for TAGs and these differences are far greater than differences observed within species, as demonstrated by the results from the pig. This implies that the method is quite robust for

differentiation between animal species, although clearly these indications are based on a fairly restricted pool of samples.

The meat products cooked by microwave, roasting and currying of different species (beef, pork, chicken and lamb) are separated well in the PCA scores plot. This work shows that the discrimination of meat from different animal species is possible for both raw and cooked meat products, and reveals that the differences produces by the various cooking methods were less than the variations observed between species. The loadings values of PC1 and PC2 for the scores plot of TAGs for raw and cooked meat products are similar to the raw meat in different animal species and have the same important descriptors for discrimination. Hence, analysis of intact TAGs in cooked food products has considerable potential for detection of adulteration of cooked meat-based food products.

The reassessed TAG profiles for curry cooked beef and chicken reveal the underlying profiles relating to the meat, indicating there is merit in this approach for meat that has been cooked. The reconstructed PCA scores plot of reassessed beef curry and chicken curry did distinguished beef from other species more effectively.

The similarity in the profiles of cooked and raw meat gives confidence regarding the ability of the method to determine the nature of the cooked meat samples from analysis of their TAGs. A significant overprint from additional TAGs derived from cooking oil was noted in the cooked meat samples. The method was tested to remove the fat. The method proved useful for regrouping the samples but not the case for chicken curry, for which the modified protocol was not necessary, despite the present of TAGs in cooking oils.

The plot of PC1 vs. PC2 for TAGs (Fig. 3.16) shows that POP and PPO are important in the discrimination of beef and pork. These two TAGs are not separated by published HPLC methods (Mottram et al., 2001; Fauconnot et al., 2004 and Dugo et al., 2006) but were separated in the present study. POP and PPO are important descriptors for beef and pork, respectively, and their separation undoubtedly leads to better discrimination of beef and pork by PCA than would otherwise have been possible. Two other components not separated before but separated in the present study are OOP and OPO, both of which are also important descriptors for discrimination of beef and pork. OLnL is nicely separated from other TAGs in the present study but was not observed in two previously published

methods (Fauconnot et al., 2004 and Dugo et al., 2006) and co-eluted with LLL in a third (Mottram et al., 2001). This component is important for discrimination of chicken. Hence, the improved method will have greater potential for separating different species than the earlier methods. Thus, it seems evident that the improved separation of TAGs by HPLC impacts favorably on the discrimination of animal fats by species.

5.2 Future work.

Aspects of this research have raised further question that need to be addressed:

a) The retention times observed for each chromatogram produced were fairly consistent, except for one batch/lot of samples running where the retention times were decreased. This might be attributed to very late eluting compounds, either TAGs or component derived from TAGs being retained on the column and not being removed efficiently. The retention of such components indicates that the HPLC column required regular additional final wash or flushes. This will be important if batch runs are to be performed.

b) The proportions of TAG isomers differ between animal species and this observation might be important for unique species identification and understanding the biosynthesis of TAGs in different animal species. The results indicate that TAG regioisomers should be analysed for different anatomical locations of beef and lamb where there is substantial variation in the isomer proportions.

c) Due to the substantial variations observed for different anatomical locations of pork (belly, ham, loin and shoulder), it is important that TAG profiles for different anatomical locations of chicken, beef and lamb are examined. The TAG profiles of different anatomical locations of all animal species will give much better underlying TAG profiles for each animal species and provide better context for discrimination of different cooked meat products.

d) Even though the chromatograms for curry cooking of beef and chicken show distinct difference to the raw meats, the analysis with PCA reveals that the difference attributed to different cooking methods were less than the variations between species, making the discrimination of both raw and cooked meat products possible. It is important, however, to include a more comprehensive range of meats and of different types of cooked meat products in order to explore the extent of variation between species and the different types of cooking.

e) Compared with the HPLC methods, the UHPLC method developed for separation of TAGs in this study has the advantages of improved speed, which reduced the analysis times to almost half, and improved resolution. Further

development is needed for better separation of OPO and POP and OSO and SOP. Due to the shorter analysis time and better resolution, it would be worthwhile to apply this method to discriminate TAGs within and between different animal species and different cooking methods.

f) The inspection of the profiles of TAGs in animal species highlighted a number of components that are important for species discrimination: POP, OOP* and OPPo* for beef; PMO*, SOS, OOS*, PPS*, OSO, SPS* and SSS for lamb; OLnO* and OLnL* for chicken and OPO, PPO*, SPO* and LPS* for pork fat. It is important to refine the PCA with regard to those important TAGs which can be expected to provide a much better context for discrimination of different species and different cooking methods since there will be no interference from other TAG variables.

g) The techniques developed and applied in the thesis for the analysis of TAGs could be useful for studying their degradation and transformation during cooking and with different cooking processes. This can only be done following comprehensive study of different anatomical locations, different species and different cooking methods.

h) This technique may find applications outside food analysis, for example, the analysis of TAGs from archaeological items such as pottery used for cooking or storage of foods. Studies in this area are of considerable interest as they can provide unique information on animal exploitation.

i) The analytical method for analysis of TAGs could be extended through development of 2D separations to improve both its speed and its resolving power.

CHAPTER 6

Experimental

6.1 Chemicals

6.1.1 Reagents and standards

The fatty acid methyl ester (FAME) standard mix C14-C22 (99.2 to 99.9% purity) was obtained from Sigma-Aldrich (Germany) together with heptadecanoic acid methyl ester (99% purity) which was used as an internal standard for gas chromatography.

The TAG standards; 1,3-dioleoyl-2-palmitoylglycerol (OPO; ≥ 99% purity) and 1,2-dioleoyl-3-palmitoyl-rac-glycerol (OOP; ≈ 99% purity) were purchased from Sigma-Aldrich (Germany), 1-oleoyl-2,3-dipalmitoyl-rac-glycerol (OPP; 98% purity) from TRC (Toronto Research Chemicals Inc., Canada) and 1,2-dipalmitoyl-3-oleoyl-rac-glycerol (PPO; 99% purity) from Larodan Fine Chemicals (Malmo, Sweden). Hexane, dichloromethane, acetonitrile, chloroform, 2-propanol and methanol used were HPLC grade and ammonium acetate, sulphuric acid, toluene, sodium chloride, potassium bicarbonate and anhydrous sodium sulphate was analytical reagent grade (Fisher Scientific, United Kingdom).

6.1.2 Sampling

6.1.2.1 Different anatomical locations of adipose tissue

Pork fat was used to study the variation of FAs and TAG in adipose tissue from different anatomical locations. The pigs were of the same breed (Tamworth), age (10 months old) and gender (male) and from the same farm (Malton, York). The pigs diet was uncontrolled but mostly consisted of sugar beet and green vegetables.

A total of 24 samples of adipose tissue were taken from four different locations from three different pigs. The four locations were; ham, shoulder, loin and belly (Fig 6.1a). The adipose tissue samples (about 5 g) were taken from subcutaneous and intermuscular sections at each of the locations, following Timon et al., 2001 (Fig 6.1b). All samples were extracted immediately.

a)

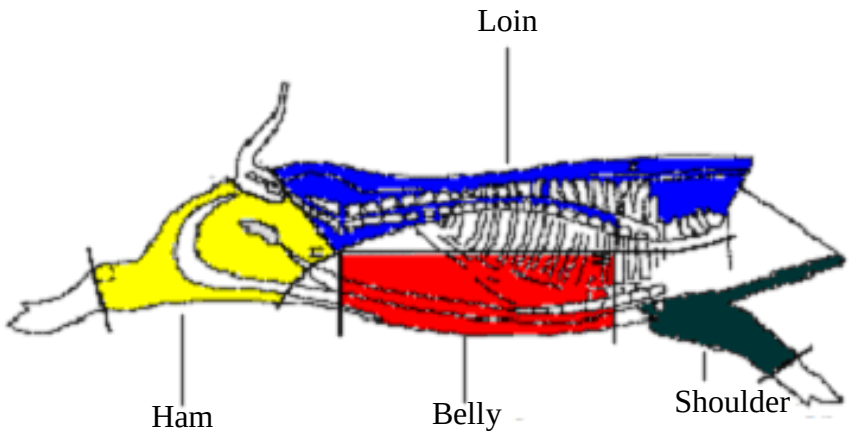

b)

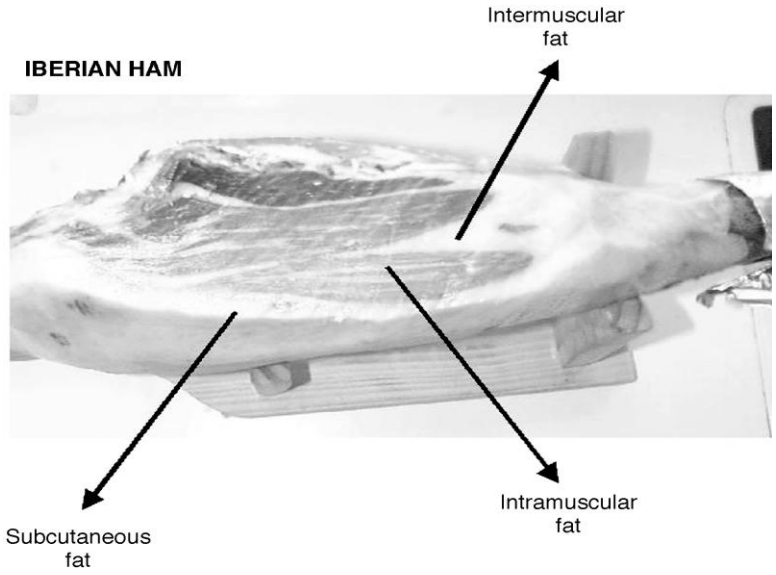

Figure 6.1: a) Diagram identifying the four different locations of pig adipose tissue (modified from Metayer and Daumas, 1998). b) Subcutaneous, intermuscular and intramuscular adipose tissues from sliced dry-cured Iberian ham (Timon et. al., 2001).

6.1.2.2 Raw/uncooked meat samples

Meat samples from beef (labelled fresh British beef sirloin steak), chicken (labelled fresh British chicken) and lamb (fresh British lamb chops) were purchased from a local supermarket (TESCO). Chicken samples were deboned (skin and muscle were used) whereas beef and lamb were used as purchased. All samples (about 5 g) were homogenised in the laboratory and extracted on the day of purchase.

6.1.2.3 Cooked meat products

Three different methods of cooking were studied to determine the effect of each on the TAG profiles in the meat products:

Microwave open cooking: Different homogenised samples (≈ 5 g) of beef, lamb and chicken as specified in Section 6.1.2.2, and pork ham were cooked in a microwave oven (700 W, full power, 4 min) and extracted immediately.

Cooked and roasted cooking: Samples of cooked and roasted pork, beef and chicken were purchased from a local supermarket (TESCO), labelled as; 'cooked and roasted pork formed from cuts of pork', 'sliced cooked and roasted beef' and 'reformed, cooked and roasted chicken with added pea fibre' on their packaging. The samples (about 5 g) were homogenised and extracted on the day of purchase.

Curry and hotpot: Samples of beef and chicken curry (labelled as 'beef curry: pieces of beef in a spicy curry sauce' and 'chicken curry: chicken pieces in a mild curry sauce') and lamb hotpot (labelled as 'Cumbrian lamb hotpot slow-cooked traditional kitchen recipes') were purchased from a local supermarket (TESCO). The samples (about 5 g) were homogenised and extracted on the day of purchase.

6.1.3 Extraction procedure

6.1.3.1 Solvent extraction (Liquid-liquid extraction).

Samples of homogenised pork fat (≈ 5 g) from the different anatomical locations identified in Section 6.1.2.1 and samples from the different meats (about 5 g) detailed in Section 6.1.2.2 were extracted with a chloroform-methanol according to a method modified from Pedro et al., 1997. Each sample was macerated in covered flasks containing a 2:1 mixture of chloroform-methanol (v/v; 20:10) and was left to extract for 24 h at ambient temperature. The macerates were then filtered through cellulose filters and the solvent was removed in a rotary evaporator.

Fat purification: The dry extract was dissolved in hexane (5 mL) and washed with water (4 mL) and the mixture allowed to separate into two phases by standing (Folch et al., 1956 for washing of crude extract). As much of the lower phase as possible was collected and filtered through a short plug of dichloromethane washed cotton wool. The remaining solvent was removed under a gentle flow of nitrogen. The extracts were stored in a freezer (-20 °C) prior to use.

6.1.3.2 Accelerated Solvent Extraction (ASE).

The samples of cooked meat products (Section 6.1.2.3) were extracted according to Dionex Application Note 334 (Rapid determination of fat in meat using accelerated solvent extraction (ASE)). About 1 g of microwave cooked sample was loaded into a 5 mL stainless steel extraction cell and about 5 to 6 g of homogenous roasted, curry and hotpot samples was loaded into a 33 mL extraction cell. Cellulose filters were placed at each end of the extraction cell.

The extraction conditions as per Dionex application note 334:

Solvent	:	hexane
Temperature	:	125°C
Pressure	:	10.3 Mpa (1500 psi)
Heat	:	6 min
Static	:	2 min
Flush	:	60%
Purge	:	60 s
Cycles	:	2
Total time	:	14 min

The extraction solvent was evaporated using a rotational vacuum concentrator (CHRIST RVC 2-25 CD) and the extracts were stored in the freezer (-20 °C) prior to analysis.

6.1.4 Hydrolysis and methylation of the fat extract.

Fatty acid methyl esters were prepared with methanolic sulphuric acid (Christie and Barnes, 1990). The fat (50 mg) was dissolved in toluene (1 mL) and 2 mL 1% sulphuric acid in methanol (2 mL) was added. The mixture was left overnight in a stoppered tube at 50°C, after which 5 mL water containing 5% sodium chloride was added. The FAMEs were extracted with hexane (2 x 5 mL), using Pasteur pipettes to remove the layers. The hexane layer was washed with water containing 2% potassium bicarbonate (4 mL) and dried by passing through a short column of anhydrous sodium sulphate. FAMEs were diluted with hexane before injection into GC (1 mg FAMEs in 1 mL hexane).

6.2 Instrumentation

6.2.1 GC/FID

The fatty acid methyl esters were analysed using a Carlo Erba HRGC 5300 Mega Series gas chromatograph (GC) with flame ionization detector (FID). The GC was equipped with a split/splitless and a cold on column injector. 1 µL of sample dissolved in hexane was injected. In the case of split injector mode the split ratio was 20:1. The separations were achieved on a WCOT fused silica capillary CP-SIL 88 for FAME column, coated with 100% cyanopropyl polysiloxane as the stationary phase (100 m x 0.25 mm, 0.2 µm film thickness; Varian, Inc. USA). The GC gradient programme for split injection is shown in Table 6.1. The detector and injector temperature were both kept at 250°C.

Table 6.1: Chromatographic conditions used in the determination of FAMEs for split injector.

Temperature ramps	Rate (°C/min)	Temperature (°C)	Duration (min)
Initial	-	160	2
Ramp 1	2	200	48

The GC gradient programme used for on column injection is shown in Table 6.2. Sample (1 µL) was injected and the starting oven temperature was at 80°C (12°C higher then the boiling point of hexane). The detector temperature was 250°C. The FID gases were hydrogen at 60 kPa, make-up gas nitrogen at 25 kPa and air at 100 kPa. The hydrogen carrier gas was set at a constant flow rate of 0.5 mL/min (80 kPa).

Table 6.2: Chromatographic conditions used in the determination of FAMEs for on column

Temperature ramps	Rate (°C/min)	Temperature (°C)	Duration (min)
Initial	-	80	-
Ramp 1	40	160	-
Ramp 2	2	200	48

6.2.2 HPLC-LCQ ion trap

Liquid chromatography-mass spectrometry was carried out using a Finnigan MAT SpectraSystem P4000 HPLC coupled to a Finnigan LCQ ion trap mass spectrometer with the APCI and ESI sources operated in the positive ion mode. The vaporiser temperature for APCI was set to 450°C, the capillary temperature to 150°C and the corona discharge current to 10 μA. Nitrogen was used as sheath gas and auxillary gas at a flow rate of 60 arbitrary units. The capillary voltage and tube lens offset are 15 and 25 V, respectively. For ESI, the spray voltage was set at 4.0 kV and the capillary temperature to 200°C. Nitrogen sheath gas was set to a flow rate of 20 arbitrary units and auxillary gas at 30 arbitrary units. Scans were obtained from *m/z* 400 – 1000 and the ion trap was set to automatically select the most abundant precursor ion and perform CID. The collision energy for CID was set at 35 eV.

For separation of TAGs, two Waters Spherisorb ODS2 (150 mm x 4.6 mm, 3 μm) columns were connected in series. The standards and samples were dissolved in hexane:acetonitrile:2-propanol mixture (1:1:1, v/v/v) and a combination of acetonitrile, dichloromethane and 10 mM ammonium acetate in methanol was employed as mobile phase. The gradients are shown in Table 6.3. The injection volume was 25 μL and the flow rate 1 mL/min.

Table 6.3: The mobile phase gradient for HPLC for separation of TAGs.

Time (min)	Flow rate (mL/min)	% acetonitrile	% dichloromethane	% ammonium acetate (10 mM)
0	1	76	20	4
82	1	75	21	4
145	1	61	35	4

Full details of the columns and the mobile phase gradients for the RP HPLC development are given in Section 2.2.3.1 (Results and discussion).

6.2.3 RSLC-HCT

Ultra high performance liquid chromatography mass spectrometry was performed using an Ultimate 3000 RS (Dionex) RSLC in combination with a Bruker HCTultra ETD II ion trap. APCI was used in positive ion mode and all conditions were exactly as in Section 6.2.4. The separation was performed on two RSLC acclaim 120 C18 2.2 μm (2.1 x 100 mm, 2.2 μm) columns connected in series. The mobile phase gradient used for HPLC was modified for UHPLC accordingly as in Table 6.4. The injection volume was 25 μL and the flow rate 0.7 mL/min.

Table 6.4: The mobile phase gradient for Ultimate 3000 RS (Dionex) RSLC for separation of TAGs (Method I).

Time (min)	Flow rate (mL/min)	% acetonitrile	% dichloromethane	% ammonium acetate (10 mM)
0	0.7	76	20	4
50	0.7	76	20	4
90	0.7	56	40	4

6.2.4 HPLC– HCT ultra ETD

An Ultimate 3000 (Dionex) HPLC was used in combination with a Bruker HCT ultra ETD II ion trap. The APCI source was operated in the positive ion mode. The vaporiser temperature was set to 450°C and drying temperature to 150°C. Nitrogen was used as a dry gas at a flow rate of 3 L/min and nebulizer gas at 50 psi. Scans were obtained from *m/z* 330 – 1000. The smart tune and auto MS^n to MS^3 were selected.

Two Waters Spherisorb ODS2 (150 mm x 4.6 mm, 3 µm) columns connected in series were used for the elution of the TAGs and a mobile phase combination of acetonitrile, dichloromethane and 10 mM ammonium acetate in methanol (gradients are in Table 6.5). The injection volume was 25 µL and the flow rate 1 mL/min.

Table 6.5: The mobile phase gradient for Dionex Ultimate 3000 HPLC for separation of TAGs (Method J).

Time (min)	Flow rate (mL/min)	% acetonitrile	% dichloromethane	% ammonium acetate (10 mM)
0	1	76	20	4
82	1	75	21	4
100	1	69	27	4
145	1	57	39	4

6.3 Statistical analysis

Two-dimensional principal component analysis (PCA) score plots were created for FAME and TAG profiles from different anatomical locations, different animal species and cooked meat products. Unnormalised data were used and each variable was scaled to unit variance and mean centred to prevent the larger variables dominating the analysis. PCA used Metabolab software, developed in-house at The Food and Environment Research Agency (FERA), York, UK.

References

Aichholz R., Spitzer V., Lorbeer E., High temperature gas chromatography and high temperature gas chromatography-negative chemical ionization mass spectrometry of derivatized triglycerides containing oxygenated fatty acid acyl groups. *J. High. Resol. Chromatogr*. 1998; **21**: 152-160.

Amaral J.S., Casal S., Seabra R.M., Oliveira B.P., Effects of roasting on hazelnut lipids. *J. Agric. Food Chem.* 2006; **54**: 1315-1321.

Andrikopoulas N.K., Chromatographic and spectroscopic methods in the analysis of triacylglycerol species and regiospecific isomers of oils and fats. *Critical Reviews in Food Sc. And Nutrition.* 2002; **42(5)**:473-505.

Aparicio R., Aparicio-Ruiz R., Authentication of vegetable oils by chromatographic techniques. *J. of Chrom. A.* 2000; **881**: 93-104.

Armero E., Navarro J.L., Nadal M.I., Baselga M., Toldra F., Lipid composition of pork muscle as affected by sire genetic type. *J. Food Biochem.* 2002; **26**: 91-102.

Asensio L., Gonzalez I., Garcia T., Martin R., Determination of food authenticity by enzyme-linked immunosorbent assay (ELISA). *Food Control*. 2008; **19(1)**: 1-8.

Barron L.J.R., SantaMaria G., Masa J.C.D., Influence of bonded-phase column type, mobile phase composition, temperature and flow-rate in the analysis of triglycerides by reverse-phase high performance liquid-chromatography. *J. Liquid Chromatogr.* 1987;**10(14)**: 3193-3212.

Bender D.A., "adulteration" A Dictionary of Food and Nutrition. Oxford University Press 2009. *Oxford Reference Online*.
http://www.oxfordreference.com/views/ENTRY.html?subview=Main&entry=t39.e78

Beynon J.H., Cooks R.G., Amy J.W., Baitinge W.E., Ridley T.Y., Design and performance of a mass analyzed ion kinetic energy (MIKE) spectrometer., *Anal. Chem.*1973; **45(12)**: 1023A.

Bligh E.G., Dyer W.J., A rapid method of total lipid extraction and purification. *Can. J. Biochem. Physiol.* 1959; **37**: 911-917.

Body D.R., The lipid composition of adipose tissue. *Prog. Lipid Res*. 1988; **27**:39-60.

Bragagnolo N., Rodriguez-Amaya D.B., Simultaneous determination of total lipids, cholesterol and fatty acids in meat and backfat of suckling and adult pig. *Food Chemistry*. 2002; **79**: 255-260.

Broncano J.M., Petron M.J., Parra V., Timon M.L., Effect of different cooking methods on lipid oxidation and formation of free cholesterol oxidation products (COPs) in *Latissimus dorsi* muscle of Iberian pigs. *Meat Sci.* 2009; **83(3)**: 431-437.

Buchgraber M., Ulberth F., Emons H., Anklam E., Triacylglycerol profiling by using chromatographic techniques. *Eur. J. Lipid Sci. Technol.* 2004; **106**: 621-648.

Byrdwell W.C., Emken E.A., Analysis of triglycerides using atmospheric pressure chemical ionization-mass spectrometry. *Lipid.* 1995; **30**: 173-175.

Byrdwell W.C., Emken E.A., Neff W.E., Adlof R.O., Quantitative analysis of triglycerides using atmospheric pressure chemical ionization-mass spectrometry. *Lipid.* 1996; **31(9)**: 919-935.

Byrdwell W.C., Neff W.E., Dual parallel electrospray ionization and atmospheric pressure chemical ionization mass spectrometry (MS), MS/MS and MS/MS/MS for the analysis of triacylglycerols and triacylglycerol oxidation products. *Rapid Commun. Mass Spectrom*. 2002; **16**:300-319.

Byrdwell W.C., Atmospheric pressure ionization techniques in modern lipid analysis. *Modern Methods for Lipid Analysis by Liquid Chromatography/Mass Spectrometry and Related Techniques*. 2005; Chapter 1: 1-18, Chapter 7: 299-412.

Cai S.S., Short L.C., Syage J.A., Potvin M., and Curtis J.M., Liquid chromatography-atmospheric pressure photoionization-mass spectrometry analysis of triacylglycerol lipids – effects of mobile phases on sensitivity. *J. Chrom. A.*2007; **1173**: 88-97.

Cheng C., Michael L.G., Complete structural elucidation of triacylglycerols by tandem sector mass spectrometry. *Anal. Chemistry*. 1998; **70**: 4417-4426.

Christie W.W., Moore J.H., A comparison of the structures of triglycerides from various pig tissues. *Biochimica Et Biophysica Acta*. 1970; **210**: 46-56.

Christie W.W., Moore J.H., Structures of triglycerides isolated from various sheep tissues. *J. Sci. Food Agric.*1971; **22**: 120-124.

Christie W.W., Barnes P.J. & Assoc. *Gas Chromatography and lipids, A practical Guide.*1990; Chapter 4:37-42.

Christie W.W., Gas chromatography: theoretical aspects and instrumentation. *Gas Chromatography and lipids, A practical Guide.* Barnes PJ. & Assoc. 1990; Chapter 3: http://lipidlibrary.aocs.org/GC_lipid/03_theor/index.htm.

Cordella C., Moussa I., Martel A.C., Sbirrazzuoli N., Louisette L.C., Recent developments in food characterization and adulteration detection: technique-oriented perspectives, *J. Agric*. & *Food Chem.*2002; **50**: 1751-1764.

Covey T.R., Lee E.D., Bruins A.P., Henion J.D., Liquid chromatography/ mass spectrometry., *Anal. Chemistry*. 1986; **58(14)**: 1451A-1461A.

Cozzolino D., and Murray I., Identification of animal meat muscles by visible and near infrared reflectance spectroscopy. *Lebensm-Wiss u-Technol.* 2004; **37**: 447-452.

Crnjar E.D., Witchwoot A., and Nawar W., Thermal oxidation of a series of saturated triacylglycerols. *J. Agric*. & *Food Chem.* 1981; **29**: 39-42.

De Boer J., Chlorobiphenyls in bound and non-bounded lipids of fishes: comparison of different extraction methods. *Chemosphere*. 1988; **17**: 1803-1810.
Defernez M., Wilson R.H., Mid infrared spectroscopy and chemometrics for determining the type of fruit used in jam. *J. Sci. Food Agric.*1995; **67**: 461-467.

Dennis M.J., Recent developments in food authentication. *Analyst*. 1998; **123**: 151-156.

De Pedro E., Casillas M., Miranda M., Microwave oven application in the extraction of fat from subcutaneous tissue of Iberian pig ham. *Meat Sc*.1997; **45(1)**:45-51.

Delgado G.L., Gomez C.S., Rubio L.M.S., Capella V.S., Mendez M.D., Labastida R.C., Fatty acid and triglyceride profiles of intramuscular and subcutaneous fat from fresh and dry-cured hams from hairless Mexican pigs. *Meat Sc.* 2002; **61**: 61-65.

Diaz I., Garcia Regueiro J.A., Casillas M., and De Pedro E., Triglyceride composition of fresh ham fat from Iberian pigs produced with different systems of animal nutrition. *Food Chemistry*.1996; **55(4)**: 383-387.

Dole M., Mach L.L., Hines R.L., Mobley R.C., Ferguson L.P., Alice M.B., Molecular beams of macroions. *J. Chemal Physic*. 1968; **49**: 2240.

Downey G., Cereals. *Food authenticity and traceability, Woodhead Publishing Limited, Cambridge, England.* 2003; Chapter **17:** 378-382.

Duckett S.K., Wagner D.G., Effect of cooking on the fatty acid composition of beef intramuscular lipid. *J. Food Composition and Analysis*. 1998; **11**: 357-362.

Duffin K.L., Henion J.D., Electrospray and tandem mass spectrometric characterization of acylglycerol mixtures that are dissolved in nonpolar solvents. *Anal. Chemistry*. 1991; **63**: 1781-1788.

Dugo P., Favoino O., Tranchida P.Q., Dugo G., and Mondello L., Off-line coupling of non-aqueous reversed-phase and silver ion high-performance liquid chromatography-mass spectrometry for the characterization of rice oil triacylglycerol positional isomer. *Journal of Chromatography A.*2004; 1041: 135-142.

Dugo F., Kumm T., Fazio A., Dugo G., Mondello L., Determination of beef tallow in lard through a multidimensional off-line non-aqueous reversed phase-argentation LC method coupled to mass spectrometry. *J. Sep. Sci*. 2006; **29**: 567-575.

Duncan W.R.H., Garton G.A., The fatty acid composition and intramuscular structure of triglycerides derived from different sites in the body of the sheep. *J. Sci. Food Agric.* 1967; **18**: 99-102.

Enser M., Hallett K., Hewitt B., Fursey G.A.J., Wood J.D., Fatty acid content and composition of English beef, lamb and pork at retail. *Meat Sc*. 1996; **42**: 443-456.

Eskin N.A.M., Vaisey-Genser M., Durance-Todd S., Przybylski R., Stability of low linolenic acid canola oil to frying temperatures. *JAOCS*. 1989; 66(**8)**: 1081-1084.

Evershed R.P., High-resolution triacylglycerol mixture analysis using high-temperature gas chromatography/mass spectrometry with a polarizable stationary phase, negative ion chemical ionization, and mass-resolved chromatography. *American Soc. for Mass Spect*. 1996; **7**: 350-361.

Fauconnot L., Hau J., Aeschlimann JM., Fay L.B., Dionisi F., Quantitative analysis of triacylglycerol regioisomers in fats and oils using reversed-phase high-performance liquid chromatography and atmospheric pressure chemical ionization mass spectrometry. *Rapid Commun. Mass Spectrom*. 2004; **18**: 218-224.

Folch J., Lees M., Sloane Stanley G.H. A simple method for the isolation and purification of total lipids from animal tissues. *J. Biological Chemistry.*1956: 497-509.

Franco I., Escamilla M.C., Garcia J., Garcia Fontan M.C., and Carballo J., Fatty acid profile of the fat from celta pig breed fattened using a traditional feed: Effect of the location in the carcass. *J. Food Composition and Analysis*. 2006; 19: 792-799.

Frede E., Thiele H. Analysis of milkfat by HPLC. *JAOCS*. 1987; 64(4): 521-528.

Galli M., Trestianu S., Benefits of a special cooling system to improve precision and accuracy in non-vaporizing on-column injection procedures. *J. Chromatogr.* 1981;**203**: 193-205.

Garcia-Olmo J., De Pedro E., Garrido A., Paredes A., Sanabria C., Santolalla M., Salas J., Garcia-Hierro J.R., Gonzalez I., Garcia-Cachan M.D., and Guirao J., Determination of the precision of the fatty acid analysis of Iberian pig fat by gas chromatography. Results of a mini collaborative study. *Meat Sc.* 2002; **60**: 103-109.

Garcia P.T., Pensel N.A., Sancho A.M., Latimori N.J., Kloster A.M., Amigone M.A., Casal J.J., Beef lipids in relation to animal breed and nutrition in Argentina. *Meat Sc.* 2008; **79**: 500-508.

Good A., Durden D.A., Kebarle P., Mechanism and rate constants of ion-molecule reactions leading to formation of $H^+(H_2O)_n$ in moist oxygen and air. *J. Chem. Phys.* 1970;**52(1)**: 222-229.

Grob K., Neukom H.P., Factors affecting the accuracy and precision of cold on-column injections in capillary gas chromatography. *J. Chromatogr. A.* 1980;**189**: 109-117.

Grob R.L., Theory of gas chromatography., *Modern Practice of Gas Chromatography. Second edition*. 1985; Chapter 2: 49-115.

Gutierrez V.R., Barron L.J.R., Methods for the analysis of triacylglycerols. *J. Chromatogr. B: Biomedical Applications.* 1995; **671**: 133-168.

Haak L., Sioen I., Raes K., Van Camp J., De Smet S., Effect of pan-frying in different culinary fats on the fatty acid profile of pork. *Food Chemistry*. 2007; **102** : 857-864.

Harris KB., Harberson TJ., Savell JW., Cross HR., Smith SB., Influences of quality grade, external fat level, and degree of doneness on beef steak fatty acids. *J. Food Composition and Analysis*. 1992; **5**: 84-89.

Haddon WF., Mclaffer FW., Metastable ion characteristics. 7. collision-induced metastables., *J. Of the American Chem. Society.*1968; **90(17)**: 4745-4746.

Hitchcock C.H.S., Crimes A.A., Methodology for meat species identification: A review. *Meat Sci*. 1985; 1**5**: 215-224.

Hlongwane C., Delves I.G., Wan L.W., Ayorinde F.O., Comparative quantitative fatty acid analysis of triacylglycerols using matrix-assisted laser desorption/ionization time-of-flight mass spectrometry and gas chromatography. *Rapid Commun. Mass Spectrom.* 2001; **15(21)**: 2027-2034.

Hoffman E.D., Tandem mass spectrometry: a primer., *J. Of Mass Spec.* 1996; **31**: 129-137.

Holcapek M., Jandera P., Zderadicka P., and Hruba L., Characterization of triacylglycerol and diacylglycerol composition of plant oils using high-performance liquid chromatography-atmospheric pressure chemical ionization mass spectrometry. *J. Chromatogr. A* 2003; **1010**: 195-215.

Holcapek M., Lisa M., Jandera P., Kabatova N., Quantitation of triacylglycerols in plant oils using HPLC with APCI-MS, evaporative light-scattering, and UV detection. *J. Sep. Sci.* 2005; **28**: 1315-1333.

Howland M.R., Corr L.T., Young S.M.M., Jones V., Jim S., Van Der Merwe N.J., Mitchell A.D., Evershed R.P., Expression of the dietary isotope signal in the compound-specific $\delta^{13}C$ values of pig bone lipids and amino acids. *Int. J. Osteoarchaeol.* 2003; **13**: 54-65.

Huerta-Leidenz N.O., Cross H.R., Savell J.W., Lunt D.K., Baker J.F., Smith S.B. Fatty acid composition of subcutaneous adipose tissue from male calves at different stages of growth. *J. Animal Sci.* 1996; **74**: 1256-1264.

Hvattum E., Analysis of triacylglycerols with non-aqueous reversed-phase liquid chromatography and positive ion electrospray tandem mass spectrometry. *Rapid Commun. Mass Spectrom.* 2001; 15: 187-190.

Iribarne J.V., Thomson B.A., Evaporation of small ions from charged droplets. *J. Chemical Physics.* 1976; **64**: 2287-2294.

IUPAC-IUB Commission on Biochemical Nomenclature The Nomenclature of Lipids., *The J. of Biological Chemistry*. 1967; **242(21):** 4845-4849.

IUPAC Compendium of Chemical Terminology, 2nd Edition. 1997. 1993, *65*, 826; O.B. 94. http://www.iupac.org/goldbook/P04436.pdf.IUPAC-IUB Commission on Biochemical Nomenclature The Nomenclature of Lipids (Recommendations 1976)., *Molecular & Cellular Biochemistry*. 1977; **17(3):** 157-171.

Jakab A., Heberger K., Forgacs E., Comparative analysis of different plant oils by high-performance liquid chromatography-atmospheric pressure chemical ionization mass spectrometry. *Journal of Chromatography A.*2002: 255-263.

Jennings K.R., Collision-induced decompositions of aromatic molecular ions., *Int. J. Of mass spec & ions Phys.* 1968: 227-235.

Jiang T., Busboom J.R., Nelson M.L., O'Fallon J., Ringkob T.P., Joos D., Piper K., Effect of sampling fat location and cooking on fatty acid composition of beef steaks. *Meat Sci.* 2010; **84(1)**: 86-92.

Jonscher K.R., Yates J.R., The quadrupole ion trap mass spectrometer – a small solution to a big challenge., *Anal. Biochemistry*. 1997; **244**: 1-15.

Juarez M., Horcada A., Alcade M.J., Valera M., Mullen A.M., Molina A. Estimation of factors influencing fatty acid profiles in light lambs. *Meat Sc*. 2008; **79**: 203-210.

Kallio H., Yli-Jokipii K., Kurvinen J.P., Sjovall O., Regioisomerism of triacylglycerols in lard, tallow, yolk, chicken skin, palm oil, palm olein, palm stearin, and a transesterified blend of palm stearin and coconut oil analyzed by tandem mass spectrometry. *J. Agric*. & *Food Chem.*2001; **49**: 3363-3369.

Kamm W., Dionisi F., Hischenhuber C., Engel K.H., Authenticity assessment of fats and oils. *Food Reviews Int*. 2001; **17(3)**: 249-290.

Kelly S, Parker I, Sharman M, Dennis J, Goodall I. Assessing the authenticity of single seed vegetable oils using fatty acid stable carbon isotope ratios ($^{13}C/^{12}C$). *Food Chemistry*. 1997; **59(2)**: 181-186.

Kouba M., Mourot J., Effect of a high linoleic acid diet on lipogenic enzyme activities and on the composition of the lipid fraction of fat and lean tissues in the pig. *Meat Sci.* 1999; **52(1)**: 39-45.

Kuksis A., McCarthy M.J., Gas-liquid chromatographic fractionation of natural triglyceride mixtures by carbon number. *Can. J. of Biochem.* & *Physiology*. 1962; **40(5)**: 679-686.

Laakso P., Mass spectrometry of triacylglycerols. *Eur. J. Lipid Sci. Technol.* 2002; 104:43-49.

Lees M., Meat and meat products. *Food authenticity and traceability, Woodhead Publishing Limited, Cambridge, England.* 2003; Chapter **15:** 347-352.

Leon-Camacho M., Viera-Alcaide I., Vicario I.M., Acorn (*Quercus spp.*) Fruit lipids: Saponifiable and unsaponifiable fractions: A detailed study. *JAOCS.* 2004; **81(5)**: 447-453.

Leskinen H., Suomela J.P., Kallio H., Quantification of triacylglycerol regioisomers in oils and fat using different mass spectrometric and liquid chromatographic methods. *Rapid Commun. Mass Spectrom.* 2007; **21**: 2361-2373.

Leskinen H., Suomela J.P., Kallio H., Quantification of triacylglycerol regioisomers by ultra-high-performance liquid chromatography and ammonia negative ion atmospheric pressure chemicalionization tandem mass spectrometry., *Rapid Commun. Mass Spectrom.* 2010; **24**: 1-5.

Litchfield C., Analysis of Triglycerides, *Academic Press, 1972*: 2-5, 243.

Li X., Evans J.J., Examining the collision-induced decomposition spectra of ammoniated triglycerides as a function of fatty acid chain length and degree of unsaturation. I. The OXO/YOY series. *Rapid Commun. Mass Spectrom.* 2005; **19**: 2528-2538.

Madron M.S., Peterson D.G., Dwyer D.A., Corl B.A., Baumgard L.H., Beermann D.H., Bauman D.E., Effect of extruded full fat soybeans on conjugated linoleic acid content of intramuscular, intermuscular, and subcutaneous fat in beef steers. *J. Animal Sci.*2002; **80**: 1135-1143.

Mahesar S.A., Sherazi S.T.H., Abro K., Kandhro A., Bhanger M.I., Van de Voort F.R., Sedman J., Application of microvawe heating for the fast extraction of fat content from poultry feeds. *Talanta*. 2008; **75**: 1240-1244.

Mahgoub O., Khan A.J., Al-Maqbaly R.S., Al-Sabahi J.N., Annamalai K., and Al-Sakry N.M., Fatty acid composition of muscle and fat tissues of Omani Jebel Akhdar goats of different sexes and weights. *Meat Sc.* 2002; **61**: 381-387.

Malone M., Evans J.J., Determining the relative amounts of positional isomers in complex mixtures of triglycerides using reversed-phase high-performance liquid chromatography-tandem mass spectrometry. *Lipids*. 2004; **39(3)**:273-284.

Manirakiza P., Covaci A., Schepens P., Comparative study on total lipid determination using soxhlet, Roese-Gottlieb, Bligh & Dyer, and modified Bligh & Dyer extraction methods. *J. Food Composition and Analysis*. 2001; **14**: 93-100.

March R.E., An introduction to quadrupole ion trap mass spectrometry. *J. Of Mass Spectrometry.* 1997; **32**: 351-369.

Marchello M.J., Cook N.K., Slanger W.D., Johnson V.K., Fischer A.G., Dinusson W.E., Fatty-acid composition of lean and fat tissue of swine fed various dietary levels of sunflower seed. *J. Of Food Sc.* 1983; **48(4)**: 1331-1334.

Marikkar J.M.N., Ghazali H.M., Che Man Y.B., Lai O.M., *Food research Int.* 2002; **35(10)**: 1007-1014.

Marikkar J.M.N., Ghazali H.M., Che Man Y.B., Peiris T.S.G., Lai O.M., Distinguishing lard from other animal fats in admixtures of some vegetable oils using liquid chromatographic data coupled with multivariate data analysis. *Food Chem.* 2005; **91(1)**: 5-14.

Marina A.M., Che Man Y.B., Nazimah S.A.H., Chemical properties of virgin coconut oil. *J. Of the American Oil Chem Society.* 2009; **86**: 301-307.

Marion J.E., Effect of age and dietary fat on the lipids of muscle chicken. *J. Nutrition.* 1965;**85**: 38-44.

Marzilli L.A., Fay L.B., Dionisi F., Vouros P., Structural characterization of triacylglycerols using electrospray ionization-MS^n ion-trap MS. JAOCS 2003; **80(30**): 195-202.

Mayer B.X., Lorbeer E., Triacylglycerol mixture for testing capillary columns for high-temperature gas chromatography. *J. Chromatogr. A.* 1997; **758**: 235-242.

Metayer A., Daumas G., Estimation, par decoupe, de la teneur en viande maigre des carcasses de porcs. *J. Rech. Porcine en France.* 1998; **30**: 7-11.

Momchilova S., Tsuji K., Itabashi Y., Damyanova B.N., Kuksis A., Resolution of triacylglycerol positional isomers by reversed-phase high-performance liquid chromatography. *J. Sep. Sci.* 2004;**27** : 1033-1036.

Momchilova S., Nikolova-Damyanova B., Quantitative TLC and gas chromatography determination of the lipid composition of raw and microwaved roasted walnuts, hazelnuts, and almonds. *J. Of Liquid Chromatography & Related Tech.* 2007; **30**: 2267-2285.

Monziols M., Bonneau M., Davenel A., Kouba M., Comparison of the lipid content and fatty acid composition of intermuscular and subcutaneous adipose tissues in pig carcasses. *Meat Science*. 2007; **76**: 54-60.

Mottram H.R, Evershed R.P. Structure analysis of triacylglycerol positional isomers using Atmospheric Pressure Chemical Ionization Mass Spectrometry. *Tetrahedron Lett*. 1996; **37**: 8593-8596.

Mottram H.R., Dudd S.N., Lawrence G.J., Stott A.W., Evershed R.P., New chromatographic, mass spectrometric and stable isotope approaches to the classification of degraded animal fats preserved in archaeological pottery. *J. Chromatogr. A* 1999; **833** : 209-221.

Mottram H.R., Crossman Z.M., Evershed R.P., Regiospecific characterisation of the triacylglycerols in animal fats using high-performance liquid chromatography-atmospheric pressure chemical ionisation mass spectrometry. *Analyst*. 2001; **126**: 1018-1024.

Mottram H.R., Evershed R.P., Practical considerations in the gas chromatography/combustion/isotope ratio monitoring mass spectrometry of ^{13}C-enriched compounds: detection limits and carryover effects. *Rapid Commun. Mass Spectrom.* 2003; **17**: 2669-2674.

Mottram H.R., Regiospecific analysis of triacylglycerols using high performance liquid chromatography/atmospheric pressure chemical ionization mass spectrometry. *Modern Methods for Lipid Analysis by Liquid Chromatography/Mass Spectrometry and Related Techniques*. 2005; Chapter 6: 276-297.

Nawar W.W., Chemical changes in lipids produced by thermal processing. *J. Of Chemical Education.* 1984; **61(4)**: 299-302.

Pamplet-standard section, Ministry Of Health, Malaysia.,
http://fsq.moh.gov.my/info/Standard_Section1.pdf

Pascual J.V., Rafecas M., Canela M.A., Boatella J., Bou R., Baucells M.D., Codony R., Effect of increasing amounts of a linoleic-rich dietary fat on the fat composition of four pig breeds. Part II: Fatty acid composition in muscle and fat tissues. *Food Chem.* 2007a; **100**: 1639-1648.

Pascual J.V., Rafecas M., Canela M.A., Boatella J., Bou R., Baucells M.D Codony R., Effect of increasing amounts of a linoleic-rich dietary fat on the fat composition of four pig breeds. Part III: Triacylglycerol composition in muscle and fat tissues. *Food Chem.* 2007b; **102**: 50-58.

Poy F., Visani S., Terrosi F., Automatic injection in high-resolution gas chromatography: A programmed temperature vaporizer as a general purpose injection system. *J. of Chromatogr.* 1981; **217**: 81-90.

Ramirez M.R., Morcuenda D., Estevez M., Lopez RC., Fatty acid profiles of intramuscular fat from pork loin chops fried in different culinary fats following refrigerated storage. *Food Chem.* 2005; **92(1)**: 159-167.

Raes K., Balcaen A., Dirinck P., Winne A. De., Claeys E., Demeyer D., Smet S. De., Meat quality, fatty acid composition and flavour analysis in Belgian retail beef. *Meat Sc.* 2003; **65**: 1237-1246.

Reid L.M., O'Donnell C.P., and Downey G., Recent technological advances for the determination of food authenticity. *Trends in Food Sc. & Tech*. 2006; **17**: 344-353.

Rezanka T., Mares P., Determination of plant triacylglycerols using capillary gas-chromatography, high-performance liquid-chromatography and mass spectrometer. *J. of Chromatogr*. 1991; **542(1)**: 145-159.

Rezanka T., Sigler K., The use of atmospheric pressure chemical ionization mass spectrometry with high performance liquid chromatography and other separation techniques for identification of triacylglycerols. *Current Analytical Chemistry*.2007; **3**: 252-271.

Romeu-Nadal M., Morera-Pons S., Castellote A.I., Lopez-Sabater M.C., Comparison of two methods for the extraction of fat from human milk. *Analytica Chimica Acta*. 2004; **513**: 457-461.

Sandra P., Medvedovici A., Zhao Y., David F., Charaterization of triglycerides in vegetable oils by silver-ion packed-column supercritical fluid chromatography coupled with mass spectroscopy with atmospheric pressure chemical ionization and coordination ion spray. *J. Chromatogr. A* 2002;**974(1-2)**: 231-241.

Segall S.D., Artz W.E., Raslan D.S., Ferraz V.P., and Takahashi J.A., Triacylglycerol analysis of pequi (caryocar brasiliensis camb.) oil by electrospray and tandem mass spectrometry. *J. Sci. Food Agric*. 2006; **86**: 445-452.

Segall S.D., Artz W.E., Raslan D.S., Ferraz V.P., Takahashi J.A., Analysis of triacylglycerol isomers in Malaysian cocoa butter using HPLC-mass spectrometry. *Food research International*. 2005; 3**8**: 167-174.

Scheeder M.R.L., Casutt M.M., Roulin M., Escher F., Dufey P.A., Kreuzer M., Fatty acid composition, cooking loss and texture of beef patties from meat of bulls fed different fats. *Meat Sci.* 2001; **58**: 321-328.

Shimizu M., Moriwaki J., Nishide T., Nakajima Y., Thermal deterioration of diacylglycerol and triacylglycerol oils during deep-frying. *J. Of the American Oil Chem Society*. 2004; **81(6)**: 571-576.

Shukla A.K., Futrell J.H., Collision activation and dissociation of polyatomic ions., *Mass Spec Review.*1993; **12**: 211-255.

Smedes F., Determination of total lipid using non-chlorinated solvents. *Analysts.* 1999; **124**: 1711-1718.

Soanes C., Stevenson A., "authenticate". The Oxford Dictionary of English (2nd edition revised) in English Dictionaries and Thesauruses. Oxford University Press, 2005; Oxford references online. <http://www.oxfordreference.com/views/ENTRY.html?subview=Main&entry=t140.e4667>

Sovova H., Lisa M., Holcapek M., Estimation of stereospecific fatty acid distribution in vegetable oils from liquid chromatography data. *Eur. J. Lipid Sci. Technol.* 2008; 110:266-276.

Stafford G.C., Kelley P.E., Syka J.E.P., Reynolds WE., and Todd JFJ., Recent improvements in and analytical applications of advanced ion trap technology., *Int. J. Mass Spect. And Ion Processes*. 1984; **60**: 85-98.

Suzuki K., Ishida M., Kadowaki H., Shibata T., Uchida H., Nishida A., Genetic correlations among fatty acid compositions in different sites of fat tissues, meat production, and meat quality traits in Duroc pigs. *J. Animal Sci.*2006; **84**: 2026-2034.

Suzuki S., Ishikawa S., Arihara K., Itoh M., Changes in molecular species composition of triacylglycerol in subcutaneous fat from beef cattle during fattening. *J. Animal Sci.*2007; **78**: 293-300.

Swartz M.E., UPLC^{TM}: An introduction and review. *J. Of Liquid Chromatography & Related Technologies.* 2005; **28(7)**:1253-1263.

Timon M.L., Ventanas J., Carrapiso A.I., Garcia J.C. , Subcutaneous and intermuscular fat characterization of dry-cured Iberian hams. *Meat Science*. 2001; **58**:85-91.

Tranchida P.Q., Donato P., Dugo P., Dugo G., Mondello L., Comprehensive chromatographic methods for the analysis of lipids. *Trends in Anal. Chem.*2007; **26(3)**: 191-205.

Tsimidou M., Macrae R., Reversed-phase chromatography of triglycerides – theoretical and practical aspects of the influence of injection solvents. *J. of Chromatogr Sci.* 1985; **23(4)**: 155-160.

Tyrefors L.N., Moulder R.X., Markides K.E., Interface for open tubular column supercritical fluid chromatography/atmospheric pressure chemical ionization mass spectrometry. *Anal. Chem.*1993; **65**: 2835-2840.

Ulberth F., Buchgraber M., Authenticity of fats and oils. *Eur. J. Lipid Sci. Technol.* 2000; **102**: 687-694.

Ulberth F., Milk and dairy products. *Food authenticity and traceability, Woodhead Publishing Limited, Cambridge, England.* 2003; Chapter **16:** 357-372.

Van der Klift E.J.C., Vivo-Truyols G., Claassen F.W., van Holthoon F.L., van Beek TA., Comprehensive two-dimensional liquid chromatography with ultraviolet, evaporative light scattering and mass spectrometric detection of triacylglycerols in corn oil. *Journal of Chromatography A.* 2008; **1178**: 43-55.

Van Heerden van S.M., Schonfeldt H.C., Smith M.F., Jansen van Rensburgz D.M., Nutrient content of South African chickens. *J. Food Composition and Analysis*. 2002; **15**: 47-64.

Van Ruth S.M., Villegas B., Akkermans W., Rozijn M., van der Kamp H., koot A., Prediction of the identity of fats and oils by their fatty acid, triacylglycerol and volatile compositions using PLS-DA. *Food Chemistry*. 2010; **118(4)**: 948-955.

Velasco S., Caneque V., Perez C., Lauzurica S., Diaz M.T., Huidobro F., Manzanares C., Gonzalez J., Fatty acid composition of adipose depots of suckling lambs raised under different production systems. *Meat Sc.* 2001; **59**: 325-333.

Viera-Alcaide I., Vicario I.M., Graciani Constante E., Leon-Camacho M., Authentication of fattening diet of Iberian pig according to their triacylglycerols profile from subcutaneous fat. *Analytica Chimica Acta*. 2007; **596**:319-324.

Warren H.E., Scollan N.D., Enser M., Hughes S.I., Richardson R.I., Wood J.D., Effects of breed and a concentrate or grass silage diet on beef quality in cattle of 3 ages. I: Animal performance, carcass quality and muscle fatty acid composition. *Meat Sc*. 2008; **78**: 256-269.

Wood J.D., Enser M., Fisher A.V., Nute G.R., Sheard P.R., Richardson R.I., Hughes S.I., Whittington F.M., Fat deposition, fatty acid composition and meat quality: A review. *Meat Sc*. 2008; **78**: 343-358.

Zhang S., Knight T.J., Stalder K.J., Goodwin R.N., Lonergan S.M., Beitz D.C., Effects of breed, sex, and halothane genotype on fatty acid composition of pork longissimus muscle. *J. Animal Sci.*2007; **85**: 583-591.